



# ROOT AND NODULE

*Lateral Organ Development in  
 $N_2$ -Fixing Plants*

TING TING XIAO

# ROOT AND NODULE

*Lateral Organ Development in  
 $N_2$ -Fixing Plants*

TING TING XIAO

## **Thesis committee**

### **Promotor**

Prof. dr. T. Bisseling  
Professor of Molecular Biology  
Wageningen University

### **Co-Promotors**

Dr. ir. R. Geurts  
Associate professor, Laboratory of Molecular Biology  
Wageningen University

Dr. H. Franssen  
Assistent professor, Laboratory of Molecular Biology  
Wageningen University

### **Other members**

Prof. dr. G.H. Immink, Wageningen University  
Prof. dr. K. Pawlowski, Stockholm University  
Dr. A. Niebel, Directeur de recherche CNRS  
Dr. J. E. M. Vermeer, Postdoc University of Lausanne

This research was conducted under the auspices of the Graduate School of Experimental Plant Sciences.

# ROOT AND NODULE

*Lateral Organ Development in  
 $N_2$ -Fixing Plants*

TING TING XIAO

## **Thesis**

submitted in fulfilment of the requirements for the degree of doctor  
at Wageningen University  
by the authority of the Rector Magnificus  
Prof. dr. M. J. Kropff,  
in the presence of the  
Thesis Committee appointed by the Academic Board  
to be defended in public  
on Wednesday 20 of May 2015  
at 1:30 p.m. in the Aula.

Ting Ting Xiao  
Root and Nodule  
Lateral Organ Development in N<sub>2</sub>-Fixing Plants  
200 pages

PhD thesis, Wageningen University, Wageningen, NL (2015)  
With references, with summaries in Dutch and English.

ISBN 978-94-6257-276-8

# CONTENTS

OUTLINE	7
CHAPTER 1	
<i>General introduction</i>	13
CHAPTER 2	
<i>Stem cells are formed from endodermis and pericycle during Medicago truncatula lateral root formation</i>	33
CHAPTER 3	
<i>Fate map of Medicago truncatula root nodules</i>	55
CHAPTER 4	
<i>MtPINs play a role in maintaining the auxin accumulation pattern during nodule development</i>	93
CHAPTER 5	
<i>Root developmental programs shape the Medicago truncatula nodule meristem</i>	133
CHAPTER 6	
<i>General discussion</i>	159
SUMMARY	183
SAMENVATTING	189
ACKNOWLEDGEMENTS	193
CURRICULUM VITAE	197





# OUTLINE

# OUTLINE

Plants are sessile organisms. This characteristic severely limits their ability of approaching nutrients. To cope with this issue, plants evolved endosymbiotic relationships with soil fungi to extend their interface with surrounding environment. In case of arbuscular mycorrhizae (AM) fungi this occurred about 400 million years ago. The AM fungi can interact with most angiosperms. In this symbiotic relationship, the plant get nutrients, especially phosphate, from the fungi, and plants provide carbohydrates to the fungi in return. About 60 million years ago, a group of plants evolved  $N_2$ -fixing nodule symbiosis. This includes interactions of legumes plants with rhizobium bacteria and actinorhizal plants with Frankia bacteria. Currently, all plant species that are able to establish a nodule symbiosis belong to the Rosid I clade. In the nodule symbioses the bacteria produce ammonia and the plant provides carbohydrates to the bacteria.

In the root nodule symbiosis, the nitrogen fixing bacteria are hosted in the cell of the root nodule. Although the function and structure of the root nodule are different from the other plant organs, it does share some features with other organs, especially the lateral root. To get further insight into the similarities and differences between root nodule and lateral root, I made use of the model legume (*Medicago truncatula*) and the non-legume Parasponia (*Parasponia andersonii*) that is the only genus outside the legumes that forms nodules with rhizobium.

In Chapter 1, I will give a general introduction on the process of root nodule formation in legume plants. I will mainly focus on nodule organogenesis and the plant hormones that are known to be important for this process. Root nodules are supposed to have a close relationship with lateral roots. Therefore a comparison between lateral root and root nodule development will be included in this introduction.

Lateral root development has especially been studied in in Arabidopsis. To be able to compare the root and root nodule developmental process, especially at the early stages, a Medicago lateral root development fate map has been made. This will be described in Chapter 2 and showed that in addition to the pericycle, endodermis and cortex are also mitotically

## OUTLINE

activated during lateral root formation. Pericycle derived cells only form part of the stem cell niche as endodermis derived cells also contribute to this.

In Chapter 3, a *Medicago* root nodule fate map is presented. In this Chapter, the contribution of different root cell layers to the mature nodule will be described. A set of molecular markers for root tissue, cell cycle and rhizobial infection have been used to facilitate this analysis. The fate map showed that nodule meristem originates from the third cortical layer and many cell layers of the base of the nodule are directly derived from cells of the inner cortical layers, root endodermis and pericycle. The inner cortical cell layers form about 8 cell layers of infected cells while the root endodermis and pericycle derived cells forms the uninfected tissues that are located at the base of the mature nodule. Nodule vascular is formed from the part of the primordium derived from the cortex. The development of primordia was divided in 6 stages. To illustrate the value of this fate map, a few published mutant nodule phenotypes are re-analyzed.

In Chapter 4, the role of auxin at early stages of *Medicago* nodule formation is studied. In this chapter auxin accumulation is studied during the 6 stages of primordium development. It is studied by using DR5::GUS as an auxin reporter. Auxin accumulation associates with mitotic activity within the primordium. Previously, it has been postulated by theoretical modelling that the accumulation of auxin during nodulation is induced by a local reduction of PIN (auxin efflux carriers) levels. We tested this theory, but this was hampered due to the low level of PIN proteins in the susceptible zone of the root. It is still possible that auxin accumulation is initiated by a decrease of PIN levels. However, the level of 2 PIN already increase before the first divisions are induced. In young primordia they accumulate in all cells. At later stages PINs mainly accumulate at the nodule periphery and the future nodule meristem. The subcellular position of PINs strongly indicates they play a key role in the accumulation of auxin in primordia.

Previous studies showed that a group of root apical meristem regulators is expressed in the nodule meristem. In Chapter 5, we tested whether the

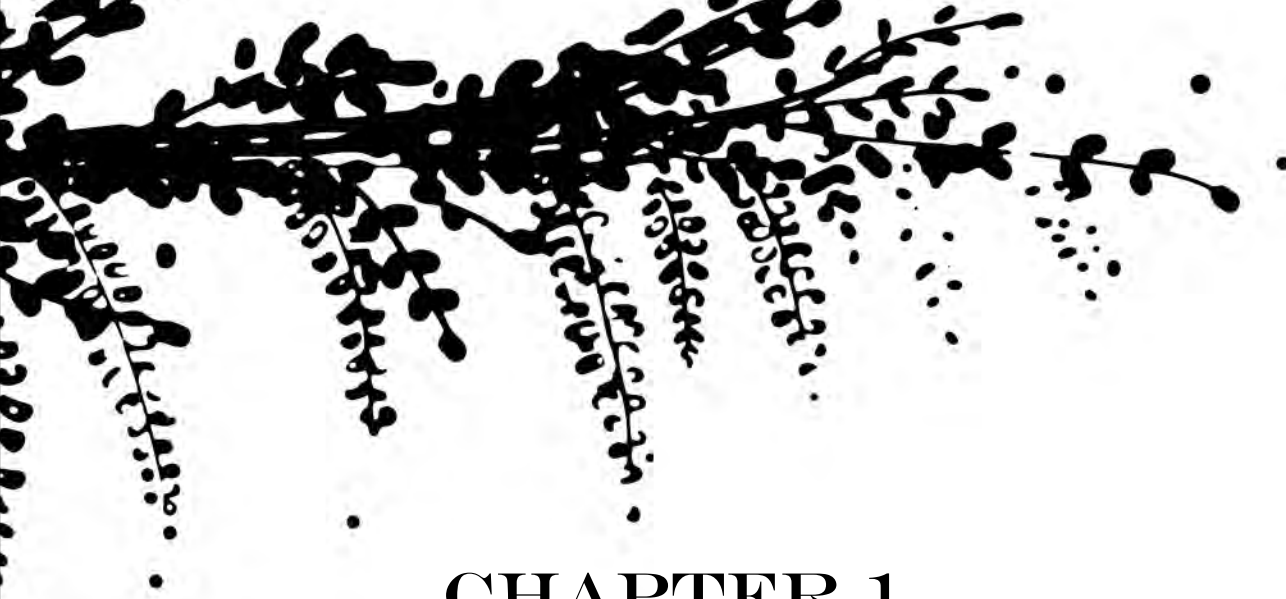
# OUTLINE

Medicago nodule meristem expresses *PLETHORA* genes that are expressed in the root meristem. These *PLETHORAs* were functionally analysed, by using RNAi approach using a nodule specific promoter. Knockdown of *PLETHORAs* expression hampers primordium formation and meristem growth. Hence, we conclude rhizobium recruited key regulators of root development for nodule development.

In Chapter 6, we first introduced the non-legume lateral root and nodule fate maps by using *Parasponia*. In *Parasponia* nodules the nodule central vascular bundle is completely derived from the pericycle similar as its lateral roots. The nodule infected cells were shown to be derived from cortex. Together with the data obtained in this thesis, this Chapter further discussed several developmental aspects of the different lateral root organs. Especially, it focused on the vasculature and meristem formation of legume and non-legume nodules.

## OUTLINE





# CHAPTER 1

## *General introduction*

**Ting Ting Xiao**

Department of Plant Sciences, Laboratory of Molecular Biology, Wageningen  
University, Droevendaalsesteeg 1, 6708 PB, Wageningen, The Netherlands

# CHAPTER 1

Legume plants are able to interact with nitrogen-fixing rhizobia which results in the formation of a unique lateral organ, the root nodule. These root nodules are made to host the bacteria and to create an environment where they can fix nitrogen (Desbrosses and Stougaard, 2011; Oldroyd et al., 2011). This symbiotic relationship between legume plants and nitrogen-fixing rhizobia brings major advantages for agriculture and environment. Inside the root nodule, bacteria convert  $N_2$  into ammonia providing a fixed nitrogen source for its host. In return, the plant supports the bacteria with carbohydrates. This symbiotic nitrogen fixation makes legume crops almost independent of nitrogen fertilizer, the use of which causes major damage to the environment. Not only legume plants profit from the fixed nitrogen, for example when legume material is eaten or when it decomposes, the fixed nitrogen becomes available to other organisms.

In this introduction, I will mainly focus on nodule organogenesis and the plant hormones that are known to be important for this process. Further, root nodules are supposed to have a close relationship with lateral roots. Therefore, a comparison between lateral root and root nodule development will be included in this introduction.

## **Root nodule formation and bacterial infection**

Legume root nodules can have either a determinate or indeterminate growth, which depends on the host plant species (Franssen et al., 1992; Maunoury et al., 2008). Determinate nodules are formed on plants like, *Lotus japonicus* (Lotus) and *Glycine max* (soybean). These nodules have a transient nodule meristem. Indeterminate root nodules are formed on plant species like, Medicago, pea, alfalfa, and clover. These nodules have a meristem at their apices and this keeps on adding cells to the nodule tissues, through the lifespan of the nodule (Franssen et al., 1992; Maunoury et al., 2008; Lotocka et al., 2012). An example of an indeterminate root nodule (Medicago nodule) is shown in Fig. 1. At the apex of the root nodule is the nodule meristem, which remains mitotically active and adds cells to the different nodule tissues. The center of the nodule is composed of two types of cells: cells that are not infected and cells that are fully infected by rhizobia. Within the infected cells bacteria are hosted as symbiosomes (Roth and Stacey, 1989). These are membrane compartments containing

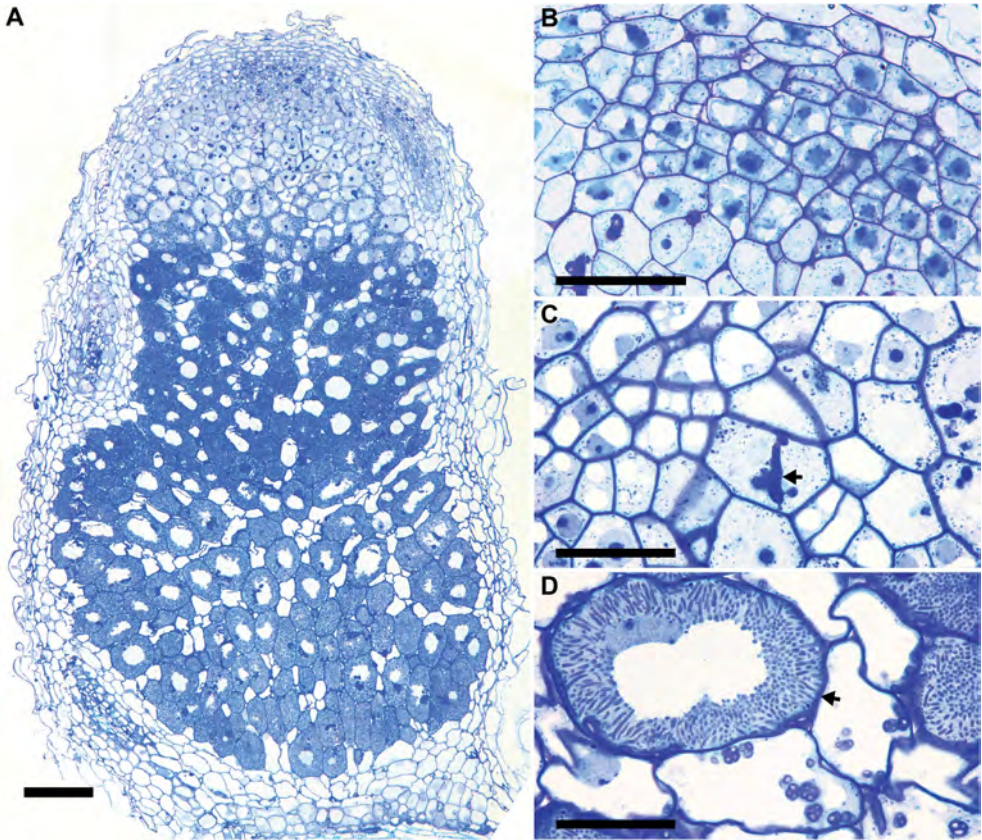


Fig. 1. Medicago root nodule. Longitudinal section of a Medicago root nodule (A) with the magnification of nodule meristem (B), infection zone (C) and fixation zone (D). Arrows indicate infection thread (C) and fully infected cell (D). Bars, 75  $\mu\text{m}$  in A, 25  $\mu\text{m}$  C-D.

a single or a few differentiated rhizobia. At the nodule periphery, there are 3 uninfected tissues. These are 2 to 3 layers of non-infected nodule parenchyma and 3 to 4 layers of cortex (Van De Wiel et al., 1990; Brewin, 1991). In between these tissues there is also one cell layer of endodermis. Nodule vascular bundles, which are connected to the root stele, are located within the nodule parenchyma.

In general, the formation of this symbiotic organ requires two processes, nodule organogenesis and bacterial infection. Both are triggered by Nodulation (Nod) factors, which are rhizobium secreted signal molecules. These are lipochito-oligosaccharides, which can have specific substitutions

# CHAPTER 1

at their terminal sugar residues. When the plant perceives Nod factors (Nod factor signalling see next section), cortical cells are mitotically activated (Libbenga and Harkes, 1973; Dudley et al., 1987; Timmers et al., 1999). This cluster of dividing cortex cells is named nodule primordium (Libbenga and Harkes, 1973; Dudley et al., 1987; Yang et al., 1992; Timmers et al., 1999). Concurrently, Nod factors induce root hair curling at the root epidermis by which closed pockets are formed that entrap the rhizobia. Within these pockets the host cell wall is locally degraded and plasma membrane starts to invaginate by which an inward growing tube is formed, the infection thread. This involves deposition of new cell wall and membrane material by the host (Brewin, 2004; Gage, 2004). By this cell wall bound infection thread, rhizobia pass the epidermis and are delivered to the nodule primordium cells. There, rhizobia are released in host cells. This involves the formation of a small region at the infection thread that lacks a cell wall, the unwalled droplet. This brings bacteria in direct contact with the host membrane. By a specific exocytosis process (Ivanov et al., 2012), bacteria become surrounded by a plant-derived membrane and are individually taken up by the host cells. In this way symbiosomes are formed. Subsequently, symbiosomes proliferate and differentiate into  $N_2$ -fixing organelles (Roth and Stacey, 1989). In case of indeterminate nodules, like those of Medicago and pea, nodule primordia are derived from inner cortex cell layers. Once the infection thread invades the nodule primordium, a meristem is formed and this starts to add cells to the developing root nodule (Timmers et al., 1999) (Chapter 3).

## **Nod factor signalling**

Nod factors are lipo-chitooligosaccharides. In general, they have a backbone of four or five *N*-acetyl glucosamine residues that are  $\beta$ -1,4-linked. A fatty acid chain (16 or 18 carbon atoms) is attached to the terminal non-reducing glucosamine residue. Depending on the rhizobium species, variations may occur in the structure of the fatty acid. Further, specific substitutions can be present on the terminal residues. The structure of Nod factors determines their biological activity and is also a major determinant of host specificity (Ardourel et al., 1994). Genetic studies on legumes have identified genes that are essential for Nod factor perception or signal transduction.

Nod factors are recognized by the plant by (at least) 2 LysM receptor-like kinases (RLKs) this are NFR1/NFR5 in Lotus and NFP/LYK3 in Medicago (Ben Amor et al., 2003; Radutoiu et al., 2003; Arrighi et al., 2007; Smit et al., 2007). Perception of Nod factors triggers calcium oscillations in and around the nucleus (Oldroyd and Downie, 2006). This requires, in addition to the Nod factor receptors, a plasma membrane located LRR-type receptor kinase, SYMRK, and an ion channel (DMI1 in Medicago; CASTOR and POLLUX in Lotus) (Endre et al., 2002; Bersoult et al., 2005; Imaizumi-Anraku et al., 2005; Limpens et al., 2005; Charpentier et al., 2008) that is localized on the nuclear envelope. These are required for Nod factor induced Ca spiking. The calcium oscillations are then perceived by a nuclear localized calcium and calmodulin-dependent kinase (CCaMK) (Levy et al., 2004; Mitra et al., 2004), which interacts and activates a transcriptional regulator (IPD3 in Medicago; CYCLOPS in Lotus) (Yano et al., 2008; Horvath et al., 2011; Ovchinnikova et al., 2011; Singh et al., 2014). Downstream of CCaMK/CYCLOPS several transcription factors are essential for Nod factor induced responses. This includes two GRAS type transcription regulator NSP1 and NSP2 (Kalo et al., 2005; Smit et al., 2005); an ethylene response factor (ERN1) (Andriankaja et al., 2007); nodule inception (NIN) (Marsh et al., 2007) and one CCAAT-binding family transcription factor NF-YA1 (Combiere et al., 2006; Laporte et al., 2014). These transcription factors are involved in nodule organogenesis as well as infection. In this symbiotic signalling pathway CCaMK/CYCLOPS plays a key role, since dominant active forms of CCaMK as well as CYCLOPS are able to trigger nodule organogenesis independent of rhizobia (Gleason et al., 2006; Tirichine et al., 2006; Yano et al., 2008). Also ectopic NIN expression induces nodule formation in the absence of bacteria (Soyano et al., 2013). Further, to induce nodule organogenesis a specific cytokinin receptor (LHK1 in Lotus and CRE1 in Medicago) is essential. Loss of function of this gene blocks nodule primordium formation and infection threads fail to enter the cortex (Murray et al., 2007; Plet et al., 2011). A gain of function LHK1 mutant is able to induce nodule-like structures, which is independent of CCaMK, but depends on NSP1/2 and NIN (Gonzalez-Rizzo et al., 2006; Murray et al., 2007; Tirichine et al., 2007; Ovchinnikova et al., 2011; Plet et al., 2011).

The involvement of a specific cytokinin receptor leads to the conclusion

# CHAPTER 1

that cytokinin plays a key role in nodule organogenesis. This creates an intriguing paradox, as it has been shown that the cytokinin antagonist auxin is most likely instrumental in triggering the cortical divisions that lead to the formation of a nodule primordium. In the following section I will summarize the current knowledge on the role of auxin and cytokinin in nodule organogenesis.

## **The role of cytokinin and auxin in nodule organogenesis**

Auxin has been shown to be involved in early steps of nodule organogenesis. The involvement of the auxin signalling in nodule primordia has been shown by using GH3 and (a more sensitive) DR5::GUS fusion reporter systems (Pacios-Bras et al., 2003; Huo et al., 2006; Van Noorden et al., 2007; Takanashi, 2011; Takanashi et al., 2011; Turner et al., 2013). Recently, auxin has even been shown to be involved at the start of nodule primordium formation in Lotus, by using a DR5 based reporter system (Suzaki et al., 2012). In the same study, auxin signalling was also shown to occur during spontaneous nodule formation, induced by CCaMK, LHK1 and NIN dominant active mutants (Suzaki et al., 2012).

The involvement of auxin in nodule organogenesis is well in line with the role of auxin as a central regulator of plant development. The formation of plant organs starts in general with the accumulation of auxin and it is a prerequisite for organ formation (Benkova et al., 2003). The formation of root nodules seems no exception, although the importance of auxin signalling at initial steps of nodule formation remains to be demonstrated. Based on the expression of auxin signalling reporters during nodule initiation (Van Noorden et al., 2007; Suzaki et al., 2012), we can hypothesise that auxin signalling is required for cortical cell reprogramming and divisions.

Cytokinin signalling is absolutely crucial for nodule organogenesis. As I described above, a specific cytokinin receptor (LHK1 and CRE1) is needed to induce nodule primordium formation. How is this receptor activated by Nod factor signalling? A recent study shows that Nod factors are able to induce cytokinin accumulation within 3 h (de Camp, 2012). Furthermore, it has been shown that exogenous cytokinin can induce nodulin gene expression in *Sesbania* (Dehio and Debruijn, 1992) and cytokinin producing nod<sup>-</sup> rhizobia (deficient in producing Nod factors) induce nodule

primordium formation in alfalfa (Cooper and Long, 1994). Together these studies strongly suggest that cytokinin that accumulates upon Nod factor perception, triggers cortical cell division. So during nodule initiation, on one hand auxin signalling correlates with cortical cell division; on the other hand, cytokinin triggers these divisions. Since, cytokinin and auxin work in an antagonistic manner to control different aspect of plant development (Laplaze et al., 2007; Dello Ioio et al., 2008; Moubayidin et al., 2009; Sablowski, 2011), the involvement of both hormones signalling during nodule initiation creates a paradox.

To further understand the mechanism behind the paradox, a theoretical computer model has bridged auxin and cytokinin signalling during nodulation (Deinum et al., 2012). The model tested 3 possible ways of achieving auxin accumulation during nodulation, which includes increased local auxin production, increased auxin transport influx and decreased auxin efflux. Model prediction suggested that auxin accumulation at the primordium site can efficiently be created by regulating auxin transport, especially by decreasing auxin efflux in a local region.

Auxin efflux is controlled by the PIN-FORMED (PIN) proteins. In general, these proteins have a hydrophobic domains of about five transmembrane regions their N and C-terminal regions and there is a distinct central hydrophilic loop (Krecek et al., 2009). These PIN proteins are located in the plasma membrane, but are asymmetrically/polarly distributed within the cell. This polar localization determines the directionality of intercellular auxin flow (Benkova et al., 2003; Vieten et al., 2005; Vieten et al., 2007; Peret et al., 2013).

In the theoretical model the concentration of PINs in the plasma membrane was locally reduced. This theory is consistent with the fact that cytokinin is able to trigger this. For example, cytokinin promotes differentiation of root meristematic cells by reducing PIN expression (Dello Ioio et al., 2008). Also, cytokinin disturbs lateral root formation by reducing PIN gene expression, stimulating PIN1 degradation and it affects PIN polar localization (Laplaze et al., 2007; Marhavy et al., 2011; Marhavy et al., 2014).

Although this model remains to be tested by experimental work, several

# CHAPTER 1

previous studies are in line with it. A block of polar auxin transport is observed in *Medicago* roots 24 h after inoculation with rhizobium (van Noorden et al., 2006; Plet et al., 2011) and this is dependent on the cytokinin receptor (CRE1) (Plet et al., 2011). Further, auxin transport inhibitors, like N-1-naphthylphthalamic acid (NPA) and 2,3,5-triiodobenzoic acid (TIBA), induce the formation of nodule-like structures (Hirsch et al., 1989; Wasson et al., 2006; Rightmyer and Long, 2011). It has been proposed that flavonoids can affect auxin polar transport and they may also contribute to the block of auxin transport during nodulation (Yang et al., 1992; Mathesius et al., 1998). These studies are in line with the idea that rhizobia affect polar auxin transport by which auxin locally accumulates. However, whether this involves the local reduction of PIN levels remains to be demonstrated. Currently, only studies have been published in which *Medicago* PIN expression is globally affected (Huo et al., 2006; Plet et al., 2011).

Reduced *MtPIN* expression by using RNAi knockdown driven by 35S promoter caused a reduction in nodule numbers (Huo et al., 2006). However, this effect on nodulation is most likely indirect as auxin homeostasis will be affected in the complete root. To identify whether PIN proteins are really targets of Nod factor signalling, extensive studies on this protein family during nodulation have to be performed (Chapter 4).

## Evolution of Nod factor signalling

The evolutionary origin of the Nod factor signalling pathway has been revealed by genetic studies on legume plants. These studies showed that a group of essential Nod factor signalling genes are also required for the endosymbiosis with arbuscular mycorrhizal (AM) fungi (Oldroyd, 2013). This symbiosis is far more ancient than the rhizobium legume symbiosis as it originated more than 400 million years ago, whereas the nodule symbiosis arose about 60 million years ago (Lavin et al., 2001; Lavin et al., 2005; Sprent and James, 2007; Swensen and Benson, 2008; Wang et al., 2009; Doyle, 2011). Therefore, at least part of the signalling pathway used by AM fungi has been co-opted in the legume rhizobium nodule symbiosis. This part of the signalling cascade has been named the common symbiotic signalling pathway. This common signalling pathway is activated in the interaction with rhizobium by the Nod factor receptors. However, in

legumes loss of function mutations in Nod factor receptors do not affect mycorrhization. Although receptors activated by mycorrhizal (Myc) factors have not yet been identified, recent studies support the hypothesis that Nod factor receptors evolved from ancestral Myc factor receptors. First, AM fungi were shown to produce lipo-chitooligosaccharides (Myc factor) with a similar structure as Nod factors. Plants treated with these Myc factors have an increased colonization by AM fungi (Maillet et al., 2011). Second, *Parasponia* is the only non-legume plant genus that also can establish nodule symbioses with rhizobia. This symbiosis evolved independent from legume and arose more recent (Doyle, 2011). In contrast to legumes, *Parasponia* has only one NFP-like gene. It was tested whether this gene is required for nodulation. Suppression of *Parasponia* NFP blocked nodulation. Further, it also blocked the formation of arbuscules (intracellular infection) by AM fungi. Arbuscules are highly branched intracellular hyphae that are surrounded by a host membrane. The fact that knockdown of NFP affects both symbiotic interactions suggests that *Parasponia* NFP has kept its ancestral function, which is recognition of Myc factors of AM fungi (den Camp et al., 2011). In legumes the Nod factor receptor genes are part of gene families. Therefore it seems probable that in legumes the Myc factor receptor genes duplicated and by neo-functionalization specialised Nod factor receptors evolved.

In addition to the common signalling pathway the intracellular colonization of host cells by rhizobia and AM fungi also share similarities. In *Medicago*, a specific exocytotic pathway has been identified that is required for symbiosome and arbuscule formation (Ivanov et al., 2012). This exocytotic pathway involves 2 symbiosis specific vesicle-associated membrane proteins *MtVAMP72*'s. The common signalling pathway and the shared cellular mechanism for intracellular infection strongly suggest that the rhizobium legume symbiosis evolved from the ancient arbuscular mycorrhizal symbiosis.

Although both Nod and Myc factors activate the common signalling pathway, legume plants are able to distinguish between the two signals, as the responses are different. Nod factors trigger division in inner cortical cells and from these a nodule primordium and subsequently, a nodule is formed. In the case of mycorrhization the fungal hyphae penetrate inner cortical cells and subsequently arbuscules are formed. Cortical cells

# CHAPTER 1

in which arbuscules are formed do not divide, although they undergo endoreduplication (Bainard et al., 2011). As we described in the previous paragraph Nod factor induced cytokinin signalling is essential for the induction of cortical cell division (nodule organogenesis). However, cytokinin signalling seems not essential for arbuscule formation (Andrea Genre, personal communication). Therefore, the integration of cytokinin signalling within Nod factor signalling might be causal to the different readouts. However, how Nod factors activate cytokinin signalling, whereas Myc factors do not, remains to be demonstrated.

## Are root nodules modified lateral roots?

As described above rhizobium symbiosis evolved from the ancient arbuscular mycorrhizal symbiosis. However, only in the rhizobium symbiosis a new organ is formed. Although the function and structure of root nodules are different from other plant organs, it shares some features with other organs (Hirsch et al., 1997), especially the lateral root (Gualtieri and Bisseling, 2000; Stougaard, 2001; Roudier et al., 2003; Bright et al., 2005; Soyano et al., 2013).

Lateral roots are derived from the pericycle (Malamy and Benfey, 1997; Lucas et al., 2013). In *Arabidopsis*, lateral roots initiate in pairs of founder cells that are located in the pericycle (Lucas et al., 2013). Both anticlinal and periclinal cell divisions of these founder cells contribute to the formation of the new lateral root primordium. Then, the primordium becomes progressively organized and a meristem including a stem cell niche is formed. When the lateral root has emerged, the meristem

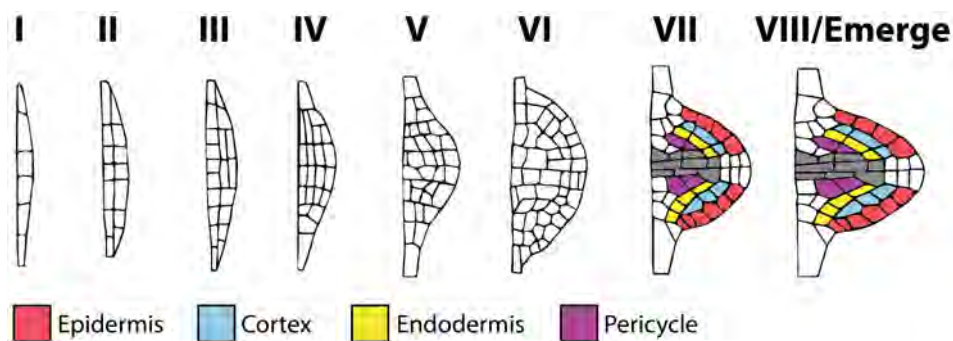


Fig. 2. Lateral root developmental stages of *Arabidopsis*.

becomes functional and adds cells to the different root tissues (Malamy and Benfey, 1997). In total, 8 anatomical stages have been described for Arabidopsis (Fig. 2) (Malamy and Benfey, 1997).

In non-legume plants, such as actinorhizal plants (Callaham and Torrey, 1977; Torrey and Callaham, 1979) or Parasponia (Lancelle and Torrey, 1985), root nodules appear to be modified lateral roots, since they have a pericycle-derived central vascular bundle (Hirsch et al., 1997). In legumes, loss of function of the Arabidopsis BLADE-ON-PETIOLE ortholog NOOT/COCH, results in the change in identity of root nodule meristem into a root meristem (Ferguson and Reid, 2005; Couzigou et al., 2012), which suggests that these meristems are closely related. Further, lateral roots and root nodules are both initiated in front of protoxylem poles in the root differentiation zone (root nodule, Libbenga and Harkes, 1973; lateral root, Sussex et al., 1995) and both start with cell divisions in the pericycle (lateral root, Malamy and Benfey, 1997; root nodule, Timmers et al., 1999). Some studies on legume plants show that also cortical cell divisions occur during lateral root development (Popham, 1955; Mallory et al., 1970; Herrbach et al., 2014), pointing to similarities in root and nodule development. Although similar tissues are activated, it is unclear whether these activated cells contribute to the newly formed organs. For example it is not known whether these activated cortical cells contribute to the newly formed lateral root or whether activated pericycle cells become part of the nodule. To study in more depth similarities and differences in the root and nodule developmental programs it will be essential to develop detailed fate maps for these 2 organs (Chapter 2, Chapter 3, Chapter 5 and Chapter 6).

## REFERENCES

**Andriankaja, A., Boisson-Demier, A., Frances, L., Sauviac, L., Jauneau, A., Barker, D. G. and de Carvalho-Niebel, F. (2007).** AP2-ERF transcription factors mediate nod factor-dependent mt ENOD11 activation in root hairs via a novel cis-regulatory motif. *Plant Cell* **19**, 2866-2885.

**Ardourel, M., Demont, N., Debelle, F. D., Maillet, F., Debilly, F., Prome, J. C., Denarie, J. and Truchet, G. (1994).** *Rhizobium meliloti* lipooligosaccharide nodulation factors: different structural requirements for bacterial entry into target root hair cells and induction of plant symbiotic developmental responses. *Plant Cell* **6**, 1357-1374.

# CHAPTER 1

**Arrighi, J. F., Barre, A., Ben Amor, B., Bersoult, A., Soriano, L. C., Mirabella, R., de Carvalho-Niebel, F., Journet, E. P., Gherardi, M., Huguet, T. et al. (2007).** The *Medicago truncatula* lysine motif-receptor-like kinase gene family includes NFP and new nodule-expressed genes. *Plant Physiol* **143**, 1078-1078.

**Bainard, L. D., Bainard, J. D., Newmaster, S. G. and Klironomos, J. N. (2011).** Mycorrhizal symbiosis stimulates endoreduplication in angiosperms. *Plant Cell Environ* **34**, 1577-1585.

**Ben Amor, B., Shaw, S. L., Oldroyd, G. E. D., Maillet, F., Penmetsa, R. V., Cook, D., Long, S. R., Denarie, J. and Gough, C. (2003).** The NFP locus of *Medicago truncatula* controls an early step of Nod factor signal transduction upstream of a rapid calcium flux and root hair deformation. *Plant J* **34**, 495-506.

**Benkova, E., Michniewicz, M., Sauer, M., Teichmann, T., Seifertova, D., Jurgens, G. and Friml, J. (2003).** Local, efflux-dependent auxin gradients as a common module for plant organ formation. *Cell* **115**, 591-602.

**Bersoult, A., Camut, S., Perhald, A., Kereszt, A., Kiss, G. B. and Cullimore, J. V. (2005).** Expression of the *Medicago truncatula* DM12 gene suggests roles of the symbiotic nodulation receptor kinase in nodules and during early nodule development. *Molecular Plant Microbe Interactions* **18**, 869-876.

**Brewin, N. J. (1991).** Development of the legume root nodule. *Annual review of cell biology* **7**, 191-226.

**Brewin, N. J. (2004).** Plant cell wall remodelling in the rhizobium-legume symbiosis. *Crit Rev Plant Sci* **23**, 293-316.

**Bright, L. J., Liang, Y., Mitchell, D. M. and Harris, J. M. (2005).** The *LATD* gene of *Medicago truncatula* is required for both nodule and root development. *Molecular Plant Microbe Interactions* **18**, 521-532.

**Callaham, D. and Torrey, J. G. (1977).** Prenodule formation and primary nodule development in roots of *Comptonia* (Myricaceae). *Canadian Journal of Botany* **55**, 2306-2318.

**Charpentier, M., Bredemeier, R., Wanner, G., Takeda, N., Schleiff, E. and Parniske, M. (2008).** *Lotus japonicus* CASTOR and POLLUX are ion channels essential for perinuclear calcium spiking in legume root endosymbiosis. *Plant Cell* **20**, 3467-3479.

**Combier, J. P., Frugier, F., de Billy, F., Boualem, A., El-Yahyaoui, F., Moreau, S., Vernie, T., Ott, T., Gamas, P., Crespi, M. et al. (2006).** MtHAP2-1 is a key transcriptional regulator of symbiotic nodule development regulated by microRNA169 in *Medicago truncatula*. *Genes & Development* **20**, 3084-3088.

**Cooper, J. B. and Long, S. R. (1994).** Morphogenetic rescue of *Rhizobium meliloti* nodulation mutants by trans-zeatin secretion. *Plant Cell* **6**, 215-225.

**Couzigou, J. M., Zhukov, V., Mondy, S., Abu el Heba, G., Cosson, V., Ellis, T. H. N., Ambrose, M., Wen, J. Q., Tadege, M., Tikhonovich, I. et al. (2012).** *NODULE ROOT* and *COCHLEATA* maintain nodule development and are legume orthologs of Arabidopsis *BLADE-ON-PETIOLE* genes. *Plant Cell* **24**, 4498-4510.

**de Camp, R. H. O. (2012).** Evolution of rhizobium symbiosis. *PhD thesis*.

**Dehio, C. and Debruijn, F. J.** (1992). The early nodulin gene *Srenod2* from *Sesbania rostrata* is inducible by cytokinin. *Plant J* **2**, 117-128.

**Deinum, E. E., Geurts, R., Bisseling, T. and Mulder, B. M.** (2012). Modeling a cortical auxin maximum for nodulation: different signatures of potential strategies. *Front in Plant Science* **3**, 96.

**Dello Ioio, R., Nakamura, K., Moubayidin, L., Perilli, S., Taniguchi, M., Morita, M. T., Aoyama, T., Costantino, P. and Sabatini, S.** (2008). A genetic framework for the control of cell division and differentiation in the root meristem. *Science* **322**, 1380-1384.

**den Camp, R. O., Streng, A., De Mita, S., Cao, Q. Q., Polone, E., Liu, W., Ammiraju, J. S. S., Kudrna, D., Wing, R., Untergasser, A. et al.** (2011). LysM-type mycorrhizal receptor recruited for rhizobium symbiosis in nonlegume *Parasponia*. *Science* **331**, 909-912.

**Desbrosses, G. J. and Stougaard, J.** (2011). Root nodulation: a paradigm for how plant-microbe symbiosis influences host developmental pathways. *Cell Host Microbe* **10**, 348-358.

**Doyle, J. J.** (2011). Phylogenetic perspectives on the origins of nodulation. *Molecular Plant Microbe Interactions* **24**, 1289-1295.

**Dudley, M. E., Jacobs, T. W. and Long, S. R.** (1987). Microscopic studies of cell divisions induced in alfalfa roots by *Rhizobium meliloti*. *Planta* **171**, 289-301.

**Endre, G., Kereszt, A., Kevei, Z., Mihacea, S., Kalo, P. and Kiss, G. B.** (2002). A receptor kinase gene regulating symbiotic nodule development. *Nature* **417**, 962-966.

**Ferguson, B. J. and Reid, J. B.** (2005). Cochleata: getting to the root of legume nodules. *Plant Cell Physiol* **46**, 1583-1589.

**Franssen, H. J., Vijn, I., Yang, W. C. and Bisseling, T.** (1992). Developmental aspects of the Rhizobium-legume symbiosis. *Plant molecular biology* **19**, 89-107.

**Gage, D. J.** (2004). Infection and invasion of roots by symbiotic, nitrogen-fixing rhizobia during nodulation of temperate legumes. *Microbiology and Molecular Biology Reviews* **68**, 280-300.

**Gleason, C., Chaudhuri, S., Yang, T. B., Munoz, A., Poovaiah, B. W. and Oldroyd, G. E. D.** (2006). Nodulation independent of rhizobia induced by a calcium-activated kinase lacking autoinhibition. *Nature* **441**, 1149-1152.

**Gonzalez-Rizzo, S., Crespi, M. and Frugier, F.** (2006). The *Medicago truncatula* CRE1 cytokinin receptor regulates lateral root development and early symbiotic interaction with *Sinorhizobium meliloti*. *Plant Cell* **18**, 2680-2693.

**Gualtieri, G. and Bisseling, T.** (2000). The evolution of nodulation. *Plant molecular biology* **42**, 181-194.

**Herrbach, V., Rembliere, C., Gough, C. and Bensmihen, S.** (2014). Lateral root formation and patterning in *Medicago truncatula*. *Journal of plant physiology* **171**, 301-310.

# CHAPTER 1

**Hirsch, A. M., Larue, T. A. and Doyle, J. (1997).** Is the legume nodule a modified root or stem or an organ sui generis? *Crit Rev Plant Sci* **16**, 361-392.

**Hirsch, A. M., Bhuvaneswari, T. V., Torrey, J. G. and Bisseling, T. (1989).** Early nodulin genes are induced in *alfalfa* root outgrowths elicited by auxin transport inhibitors. *P Natl Acad Sci USA* **86**, 1244-1248.

**Horvath, B., Yeun, L. H., Domonkos, A., Halasz, G., Gobbato, E., Ayaydin, F., Miro, K., Hirsch, S., Sun, J. H., Tadege, M. et al. (2011).** *Medicago truncatula* IPD3 Is a member of the common symbiotic signaling pathway required for rhizobial and mycorrhizal symbioses. *Molecular Plant Microbe Interactions* **24**, 1345-1358.

**Huo, X., Schnabel, E., Hughes, K. and Frugoli, J. (2006).** RNAi phenotypes and the localization of a protein::GUS fusion imply a role for *Medicago truncatula* PIN genes in nodulation. *Journal of plant growth regulation* **25**, 156-165.

**Imaizumi-Anraku, H., Takeda, N., Charpentier, M., Perry, J., Miwa, H., Umehara, Y., Kouchi, H., Murakami, Y., Mulder, L., Vickers, K. et al. (2005).** Plastid proteins crucial for symbiotic fungal and bacterial entry into plant roots. *Nature* **433**, 527-531.

**Ivanov, S., Fedorova, E. E., Limpens, E., De Mita, S., Genre, A., Bonfante, P. and Bisseling, T. (2012).** Rhizobium-legume symbiosis shares an exocytotic pathway required for arbuscule formation. *P Natl Acad Sci USA* **109**, 8316-8321.

**Kalo, P., Gleason, C., Edwards, A., Marsh, J., Mitra, R. M., Hirsch, S., Jakab, J., Sims, S., Long, S. R., Rogers, J. et al. (2005).** Nodulation signaling in legumes requires NSP2, a member of the GRAS family of transcriptional regulators. *Science* **308**, 1786-1789.

**Krecek, P., Skupa, P., Libus, J., Naramoto, S., Tejos, R., Friml, J. and Zazimalova, E. (2009).** The PIN-FORMED (PIN) protein family of auxin transporters. *Genome biology* **10**, 249.

**Lancelle, S. A. and Torrey, J. G. (1985).** Early development of rhizobium induced root nodules of *Parasponia rigida*. 2. nodule morphogenesis and symbiotic development. *Canadian Journal of Botany* **63**, 25-35.

**Laplace, L., Benkova, E., Casimiro, I., Maes, L., Vanneste, S., Swarup, R., Weijers, D., Calvo, V., Parizot, B., Herrera-Rodriguez, M. B. et al. (2007).** Cytokinins act directly on lateral root founder cells to inhibit root initiation. *Plant Cell* **19**, 3889-3900.

**Laporte, P., Lepage, A., Fournier, J., Catrice, O., Moreau, S., Jardinaud, M. F., Mun, J. H., Larrainzar, E., Cook, D. R., Gamas, P. et al. (2014).** The CCAAT box-binding transcription factor NF-YA1 controls rhizobial infection. *Journal of experimental botany* **65**, 481-494.

**Lavin, M., Herendeen, P. S. and Wojciechowski, M. F. (2005).** Evolutionary rates analysis of Leguminosae implicates a rapid diversification of lineages during the tertiary. *Syst Biol* **54**, 575-594.

**Lavin, M., Pennington, R. T., Klitgaard, B. B., Sprent, J. I., de Lima, H. C. and Gasson, P. E. (2001).** The dalbergioid legumes (Fabaceae): Delimitation of a pantropical monophyletic clade. *Am J Bot* **88**, 503-533.

Levy, J., Bres, C., Geurts, R., Chalhoub, B., Kulikova, O., Duc, G., Journet, E. P., Ane, J. M., Lauber, E., Bisseling, T. et al. (2004). A putative Ca<sup>2+</sup> and calmodulin-dependent protein kinase required for bacterial and fungal symbioses. *Science* **303**, 1361-1364.

Libbenga, K. R. and Harkes, P. A. (1973). Initial proliferation of cortical cells in the formation of root nodules in *Pisum sativum* L. *Planta* **114**, 17-28.

Limpens, E., Mirabella, R., Fedorova, E., Franken, C., Franssen, H., Bisseling, T. and Geurts, R. (2005). Formation of organelle-like N<sub>2</sub>-fixing symbiosomes in legume root nodules is controlled by DMI2. *P Natl Acad Sci USA* **102**, 10375-10380.

Lotocka, B., Kopcinska, J. and Skalniak, M. (2012). The meristem in indeterminate root nodules of Faboideae. *Symbiosis* **58**, 63-72.

Lucas, M., Kenobi, K., von Wangenheim, D., Voss, U., Swarup, K., De Smet, I., Van Damme, D., Lawrence, T., Peret, B., Moscardi, E. et al. (2013). Lateral root morphogenesis is dependent on the mechanical properties of the overlaying tissues. *P Natl Acad Sci USA* **110**, 5229-5234.

Maillet, F., Poinso, V., Andre, O., Puech-Pages, V., Haouy, A., Gueunier, M., Cromer, L., Giraudet, D., Formey, D., Niebel, A. et al. (2011). Fungal lipochitooligosaccharide symbiotic signals in *arbuscular mycorrhiza*. *Nature* **469**, 58-63.

Malamy, J. E. and Benfey, P. N. (1997). Organization and cell differentiation in lateral roots of *Arabidopsis thaliana*. *Development* **124**, 33-44.

Mallory, T. E., Chiang, S. H., Cutter, E. G. and Gifford, E. M. (1970). Sequence and pattern of lateral root formation in 5 selected species. *Am J Bot* **57**, 800-809.

Marhavy, P., Duclercq, J., Weller, B., Feraru, E., Bielach, A., Offringa, R., Friml, J., Schwechheimer, C., Murphy, A. and Benkova, E. (2014). Cytokinin controls polarity of PIN1-dependent auxin transport during lateral root organogenesis. *Curr Biol* **24**, 1031-1037.

Marhavy, P., Bielach, A., Abas, L., Abuzeineh, A., Duclercq, J., Tanaka, H., Parežova, M., Petršsek, J., Friml, J., Kleine-Vehn, J. et al. (2011). Cytokinin modulates endocytic trafficking of PIN1 auxin efflux carrier to control plant organogenesis. *Dev Cell* **21**, 796-804.

Marsh, J. F., Rakocevic, A., Mitra, R. M., Brocard, L., Sun, J., Eschstruth, A., Long, S. R., Schultze, M., Ratet, P. and Oldroyd, G. E. D. (2007). *Medicago truncatula* NIN is essential for rhizobial-independent nodule organogenesis induced by autoactive calcium/calmodulin-dependent protein kinase. *Plant Physiol* **144**, 324-335.

Mathesius, U., Schlaman, H. R. M., Spaink, H. P., Sautter, C., Rolfe, B. G. and Djordjevic, M. A. (1998). Auxin transport inhibition precedes root nodule formation in white clover roots and is regulated by flavonoids and derivatives of chitin oligosaccharides. *Plant J* **14**, 23-34.

Maunoury, N., Kondorosi, A., Kondorosi, E. and Mergaert, P. (2008). Cell biology of nodule infection and development. In *Nitrogen-fixing leguminous symbioses*, (ed. M. J. Dilworth E. K. James J. I. Sprent and W. E. Newton), pp. 153-189. Dordrecht, the Netherlands: Springer.

# CHAPTER 1

**Mitra, R. M., Gleason, C. A., Edwards, A., Hadfield, J., Downie, J. A., Oldroyd, G. E. D. and Long, S. R.** (2004). A Ca<sup>2+</sup>/calmodulin-dependent protein kinase required for symbiotic nodule development: Gene identification by transcript-based cloning. *P Natl Acad Sci USA* **101**, 4701-4705.

**Moubayidin, L., Di Mambro, R. and Sabatini, S.** (2009). Cytokinin-auxin crosstalk. *Trends in plant science* **14**, 557-562.

**Murray, J. D., Karas, B. J., Sato, S., Tabata, S., Amyot, L. and Szczyglowski, K.** (2007). A cytokinin perception mutant colonized by *Rhizobium* in the absence of nodule organogenesis. *Science* **315**, 101-104.

**Oldroyd, G. E. D.** (2013). Speak, friend, and enter: signalling systems that promote beneficial symbiotic associations in plants. *Nat Rev Microbiol* **11**, 252-263.

**Oldroyd, G. E. D. and Downie, J. A.** (2006). Nuclear calcium changes at the core of symbiosis signalling. *Curr Opin Plant Biol* **9**, 351-357.

**Oldroyd, G. E. D., Murray, J. D., Poole, P. S. and Downie, J. A.** (2011). The rules of engagement in the legume-rhizobial symbiosis. *Annual Review Genetics* **45**, 119-144.

**Ovchinnikova, E., Journet, E. P., Chabaud, M., Cosson, V., Ratet, P., Duc, G., Fedorova, E., Liu, W., Camp, R. O. d., Zhukov, V. et al.** (2011). IPD3 controls the formation of nitrogen-fixing symbiosomes in pea and *Medicago* spp. *Molecular Plant Microbe Interactions* **24**, 1333-1344.

**Pacios-Bras, C., Schlaman, H. R. M., Boot, K., Admiraal, P., Langerak, J. M., Stougaard, J. and Spaik, H. P.** (2003). Auxin distribution in *Lotus japonicus* during root nodule development. *Plant molecular biology* **52**, 1169-1180.

**Peret, B., Middleton, A. M., French, A. P., Larrieu, A., Bishopp, A., Njo, M., Wells, D. M., Porco, S., Mellor, N., Band, L. R. et al.** (2013). Sequential induction of auxin efflux and influx carriers regulates lateral root emergence. *Molecular systems biology* **9**, 699.

**Plet, J., Wasson, A., Ariel, F., Le Signor, C., Baker, D., Mathesius, U., Crespi, M. and Frugier, F.** (2011). MtCRE1-dependent cytokinin signaling integrates bacterial and plant cues to coordinate symbiotic nodule organogenesis in *Medicago truncatula*. *Plant J* **65**, 622-633.

**Popham, R. A.** (1955). Zonation of primary and lateral root apices of *Pisum sativum*. *Am J Bot* **42**, 267-273.

**Radutoiu, S., Madsen, L. H., Madsen, E. B., Felle, H. H., Umehara, Y., Gronlund, M., Sato, S., Nakamura, Y., Tabata, S., Sandal, N. et al.** (2003). Plant recognition of symbiotic bacteria requires two LysM receptor-like kinases. *Nature* **425**, 585-592.

**Rightmyer, A. P. and Long, S. R.** (2011). Pseudonodule formation by wild-type and symbiotic mutant *Medicago truncatula* in response to auxin transport inhibitors. *Molecular Plant Microbe Interactions* **24**, 1372-1384.

**Roth, L. E. and Stacey, G.** (1989). Bacterium release into host cells of nitrogen-fixing soybean nodules the symbiosome membrane comes from three sources.

*European Journal of Cell Biology* **49**, 13-23.

**Roudier, F., Fedorova, E., Lebris, M., Lecomte, P., Gyorgyey, J., Vaubert, D., Horvath, G., Abad, P., Kondorosi, A. and Kondorosi, E.** (2003). The *Medicago* species A2-type cyclin is auxin regulated and involved in meristem formation but dispensable for endoreduplication-associated developmental programs. *Plant Physiol* **131**, 1091-1103.

**Sablowski, R.** (2011). Plant stem cell niches: from signalling to execution. *Curr Opin Plant Biol* **14**, 4-9.

**Singh, S., Katzer, K., Lambert, J., Cerri, M. and Parniske, M.** (2014). CYCLOPS, a DNA-binding transcriptional activator, orchestrates symbiotic root nodule development. *Cell Host Microbe* **15**, 139-152.

**Smit, P., Raedts, J., Portyanko, V., Debelle, F., Gough, C., Bisseling, T. and Geurts, R.** (2005). NSP1 of the GRAS protein family is essential for rhizobial Nod factor-induced transcription. *Science* **308**, 1789-1791.

**Smit, P., Limpens, E., Geurts, R., Fedorova, E., Dolgikh, E., Gough, C. and Bisseling, T.** (2007). Medicago LYK3, an entry receptor in rhizobial nodulation factor signaling. *Plant Physiol* **145**, 183-191.

**Soyano, T., Kouchi, H., Hirota, A. and Hayashi, M.** (2013). NODULE INCEPTION directly targets NF-Y subunit genes to regulate essential processes of root nodule development in *Lotus japonicus*. *Plos Genet* **9**.

**Sprent, J. I. and James, E. K.** (2007). Legume evolution: where do nodules and mycorrhizas fit in? *Plant Physiol* **144**, 575-581.

**Stougaard, J.** (2001). Genetics and genomics of root symbiosis. *Curr Opin Plant Biol* **4**, 328-335.

**Sussex, I. M., Godoy, J. A., Kerk, N. M., Laskowski, M. J., Nusbaum, H. C., Welsch, J. A. and Williams, M. E.** (1995). Cellular and molecular events in a newly organizing lateral root-meristem. *Philos T Roy Soc B* **350**, 39-43.

**Suzaki, T., Yano, K., Ito, M., Umehara, Y., Suganuma, N. and Kawaguchi, M.** (2012). Positive and negative regulation of cortical cell division during root nodule development in *Lotus japonicus* is accompanied by auxin response. *Development* **139**, 3997-4006.

**Swensen, S. M. and Benson, D. R.** (2008). Evolution of actinorhizal host plants and frankia endosymbionts. In *Nitrogen-fixing actinorhizal symbioses*, (ed. K. Pawlowski and W. E. Newton), pp. 73-104. Dordrecht, the Netherlands: Springer.

**Takanashi, K.** (2011). Involvement of auxin distribution in root nodule development of *Lotus japonicus*. *Sustainable Humanosphere*, 21-22.

**Takanashi, K., Sugiyama, A. and Yazaki, K.** (2011). Auxin distribution and lenticel formation in determinate nodule of *Lotus japonicus*. *Plant. Signal. Behav.* **6**, 1405-1407.

**Timmers, A. C. J., Auriac, M. C. and Truchet, G.** (1999). Refined analysis of early symbiotic steps of the Rhizobium-Medicago interaction in relationship with microtubular cytoskeleton rearrangements. *Development* **126**, 3617-3628.

# CHAPTER 1

**Tirichine, L., Sandal, N., Madsen, L. H., Radutoiu, S., Albrektsen, A. S., Sato, S., Asamizu, E., Tabata, S. and Stougaard, J.** (2007). A gain-of-function mutation in a cytokinin receptor triggers spontaneous root nodule organogenesis. *Science* **315**, 104-107.

**Tirichine, L., Imaizumi-Anraku, H., Yoshida, S., Murakami, Y., Madsen, L. H., Miwa, H., Nakagawa, T., Sandal, N., Albrektsen, A. S., Kawaguchi, M. et al.** (2006). Deregulation of a Ca<sup>2+</sup>/calmodulin-dependent kinase leads to spontaneous nodule development. *Nature* **441**, 1153-1156.

**Torrey, J. G. and Callaham, D.** (1979). Early nodule development in *Myrica gale*. *Botanical Gazette* **140**, S10-S14.

**Turner, M., Nizampatnam, N. R., Baron, M., Coppin, S., Damodaran, S., Adhikari, S., Arunachalam, S. P., Yu, O. and Subramanian, S.** (2013). Ectopic expression of miR160 Results in auxin hypersensitivity, cytokinin hyposensitivity, and inhibition of symbiotic nodule development in soybean. *Plant Physiol* **162**, 2042-2055.

**Van De Wiel, C., Norris, J. H., Bochenek, B., Dickstem, R., Bisseling, T. and Hirsch, A. M.** (1990). Nodulin gene expression and ENOD2 localization in effective, nitrogen-fixing and ineffective, bacteria-free nodules of *alfalfa*. *Plant Cell* **2**, 1009-1017.

**van Noorden, G. E., Ross, J. J., Reid, J. B., Rolfe, B. G. and Mathesius, U.** (2006). Defective long-distance auxin transport regulation in the *Medicago truncatula* super numeric nodules mutant. *Plant Physiol* **140**, 1494-1506.

**Van Noorden, G. E., Kerim, T., Goffard, N., Wiblin, R., Pellerone, F. I., Rolfe, B. G. and Mathesius, U.** (2007). Overlap of proteome changes in *Medicago truncatula* in response to auxin and *Sinorhizobium meliloti*. *Plant Physiol* **144**, 1115-1131.

**Vieten, A., Sauer, M., Brewer, P. B. and Friml, J.** (2007). Molecular and cellular aspects of auxin-transport-mediated development. *Trends in plant science* **12**, 160-168.

**Vieten, A., Vanneste, S., Wisniewska, J., Benkova, E., Benjamins, R., Beeckman, T., Luschnig, C. and Friml, J.** (2005). Functional redundancy of PIN proteins is accompanied by auxin-dependent cross-regulation of PIN expression. *Development* **132**, 4521-4531.

**Wang, H. C., Moore, M. J., Soltis, P. S., Bell, C. D., Brockington, S. F., Alexandre, R., Davis, C. C., Latvis, M., Manchester, S. R. and Soltis, D. E.** (2009). Rosid radiation and the rapid rise of angiosperm-dominated forests. *P Natl Acad Sci USA* **106**, 3853-3858.

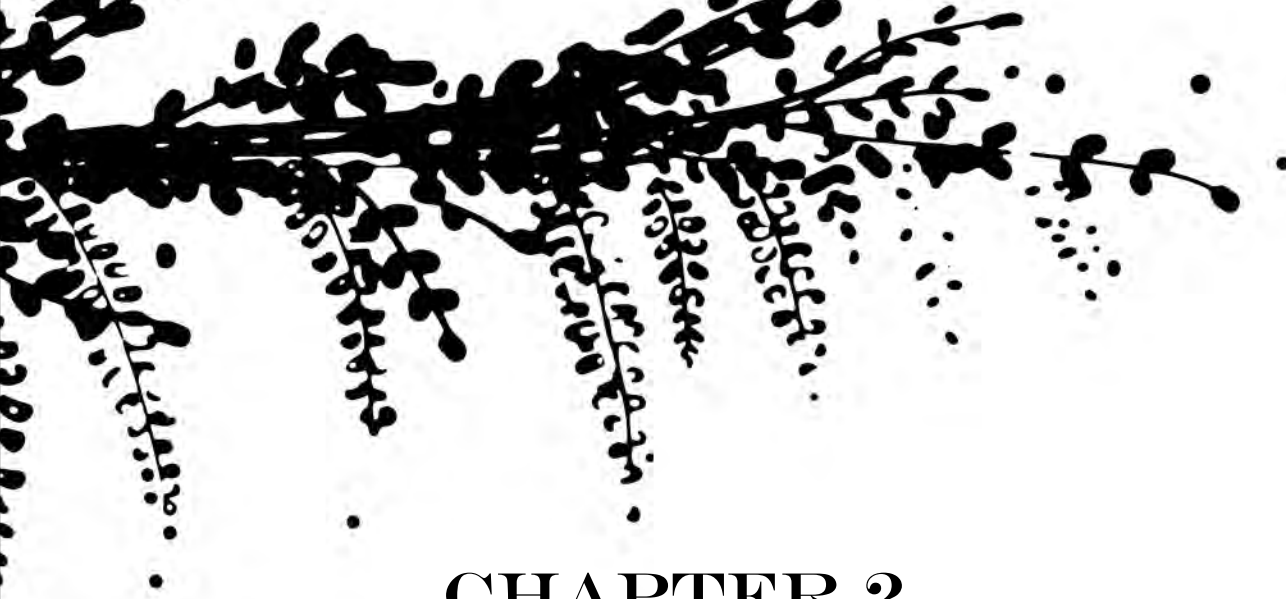
**Wasson, A. P., Pellerone, F. I. and Mathesius, U.** (2006). Silencing the flavonoid pathway in *Medicago truncatula* inhibits root nodule formation and prevents auxin transport regulation by rhizobia. *Plant Cell* **18**, 1617-1629.

**Yang, W. C., Cremers, H. C. J. C., Hogendijk, P., Katinakis, P., Wijffelman, C. A., Franssen, H., Vankammen, A. and Bisseling, T.** (1992). In situ localization of chalcone synthase messenger RNA in pea root nodule development. *Plant J* **2**, 143-151.

**Yano, K., Yoshida, S., Muller, J., Singh, S., Banba, M., Vickers, K., Markmann, K., White, C., Schuller, B., Sato, S. et al.** (2008). CYCLOPS, a mediator of symbiotic

intracellular accommodation. *P Natl Acad Sci USA* **105**, 20540-20545.





## CHAPTER 2

### *Stem cells are formed from endodermis and pericycle during Medicago truncatula lateral root formation*

**Ting Ting Xiao<sup>1</sup>, Olga Kulikova<sup>1</sup> and Ton Bisseling<sup>1,2,3</sup>**

<sup>1</sup> Department of Plant Sciences, Laboratory of Molecular Biology, Wageningen University, Droevendaalsesteeg 1, 6708 PB, Wageningen, The Netherlands.

<sup>2</sup> College of Science, King Saud University, Post Office Box 2455, Riyadh 11451, Saudi Arabia.

<sup>3</sup> To whom correspondence should be addressed: [ton.bisseling@wur.nl](mailto:ton.bisseling@wur.nl)

Manuscript in preparation

## CHAPTER 2

### SUMMARY

Lateral root development involves the formation of a new stem cell niche, which is composed of a quiescent center that is surrounded by initials (stem cells). In *Arabidopsis* the lateral root, including its stem cell niche, completely originates from pericycle cells. As lateral root formation is an important function of the pericycle, it is assumed that pericycle has a stem cell like nature. Therefore, during lateral root formation the formation of a new stem cell niche from pericycle cells most likely does not involve cell dedifferentiation. In many other species endodermis and cortex cells also divide during lateral root formation. However, it is assumed that they do not contribute to the lateral root. The exceptions are some monocots in which endodermis derived cells contribute to the root cap of the lateral root. We studied lateral root formation in the dicot *Medicago* and addressed the question whether cortex and endodermis derived cells contribute to the formation of the stem cell niche. We showed that in *Medicago* endodermis derived cells form about half of the stem cell initials of the lateral root stem cell niche. This shows for the first time that dedifferentiation of fully differentiated cells into stem cells occurs during lateral root formation in a dicot.

**Key words:** *Medicago*, lateral root, primordium, endodermis, quiescent center, stem cell initials

## INTRODUCTION

The architecture of plants is controlled by embryonic as well as post-embryonic development. Examples of post-embryonic development are the indeterminate growth of roots by their apical meristem and the formation of lateral roots. Root apical meristems contain a stem cell niche that by division maintains itself and adds cells to different tissues (van den Berg et al., 1997). Lateral root formation is best studied in *Arabidopsis*. It is initiated from pairs of founder cells in the pericycle. Further division forms a primordium in which a new stem cell niche is created (Malamy and Benfey, 1997; Benkova et al., 2003; Benkova and Bielach, 2010; Lucas et al., 2013). The pericycle is (most likely) kept in an undifferentiated state with a stem cell like nature (Laplaze et al., 2007; Sugimoto et al., 2011) by which it is specialized to form a new stem cell niche. Whereas it is textbook knowledge that lateral roots are solely derived from pericycle cells (Sugimoto et al., 2011; Roberts, 2007), in several plant species endodermis or endodermis/cortex cells can also be mitotically activated during lateral root formation (Bell and Mccully, 1970; Mallory et al., 1970; Byrne et al., 1977; Casero et al., 1995; Casero et al., 1996; den Camp et al., 2011). However, whether these fully differentiated cells can form stem cells is not known. *Medicago truncatula* (*Medicago*) is a model legume especially used to study the rhizobium nodule symbiosis. During *Medicago* lateral root development, in addition to pericycle cells, fully differentiated endodermis and inner cortical cells also divide (den Camp et al., 2011; Herrbach et al., 2014). Here, we use *Medicago* to address the question whether such fully differentiated cortical and endodermis cells can form stem cells.

Recently, early stages of *Medicago* lateral root formation have been described. Like in *Arabidopsis* *Medicago* lateral root development starts with divisions in a few pericycle cells, named founder cells (stage I in *Arabidopsis* and *Medicago*) (Malamy and Benfey, 1997; Herrbach et al., 2014). However, subsequently it diverges from *Arabidopsis* lateral root development, as endodermis and inner cortex cells also undergo some anticlinal and periclinal divisions and add cells to the primordium (stage II, III) according to Herrbach et al. (2013). At stage I to III a new stem cell niche is not yet formed, but at later stages of *Medicago* lateral root development it is not possible to trace from which root layers

## CHAPTER 2

the primordium cells are derived (Herrbach et al., 2014). So, it remains unclear from which cells the lateral root stem cell niche is derived. Here, we will use specific markers for the endodermis and the Quiescent Center (QC), that organizes the stem cell niche to answer the question whether the endodermis/inner cortex derived cells contribute to the stem cell niche.

The root stem cell niche of *Arabidopsis* has been well characterized. It has a QC, composed of 4 cells, located at its center. The QC is surrounded by 4 sets of stem cells initials. These initials divide and by a stereotypical division pattern add cells to stele, endodermis/cortex, epidermis/lateral-rootcap and columella, respectively (van den Berg et al., 1997). These stem cells are maintained by signals from the QC. In the QC cells, certain genes are essential for the stem cell maintenance, e.g. *AtWOX5* (De Smet et al., 2008; Forzani et al., 2014) and *AtSCR* (Benfey et al., 1993; Di Laurenzio et al., 1996; Heidstra et al., 2004; Lee et al., 2008). They can be used as markers to identify the QC cells. The presence of stem cells is frequently studied by using a prominent marker of differentiated columella cells, the accumulation of amyloplasts (Bennett et al., 2014). These amyloplast are absent in the layer of columella initials.

In this study we used markers for QC, endodermis and columella to determine whether cells derived from fully differentiated endodermis and cortex cells can contribute to the newly formed stem cell niche. This shows that endodermis derived cells form initials from which the columella, lateral root cap, epidermis and outer cortical cell layers are formed, respectively. In contrast, the cortex derived cells do not form initials. So, this study shows that in addition to the stem cell-like pericycle cells, fully differentiated root cells also can form stem cells. This implies that these cells must fully dedifferentiate.

## RESULTS

### Medicago root structure

To study *Medicago* lateral root formation, we first describe the stem cell niche and tissue organization of roots. Whereas the *Arabidopsis* root cortex is composed of a single layer, *Medicago* has 5 cortical cell layers (Chapter 2) (Xiao et al., 2014). Epidermis, endodermis and pericycle are

in both species composed of a single layer (Fig. 1). In a parallel study the Medicago QC has been identified. In this study the Arabidopsis specific QC gene *AtWOX5* was expressed in transgenic Medicago roots (Henk Franssen personal communication) and shown to be active in 1-2 tiers that are located below the stele pole. Based on position and expression of *AtWOX5* it is concluded that these tiers represent the QC. Previously, we used *AtSCR* as a marker for the Medicago endodermis (Xiao et al., 2014). In Arabidopsis *AtSCR* is expressed in the root endodermis and QC (Di Laurenzio et al., 1996). Therefore, we determined the expression pattern of this gene in the root tip. Indeed *AtSCR::GUS* is also expressed in the 1-2 cell layers that form the Medicago QC (Fig. 6A).

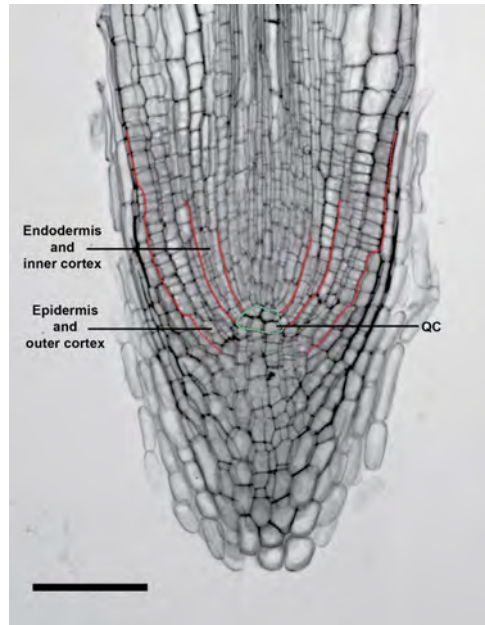


Fig. 1. Medicago root tip.

Median longitudinal section of a Medicago root tip. The QC is indicated with green dash line. The cell files of endodermis and inner cortex are linked to the QC. Files of the outer cortex and epidermis convolve to the 3rd cell trailer below QC.

Red lines indicate the border between tissues that are described in the figure.

Bar, 75  $\mu$ m.

To obtain a first characterization of the stem cells around the QC, median sections were made of root tips of Medicago lateral roots. This showed

# CHAPTER 2

that the endodermis and inner cortex cell layers are linked to the QC. This indicates that cells lateral to the QC are the endodermis/inner-cortex initials (Fig. 1). To identify the columella initials, starch granules were stained with lugol, which showed that about 3 cell layers below the QC lack starch (Chapter 5). In analogy with *Arabidopsis* these layers might all represent columella stem cells. However, it is also possible that only the cells directly adjacent to the QC are stem cells and the other 2 cell layers are at an early stage of columella differentiation in which amyloplasts remain to be formed. The outer cortex and epidermis can be traced to these 2<sup>nd</sup> and 3<sup>rd</sup> cell layers below the QC (Fig. 1). This indicates that these layers are also the origin of the outer cortex, epidermis and lateral root cap. Therefore, we decided that the cell layers that are linked to outer cortex and epidermis are the outer-cortex/epidermis/lateral-rootcap/columella initials. These layers are located below the QC and absent of amyloplasts.

A schematic overview of *Medicago* root tissue organization is shown in Fig.

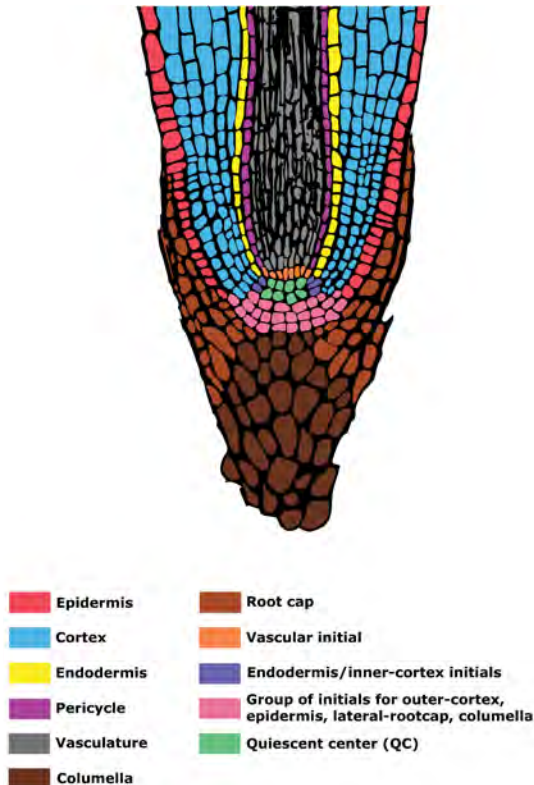


Fig. 2. Histology of *Medicago* root. Cell layers from left to right are epidermis, 5 cortex layers (C1, C2, C3, C4 and C5) (Xiao et al., 2014 and Fig. 3B), endodermis, pericycle and vasculature. All cell files can be traced to the root stem cell niche. Two tiers of cells located at the stele pole are/form the quiescent center (QC); at the side of the QC region is the endodermis/inner-cortex initial; on the top of the QC is the vascular initial; three trailers of cells adjacent and below the QC region are a group of stem cells that are give cells to the outer-cortex, epidermis, lateral-rootcap and columella. Schematic longitudinal section was made by tracing cells from median plastic sections of *Medicago* roots.

2. The characterization of the Medicago stem cell niche was subsequently used to determine which cells form the stem cell niche during lateral root development.

### **Cortex and endodermis contribute 6-7 cell layers to lateral root primordia**

We aimed to determine the Medicago lateral root fate map and especially studied whether pericycle, endodermis and/or inner cortex derived cells contribute to the stem cell niche. To study this, *AtCASP::GUS* was used to trace cells derived from the endodermis (Xiao et al., 2014). This gene is induced in the mature Medicago root endodermis cells (Fig. 3A). Further, during nodule primordium formation this gene remains active after mitotic activity has induced in the endodermis. As the endodermis is located in between cortex and pericycle this endodermis marker allows tracing of cells of all three tissues. Medicago roots expressing *AtCASP::GUS* were harvested. Median longitudinal sections (7  $\mu$ m) were made and analysed by light microscopy. Based on these analyses lateral root development was divided into 7 stages. At stage 7 the lateral roots had just emerged (Fig. 3B-H). For stage I-III we followed the classification as proposed by Herrbach et al. (2013). For the subsequent stages we defined how the root tissues had contributed to the primordium, as this is not possible by the cytological analyses published by Herrbach et al. (2013).

At stage I (Fig. 3B), anticlinal divisions are induced in the pericycle and the first anticlinal division can occur in the endodermis. At stage II (Fig. 3C), anticlinal divisions in the endodermis have continued and cells of the inner most cortical layer (C5) started to divide anticlinally. Furthermore, periclinal divisions have occurred in the pericycle by which 2 cell layers are formed. These cell layers are named pericycle derived inner layer (PIL) and pericycle derived outer layer (POL). Note that, in these dividing endodermis cells *AtCASP::GUS* remains active. At stage III (Fig. 3D), anticlinal divisions in C5 have occurred more abundantly and anticlinal divisions in C4 have started. PIL, POL and endodermis have divided periclinally, and collectively form 6 cell layers. The 2 cell layers derived from endodermis are named endodermis derived inner layer (EIL) and endodermis derived outer layer (EOL), respectively. At stage IV (Fig. 3E), C5 derived cells have divided periclinally and PIL has gone through several

## CHAPTER 2

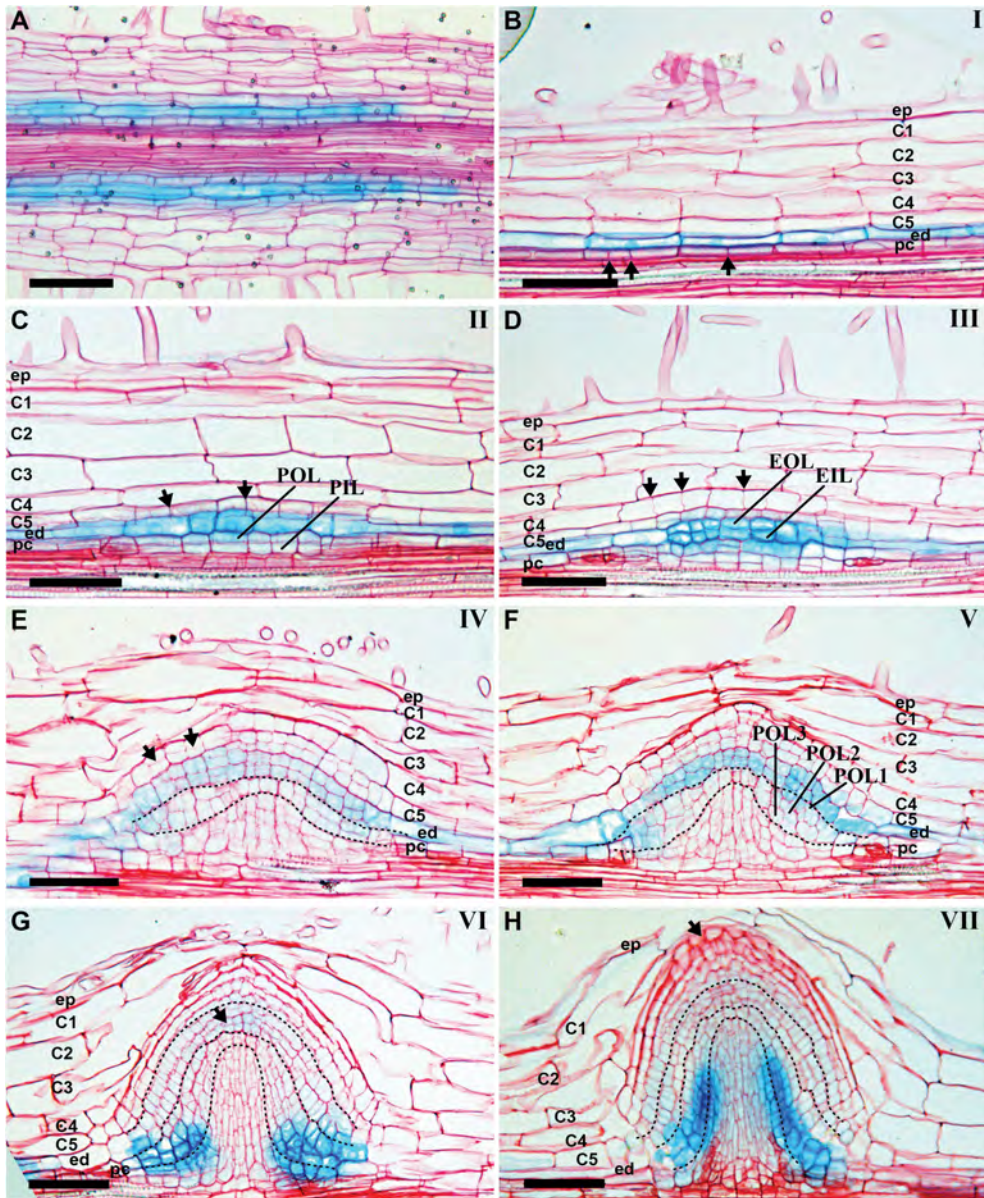


Fig. 3. Subsequent stages of Medicago lateral root development.

*AtCASP::GUS*, which is used to trace endodermis derived cells. It is expressed in the endodermis of a Medicago root (A). At stage I (B), anticlinal divisions are induced in the pericycle (arrows). At stage II (C), anticlinal divisions continued in endodermis and are induced in the most inner cortical layer (C5, arrows); periclinal divisions are induced in pericycle by which 2 cell layers are formed. This are the pericycle derived inner layer (PIL) and outer layer (POL). At stage III (D), periclinal divisions continued in PIL and

POL and are induced in endodermis. The latter results in endodermis derived inner layer (EIL) and outer layer (EOL). *AtCASP::GUS* remains active in EIL and EOL. Further, anticlinal divisions are induced in C4 (arrows). At stage IV (E), periclinal divisions are induced in C5 (arrows) and endodermis and cell division continued in PIL forms a cone. At stage V (F), periclinal divisions continued in PIL. An additional periclinal division occurs in one of the POL derived cell layers. At this stage 3 POL layers are formed; POL1, POL2 and POL3. C1, C2 and C3 collapse. At stage VI (G), periclinal divisions induced in EIL and EOL form 4 cell layers (arrow). *AtCASP::GUS* expression is reduced in EIL and EOL and is induced in POL at the base of the primordium (arrows). At stage VII (H), primordium emerges through the epidermis and cells derived from C4/5 at the apex of the primordium start to enlarge (arrow).

In E, F, G and H black lines indicate the border between cells derived from PIL, POL, endodermis and C5, respectively.

Epidermis (ep), Cortical cell layer 1 (C1), 2 (C2), 3 (C3), 4 (C4), 5 (C5), Endodermis (ed), Pericycle (pc).

Bars, 75  $\mu$ m.

periclinal divisions and forms a cone. The 2 cell layers derived from POL have only divided a few times anticlinally. At stage V (Fig. 3F), PIL derived cells have continued to divide. One cell layer of the POL derived cell layers has divided periclinally once more by which 3 POL derived cell layers are formed. The few POL derived cells adjacent to the tip of the cone remained 2 cell layers. We name the POL derived layers POL1 to POL3 and POL1 is adjacent to the endodermis derived cells. At this stage, cells of the outer cortical layers start to collapse. At stage VI (Fig. 3G), EIL and EOL cells located on top of the cone have divided periclinally and form 4 cell layers. This is the last stage that endodermis derived cells can still be recognized by *AtCASP::GUS* expression, since the expression of *AtCASP::GUS* is markedly reduced. At this stage *AtCASP::GUS* is induced in the few cells that belong to POLs at the lateral root base. At stage VII (Fig. 3H), lateral root primordia have emerged from the main root and at the apex of the primordia, C4 and C5 derived cells start to enlarge. *AtCASP::GUS* is expressed in 3 cell layers POL2, POL3 and the outer most PIL layer. The *AtCASP::GUS* expression level in POL3 is clearly higher than in the other two layers.

To determine whether *AtCASP::GUS* expressing cells in the primordium are functional endodermis cells, we studied whether casparian strips are present (Fig. 4). At stage I-V, *AtCASP::GUS* is still expressed in the endodermis derived cells, since GUS signal is at least as intense,

## CHAPTER 2

despite cell division and increase in cytoplasmic density as non-dividing endodermis. However, casparian strips are not present (Fig. 4A, B). At stage VII (Fig. 4C, D), casparian strips are formed in POL3, the cell layer with the highest *AtCASP::GUS* expression. So, POL3 forms the lateral root endodermis.

So far we have shown that endodermis and inner cortex contribute 6-7 cell layers to the apex of the lateral root primordia. This is the region that contributes to the apex of the lateral root. Therefore, we addressed the question whether endodermis and inner cortex derived cells contribute to the stem cell niche.

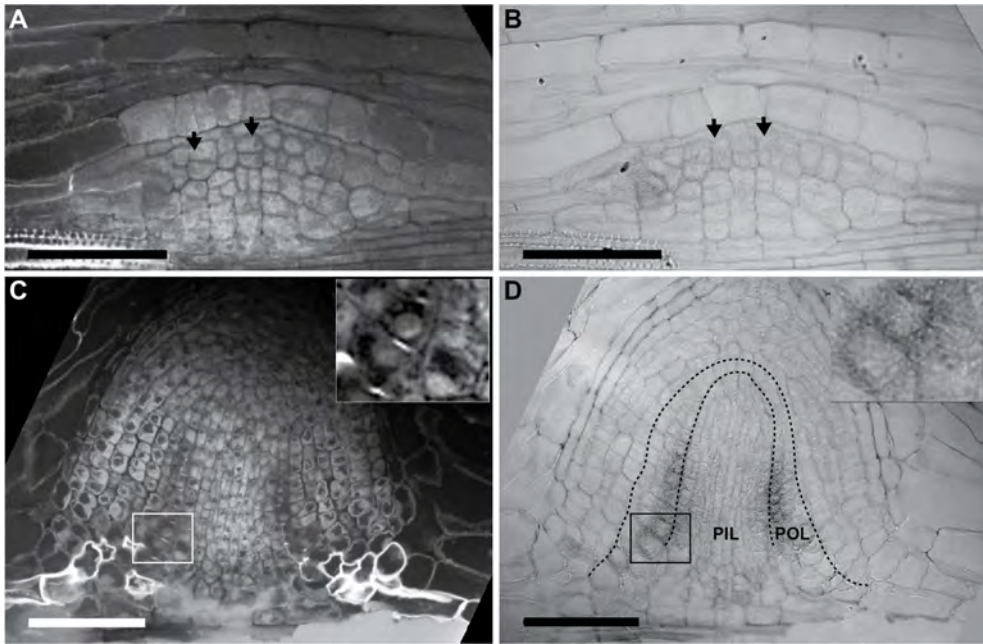


Fig. 4. PLO3 differentiates into endodermis of the lateral root at developmental stage VII.

Casparian strips are absent in dividing endodermis cells stage III-IV (A), although *AtCASP::GUS* marker is expressed in these cells (B). At lateral root development stage VII, casparian strips are formed in the POL3 cell layer (C). In this layer *AtCASP::GUS* is highest expressed (D). Magnifications of POL3 cells for figure C and D are shown on the top right corners.

In D black lines indicate the border between cells derived from PIL, POL and endodermis, respectively.

Bars, 75  $\mu$ m.

## Origin of the lateral root stem cell niche

Auxin is essential for maintaining the stem cell niche. It is present at a high concentration in the stem cell niche as well as columella cells. To identify where the stem cell niche is located, we first used a *DR5::GUS* line. The *DR5::GUS* expression pattern during lateral root primordium formation is shown in Fig. 5. At early stages (stage IV, Fig. 5A) of development *DR5::GUS* is expressed in more or less all primordium cells. At stage V (Fig. 5B), *DR5::GUS* expression pattern gradually becomes more restricted to the central part at the apex of the primordia. At stage VI (Fig. 5C), *DR5::GUS* is highly expressed at the apex of the lateral root primordium, in a group of cells derived from POL, endodermis and C5. This suggests that this group of cells forms the future stem cell niche and columella.

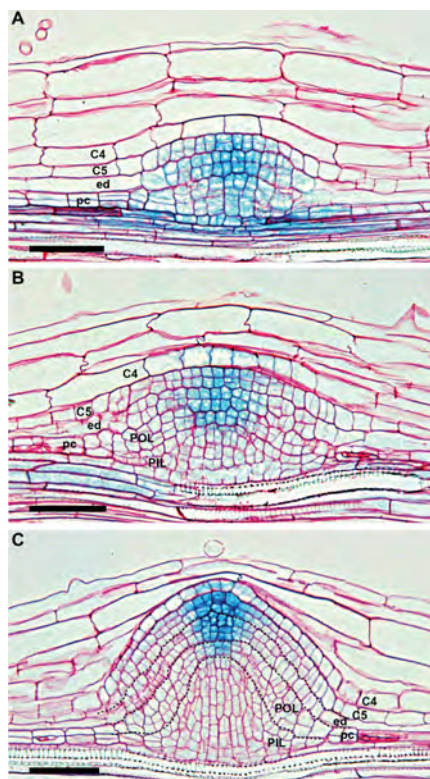


Fig. 5. Cells derived from POL, endodermis and C5, at the apex of the primordium form the stem cell niche and root cap.

*DR5::GUS* is expressed in all dividing primordia cells until stage IV (A). Then the expression gradually confined to the apex of the primordium (stage V, B). At stage VI (C), it is highest expressed at the apex of the primordium, which includes cells derived from POL, endodermis and C5. At this stage, *DR5::GUS* is also expressed in C4 derived cells at a relatively low level.

In C black lines indicate the border between cells derived from PIL, POL, endodermis and C5, respectively.

Bars, 75  $\mu$ m.

To identify the QC within the group of cells with high *DR5* expression,

## CHAPTER 2

we used *Medicago* roots expressing the promoter fusion construct *AtSCR::GUS*. *AtSCR* encodes an Arabidopsis GRAS transcription factor and is specifically expressed in endodermis and QC (Di Laurenzio et al., 1996). In *Medicago* roots (Fig. 6A), *AtSCR::GUS* is also expressed in endodermis and QC. At stage VI (Fig. 6B), *AtSCR::GUS* is highly expressed in POL3 (lateral root endodermis) and the few POL cells that are on the top of PIL derived “cone”. Therefore these cells form the QC of the lateral root primordium. It also implies that the stem cells giving rise to epidermis, outer cortex and columella of the lateral root can be formed from endodermis and cortex derived cells.

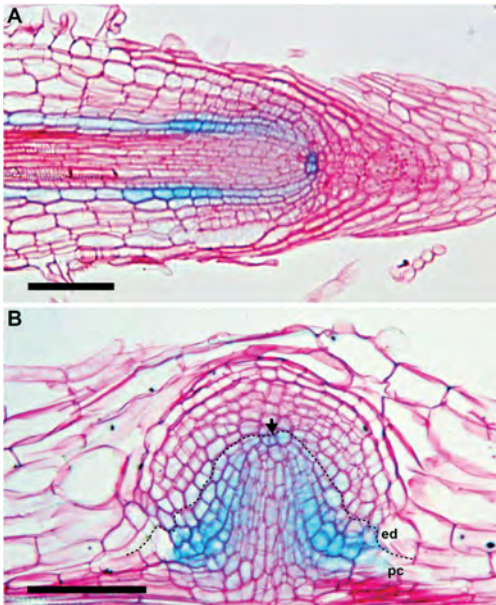


Fig. 6. POL forms the QC of the lateral root at development stage VI.

*AtSCR::GUS* is highly expressed in QC and the endodermis of the *Medicago* root (A) and weakly expressed in the pericycle and C5 cell layer in the root meristem region. At stage VI (B), *AtSCR::GUS* is highly expressed in the few POL cells (arrow) that are on the top of PIL derived “cone” and POL3. It is also expressed in POL1, POL2 and the most outer layer of PIL but at a lower level. In B black line indicates the border between cells derived from pericycle and endodermis.

Bars, 75  $\mu$ m.

Starch accumulates in columella cells and it is absent in the stem cells (Ding and Friml, 2010; Bennett et al., 2014). To distinguish the group of stem cell initials that give cells to the outer-cortex, epidermis, lateral-rootcap and columella from differentiated columella cells, we used lugol staining to visualise the starch granules. This shows that at stage VI (Fig. 7A) to VII (Fig. 7B) starch is present at the apex of the primordium in 4-5 cell layers of which are derived from C4/5 and one from EOL. So, these cells form the columella of the root cap. In between the root cap and QC there are 3 cell layers, which form the stem cell cluster. So, the group of

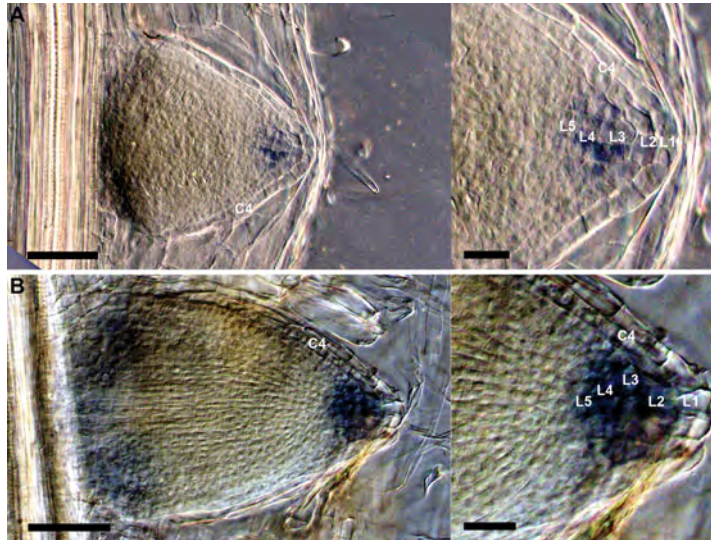


Fig. 7. Endodermis derived inner layers form the group of stem cells that are adding cells to the outer-cortex, epidermis, lateral-rootcap and columella.

Starch granules start to appear in 4-5 cell layers (L1-L5) in the columella of the primordium at stage VI-VII (A). C4 derived cells are not connected with the lateral root epidermis and it only contribute to the lateral root cap (B). Magnifications of apex of the primordium for figure A and B are shown on the right.

Bars in A-B equal to 75  $\mu$ m; in C and D magnifications equal to 25  $\mu$ m.

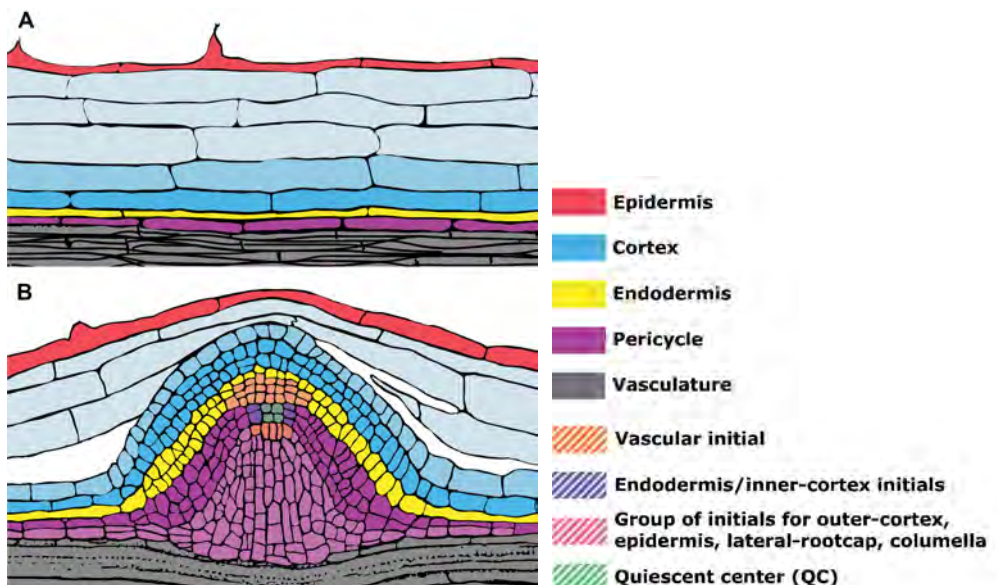


Fig. 8. The Medicago lateral root fate map.

## CHAPTER 2

stem cell initials that give cells to the outer-cortex, epidermis, lateral-rootcap and columella is formed from cells of endodermis derived cells. Furthermore, although C4 cell divide during lateral root formation, those cells do not integrate with the newly formed primordium or lateral root and they gradually falling off after the lateral root emerged (Fig. 7B).

### DISCUSSION

We showed that during Medicago lateral formation endodermis and pericycle derived cells form the stem cell niche (Fig. 8). This is the first time that it is shown that endodermis derived cells form initials of the newly formed stem cell niche in a dicot.

Lateral root formation is best studied in Arabidopsis and the lateral root is completely formed from founder cells of the pericycle. Neither endodermis nor cortex is mitotically activated. It is assumed that the pericycle cells are specialised cells with a stem cell like nature (Laplace et al., 2007; Sugimoto et al., 2011). Therefore the formation of the lateral root stem cell niche most likely does not involve the (partial) dedifferentiation of a differentiated cell into a cell with stem cell properties.

In several dicots it has been shown that endodermis cells divide during lateral root development (Popham, 1955; Mallory et al., 1970; den Camp et al., 2011; Herrbach et al., 2014). However, in none of these cases was shown that endodermis derived cell develop into stem cells. We used *AtCASP1* as a marker to trace endodermis derived cells. This allowed us to show that the columella stem cells as well as the stem cells that form epidermis, outer cortex and lateral root cap are all endodermis derived. This implies that the fully differentiated endodermis cells have to dedifferentiate to form stem cells. When the endodermis cells are mitotically activated they lose their casparian strips. However, the *AtCASP1::GUS* remains active upto stage V (Fig. 3F). This suggests that endodermis derived cells in part maintain their endodermis identity upto this stage. At stage VI (Fig. 3G), the *CASP1* gene is switched off and a subset of these cells dedifferentiate into various stem cells at the apex of the primordium. The other endodermis derived cells differentiate in outer cortex cells. It is unlikely that this involves a transient stem cell fate. Therefore it is probable that it involve a transdifferentiation (Jopling et al.,

2011) from endodermis into another differentiated form. Also the cortex derived cells most likely undergo transdifferentiation as these do not form stem cells, but become epidermis and outer layer of root cap cells.

Although it is the first time shown that in dicot endodermis derived cells contribute to the lateral root stem cell niche, this feature might be more wide spread in angiosperm than previously assumed. In monocots, like maize, rice, barley, wheat, it is already known that endodermis derived cells form the root cap and this includes some initials cells (Bell and McCully, 1970; Orman-Ligeza et al., 2013). Within the legumes, *Arachis hypogaea* L. and *Pisum sativum* endodermis derived cells also integrate into the lateral root primordium (Popham, 1955; Mallory et al., 1970). However, it has not been studied whether these cells form initials. Based on our study in *Medicago* and a reanalysis of the *Pisum sativum* lateral root primordia (Popham, 1955), we hypothesize that it is common in legumes that endodermis derived cells form stem cells. Also in dicots outside the legume family, like *Cucurbita maxima*, it was shown that endodermis and cortex derived cells contribute to lateral root primordia (Mallory et al., 1970), which is grouped outside of monocots and dicots. Taken together our studies on *Medicago* and previous reports indicate that lateral roots are not exclusively formed from pericycle perhaps rather wide spread among angiosperms species. In several plant species, in addition to pericycle also endodermis and cortex contributes to the formation of lateral roots and this might include part of the stem cell niche.

The involvement of endodermis in the formation of the initials of the lateral root is not a feature that only occurs in angiosperm plants. In ferns, which are the most basic vascular plants and belong to lycophytes, lateral roots are even completely formed from the endodermis (Lin and Raghavan, 1991; Hou et al., 2004). It is unknown whether lateral root formation in different land plant lineages (lycophytes and euphyllophytes) evolved independently. Studies on the involvement of the endodermis with more species in these plant lineages might provide insight in the evolution of lateral root formation.

## **MATERIALS AND METHODS**

### **Plant materials**

## CHAPTER 2

*M. truncatula* accession Jemalong A17 wt plants were used to study root tip structure. This accession is also used to generate *AtCASP1::GUS* and *AtSCR::GUS* *Agrobacterium rhizogenes* (strain MSU440) mediated transgenic roots as previously described by Limpens et al. (2004). *M. truncatula* accession R108 was used to make the stable *DR5::GUS* transgenic line by using *Agrobacterium tumefaciens* (strain AGL1) according to Chabaud et al. (2003). The formation of lateral root primordia in R108 is similar as described for A17. The surface-sterilization and germination of Medicago seeds were performed as previously described by Limpens et al. (2004).

### Constructs

The *AtCASP1::GUS* and *AtSCR::GUS* constructs are described in Roppolo et al. (2011) and Xiao et al. (2014), respectively. To create the *DR5::GUS* construct, pENTR™/D-TOPO® Cloning Kits (Invitrogen) and Gateway® technology (Invitrogen) were used to generate the entry clone and genetic promoter-GUS construct (Karimi et al., 2002), respectively. First, 14 synthetic DR5 DNA fragments repeats (Ulmasov et al., 1997) were included in the entry clone. Then, the entry vector was recombined into Gateway®-compatible binary vector pKGW-RR, that contains GUS reporter gene and *AtUBQ10::DsRED1* as a selection marker (Limpens et al., 2004), by using Gateway® LR Clonase® II enzyme mix (Invitrogen).

### Histochemical $\beta$ -glucuronidase (GUS) staining

Transgenic plant material containing GUS constructs were incubated in GUS buffer (3% sucrose, 2 mM  $K_3Fe(CN)_6$ , 2 mM  $K_4Fe(CN)_6$ , 10 mM EDTA, and 1 mg/ml X-Gluc salt in 100 mM phosphate buffer solution, pH 7.0) under vacuum for 30 min and then at 37 °C for 3 to 24 h (Jefferson et al., 1987).

### Tissue embedding, sectioning and section staining

Root segments were fixed at 4 °C overnight with 4% paraformaldehyde (w/v), 5% glutaraldehyde (v/v) in 0.05 M sodium phosphate buffer (pH7.2). The fixed material was dehydrated in an ethanol series and subsequently embedded in Technovit 7100 (Heraeus Kulzer) according to the manufacturer's protocol. Sections (7  $\mu$ m) were made with a RJ2035

microtome (Leica Microsystems, Rijswijk, The Netherlands), stained 5 min in 0.05% toluidine blue O for wt material and 15 min in 0.1% ruthenium red for transgenic GUS material. Sections were analysed by using a DM5500B microscope equipped with a DFC425C camera (Leica Microsystems, Wetzlar, Germany).

### **Lugol staining**

Root segments were stained with Lugol's solution (Merck, Germany) to visualize starch grains and tissues were cleared in chloral hydrate solution, which contains 2 ml water, 1 ml glycerol and 8 g chloral hydrate (VWR BDH Prolabo, Belgium). Whole mount root segments were analysed by an Axio Imager A1 microscope (Zeiss) supplied with Nomarski optics.

### **ACKNOWLEDGEMENTS**

This research is funded by European Research Council (ERC-2011-AdG-294790) and Graduate School 'Experimental Plant Science'.

### **REFERENCES**

- Bell, J. K. and McCully, M. E.** (1970). A histological study of lateral root initiation and development in *Zea Mays*. *Protoplasma* **70**, 179-205.
- Benfey, P. N., Linstead, P. J., Roberts, K., Schiefelbein, J. W., Hauser, M. T. and Aeschbacher, R. A.** (1993). Root development in *Arabidopsis*: four mutants with dramatically altered root morphogenesis. *Development (Cambridge)* **119**, 57-70.
- Benkova, E. and Bielach, A.** (2010). Lateral root organogenesis: from cell to organ. *Current Opinion in Plant Biology* **13**, 677-683.
- Benkova, E., Michniewicz, M., Sauer, M., Teichmann, T., Seifertova, D., Jurgens, G. and Friml, J.** (2003). Local, efflux-dependent auxin gradients as a common module for plant organ formation. *Cell* **115**, 591-602.
- Bennett, T., van den Toorn, A., Willemsen, V. and Scheres, B.** (2014). Precise control of plant stem cell activity through parallel regulatory inputs. *Development (Cambridge)* **141**, 4055-4064.
- Byrne, J. M., Pesacreta, T. C. and Fox, J. A.** (1977). Development and structure of the vascular connection between the primary and secondary roots of *Glycine max* (L.) Merr. *American Journal of Botany* **64**, 946-959.
- Casero, P. J., Casimiro, I. and Lloret, P. G.** (1995). Lateral root initiation by asymmetrical transverse divisions of pericycle cells in 4 plant species: *Raphanus*

## CHAPTER 2

*Sativus*, *Helianthus Annuus*, *Zea Mays*, and *Daucus Carota*. *Protoplasma* **188**, 49-58.

**Casero, P. J., Casimiro, I. and Lloret, P. G.** (1996). Pericycle proliferation pattern during the lateral root initiation in adventitious roots of *Allium cepa*. *Protoplasma* **191**, 136-147.

**Chabaud, M., De Carvalho-Niebel, F. and Barker, D. G.** (2003). Efficient transformation of *Medicago truncatula* cv Jemalong using the hypervirulent *Agrobacterium tumefaciens* strain AGL1. *Plant Cell* **22**, 46-51.

**De Smet, I., Vassileva, V., De Rybel, B., Levesque, M. P., Grunewald, W., Van Damme, D., Van Noorden, G., Naudts, M., Van Isterdael, G., De Clercq, R. et al.** (2008). Receptor-like kinase ACR4 restricts formative cell divisions in the Arabidopsis root. *Science* **322**, 594-597.

**den Camp, R. H. M. O., De Mita, S., Lillo, A., Cao, Q. Q., Limpens, E., Bisseling, T. and Geurts, R.** (2011). A phylogenetic strategy based on a legume-specific whole genome duplication yields symbiotic cytokinin type-A response regulators. *Plant Physiology* **157**, 2013-2022.

**Di Laurenzio, L., Wysocka Diller, J., Malamy, J. E., Pysh, L., Helariutta, Y., Freshour, G., Hahn, M. G., Feldmann, K. A. and Benfey, P. N.** (1996). The SCARECROW gene regulates an asymmetric cell division that is essential for generating the radial organization of the Arabidopsis root. *Cell* **86**, 423-433.

**Ding, Z. J. and Friml, J.** (2010). Auxin regulates distal stem cell differentiation in Arabidopsis roots. *Proceedings of the National Academy of Sciences of the United States of America* **107**, 12046-12051.

**Forzani, C., Aichinger, E., Sornay, E., Willemsen, V., Laux, T., Dewitte, W. and Murray, J. A. H.** (2014). WOX5 suppresses CYCLIN D activity to establish quiescence at the center of the root stem cell niche. *Current Biology* **24**, 1939-1944.

**Heidstra, R., Welch, D. and Scheres, B.** (2004). Mosaic analyses using marked activation and deletion clones dissect Arabidopsis SCARECROW action in asymmetric cell division. *Genes & Development* **18**, 1964-1969.

**Herrbach, V., Rembliere, C., Gough, C. and Bensmihen, S.** (2014). Lateral root formation and patterning in *Medicago truncatula*. *J Plant Physiol* **171**, 301-310.

**Hou, G. C., Hill, J. P. and Blancaflor, E. B.** (2004). Developmental anatomy and auxin response of lateral root formation in *Ceratopteris richardii*. *Journal of Experimental Botany* **55**, 685-693.

**Jefferson, R. A., Kavanagh, T. A. and Bevan, M. W.** (1987). Gus fusions: b-glucuronidase as a sensitive and versatile gene fusion marker in higher-plants. *EMBO Journal* **6**, 3901-3907.

**Jopling, C., Boue, S. and Belmonte, J. C. I.** (2011). Dedifferentiation, transdifferentiation and reprogramming: three routes to regeneration. *Nature Reviews Molecular Cell Biology* **12**, 79-89.

**Karimi, M., Inze, D. and Depicker, A.** (2002). GATEWAY™ vectors for *Agrobacterium*-mediated plant transformation. *Trends in Plant Science* **7**, 193-195.

**Laplaze, L., Benkova, E., Casimiro, I., Maes, L., Vanneste, S., Swarup,**

**R., Weijers, D., Calvo, V., Parizot, B., Herrera-Rodriguez, M. B. et al.** (2007). Cytokinins act directly on lateral root founder cells to inhibit root initiation. *Plant Cell* **19**, 3889-3900.

**Lee, H., Kim, B., Song, S. K., Heo, J. O., Yu, N. I., Lee, S. A., Kim, M., Kim, D. G., Sohn, S. O., Lim, C. E. et al.** (2008). Large-scale analysis of the GRAS gene family in *Arabidopsis thaliana*. *Plant Molecular Biology* **67**, 659-670.

**Limpens, E., Ramos, J., Franken, C., Raz, V., Compaan, B., Franssen, H., Bisseling, T. and Geurts, R.** (2004). RNA interference in *Agrobacterium rhizogenes*-transformed roots of *Arabidopsis* and *Medicago truncatula*. *Journal of Experimental Botany* **55**, 983-992.

**Lin, B. L. and Raghavan, V.** (1991). Lateral root initiation in *Marsilea quadrifolia*. I. Origin and histogenesis of lateral roots. *Canadian journal of botany* **69**, 123-135.

**Lucas, M., Kenobi, K., von Wangenheim, D., Voss, U., Swarup, K., De Smet, I., Van Damme, D., Lawrence, T., Peret, B., Moscardi, E. et al.** (2013). Lateral root morphogenesis is dependent on the mechanical properties of the overlaying tissues. *Proceedings of the National Academy of Sciences of the United States of America* **110**, 5229-5234.

**Malamy, J. E. and Benfey, P. N.** (1997). Organization and cell differentiation in lateral roots of *Arabidopsis thaliana*. *Development (Cambridge)* **124**, 33-44.

**Mallory, T. E., Chiang, S. H., Cutter, E. G. and Gifford, E. M.** (1970). Sequence and Pattern of Lateral Root Formation in 5 Selected Species. *American Journal of Botany* **57**, 800-809.

**Orman-Ligeza, B., Parizot, B., Gantet, P. P., Beeckman, T., Bennett, M. J. and Draye, X.** (2013). Post-embryonic root organogenesis in cereals: branching out from model plants. *Trends in Plant Science* **18**, 464-467.

**Popham, R. A.** (1955). Zonation of Primary and Lateral Root Apices of *Pisum Sativum*. *American Journal of Botany* **42**, 267-273.

Roberts, K. (2007) *Handbook of plant science*, Chichester, West Sussex, England ; Hoboken, NJ, USA: Wiley.

**Roppolo, D., De Rybel, B., Tendon, V. D., Pfister, A., Alassimone, J., Vermeer, J. E., Yamazaki, M., Stierhof, Y. D., Beeckman, T. and Geldner, N.** (2011). A novel protein family mediates Casparian strip formation in the endodermis. *Nature* **473**, 380-383.

**Sugimoto, K., Gordon, S. P. and Meyerowitz, E. M.** (2011). Regeneration in plants and animals: dedifferentiation, transdifferentiation, or just differentiation? *Trends in Cell Biology* **21**, 212-218.

**Ulmasov, T., Murfett, J., Hagen, G. and Guilfoyle, T. J.** (1997). Aux/IAA proteins repress expression of reporter genes containing natural and highly active synthetic auxin response elements. *Plant Cell* **9**, 1963-1971.

**van den Berg, C., Willemsen, V., Hendriks, G., Weisbeek, P. and Scheres, B.** (1997). Short-range control of cell differentiation in the *Arabidopsis* root meristem. *Nature* **390**, 287-289.

## CHAPTER 2

Xiao, T. T., Schilderink, S., Moling, S., Deinum, E. E., Kondorosi, E., Franssen, H., Kulikova, O., Niebel, A. and Bisseling, T. (2014). Fate map of *Medicago truncatula* root nodules. *Development (Cambridge)* **141**, 3517-3528.







## CHAPTER 3

### *Fate map of Medicago truncatula root nodules*

**Ting Ting Xiao<sup>1</sup>, Stefan Schilderink<sup>1</sup>, Sjef Moling<sup>1</sup>, Eva E. Deinum<sup>1,2,3</sup>, Eva Kondorosi<sup>4</sup>, Henk Franssen<sup>1</sup>, Olga Kulikova<sup>1</sup>, Andreas Niebel<sup>5,6</sup> and Ton Bisseling<sup>1,7,8</sup>**

<sup>1</sup> Department of Plant Sciences, Laboratory of Molecular Biology, Wageningen University, Droevendaalsesteeg 1, 6708 PB, Wageningen, The Netherlands.

<sup>2</sup> Department of Systems Biophysics, FOM institute AMOLF, Science Park 104, 1098 XG, Amsterdam, The Netherlands.

<sup>3</sup> Institute of Evolutionary Biology, The University of Edinburgh, Edinburgh, UK (present address)

<sup>4</sup> Institute of Biochemistry, Biological Research Centre, Hungarian Academy of Sciences, 6726 Szeged, Hungary.

<sup>5</sup> INRA, Laboratoire des Interactions Plantes-Microorganismes (LIPM), UMR441, Castanet-Tolosan, F-31326, France.

<sup>6</sup> CNRS, Laboratoire des Interactions Plantes-Microorganismes (LIPM), UMR2594, Castanet-Tolosan, F-31326, France.

<sup>7</sup> College of Science, King Saud University, Post Office Box 2455, Riyadh 11451, Saudi Arabia.

<sup>8</sup> To whom correspondence should be addressed: [ton.bisseling@wur.nl](mailto:ton.bisseling@wur.nl)

Published in *Development (Cambridge)* 141, 3517-3528

# CHAPTER 3

## SUMMARY

Legume root nodules are induced by  $N_2$ -fixing rhizobium bacteria which are hosted in an intracellular manner. These nodules are formed by reprogramming differentiated root cells. The model legume *Medicago truncatula* forms indeterminate nodules with a meristem at their apex. This organ grows by the activity of the meristem that adds cells to the different nodule tissues. In *Medicago sativa* it has been shown that the nodule meristem is derived from the root middle cortex. During nodule initiation also inner cortical cells and pericycle cells are mitotically activated. However, whether and how these cells contribute to the mature nodule has not been studied. Here we produce a nodule fate map precisely describing the origin of the different nodule tissues based on sequential longitudinal sections and the use of marker genes allowing to distinguish between cells originating from different root tissues. We show that nodule meristem originates from the third cortical layer while several cell layers of the base of the nodule are directly formed from cells of the inner cortical layers, root endodermis and pericycle. The latter 2 differentiate into the uninfected tissues that are located at the base of the mature nodule whereas the cells derived of the inner cortical cell layers form about 8 cell layers of infected cells. This nodule fate map has then been used to re-analyse several mutant nodule phenotypes. This showed for example that intracellular release of rhizobia in primordium cells and meristem daughter cells are regulated in a different manner.

**Key words:** *Medicago*, indeterminate root nodule, nodule primordium, nodule meristem, endodermis, inner cortex

## INTRODUCTION

The symbiosis of rhizobium and legumes results in the formation of N<sub>2</sub>-fixing root nodules, which can have a determinate or indeterminate growth. Determinate nodules lose their meristem at an early stage of development. In contrast, indeterminate legume nodules have a persistent meristem at their apexes by which they add cells to the different nodule tissues throughout their lifetime (Hadri et al., 1998). The model legume *Medicago truncatula* (Medicago) forms indeterminate nodules, so their nodule tissues are of graded age with the youngest cells near the meristem. The central tissue of the nodule is composed of 2 cell types, the infected cells that harbour the rhizobia, interspersed with specialized uninfected cells. This central tissue is surrounded by 3 uninfected peripheral tissues, the nodule parenchyma, endodermis and cortex (Bond, 1948; Van de Wiel et al., 1990; Brewin, 1991). Uninfected tissues are also present at the basal part of the nodule (See Fig. 7A).

In general it is assumed that in indeterminate nodules the cells along the complete apical-basal axis are derived from the apical meristem. However, this assumption creates some paradoxes. For example, how can the uninfected tissues at the basal part of the nodule be formed from the meristem and not be infected by rhizobium, whereas the layers that are subsequently formed do become infected? Further, the *nf-ya1* mutant forms nodules lacking a meristem or have a meristem that gives rise to daughter cells in which intracellular infection is blocked. However, several cell layers with fully infected cells are present at the base of these nodules (Combiér et al., 2006; Laporte et al., 2014).

Root nodule formation is initiated by mitotic activation of root cells. The most detailed analysis of which root tissue cells are activated has been performed on *Medicago sativa* (Timmers et al., 1999). This study showed that inner and middle cortical cells as well as pericycle cells become mitotically active upon rhizobial inoculation. Further, it was shown that the cells of the middle cortex form the nodule meristem. However, whether cells derived from the inner cortex and pericycle contribute to the mature nodule has not been studied. Based on the mutant nodule phenotype of *nf-ya1-1*, we hypothesize that cells derived from inner cortex form several cell layers of infected cells at the base of the nodule and intracellular

## CHAPTER 3

infection of these cells is less strictly controlled than infection of cells derived from nodule meristem. To test this hypothesis, we selected *Medicago* (*M. truncatula* A17) to generate a detailed nodule fate map.

The infection process in *Medicago* starts with the formation of an infection thread in a root hair and it grows to the base of the infected root hair cell. Subsequently, infection threads traverse outer cortical cells allowing rhizobia to reach the dividing cortical cells. This cluster of dividing cells is named nodule primordium and at its apex a meristem is formed (Libbenga and Harkes, 1973; Yang et al., 1994). Infection threads penetrate host cells derived from the meristem and rhizobia are internalised. During this release from infection threads, rhizobia become surrounded by the host membrane, a process controlled by a specific exocytotic pathway (Ivanov et al., 2012), leading to the formation of nitrogen-fixing symbiosomes (Roth and Stacey, 1989; Brewin, 2004). Symbiosomes then divide, differentiate and ultimately fill the infected cells.

Nodule formation as well as the infection process is controlled by specific lipochito-oligosaccharides, Nod factors, which are secreted by rhizobia (Lerouge et al., 1990). Nod factors mitotically activate root cells and such a cluster of dividing cells forming nodule primordium (Bond, 1948; Nutman, 1948; Libbenga and Harkes, 1973; Lancelle and Torrey, 1985; Dudley et al., 1987; Nap and Bisseling, 1990; Brewin, 1991; Yang et al., 1994; Timmers et al., 1999). However, the difference between a primordium and a young nodule is not well defined.

Our fate map studies confirmed that in *Medicago*, like in *M. sativa*, the inner and middle cortical and pericycle cells are mitotically activated upon rhizobium infection and the nodule meristem is derived from the middle cortex (Timmers et al., 1999). We have in addition established, that the first and second cortical layers only have a limited role in nodule ontogeny, that the third cortical layer gives rise to the nodule meristem and about 8 cell layers with fully infected cells at the base of the central tissue are derived from the inner cortex (4<sup>th</sup> and 5<sup>th</sup> cortical layer). Furthermore, cell divisions are also induced in the root endodermis and the endodermis/pericycle derived cells form the uninfected cell layers at the base of the nodule. Using this nodule fate map we re-analysed several *Medicago* mutants.

## RESULTS

### **Pericycle, endodermis and cortical layers contribute to the Medicago nodule primordium**

Medicago roots have in general 5 cortical cell layers, although also roots with 4 and 6 layers do occur. We will name the outer most layer C1 and the inner most C5. The inner most cortical cells are about 15  $\mu\text{m}$  thick, whereas the cells of the other 4 cortical layers are about twice as thick (30  $\mu\text{m}$ ). The epidermis, endodermis and pericycle each contain a single cell layer (Fig. 1A).

To determine which cell layers of the root contribute to the formation of a nodule primordium, Medicago seedlings were inoculated with *S. meliloti* 2011 and root segments were collected at different time points within 1-5 days after inoculation. These were fixed and embedded in Technovit 7100. Longitudinal sections of about 50 root segments were made and analyzed by light microscopy. Based on these analyses we divided nodule development in 6 stages (Fig. 1). At stage I (Fig. 1A), anticlinal divisions are induced in the pericycle. This is rapidly followed by anticlinal divisions first in C5 and slightly later in C4 (stage II) (Fig. 1B). During stage III (Fig. 1C), periclinal divisions are induced in C5 and C4 and anticlinal divisions occur in C3 and endodermis. At stage IV (Fig. 1D), periclinal divisions occur in C3, pericycle and endodermis, cell divisions continued in C5 and C4 and some anticlinal divisions are induced in C2. At stage V (Fig. 1E), C3 derived cells have formed a multi layered (future) meristem, C4 and C5 have formed about 8 cell layers and the endodermis and pericycle 6-8 cell layers. At this stage of nodule development mitotic activity in the non-meristematic (C4/5) cells stops. These cells start to enlarge and are penetrated by infection threads. These characteristics distinguish them morphologically from the (future) meristem cells (C3) which are small and not infected. At stage V it still can be traced from which root cell layers the primordium cells are derived. At stage VI (Fig. 1F) this is not well possible due to the formation of peripheral tissues, but meristem and C4/5 derived cells can be recognized based on their distinguishing morphological characteristics. At stage VI, vascular bundles are established at the periphery. Further, the meristem starts now to add cells to the nodule tissues, this is why we named it (future) meristem at stage V. We propose to name the clusters

## CHAPTER 3

of cells a nodule primordium up to stage V and nodule from stage VI on. Previously, it was proposed to call the clusters of dividing cells at stage I and II an initial primordium (Timmers et al., 1999). However, as these cells become part of the mature nodule (see below) there is no reason to distinguish these primordia stages from III-V.

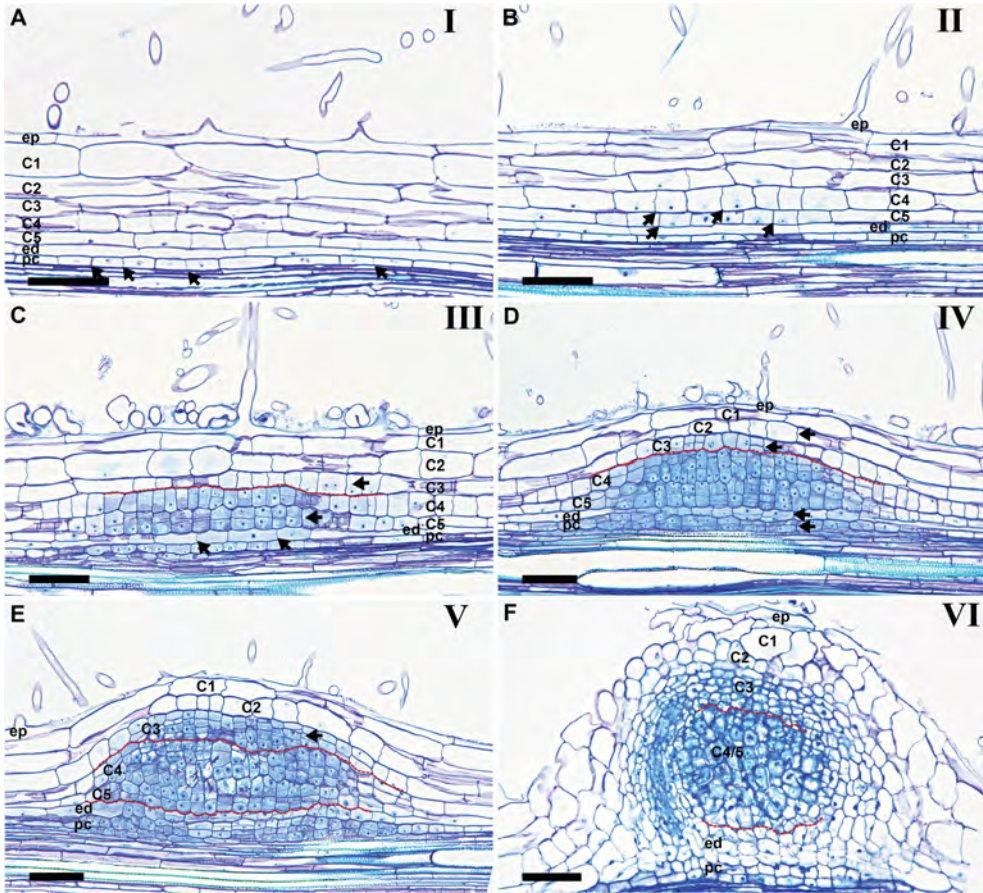


Fig. 1. Medicago nodule primordia at subsequent stages of development. Longitudinal sections of Medicago root segments. (A) Stage I: Anticlinal cell divisions are induced in the pericycle (arrows) and that occasionally occur in C5 and C4. (B) Stage II: Cell divisions (anticlinal) extend to C5 and C4 (arrows); anticlinal divisions occasionally occur in C3. The higher frequency of divisions in the inner layers reflects that the divisions start from there. (C) Stage III: Anticlinal divisions occur in C3 (arrow) and endodermis (arrows); periclinal divisions are induced in C4 and C5 derived cells (arrow); anticlinal cell divisions occasionally occur in C2. (D) Stage IV: Periclinal cell divisions are induced in C3 (arrow), endodermis (arrow) and pericycle (arrow); C4 and C5 cell division continue; anticlinal cell divisions occur in C2 (arrow). (E) Stage

V: C3 derived cells form multiple cell layers (arrow); C4/5 have form about 8 cell layers; pericycle and endodermis contribute about 6 cell layers to the basal part of the primordium; C2 and C1 have divided a few times anticlinally. (F) Stage VI: vascular bundles are formed at the periphery of the primordia; meristem starts functioning. From this moment on a nodule primordium become a nodule.

In C, D, E and F a red line indicates the border between cells derived from C3 and C4/5 and endodermis, respectively.

Epidermis (ep), Cortical cell layers 1st (C1), 2nd (C2), 3rd (C3), 4th (C4), 5th (C5), Endodermis (ed), Pericycle (pc).

Bars, 75  $\mu$ m.

To obtain better insight in the timing of the different stages of nodule primordium formation, we also spot inoculated *Medicago* roots with *S. meliloti*. Stage I starts at about 24 hours post inoculation (hpi); stage II at 27-33 hpi; stage III at 33-35 hpi; stage IV at 42-48 hpi; stage V at 65-70 hpi; stage VI after 80 hpi.

*Medicago* lateral root formation also starts with divisions in the pericycle, endodermis and cortex cells (den Camp et al., 2011; Herrbach et al., 2014), which is very similar to nodule primordium initiation. To distinguish a young lateral root primordium from an early stage (I-III) nodule primordium, we made use of transgenic *Medicago* roots expressing *MtENOD40::GUS*. This reporter is strongly induced in rhizobium activated pericycle, endodermis, cortical cells and vascular tissue and markedly less and restricted in pericycle and vascular tissues of the lateral root

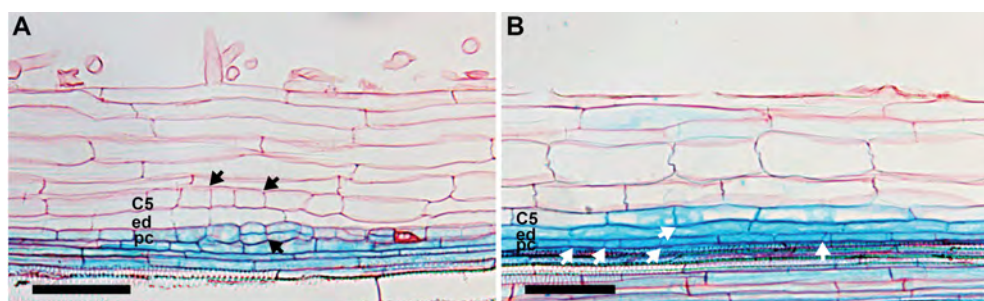


Fig. 2. *MtENOD40::GUS* is a marker to distinguish between early lateral root primordium and nodule primordium.

The root (A) and nodule (B) primordia are initiated on the same *MtENOD40::GUS* transgenic root. In both primordia C5 and pericycle cells have divided (black and white arrows), *MtENOD40* is markedly higher expressed in the nodule primordium (B).

Bars, 75  $\mu$ m.

## CHAPTER 3

primordia (Fig. 2). At stage I a marker like *MtENOD40* is essential to distinguish lateral root and nodule primordia. However, at later stages this is not essential as in nodule primordia the frequency of divisions is highest in cortical layers whereas in lateral root primordia mitotic activity is higher in pericycle and endodermis (Xiao, pers. comm.).

We showed that in *Medicago* the mitotic activation of root cells by rhizobium starts in the pericycle and extends outwards to the cortical cell layers. The middle cortical cell layer (C3) ultimately forms the nodule meristem. This is similar to nodule primordium initiation in *M. sativa* (Timmers et al., 1999). In addition, we showed that the endodermis also divides and together with pericycle and inner cortex cell layers (C4/5) contribute about 16 cell layers to the nodule primordium. Based on these observations we addressed the question whether primordium cell that originate from pericycle up to C4 contribute to mature nodule tissues?

### **Do primordium cells derived from C4/5 become part of the mature nodule?**

First we determined whether rhizobia can infect C4/5derived cells. Serial sections of 30 primordia at stage III-IV were analyzed. In 5 primordia (stage III), the infection thread was still in C1 or C2 and in 10 (stage III) primordia, the infection thread had just reached C3 (Fig. 3A). In 15 primordia, the infection thread was present in cells derived from C4 and C5 (Fig. 3B). In 10 of these latter primordia, C3 cells had divided several times including both anticlinal and periclinal divisions (stage IV). Therefore it is likely that cells derived from C3 can still be penetrated by an infection thread after the first anticlinal divisions (stage III). As nodule meristematic cells are not penetrated by infection threads it is probable that infection threads have to reach C4 and C5 derived cells before stage IV, i.e. before periclinal divisions are initiated in the C3 layer.

To determine the timing of the infection of the primordium more precisely, spot inoculated *Medicago* roots were analyzed. At 42-48 hpi, the infection thread had reached C4/5 derived cells (stage IV). Around 80 hpi (stage VI) bacterial release had taken place in cells derived from C4/5 (Fig. 3C-D). This means that release occurs about 32 h after the infection thread reached the primordium cells.

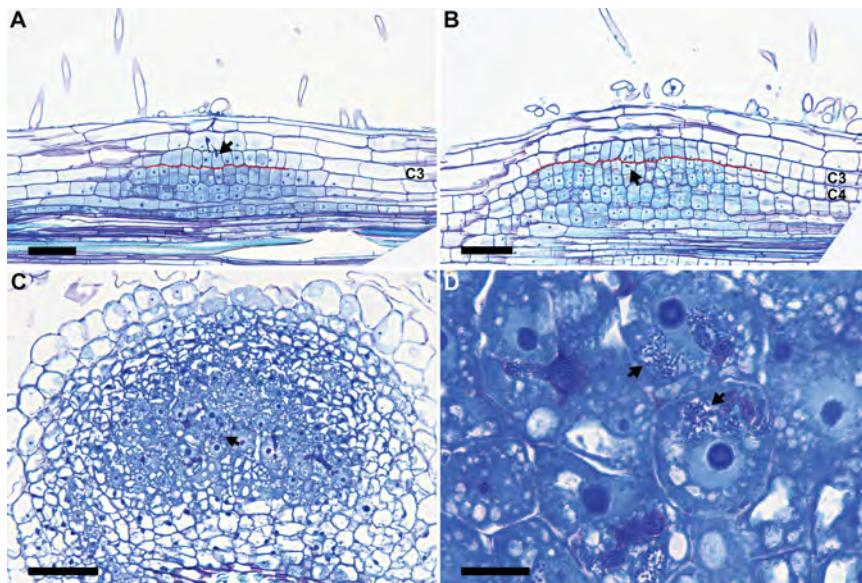


Fig. 3. Infection threads reach C4/5 derived cells before stage IV.

(A) At stage III of primordium development, anticlinal divisions are induced in C3 and the tip of the infection thread (arrow) reached C3. (B) At stage IV, the tip of the infection thread has reached the cells derived from C4/5 (arrow). (C) At stage VI (80 hpi), rhizobia are released in C4/5 derived cells. (D) Magnification of C shows the released rhizobia (arrows).

In A and B a red line indicates the border between cells derived from C3 and C4. Bars, 75 µm in A-C; 10 µm in D.

C4/5 derived cells that are infected by rhizobia develop into large infected cells. So, in a mature nodule about 8 cell layers of the central tissue directly developed from C4/5 derived cells and not from the meristem (C3).

### **Do primordium cells derived from pericycle/endodermis become part of the mature nodule?**

The analysis of nodule primordia showed that C4 and C5 derived cells can be infected by rhizobia. However, whether endodermis and pericycle derived cells may also become infected cannot be excluded. In order to trace primordium cells derived from endodermis and pericycle more precisely, we made use of *CASP1*, an Arabidopsis gene that is specifically expressed in the root endodermis. It encodes a transmembrane protein that is involved in the formation of casparian strips (Roppolo et al., 2011).

## CHAPTER 3

To determine whether this gene can be used as an endodermis marker in *Medicago*, we transformed *Medicago* roots with *AtCASP1::GUS* (Vermeer et al., 2014) and showed that this construct is expressed in endodermis and also in pericycle but at low level (Fig. 4A).

In general, it is presumed that root cells that are mitotically activated are completely de-differentiated. Therefore we expected that *AtCASP1::GUS* would be repressed when cell divisions are induced in the endodermis. However, when the endodermis had undergone several periclinal as well as anticlinal divisions all endodermis derived cells displayed GUS activity. Therefore we were able to trace endodermal cells during the formation of a nodule primordium and could distinguish them from cortex derived cells (Fig. 4B). The intensity of the signal in the endodermis derived cells is (at least) as high as in the endodermis before division. On that account, it is not simply a dilution of GUS present in the root endodermis and the *AtCASP1* promoter must have remained active during endodermal cell

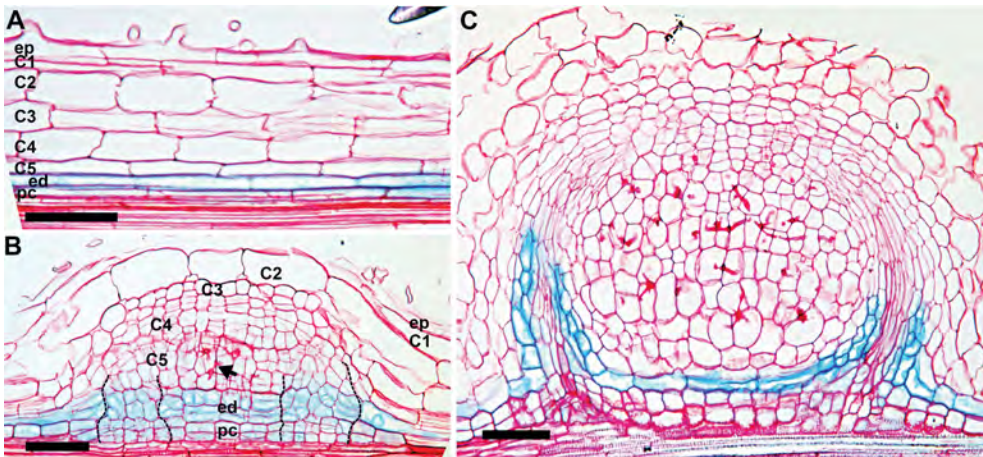


Fig. 4. Endodermis and pericycle derived cells of the primordium are not infected. *AtCASP1::GUS* (A) is specifically expressed in the *Medicago* root endodermis and also in pericycle but at low level. *AtCASP1::GUS* (B) remains in endodermis derived cells at stage IV. Cells at the periphery region (indicated in between black lines) will differentiate into nodule parenchyma include vascular bundles and endodermis. These cells show different division pattern with their neighboring cells which derived from the same tissue. Infection threads (arrow) never reach endodermis and pericycle derived cells. (C) At stage VI, *AtCASP1::GUS* expression is restricted to a single cell layer surrounding the nodule vascular bundle (endodermis).

Bars, 75  $\mu$ m.

divisions. Analyses of serial sections of 30 stage IV-V primordia showed that infection threads do not penetrate endodermis and pericycle derived cells in contrast to C4 and C5 derived cells. For that reason, the origin of the primordial cells appears to determine whether they can be penetrated by an infection thread or not.

At stage VI the expression of *AtCASP1::GUS* is repressed in most of the endodermis derived cells and becomes restricted to a single cell layer. Further, it is induced in vascular endodermis (Fig. 4C).

The maintenance of endodermal specific gene expression in nodule primordium is also illustrated by the expression of *Scarecrow (SCR)*. Arabidopsis SCR is a GRAS type transcription factor that is specifically expressed in the root endodermis and is essential for the formation of this tissue (Di Laurenzio et al., 1996). *AtSCR::GUS* is also specifically expressed in the endodermis of transgenic Medicago roots (Fig. S1A). Like *AtCASP1*, it remains active in divided endodermal cells in a nodule primordium up to the stage when vascular bundles start to be formed (Fig. S1B). It is also activated in cells around the vasculature (Fig. S1C).

So, *AtCASP1* and *AtSCR* promoters are expressed in the root endodermis and remain active when cell division is induced. Therefore we studied whether casparian strips, the hallmark of endodermal cells, are formed in the dividing endodermis cells (Fig. 5). Casparian strips are present in the Medicago root endodermis (Fig. 5A), but upon the first divisions induced by rhizobium, these are lost (Fig. 5B). They are again formed in the single cell layer at the base of the nodule, where expression of *AtCASP1::GUS* is maintained (Fig. 5C). *AtCASP1::GUS* is also expressed in the endodermis around the nodule vascular bundles, and there casparian strips are present (Fig. 5D; Fig. S2). In contrast, *AtCASP1::GUS* is not expressed in the nodule endodermis and casparian strips are not formed (Fig. 5D; Fig. S2). A “real” endodermis is only formed at the base of the nodule and around nodule vascular bundles. The fact that the casparian strips are (have to be?) removed before cell division is induced could be a reason why induction of mitotic activity in this tissue is slightly delayed compare to C4 and 5 cells.

These results show that primordium cells derived from pericycle and

## CHAPTER 3

endodermis, in contrast to those with a cortical origin, cannot be infected by rhizobia. As the endodermis derived primordium cells maintain expression of endodermal genes, it is most likely that these cells do not completely de-differentiate, but switch from one differentiated cell type into another, a process named trans-differentiation (Sugimoto et al., 2011). By which mechanism infection in these endodermis derived cells is prohibited is unclear. We hypothesise that the (partial) maintenance of the endodermal

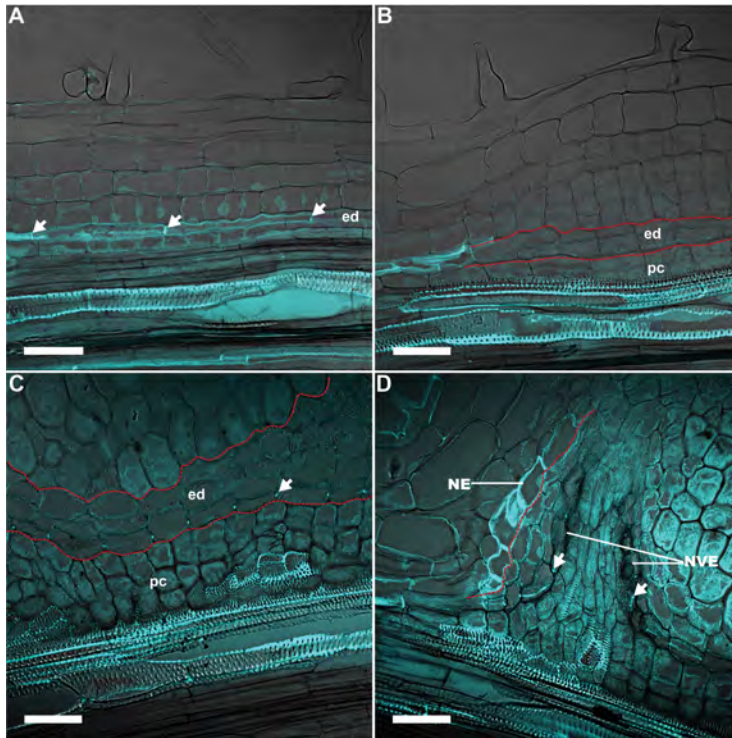


Fig. 5. Casparian strips disappear in the dividing endodermis of nodule primordium. (A) Casparian strips (arrows) in the root endodermis. (B) Casparian strips are absent in dividing endodermal cells. (C) At stage VI, casparian strips (arrow) are formed in the single cell layer at the base of which *AtCASP1* are expressed. (D) Casparian strips (arrows) are formed in the endodermis of nodule vascular bundles but not in the nodule endodermis (split channels in Fig. S2).

In B and C red lines indicate the border between cells derived from endodermis and C5 or pericycle, respectively; in D a red line indicates the border between nodule endodermis and nodule parenchyma.

Casparian strips are detected as autofluorescence under UV light.

Nodule vascular endodermis (NVE), Nodule endodermis (NE).

Bars, 50 µm.

fate can contribute to this.

In primordia, infection threads are restricted to the central region of the C4/5 derived cells (Fig. 4B; Fig. S1B). At the transition from stage V to VI the peripheral tissues and vascular bundles start to be formed. These are cells derived from the periphery of the nodule primordium, which includes cells derived from C4, C5, endodermis and pericycle (Fig. 4B; Fig. S1B). In nodules, the pericycle and endodermis derived cells form the peripheral tissues at the base of the nodule. These are the nodule parenchyma and the few cell layers that are adjacent to the root vascular bundle. In between these two tissues an endodermis containing casparian strips is present.

### **Markers to distinguish C4/5 derived cells and meristem**

We searched for molecular markers enabling us to distinguish between C4/5 derived cells and (future) meristem cells. Infected cells in the infection zone of a mature nodule undergo endoreduplication. Therefore, we expected that C4 and C5 derived cells enter endoreduplication when they stop dividing (stage V or VI). In this case markers for mitosis and endoreduplication could be used to distinguish these cells from (future) meristem cells. To identify mitotically active and endoreduplicating cells we used Medicago lines containing an Arabidopsis Cyclin B1 reporter (*AtCyclB1.1::GUS*) which is active during mitosis and *MtCCS52A::GUS* which is expressed in endoreduplicating cells (Vinardell et al., 2003). *AtCyclB1.1* is active in (future) meristem and not in C4/5 derived cells at stage V and later stages (Fig. 6A). The endoreduplication reporter is not expressed in nodule primordia before stage V and has an expression pattern that is complementary to that of *AtCyclB1* at stage VI; when the latter is switched off in the C4/5 derived cells, *MtCCS52A::GUS* is switched on in these cells (Fig. 6B).

We also tested whether the nodule specific remorin (*MtSYMREM1*) that is involved in bacterial release (Lefebvre et al., 2010) can be an extra marker. *MtSYMREM1::GUS* is first induced in C4/5 derived cells and it is not active in cells derived from C3 at stage V/VI (Fig. 6C).

## CHAPTER 3

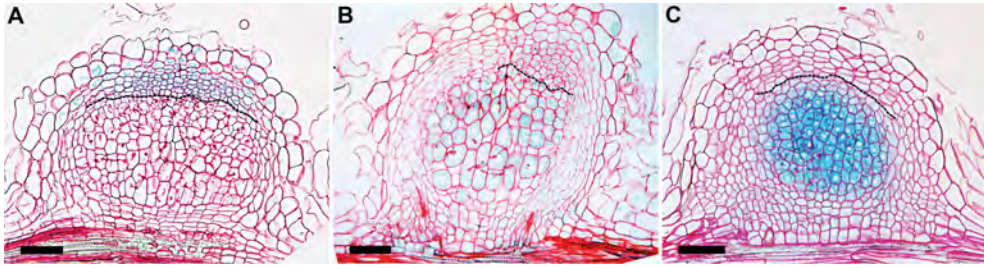


Fig. 6. Molecular markers to distinguish C4/5 derived cells from the nodule meristem (C3).

(A) At stage VI, *AtCycB1.1::GUS* is expressed in C3 derived cells, but not in C4/5 derived cells. (B) At stage VI, the cell endoreduplication marker *MtCCS52A::GUS* is expressed in C4/5 derived cells and some C1/2 and epidermis derived cells, but not in C3 derived cells. (C) In transition from stage V to VI, *MtSYMREM1::GUS* is detected in C4/5 derived cells.

A black line indicates the border between cells derived from C3 and C4.

Bars, 75  $\mu$ m.

We thus have identified three markers allow to distinguish between C4/5 and C3 derived cells at stage V/ VI.

## DISCUSSION

### Analyses of symbiotic mutants

To illustrate the value of our Medicago nodule fate map we have re-analyzed four previously characterized mutants with greater accuracy, namely *nf-ya1-1* (Combiér et al., 2006; Laporte et al., 2014), *sickle* (Penmetsa and Cook, 1997), *ipd3* (Horvath et al., 2011; Ovchinnikova et al., 2011; Singh et al., 2014) and *lin* (Kuppusamy et al., 2004; Kiss et al., 2009; Guan et al., 2013), respectively.

#### *nf-ya1-1*

*nf-ya1-1* (Combiér et al., 2006; Laporte et al., 2014) forms nodules of variable size, but all are markedly smaller than wild type (wt) nodules. The largest *nf-ya1-1* nodules (Fig. 7B) have about 8 cell layers with well infected cells at their basal part. In these cells development of rhizobium into N<sub>2</sub>-fixing symbiosomes (Fig. S3) is like in wt, as described in Laporte

et al (2014). These nodules have a relatively small meristem. In cells derived from it, infection threads are present, but release is blocked. This phenotype suggests that during primordium formation, cell divisions in C4 and C5 have occurred and rhizobia are released in these cells. However, the formation of a wt-sized meristem that can produce daughter cells competent for bacterial release requires NF-YA1. In addition to these relatively large *nf-ya1-1* nodules also smaller nodules are formed. These can have only a few layers with fully infected cells (Fig. 7C), a nodule meristem is absent and the nodule is completely surrounded by the nodule endodermis. In these nodules, divisions in C4 and C5 have most likely occurred to a certain extend and these cells differentiate into wt-like

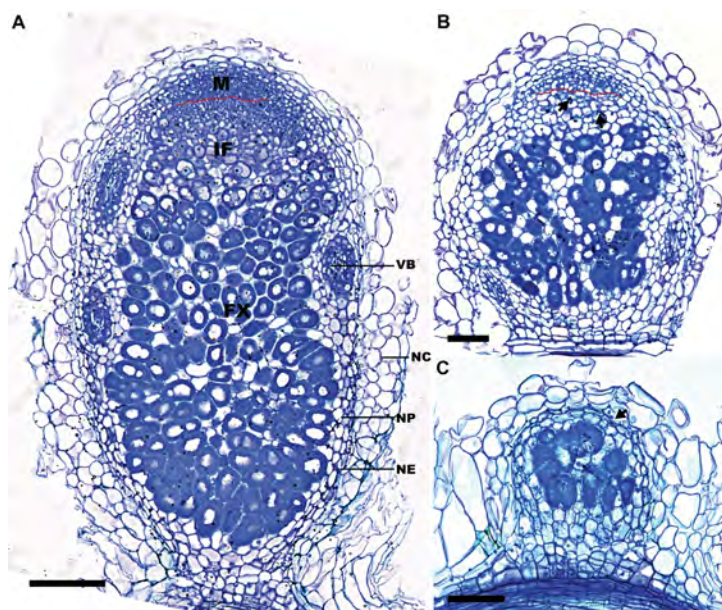


Fig. 7. Mutant *nf-ya1-1* forms nodules with a small nodule meristem or no nodule meristem.

Two weeks old wt (A) and *nf-ya1-1* (B-C) nodules have a central part well infected by rhizobia. (B) A relatively large *nf-ya1-1* nodule has a small nodule meristem (Infection threads are indicated by arrows). (C) A small *nf-ya1-1* nodule does not have a nodule meristem and develops closed nodule endodermis (arrow).

Meristem (M), Infection zone (IF), Fixation zone (FX), Vascular bundle (VB), Nodule parenchyma (NP), Nodule cortex (NC).

In A and B a red line indicates the border between nodule meristem and infection zone. Bars, 75  $\mu$ m.

## CHAPTER 3

infected cells. However, the formation of a meristem (from C3) appears to be blocked.

To test these hypotheses we studied nodule primordia of the *nf-ya1-1* mutant. Roots were sectioned at 1-5 dpi. This showed that primordia are rather diverse, which is well in line with the diverse nodule phenotypes. The largest primordia are composed of cells derived from pericycle up to C3 (Fig. 8A). Cells derived from C4/5 are infected and contain released bacteria which in wt is a hall mark of stage VI (Fig. 8B) and several of these infected cells have already enlarged (Fig. 8A). In such primordia, some periclinal divisions have occurred in C3 derived cells, but markedly less than in wt stage VI. It seems that such primordia can develop into the relatively large *nf-ya1-1* nodules with a small meristem and hampered bacterial release in its daughter cells. In addition, markedly smaller primordia are formed, where cell divisions have occurred in C4 and C5, albeit with a lower frequency. Further, only a few anticlinal and no periclinal divisions or bacteria release have occurred in C3 (Fig. 8C). Probably, such primordia develop into the small nodules that lack a meristem.

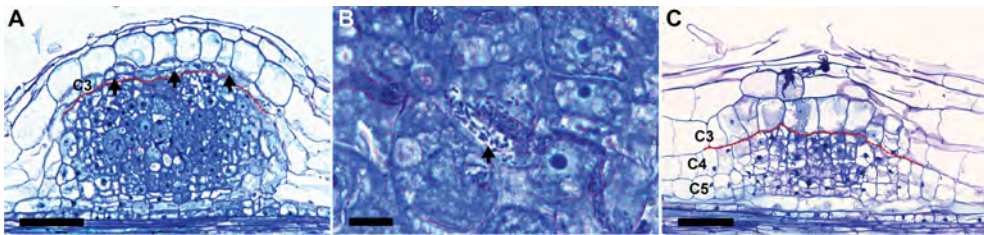


Fig. 8. Reduced cell division in C3 of *nf-ya1-1* nodule primordia.

(A) Relatively large *nf-ya1-1* nodule primordium with bacteria release in C4/5 derived cells; the number of C3 derived cells is less than in wt at stage III or VI (arrows). (B) Bacteria are released from infection threads (arrow) (magnification of the primordium A). (C) A *nf-ya1-1* nodule primordium with about 8 cell layers derived from C4/5 and no periclinal division in C3.

In A and C a red line indicates the border between cells derived from C3 and C4.

Bars, 75  $\mu$ m in A and C; 10  $\mu$ m in B.

Using our fate map we have thus been able not only to confirm and to describe more thoroughly that meristem formation is hampered in the *nf-ya1-1* mutant but we have also shown the well infected cells inside

mutant nodules are derived from C4 and C5. Further the cells that are derived from the (small) nodule meristem cells cannot differentiate into cells competent for bacterial release. The latter implies that release of rhizobia in primordia cells derived from C4/5 is not affected in the *nf-ya1-1* mutant, whereas in daughter cells derived from the meristem release requires NF-YA1. Our data also suggest that NF-YA1 is required for proper nodule meristem formation.

### *sickle*

*sickle* makes markedly more root nodules than wt as it is mutated in an ethylene signalling gene. The nodule histology of this mutant is in general considered to be wt-like (Penmetsa and Cook, 1997). We sectioned about 50 *sickle* nodules that are formed at the “sickle” shaped zone (Fig.

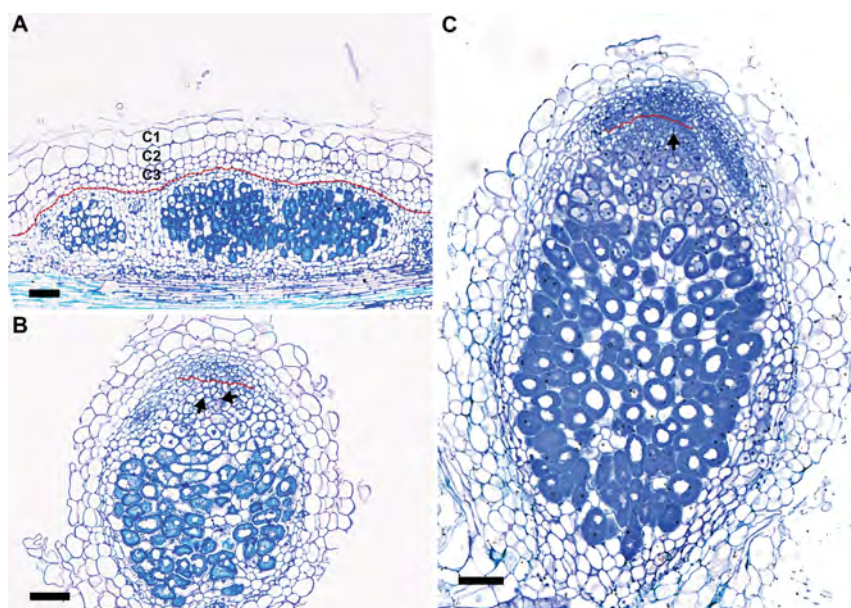


Fig. 9. Meristem formation is hampered in some *sickle* nodules.

Two weeks old *sickle* (A-B) and wt (C) nodules. (A) *sickle* nodules that are “fused” have no meristem and are surrounded by an endodermis. (B) A *sickle* nodule is smaller than (C) wt nodule.

In A a red line indicates the border between cells derived from C3 and C4 and nodule meristem and infection zone in B and C. Infection threads are indicated by arrows (B-C).

Bars, 75  $\mu$ m.

## CHAPTER 3

S4A) (Penmetsa and Cook, 1997). The vast majority has about 8 (or less) layers with well infected cells. These nodules have no meristem and are surrounded by the endodermis (Fig. 9A). This mutant also forms a few nodules morphologically more similar to wt (Fig. 9B; Fig. S4B). However, their size is much smaller compared to wt, indicating a sub-optimal functioning meristem (Fig. 9C; Fig. 4C). So, the defect in ethylene signalling has a positive effect on nodule primordium formation, but directly or indirectly has a strong negative effect on nodule meristem formation.

*sickle* was previously used by Timmers et al. (1999) to study the timing of meristem formation and infection thread growth. However, as the *sickle* mutant is disturbed in nodule meristem formation these studies might not provide reliable insight in the timing of these processes in wt nodules.

### *ipd3*

The fate map studies show that infection threads have passed C3 before periclinal divisions are induced. This suggests that nodule primordia will not be infected when infection thread growth is delayed in comparison to divisions in C3. IPD3 is a transcriptional regulator that interacts with the kinase CCaMK and is essential for release of bacteria from infection threads (Horvath et al., 2011; Ovchinnikova et al., 2011; Singh et al.,

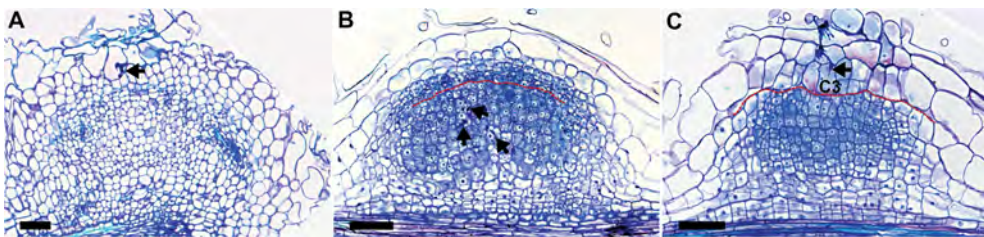


Fig. 10. Infection thread failed to pass the future nodule meristem cells (C3) before stage IV in *ipd3* mutant.

(A) Small non-infected *ipd3* nodule with infection thread (arrow) arrested in outer cortex layers. Nodule primordia (B) with infection threads (arrows) successfully reached cells derived from C4/5 and (C) with infection thread (arrow) failed to pass through C3 at stage IV.

In B and C a red line indicates the border between cells derived from C3 and C4.

Bars, 75 μm.

2014). The *Medicago ipd3* (*Mtsym1-1/TE7*) mutant can form nodules with a meristem and numerous infection threads from which rhizobia are not released. However, many nodules remain very small and lack infection threads (Fig. 10A) (Ovchinnikova et al., 2011).

To test whether lack of infection threads in primordia is due to delayed infection thread growth in the outer cortex, serial sections of roots (1-5 dpi) were made. Two types of primordia were detected. One type is similar to wt (Fig. 10B), C4 and C5 have formed about 8 cell layers and these cells contain infection threads. So, the infection threads have successfully passed C3. These primordia probably develop into nodules containing numerous infection threads. The other type of primordium is composed of cells derived from C5, C4 and C3. C3 has already periclinal divided several times whereas the infection thread has just reached the outer cortex (Fig. 10C). These primordia probably result in small non-infected nodules (Fig. 10A) and this is consistent with the hypothesis that infection threads no longer can traverse C3 when periclinal divisions have been induced (stage IV). In this way, a few hours difference in reaching or passing C3 can cause a major difference in nodule development.

### *lin*

Rhizobium induced cell division in pericycle and endodermis is arrested at an early stage (IV-V) of development. Some *Medicago* mutants form nodules with central vascular bundles, whereas wt nodules have peripheral vascular bundles. We hypothesize that this is due to more extensive divisions in pericycle and endodermis. An example is *LIN*, which is essential for infection (Kuppusamy et al., 2004; Kiss et al., 2009; Guan et al., 2013) and codes for a E3 ubiquitin ligase. *lin-1* (Kuppusamy et al., 2004) forms non-infected nodules with central vascular bundles (Fig. 11A).

We tested our hypothesis in *lin-1* primordia by using the endodermis marker (*AtCASP1::GUS*). In several primordia, cortical divisions (C4/5) are at stage III-IV, while pericycle and endodermis divisions are at stage V or have divided even more frequently (Fig. 11B). In addition to that, C3 divisions are in between stage II-IV and never go further than stage IV. This indicates that the higher mitotic activity of pericycle and endodermis

## CHAPTER 3

probably leads to the formation of central vascular bundles (Fig. 11C). The phenotype of the *lin-1* mutant suggests that the expression of this gene is important to block at an early stage of development cell divisions in endodermis/pericycle derived cells.

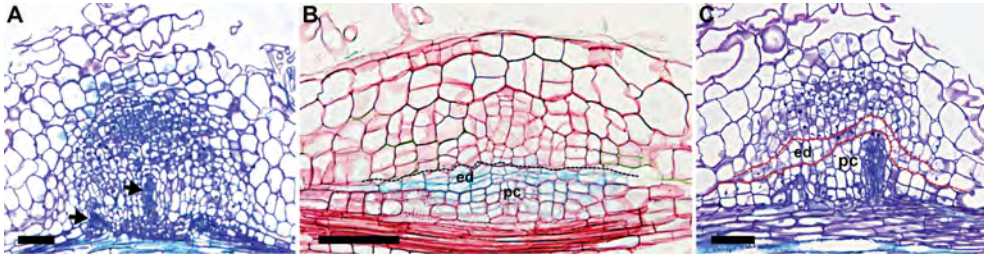


Fig. 11. Extensive cell divisions in root pericycle and endodermis during *lin1-1* nodule primordium development correlates with formation of central vascular bundle.

Two weeks old *lin1-1* nodule (A), which have a few central vascular bundles (arrows) and does not have a meristem. (B) In *AtCASP1::GUS* expressing *lin1-1* roots, a nodule primordium has more endodermis and pericycle divisions than the wt stage V primordium. The number of C3 and C4/5 derived cells are less or comparable to wt cell numbers at stage IV. (C) Central vascular bundles of *lin1-1* nodules are derived from pericycle.

In B and C the lines confine cells derived from endodermis.

Bars, 75 µm.

### Integrated model for cell fate control and initiation of cell division

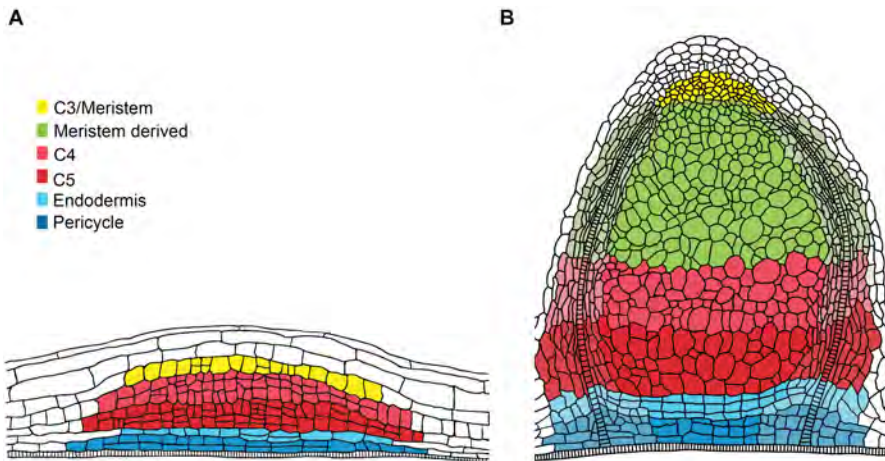


Fig. 12. Indeterminate root nodule fate map, (A) nodule primordium and (B) nodule. The origins of cells in primordium and nodule are indicated by the same colour. The origin of nodule cortex are not shown.

Table 1. Characteristics of the Medicago nodule primordia developmental stages.

Stages	Primordia Characteristics	Infection Thread Tip
I	1) Pericycle: anticlinal divisions	---
II	1) C4/5: anticlinal divisions	---
III	1) C3: anticlinal divisions 2) C4/5: first periclinal division 3) Endodermis: anticlinal divisions	C3 or C4
IV	1) C2: anticlinal divisions 2) C3: first periclinal divisions 3) C4/5: cell division continued 4) Endodermis/pericycle: first periclinal divisions	C4/5
V	1) C3: multi layered (future) meristem 2) C4/5: i. central part cell division stops ii. 6-8 cell layers iii. central cells start to enlarge iv. peripheral cells start to differentiate into vascular bundles and peripheral tissues 3) Endodermis/pericycle: i. central part cell division stops ii. 6-8 cell layers iii. peripheral cells start to differentiate into vascular bundles and peripheral tissues	Central part of C4/5 derived cells
VI	1) C3: functional meristem start adding cells to the nodule 2) C4/5: i. central cells enlarged ii. peripheral cells differentiated into vascular bundles and peripheral tissues 3) Endodermis/pericycle: i. central cells differentiated to parenchyma and an endodermis layer with casparian strips ii. peripheral cells differentiated to vascular bundles and peripheral tissues	Central part of C4/5 derived cells (bacteria released)

## CHAPTER 3

In this study we produced a fate map for *Medicago* root nodules. This fate map is summarized in the cartoon shown in Fig. 12 and Table 1. In a mature nodule, about 8 cell layers of the basal part of the nodule tissue are derived directly from the nodule primordium (C4/5 derived) and not from the meristem. The uninfected basal tissues develop from primordium cells, which are derived from endodermis and pericycle. The nodule meristem is derived from a single central cortical layer (C3) and when the meristem becomes functional at stage VI, it continuously adds cells to the different nodule tissues.

Nodule primordium formation starts with cell divisions in the pericycle and subsequently extends towards more outer layers. When pericycle cells are mitotically activated by Nod factors secreted by rhizobia the bacteria are still present at or in the epidermis. As Nod factors are rather immobile signal molecules (Goedhart et al., 2000), perception of Nod factors at the epidermis most likely triggers mitotic activity in inner root cell layers. So how could an exogenously applied signal lead to cell division starting in the cell layer that is most remote, while the cells closest to the signal respond last?

Previously, we made a theoretical model to investigate how Nod factors can induce cortical cell divisions (Deinum et al., 2012). It is known that Nod factor perception leads to cytokinin signaling (den Camp et al., 2011), while cortical cell division is associated with increased auxin (Mathesius et al., 1998). Cytokinin is known to affect negatively the accumulation of auxin efflux carriers (PIN) in the plasma membrane (Dello Ioio et al., 2008; Marhavy et al., 2011). Therefore we simulated that Nod factor signaling induces the decrease of the level of PIN protein in all cortical cell layers of the region responding to Nod factors. This block of cortical cells was named "controlled area". This resulted, in the model, in a local increase of auxin in the cortex which coincided with the site where cortical cell divisions are induced. Here we included the pericycle and endodermis into the "controlled area" (Fig. 13A) and further we focused on the early dynamics of the predicted auxin accumulation in the cell layers where cell division is induced.

For our current simulations we start from a PIN layout that gave rise to auxin accumulation in inner root layers (Fig. 13B), as divisions have been

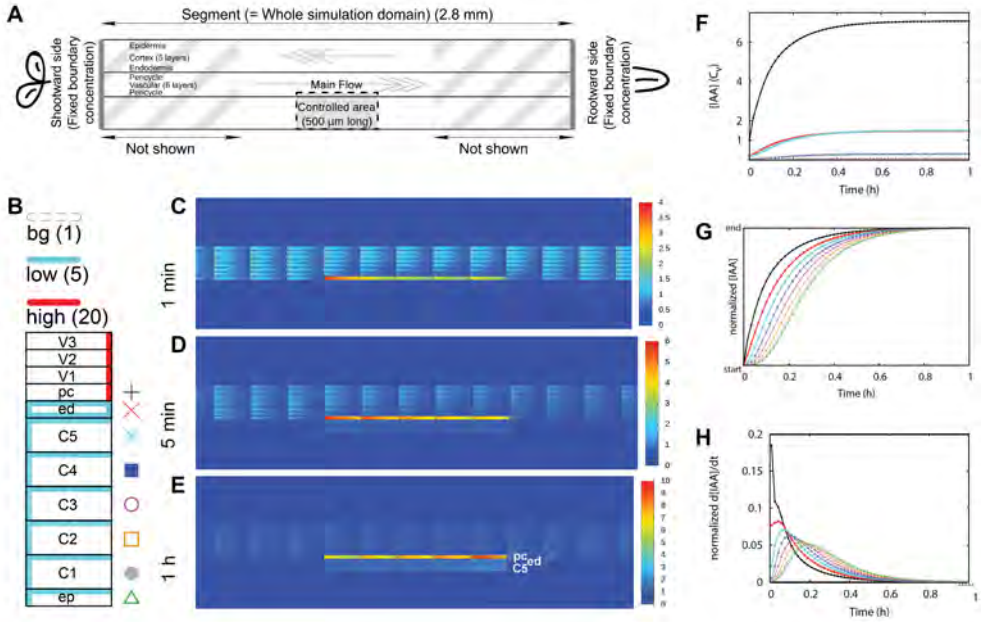


Fig. 13. Auxin accumulation following a local reduction of the effective efflux permeability starts from the inner root layers.

Simulations are based on a root segment representing the susceptible zone of *Medicago* roots (A) (Deinum et al., 2012). At  $T = 0$  s, the efflux is reduced in a block of cells that is 5 cells long and comprises all cell files from epidermis to pericycle. This we call the “controlled area”. The PIN distribution (B) of this root segment is such that the main auxin flux in the vascular tissue is rootward and reversed in the cortex. The starting concentration of PINs in each membrane segment is one of three levels: “high” (red,  $P_{eff} = 20 \mu\text{m s}^{-1}$ ), “low” (cyan,  $P_{eff} = 5 \mu\text{m s}^{-1}$ ), or “bg” (background level; white,  $P_{eff} = 1 \mu\text{m s}^{-1}$ ) (Laskowski et al., 2008; Deinum et al., 2012). The colored symbols serve as a legend for F-H. (C-E) Concentration heat maps of the middle part of the root segment including the controlled area at  $T = 1$  min (C),  $T = 5$  min (D) and  $T = 1$  h (E) (Movie 1). (F) The concentration in the middle row of cells is tracked for all cell files in the controlled area. The concentration in the pericycle remains highest, followed by endodermis and inner cortex (C5). (G) When rescaling the concentration in each file from its starting level to the level reached at the end of the simulation ( $T = 1$  h), it becomes clear that the concentration in the pericycle increased first, followed by the other layers in an interior to exterior order. The moment of fastest concentration increase, the peaks of the curves in H (time derivative of G, expressed in rescaled concentration units per minute), showed the same relative order. Start from pericycle, vasculature cell layer 1st (V1); 2nd (V2); 3rd (V3).

## CHAPTER 3

observed to coincide with an auxin maximum (Mathesius et al., 1998; own observations). This layout, and all variants that we have used, produce a root-ward auxin flux in the stele/vascular tissue and a shoot-ward and inward flux in the cortex.

The reduction of membrane PINs resulted in an increase of the auxin concentration in all cell layers. However, only in the pericycle, endodermis and inner cortical layers the auxin concentration in the controlled area reached a level similar to or higher than the vascular starting level. Furthermore, in the outer layers the absolute increase was very small compared to this (Fig. 13C-F). A detailed modeling study of the auxin sensing system of TIR1-SCF controlled ubiquitination of Aux/IAA proteins showed it has the potential to detect changes in auxin concentration (Middleton et al., 2010). We therefore plotted the concentration increase in each layer normalized by the concentrations at the beginning and the end of the simulation (Fig. 13G) and the time derivative of these curves (Fig. 13H). This shows that the auxin concentration increased first and fastest in the pericycle, followed by the endodermis and C5 and then by other layers in an outward fashion. The time derivatives (Fig. 13H) clearly show that the pericycle was also the first layer where the increase of concentration started slowing down; the peaks of these curves occurred in an interior to exterior order. Two sets of control simulations, slowing down the dynamics by decreasing all influx and efflux parameters (Fig. S5) and changing the cortical auxin distribution of the segment by varying the inward: outward ratio of the cortical PINs (Fig. S6), show that auxin accumulation from the inner layers is a robust feature of the model.

If we use auxin as a proxy for the induction of cell divisions, these results predict that the divisions would start from the interior layers and proceed outward. This would happen both when absolute auxin concentration controls divisions, and when the change in auxin concentration does it. So this model can explain the initial steps (stage I and II) of nodule primordium formation, although this does not address the later stages.

Divisions in pericycle and endodermis are arrested when a few layers are formed. In the *lin* mutant the arrest of division in these cell layers is delayed and this is correlated with the formation of vasculature in the central region of the nodules. As this vasculature is not well integrated

into nodule tissue derived from cortical cells, it underlines the importance of an early block of division in pericycle and endodermis.

In nodule primordia where rhizobia are not released central tissue cells (and their nuclei) remain small as in *ipd3* and *lin*. Therefore it is probable that induction of endoreduplication requires release of rhizobia from infection threads or vice versa.

Our nodule fate map underlines the impact of the multistep nature of nodule formation as well as the involvement of different root tissues in nodule formation. Similar processes can occur at different time points and in different cell types. A clear example is the release of rhizobia from infection threads in nodule primordium cells and in daughter cells of the meristem. In the latter case, NF-YA1 appeared to be essential for release, whereas release is not affected in primordium cells of the *nf-ya1-1* mutant. This shows that similar processes can be controlled by different mechanisms (or with different stringency) during subsequent steps of nodule development.

In conclusion we have shown that a nodule fate map is indispensable for identification of the affected developmental steps in nodulation mutants.

## **MATERIALS AND METHODS**

### **Plant materials and bacterial strains**

*M. truncatula* accession Jemalong A17 plants were used to study nodule primordium formation. This accession is also used to generate *Agrobacterium rhizogenes* (strain MSU440) mediated transgenic roots as previously described by Limpens et al. (2004). Another *M. truncatula* accession that is used is R108. This accession has roots with 5 or 4 cortical layers. In both root types nodule meristem is derived from C3. Root with 5 cortical cell layers the formation of primordia is similar as described for A17 in Fig.1. *M. truncatula* accession R108 seedlings were used to make the stable *AtCyclB1.1::GUS* (Bursens et al., 2000) transgenic line by using *Agrobacterium tumefaciens* (strain AGL1) and followed the protocol described by Chabaud et al. (2003). *MtCCS52A::GUS* is also introduced in R108 (Vinardell et al., 2003). The symbiotic mutants re-analyzed in this study were described previously, namely *nf-ya1-1* in Laporte et al.

## CHAPTER 3

(2014), *sickle* in Penmetsa and Cook (1997), *ipd3* in Ovchinnikova et al. (2011) and *lin1-1* in Kuppusamy et al. (2004). The surface-sterilization and germination of Medicago seeds were performed as previously described by Limpens et al. (2004). Roots of A17 were inoculated with *Sinorhizobium meliloti* (*S. meliloti*) strain 2011 and R108 with *S. meliloti* Rm41.

### Constructs

The *AtCASP1::GUS* construct is described in Roppolo et al. (2011). For *MtENOD40::GUS* and *AtSCR::GUS* constructs, DNA fragments of putative promoters were amplified from *M. truncatula* and *A. thaliana* genomic DNA respectively using primer combinations listed in Table S2 and *Phusion™ High-Fidelity DNA Polymerase* (Finnzymes). Then, the Gateway® technology (Invitrogen) was used to create genetic promoter-GUS constructs (Karimi et al., 2002). For *MtENOD40::GUS*, the pENTR™/D-TOPO® Cloning Kits (Invitrogen) was used to create entry clones. The entry vector was recombined into Gateway®-compatible binary vector pKGW-RR, that contains GUS reporter gene and *AtUBQ10::DsRED1* as a selection marker (Limpens et al., 2004), by using Gateway® LR Clonase® II enzyme mix (Invitrogen). For *AtSCR::GUS*, the *AtSCR* DNA fragment was introduced into Gateway® donor vector pENTR4-1, GUS reporter gene into pENTR1-2 and 35S CaMV terminator into pENTR2-3, using Gateway® BP Clonase® II enzyme mix. These entry vectors were recombined into Gateway®-compatible binary vector pKGW-RR-MGW, that contains *AtUBQ10::DsRED1* as a selection marker using Gateway® LR Clonase® II Plus enzyme mix (Invitrogen).

### Histochemical $\beta$ -glucuronidase (GUS) staining

Transgenic plant material (nodules and part of roots) containing GUS constructs were incubated in GUS buffer (3% sucrose, 2 mM  $K_3Fe(CN)_6$ , 2 mM  $K_4Fe(CN)_6$ , 10 mM EDTA, and 1 mg/ml X-Gluc salt in 100 mM phosphate buffer solution, pH 7.0) under vacuum for 30 min and then at 37 °C for 3 to 24 h (Jefferson et al., 1987).

### Tissue embedding, sectioning and section staining

Root segments and nodules were fixed at 4 °C overnight with 4%

paraformaldehyde (w/v), 5% glutaraldehyde (v/v) in 0.05 M sodium phosphate buffer (pH 7.2). The fixed material was dehydrated in an ethanol series and subsequently embedded in Technovit 7100 (Heraeus Kulzer) according to the manufacturer's protocol. Five  $\mu\text{m}$  thin longitudinal sections were made by using a RJ2035 microtome (Leica Microsystems, Rijswijk, The Netherlands), stained 5 min in 0.05% toluidine blue O. For GUS stained plant material 9-10  $\mu\text{m}$  thick longitudinal sections were stained for 15 min in 0.1% ruthenium red. Sections were analysed by using a DM5500B microscope equipped with a DFC425C camera (Leica Microsystems, Wetzlar, Germany).

### **Simulation methods**

We used our previously described simulation platform (Deinum et al., 2012) to simulate changes in auxin transport in root segments representing the susceptible zone of legume roots. Inside cells and within the apoplast, auxin moves by diffusion with diffusion constants  $300 \mu\text{m}^2 \text{s}^{-1}$  and  $44 \mu\text{m}^2 \text{s}^{-1}$ , respectively. Auxin transport over membranes is modeled using effective permeabilities. This results in an outward flux of  $J_{\text{mem}} = C_{\text{cell}} P_{\text{eff}} - C_{\text{wall}} P_{\text{inf}}$ , with negative values indicating a net inward flux. In this,  $C_{\text{cell}}$  and  $C_{\text{wall}}$  are the concentrations in the pixels on either side of the membrane,  $P_{\text{eff}}$  is the local effective efflux permeability, which starts at one of three levels ("high" =  $20 \mu\text{m s}^{-1}$ , "low" =  $5 \mu\text{m s}^{-1}$ , or "bg" (background level) =  $1 \mu\text{m s}^{-1}$  as shown in fig. 3B), and  $P_{\text{inf}} = 20 \mu\text{m s}^{-1}$  the effective influx permeability, as shown in figure 13A.

The PIN layout of these root segments is derived from the model of (Laskowski et al., 2008), which is based on their experimental observations in *Arabidopsis*, with cell sizes and number of cortical layers adapted to the *Medicago* geometry. Individual cells are  $100 \mu\text{m}$  long and  $20 \mu\text{m}$  (cortex) or  $10 \mu\text{m}$  (all others) wide.

In the middle of the segment we have indicated a five cell long block of cells, comprising epidermis to pericycle on one side of the root, which we call the "controlled area". At  $T = 0$  we reduce all  $P_{\text{eff}}$  parameters in the controlled area by a factor 10. Using larger factors did not affect the qualitative behaviour of the model, i.e., any of the effects described in the main text. It only resulted in larger absolute increases of the auxin

## CHAPTER 3

concentration and corresponding increases of the time to reach the new steady state concentration (not shown).

The full segments are 28 cells long to avoid boundary effects near the controlled area. For further details and references, see (Deinum et al., 2012). Because we focus on early events we used a smaller integration time step of 0.1 second.

### ACKNOWLEDGEMENTS

We thank Niko Geldner for providing the *AtCASP1* promoter GUS fusion vector; Dirk Inzé for the *AtCyc1B1.1* promoter GUS fusion vector; Thomas Ott for the *MtSYMREM* promoter GUS fusion vector. TB and SM are supported by ERC-2011-AdG-294790.

### REFERENCES

- Bond, L.** (1948). Origin and developmental morphology of root nodules of *Pisum Sativum*. *Bot Gaz* **109**, 411-434.
- Brewin, N. J.** (1991). Development of the legume root nodule. *Annu Rev Cell Biol* **7**, 191-226.
- Brewin, N. J.** (2004). Plant cell wall remodelling in the rhizobium-legume symbiosis. *Crit Rev Plant Sci* **23**, 293-316.
- Burssens, S., Himanen, K., Van de Cotte, B., Beeckman, T., Van Montagu, M., Inze, D. and Verbruggen, N.** (2000). Expression of cell cycle regulatory genes and morphological alterations in response to salt stress in *Arabidopsis thaliana*. *Planta* **211**, 632-640.
- Chabaud, M., De Carvalho-Niebel, F. and Barker, D. G.** (2003). Efficient transformation of *Medicago truncatula* cv Jemalong using the hypervirulent *Agrobacterium tumefaciens* strain AGL1. *Plant Cell* **22**, 46-51.
- Combier, J. P., Frugier, F., de Billy, F., Boualem, A., El-Yahyaoui, F., Moreau, S., Vernie, T., Ott, T., Gamas, P., Crespi, M. et al.** (2006). MtHAP2-1 is a key transcriptional regulator of symbiotic nodule development regulated by microRNA169 in *Medicago truncatula*. *Genes & Development* **20**, 3084-3088.
- Deinum, E. E., Geurts, R., Bisseling, T. and Mulder, B. M.** (2012). Modeling a cortical auxin maximum for nodulation: different signatures of potential strategies. *Front in Plant Science* **3**, 96.
- Dello Ioio, R., Nakamura, K., Moubayidin, L., Perilli, S., Taniguchi, M., Morita, M. T., Aoyama, T., Costantino, P. and Sabatini, S.** (2008). A genetic framework for the control of cell division and differentiation in the root meristem.

*Science* **322**, 1380-1384.

**den Camp, R. H. M. O., De Mita, S., Lillo, A., Cao, Q., Limpens, E., Bisseling, T. and Geurts, R.** (2011). A phylogenetic strategy based on a legume-specific whole genome duplication yields symbiotic cytokinin type-A response regulators. *Plant Physiol* **157**, 2013-2022.

**Di Laurenzio, L., Wysocka-Diller, J., Malamy, J. E., Pysh, L., Helariutta, Y., Freshour, G., Hahn, M. G., Feldmann, K. A. and Benfey, P. N.** (1996). The SCARECROW gene regulates an asymmetric cell division that is essential for generating the radial organization of the Arabidopsis root. *Cell* **86**, 423-433.

**Dudley, M. E., Jacobs, T. W. and Long, S. R.** (1987). Microscopic studies of cell divisions induced in alfalfa roots by *Rhizobium meliloti*. *Planta* **171**, 289-301.

**Goedhart, J., Hink, M. A., Visser, A. J. W. G., Bisseling, T. and Gadella, T. W. J., Jr.** (2000). *In vivo* fluorescence correlation microscopy (FCM) reveals accumulation and immobilization of Nod factors in root hair cell walls. *Plant Journal* **21**, 109-119.

**Guan, D., Stacey, N., Liu, C., Wen, J. Q., Mysore, K. S., Torres-Jerez, I., Vernie, T., Tadege, M., Zhou, C. N., Wang, Z. et al.** (2013). Rhizobial infection is associated with the development of peripheral vasculature in nodules of *Medicago truncatula*. *Plant Physiol* **162**, 107-115.

**Hadri, A. E., Spaink, H. P., Bisseling, T. and Brewin, N. J.** (1998). Diversity of root nodulation and rhizobial infection processes. In *The Rhizobiaceae*, (ed. H. P. Spaink A. Kondorosi and P. J. J. Hooykaas), pp. 347-359. Dordrecht, the Netherlands: Springer.

**Herrbach, V., Rembliere, C., Gough, C. and Bensmihen, S.** (2014). Lateral root formation and patterning in *Medicago truncatula*. *Journal of plant physiology* **171**, 301-310.

**Horvath, B., Yeun, L. H., Domonkos, A., Halasz, G., Gobbato, E., Ayaydin, F., Miro, K., Hirsch, S., Sun, J. H., Tadege, M. et al.** (2011). *Medicago truncatula* IPD3 Is a member of the common symbiotic signaling pathway required for rhizobial and mycorrhizal symbioses. *Molecular Plant Microbe Interactions* **24**, 1345-1358.

**Ivanov, S., Fedorova, E. E., Limpens, E., De Mita, S., Genre, A., Bonfante, P. and Bisseling, T.** (2012). *Rhizobium*-legume symbiosis shares an exocytotic pathway required for arbuscule formation. *Proceedings of the National Academy of Sciences of the United States of America* **109**, 8316-8321.

**Jefferson, R. A., Kavanagh, T. A. and Bevan, M. W.** (1987). Gus fusions: b-glucuronidase as a sensitive and versatile gene fusion marker in higher-plants. *The EMBO journal* **6**, 3901-3907.

**Karimi, M., Inze, D. and Depicker, A.** (2002). GATEWAY™ vectors for *Agrobacterium*-mediated plant transformation. *Trends in plant science* **7**, 193-195.

**Kiss, E., Olah, B., Kalo, P., Morales, M., Heckmann, A. B., Borbola, A., Lozsa, A., Kontar, K., Middleton, P., Downie, J. A. et al.** (2009). LIN, a novel type of U-Box/WD40 protein, controls early infection by rhizobia in legumes. *Plant Physiol* **151**, 1239-1249.

**Kuppusamy, K. T., Endre, G., Prabhu, R., Penmetsa, R. V., Veereshlingam,**

## CHAPTER 3

**H., Cook, D. R., Dickstein, R. and Van den Bosch, K. A.** (2004). LIN, a *Medicago truncatula* gene required for nodule differentiation and persistence of rhizobial infections. *Plant Physiol* **136**, 3682-3691.

**Lancelle, S. A. and Torrey, J. G.** (1985). Early development of *Rhizobium*-induced root nodules of *Parasponia rigida*. II. Nodule morphogenesis and symbiotic development. *Canadian Journal of Botany* **63**, 25-35.

**Laporte, P., Lepage, A., Fournier, J., Catrice, O., Moreau, S., Jardinaud, M. F., Mun, J. H., Larrainzar, E., Cook, D. R., Gamas, P. et al.** (2014). The CCAAT box-binding transcription factor NF-YA1 controls rhizobial infection. *Journal of experimental botany* **65**, 481-494.

**Laskowski, M., Grieneisen, V. A., Hofhuis, H., Hove, C. A. t., Hogeweg, P., Maree, A. F. M. and Scheres, B.** (2008). Root system architecture from coupling cell shape to auxin transport. *PLoS Biology* **6**.

**Lefebvre, B., Timmers, T., Mbengue, M., Moreau, S., Herve, C., Toth, K., Bittencourt-Silvestre, J., Klaus, D., Deslandes, L., Godiard, L. et al.** (2010). A remorin protein interacts with symbiotic receptors and regulates bacterial infection. *Proceedings of the National Academy of Sciences of the United States of America* **107**, 2343-2348.

**Lerouge, P., Roche, P., Faucher, C., Maillet, F., Truchet, G., Prome, J. C. and Denarie, J.** (1990). Symbiotic host-specificity of *Rhizobium meliloti* is determined by a sulphated and acylated glucosamine oligosaccharide signal. *Nature* **344**, 781-784.

**Libbenga, K. R. and Harkes, P. A. A.** (1973). Initial proliferation of cortical cells in the formation of root nodules in *Pisum sativum* L. *Planta* **114**, 17-28.

**Limpens, E., Ramos, J., Franken, C., Raz, V., Compaan, B., Franssen, H., Bisseling, T. and Geurts, R.** (2004). RNA interference in *Agrobacterium rhizogenes*-transformed roots of *Arabidopsis* and *Medicago truncatula*. *Journal of experimental botany* **55**, 983-992.

**Marhavy, P., Bielach, A., Abas, L., Abuzeineh, A., Duclercq, J., Tanaka, H., Parezova, M., Petrasek, J., Friml, J., Kleine-Vehn, J. et al.** (2011). Cytokinin modulates endocytic trafficking of PIN1 auxin efflux carrier to control plant organogenesis. *Developmental cell* **21**, 796-804.

**Mathesius, U., Bayliss, C., Weinman, J. J., Schlaman, H. R. M., Spaink, H. P., Rolfe, B. G., McCully, M. E. and Djordjevic, M. A.** (1998). Flavonoids synthesized in cortical cells during nodule initiation are early developmental markers in white clover. *Molecular Plant Microbe Interactions* **11**, 1223-1232.

**Middleton, A. M., King, J. R., Bennett, M. J. and Owen, M. R.** (2010). Mathematical modelling of the Aux/IAA negative feedback loop. *Bulletin of mathematical biology* **72**, 1383-1407.

**Nap, J. P. and Bisseling, T.** (1990). Developmental biology of a plant-prokaryote symbiosis: the legume root nodule. *Science* **250**, 948-954.

**Nutman, P. S.** (1948). Physiological studies on nodule formation.1. The relation between nodulation and lateral root formation in red clover. *Ann Bot-London* **12**, 81-96.

**Ovchinnikova, E., Journet, E. P., Chabaud, M., Cosson, V., Ratet, P., Duc, G., Fedorova, E., Liu, W., Op den Camp, R., Zhukov, V. et al.** (2011). IPD3 controls the formation of nitrogen-fixing symbiosomes in pea and *Medicago* spp. *Molecular Plant Microbe Interactions* **24**, 1333-1344.

**Penmetsa, R. V. and Cook, D. R.** (1997). A legume ethylene-insensitive mutant hyperinfected by its rhizobial symbiont. *Science* **275**, 527-530.

**Roppolo, D., De Rybel, B., Tendon, V. D., Pfister, A., Alassimone, J., Vermeer, J. E., Yamazaki, M., Stierhof, Y. D., Beeckman, T. and Geldner, N.** (2011). A novel protein family mediates Casparian strip formation in the endodermis. *Nature* **473**, 380-383.

**Roth, L. E. and Stacey, G.** (1989). Bacterium release into host cells of nitrogen-fixing soybean nodules the symbiosome membrane comes from three sources. *European Journal of Cell Biology* **49**, 13-23.

**Singh, S., Katzer, K., Lambert, J., Cerri, M. and Parniske, M.** (2014). CYCLOPS, a DNA-binding transcriptional activator, orchestrates symbiotic root nodule development. *Cell host & microbe* **15**, 139-152.

**Sugimoto, K., Gordon, S. P. and Meyerowitz, E. M.** (2011). Regeneration in plants and animals: dedifferentiation, transdifferentiation, or just differentiation? *Trends in Cell Biololgy* **21**, 212-218.

**Timmers, A. C. J., Auriac, M. C. and Truchet, G.** (1999). Refined analysis of early symbiotic steps of the *Rhizobium-Medicago* interaction in relationship with microtubular cytoskeleton rearrangements. *Development* **126**, 3617-3628.

**Van de Wiel, C., Norris, J. H., Bochenek, B., Dickstein, R., Bisseling, T. and Hirsch, A. M.** (1990). Nodulin gene-expression and Enod2 localization in effective, nitrogen-fixing and ineffective, bacteria-free nodules of alfalfa. *Plant Cell* **2**, 1009-1017.

**Vermeer, J. E. M., Von Wangenheim, D., Barberon, M., Lee, Y., Stelzer, E. H. K., Maizel, A. and Geldner, N.** (2014). A spatial accommodation by neighboring cells is required for organ initiation in *Arabidopsis*. *Science* **343**, 178-183.

**Vinardell, J. M., Fedorova, E., Cebolla, A., Kevei, Z., Horvath, G., Kelemen, Z., Tarayre, S., Roudier, F., Mergaert, P., Kondorosi, A. et al.** (2003). Endoreduplication mediated by the anaphase-promoting complex activator CCS52A is required for symbiotic cell differentiation in *Medicago truncatula* nodules. *Plant Cell* **15**, 2093-2105.

**Yang, W. C., Deblank, C., Meskiene, I., Hirt, H., Bakker, J., Vankammen, A., Franssen, H. and Bisseling, T.** (1994). *Rhizobium* Nod factors reactivate the cell-cycle during infection and nodule primordium formation, but the cycle is only completed in primordium formation. *Plant Cell* **6**, 1415-1426.

# CHAPTER 3

## SUPPLEMENTARY FIGURES AND TABLE

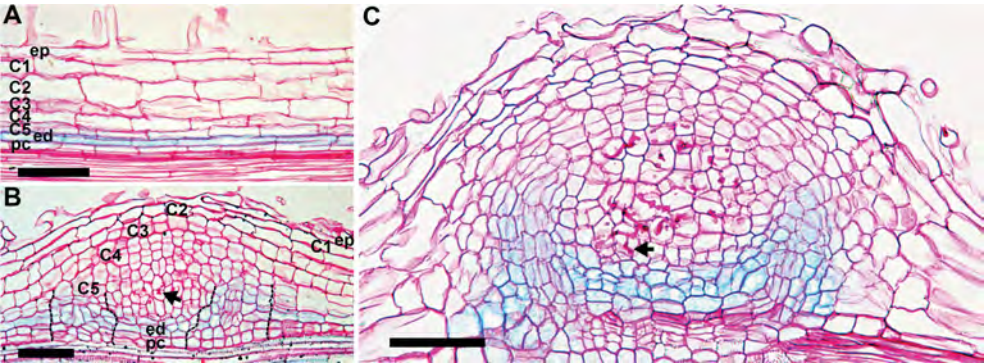


Fig. S1. *AtSCR::GUS* is expressed in endodermis (A) and cells derived from endodermis (B) and these cells are not infected by rhizobium (B-C). Infection threads are indicated by arrows.

In B, cells at the periphery region (indicated in between black lines) will differentiate into nodule parenchyma include vascular bundles and endodermis.

Bars, 75  $\mu$ m.

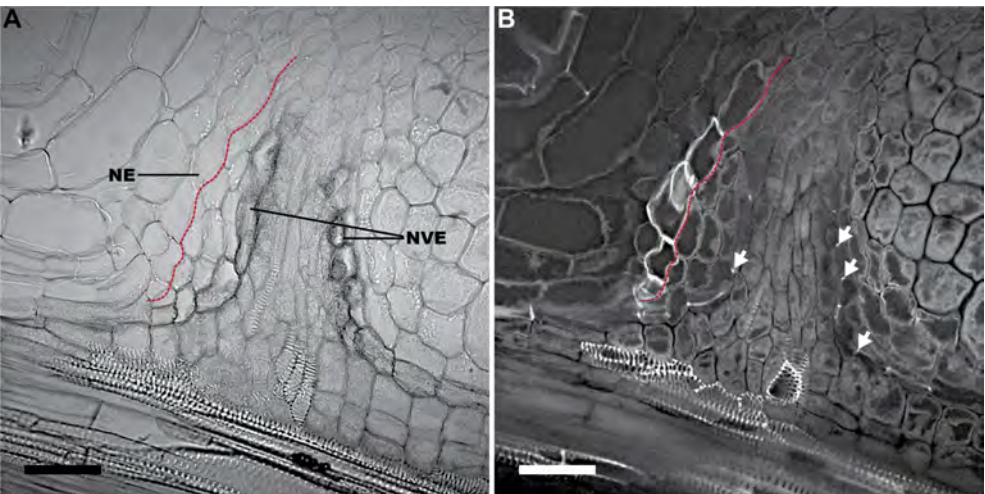


Fig. S2. Casparian strips are present in cells where *AtCASP1::GUS* is expressed.

Split channels of Fig. 5D. (A) *AtCASP1::GUS* is expressed in NVE but not in NE; (B) Casparian strips (arrows) are present in NVE but not in NE.

Bars, 50  $\mu$ m.

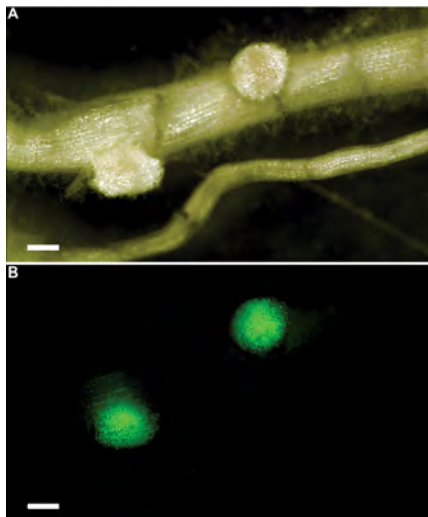


Fig. S3. *S. meliloti* strain 2011 expresses *nifH::GFP* in *nf-ya1-1* nodules. Bars, 250  $\mu$ m.

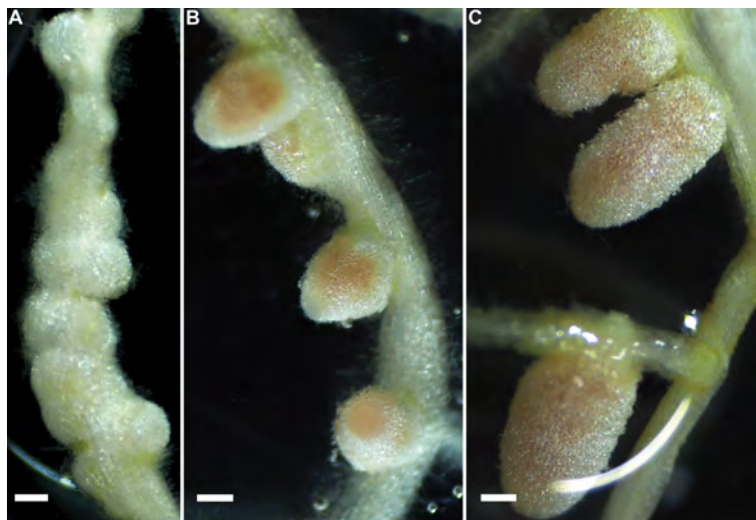


Fig. S4. Three weeks old *sickle* nodules (A-B) in comparison to wt nodules (C). (A) Nodules formed at the "sickle" shaped zone. (B) Small pink nodules. Bars, 250  $\mu$ m.

## CHAPTER 3

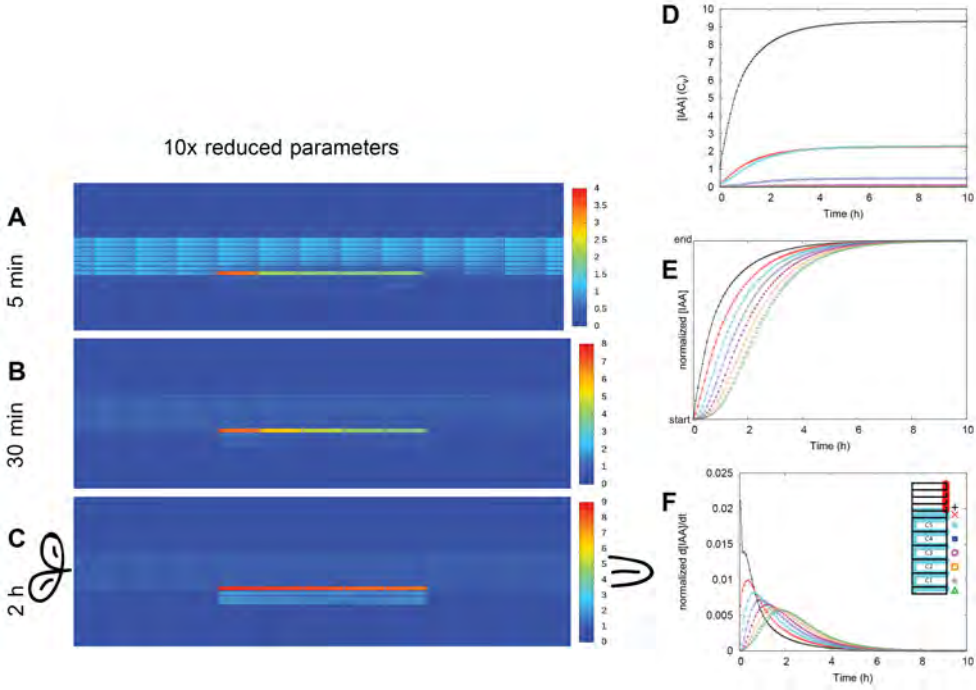


Fig. S5. Also with slowed down auxin dynamics, auxin accumulation following a local 10x reduction of the effective efflux permeability starts from the inner root layers. The starting concentration of PINs in each membrane segment is one of three levels: “high” (red,  $P_{eff} = 2 \mu\text{m s}^{-1}$ ), “low” (cyan,  $P_{eff} = 0.5 \mu\text{m s}^{-1}$ ), or “bg” (white,  $P_{eff} = 0.1 \mu\text{m s}^{-1}$ ) (Deinum et. al, 2012). (A-C) Concentration heat maps of the part of the root segment including the controlled area at  $T = 5$  min (A),  $T = 30$  min (B) and  $T = 2$  h (C). (D) The concentration in the middle row of cells is tracked for all cell files in the controlled area. The concentration in the pericycle remains highest, followed by endodermis and inner cortex (C5). (E) When rescaling the concentration in each file from its starting level to the level reached at the end of the simulation ( $T = 20$  h), it becomes clear that the concentration in the pericycle increased first, followed by the other layers in an interior to exterior order. The moment of fastest concentration increase, the peaks of the curves in F (time derivative of E, expressed in rescaled concentration units per minute), showed the same relative order.

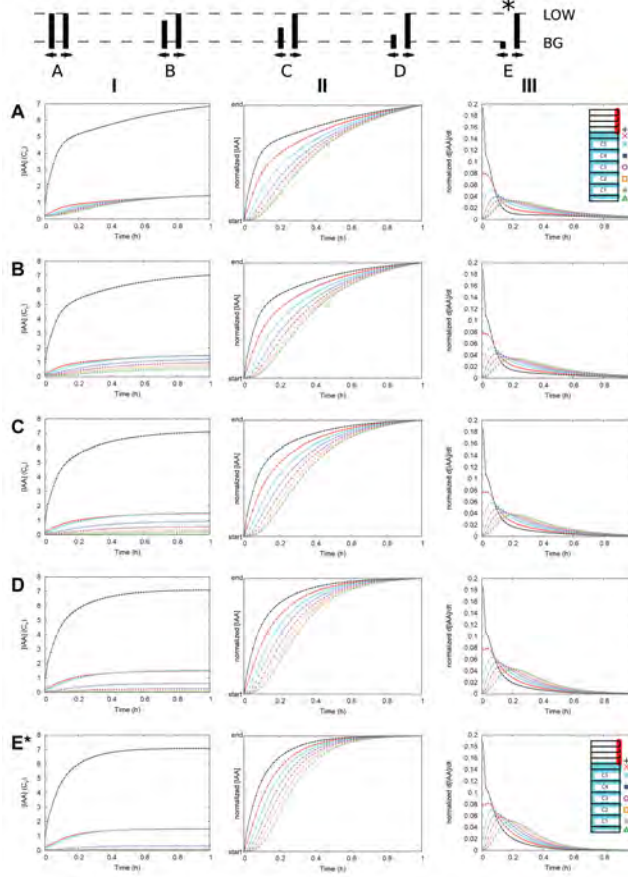


Fig. S6. Auxin accumulation always starts from the interior layers, regardless of inward: outward PIN bias in the cortex.

The amount of PIN ( $P_{eff}$ ) before efflux reduction in the abaxial membrane of the cortical cells decreases from A, with  $P_{eff} = 5 \mu\text{m s}^{-1}$  ("low") for abaxial and adaxial cell faces, to E, with  $P_{eff} = 1 \mu\text{m s}^{-1}$  ("bg") for the abaxial cell face. This is illustrated in the cartoon on top. The root from Fig. 13, E in this figure, is marked with an asterisk (\*). The full PIN distribution pattern is illustrated for A and E similar to Fig. 13B. This also shows the markers for the different cell layers. I: Concentration in the controlled area from the moment of efflux reduction (c.f. Fig. 13F). II: Concentration, rescaled from the initial value to the concentration at the end of the simulation ( $T = 1 \text{ h}$ ; c.f. Fig. 13G). III: Concentration change. This is the time derivative of II, expressed in rescaled concentration units per minute (c.f. Fig. 13H). In all cases (A-E) the same relative order occurs: the first, strongest and fastest increase occurs in the pericycle, followed by endodermis, C5, etc. towards outer layers. The stronger the inward bias of the cortical PINs, the lower the steady state concentrations reached in the exterior root layers epidermis and outer cortex. It is likely that with a strong inward bias, i.e., towards the bottom of the figure, the maximum concentration reached in the outer cortex is insufficient to trigger a cell division response.

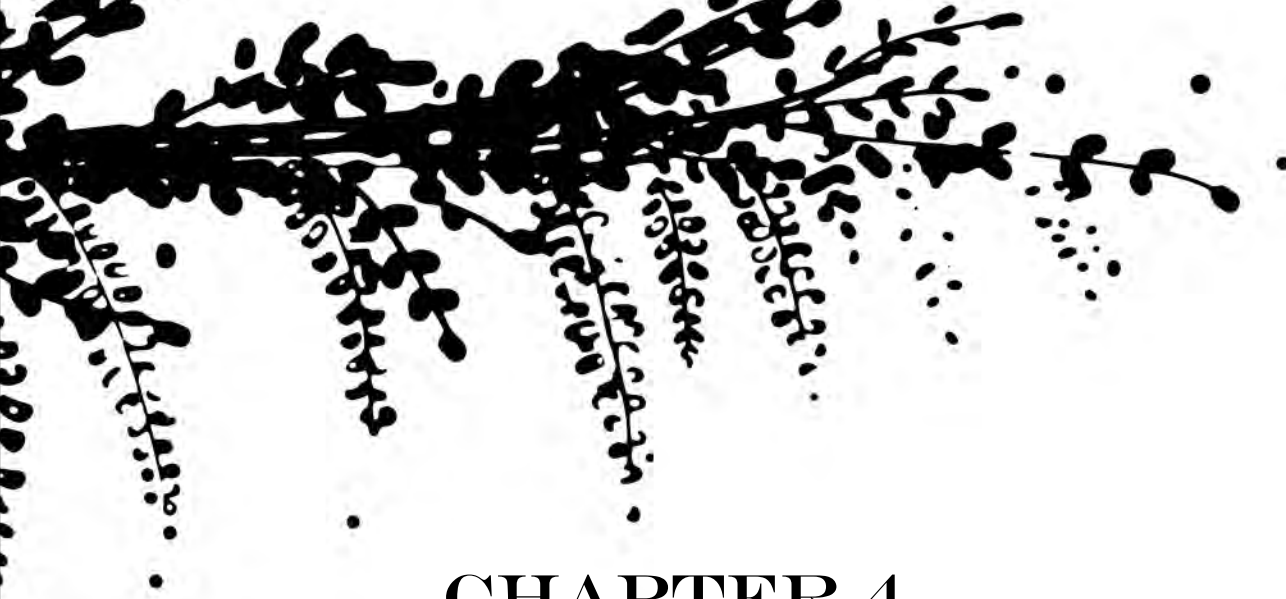
# CHAPTER 3

Table S1. List of primers used for *MtENOD40* and *AtSCR* promoter amplification.

Gene name	Corresponding gene locus	Primer name	Primer sequence (5'-3')
<i>MtENOD40</i>	AJ388939.1	pMtENOD40-F	cacctaaattgtcagtctcgtaaaatagc
		pMtENOD40-R	tctctgatcattgttttaaatacttg
<i>AtSCARECROW</i>	At3g54210	pAtSCR-F	gaacacgtcgtccgtgtctc
		pAtSCR-R	gtaagaaaagggttaaataccaaaatcg







## CHAPTER 4

### *MtPINs play a role in maintaining the auxin accumulation pattern during nodule development*

**Ting Ting Xiao<sup>1</sup>, Henk Franssen<sup>1</sup>, Rene Geurts<sup>1</sup>, Robin van Velzen<sup>1</sup>, Rujin Chen<sup>2</sup> and Ton Bisseling<sup>1,3,4</sup>**

<sup>1</sup> Department of Plant Sciences, Laboratory of Molecular Biology, Wageningen University, Droevendaalsesteeg 1, 6708 PB, Wageningen, The Netherlands.

<sup>2</sup> Plant Biology Division, The Samuel Roberts Noble Foundation, Ardmore, Oklahoma 73401, USA

<sup>3</sup> College of Science, King Saud University, Post Office Box 2455, Riyadh 11451, Saudi Arabia.

<sup>4</sup> To whom correspondence should be addressed: [ton.bisseling@wur.nl](mailto:ton.bisseling@wur.nl)

Manuscript in preparation

## CHAPTER 4

### SUMMARY

Legumes can establish a symbiosis with rhizobium by forming a novel plant organ, the root nodule. There are indications that auxin is involved in nodule organogenesis. Some studies showed that auxin accumulates during nodulation by using reporter constructs. However, how this auxin landscape is created is not known. In this chapter, we studied how the auxin accumulation pattern is created and maintained during nodulation by analysing the expression and accumulation of auxin efflux carriers, PIN proteins. We first analysed the auxin accumulation pattern during subsequent nodule primordium developmental stages by using *DR5::GUS* as reporter system. This showed that auxin accumulation associates with mitotic activity within the primordium. Further, we tested whether the accumulation of auxin during nodulation is induced by a local reduction of PIN activity. However, this was hampered due to the low level of PIN proteins present in the susceptible zone of the root. It is still possible that auxin accumulation is initiated by a decrease of PIN levels. However, *MtPIN2* and *MtPIN10* proteins accumulate in cells that will form a primordium prior cell division. At initial stages (I-III) these *MtPINs* accumulate in all primordium cells. At later stages (IV-VI), *MtPIN10* mainly accumulates at the nodule periphery and *MtPIN2* mainly at the future meristem (C3 derived cells). Further, a *Mtpin10-1* mutant forms nodule primordia with more cell layers. Based on these observations we conclude that *MtPINs* play a role in the accumulation of auxin in primordia at early stages and the formation of an auxin maximum in the nodule meristem at later stages (IV-VI).

**Keywords:** Medicago, root nodule, nodule primordium, auxin, DR5, *MtPIN*

## INTRODUCTION

Rhizobium can establish a symbiotic relationship with legume plants and this leads to the formation of root nodules. This involves the mitotic reactivation of cortex, endodermis and pericycle cells, by which a nodule primordium is formed (Xiao et al., 2014). Within these primordia an increased auxin response occurs (Mathesius et al., 1998; Huo et al., 2006; Suzaki et al., 2012; Turner et al., 2013). It has been hypothesised that this is caused by a local increase in auxin levels, which is triggered by a local reduction of auxin efflux (Deinum et al., 2012). In a theoretical model this is the most efficient way to increase the auxin levels in cells that form the nodule primordium. However, this hypothesis remains to be tested experimentally. To test this, we characterized the *Medicago truncatula* (Medicago) auxin efflux carriers (*MtPINs*) and determined during nodule primordium formation, the dynamics of *MtPIN* expression as well as their subcellular localization. Further, the importance of *MtPINs* was studied in a loss of function mutant of one abundantly expressed *MtPIN* gene.

On the roots of legume plants, soil-borne bacteria, collectively known as rhizobium are able to induce the formation of organised structures, called root nodules. Rhizobia become hosted herein and provide ammonia to the plant. In return the host provides rhizobium with sugars and other nutrients. Nodule formation is initiated by lipo-oligosaccharides, called Nod factors, secreted by rhizobia. These signal molecules are also required for rhizobial infection. Rhizobia penetrate the root via root hairs, where tubular structures called infection threads are formed. Concomitantly, differentiated root cells are mitotically activated in an organised manner by which the nodule primordium is formed (Xiao et al., 2014). The infection thread that contains rhizobia, grows towards the primordium and there bacteria are released into the host cells. During this process bacteria become surrounded by a host-derived membrane and in this way transient organelles, designated symbiosomes, are formed (Roth and Stacey, 1989). In the primordium a meristem is formed by which facilitates further growth of the nodule. In general, two types of nodules can be distinguished based on the lifespan of the meristem, determinate and indeterminate nodules. In determinate nodules (e.g. Lotus) the meristem is active for a short time, while in indeterminate nodules (e.g. Medicago) a persistent meristem is formed.

## CHAPTER 4

Medicago is the model legume to study indeterminate nodule development. A detailed Medicago nodule fate map has recently been made (Xiao et al., 2014). It describes how cells of the cortical cell layers, endodermis and pericycle contribute to the development of a nodule. We hypothesise that an increased auxin response during primordium formation correlates with mitotic activity. Therefore, we will summarize the fate map and focus on where and when cell division occurs during the 6 stages of primordium development. Cell division starts in pericycle cells (stage I) and immediately extends to (inner) cortical cell layers 4 and 5 (C4/5) (stage II). From stage III until stage IV cell division is maintained in C4/5 and this leads to 6-8 cells layers. Further, C3 and endodermis also divide but with a lower frequency. At stage V, cell division continues in C3 (meristem), whereas division stops in the cells derived of pericycle, endodermis, C4/5 that are located in the central part of the primordium. At the periphery of the primordium some groups of cells continue with a few additional anticlinal divisions (from Stage IV) and will develop into nodule vascular bundles.

In both determinate and indeterminate nodule formation, auxin responsive promoter activity suggests that auxin accumulates during nodule formation (Mathesius et al., 1998; Huo et al., 2006; Suzaki et al., 2012; Turner et al., 2013). Most studies have made use of the auxin responsive promoter *DR5* (Huo et al., 2006; Suzaki et al., 2012; Turner et al., 2013) or *GH3* (Mathesius et al., 1998). For determinate nodule development detailed *DR5* expression patterns have been obtained in Lotus (Suzaki et al., 2012) and Soybean (Turner et al., 2013). In the case of Lotus nodule development, the *DR5* promoter is first activated in the cells that divide, which are the outer cortical cells, and also at later stages *DR5* expression seems to correlate (more or less) with mitotic activity (Suzaki et al., 2012). During indeterminate nodule primordium development auxin response promoter activity has also been shown to be increased (Mathesius et al., 1998; Huo et al., 2006). However, whether it correlates with mitotic activity at all stages of development, has not been studied. The detailed fate map for Medicago nodule development allows us to study this.

Genetic studies on model legumes have revealed a group of genes that are important for Nod factor perception and the signalling pathway that

is activated. This includes 2 LysM receptor-like kinases (NFR1 /NFR5 in lotus, and NFP/ LYK3 in Medicago) located at the plasma membrane (Ben Amor et al., 2003; Radutoiu et al., 2003; Arrighi et al., 2007; Smit et al., 2007); a plasma membrane located LRR-type receptor kinase (SYMRK or DMI2), a nuclear envelop localized ion channel (CASTOR and POLLUX or DMI1) that is essential for the induction of calcium spiking (Endre et al., 2002; Bersoult et al., 2005; Imaizumi-Anraku et al., 2005; Limpens et al., 2005; Charpentier et al., 2008); a calcium and calmodulin-dependent kinase (CCaMK or DMI3) to recognize the oscillating calcium signal (Levy et al., 2004; Mitra et al., 2004) and to activate a transcriptional regulator (CYCLOPS or IPD3) (Yano et al., 2008; Horvath et al., 2011; Ovchinnikova et al., 2011; Singh et al., 2014). Downstream of CCaMK/CYCLOPS, several other transcription factors are active. This includes two GRAS type transcription regulators (NSP1 and NSP2) (Kalo et al., 2005; Smit et al., 2005); an ethylene response factor (ERN1) (Andrianakaja et al., 2007) and nodule inception (NIN) (Marsh et al., 2007). These transcription factors are involved in nodule organogenesis as well as infection. Further, Nod factor signalling induced nodule organogenesis requires a specific cytokinin receptor, CRE1 (Murray et al., 2007; Plet et al., 2011). This indicates that Nod factor induced cytokinin signaling is essential for nodule organogenesis.

The importance of cytokinin signalling in nodule organogenesis seems contradictory to the involvement of auxin. Recently, they were theoretically brought together by a computer simulation, which proposed that Nod factor induced cytokinin signalling triggers local reduction of the level of auxin efflux proteins (PINs). PINs are generally polar localized in cells and export auxin directionally (Benkova et al., 2003; Vieten et al., 2005; Petrasek et al., 2006; Wisniewska et al., 2006; Vieten et al., 2007; Krecek et al., 2009; Peret et al., 2013). This model showed that in this way a local auxin maximum is formed that could initiate primordium formation (Deinum et al., 2012).

In this study, we shows that during Medicago nodule primordium development mitotic activity and high auxin response strictly correlate. At a very early stage the expression level of *MtPINs* is transiently decreased preceding the first mitotic activity. Subsequently, *MtPIN2* and *MtPIN10* were shown to be induced during all stages of primordium formation.

## CHAPTER 4

Their function is studied by determining their subcellular location and the effect of a loss of function mutation in *MtPIN10*.

### RESULTS

#### **Auxin accumulation coincides with cell divisions during root nodule primordium formation**

To determine the dynamics of auxin accumulation during different stages of nodule primordium development, we used a transgenic *Medicago* line containing the auxin-response promoter *DR5* fused to *GUS* gene ( $\beta$ -glucuronidase). After inoculation with *Sinorhizobium meliloti* 2011, roots were harvested at different time points and sectioned (Fig. 1). At stage I (Fig. 1A), *DR5* is expressed in the dividing pericycle cells and it is also active in not yet dividing cells of endodermis and cortex. At stage II (Fig. 1B) *DR5* expression is maintained in these inner layers and has extended to outer layers. At stage III and IV (Fig. 1C, D), *DR5* expression is high in C4/5 derived cells. Although cell division has started in C3, the GUS signal is lower than in the C4/5 derived cells. This might be because C3 cells still contain relatively large vacuoles, whereas the C4/5 derived cells are more cytoplasmic rich. *DR5* expression starts to reduce in pericycle and endodermis, which correlates with decreased cell division at those stage. At stage V and VI (Fig. 1E, G), *DR5* is highly expressed in the (future) meristem (C3 derived cells). During stage V the expression level in the C4/5 derived cells of the central part of the primordium markedly decreases and at stage VI it is no longer detectable (Fig. 1G). In young (non-dividing) infected cells directly adjacent to the meristem some GUS protein is present. This might be due to the relatively stable nature of GUS. Further, at the periphery vascular bundles start to be formed and in these dividing cells *DR5::GUS* is (weakly) expressed. So, mitotic activity in primordia and young nodules correlates with *DR5* expression, whereas endoreduplication in the C4/5 derived cells does not.

#### **Characterization of the *Medicago PIN* family**

Our theoretical model indicated that auxin accumulation in the nodule primordium can be triggered by a local reduction of the PIN proteins (Deinum et al., 2012). To be able to test this model, we identified all *Medicago* homologs in the *Mt4.0* genome database by reciprocal BLAST

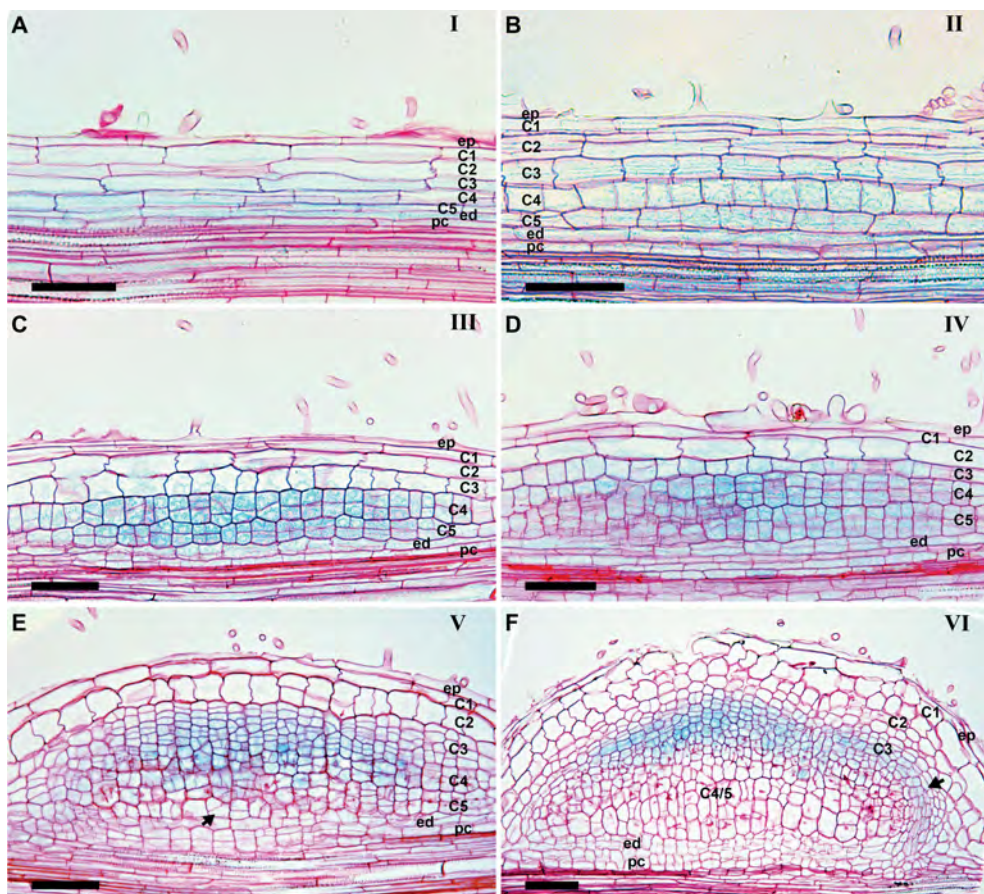


Fig. 1. *DR5::GUS* expression in different root nodule development stages.

(A) Stage I, *DR5* is expressed in the dividing pericycle cells and not yet dividing endodermis and inner cortex (C5 and C4) cells. (B) Stage II, *DR5* is expressed in pericycle, endodermis and all cortical cell layers. (C-D) Stage III-IV, *DR5* expression is high in C4/5 derived cells and it is also expressed in C3 (and outer cortex). (E) Stage V, *DR5* is highest expressed in the (future) meristem (C3 derived cells) and expression level in the pericycle, endodermis and C4/5 derived cells markedly decreases (arrow). (F) Stage VI, *DR5* is highly expressed in nodule meristem and (non-dividing) infected cells directly adjacent to the meristem. It is also weakly expressed in the developing nodule vascular tissue.

ep, epidermis; C1, 1st cortical cell layer; C2, 2nd cortical cell layer; C3, 3rd cortical cell layer; C4, 4th cortical cell layer; C5, 5th cortical cell layer; ed, endodermis; pc, pericycle

Bar equal to 75  $\mu$ m.

## CHAPTER 4

using the Arabidopsis *PIN* genes. In this way we identified 12 putative *PIN* genes in the Medicago genome. Two of these have not been reported previously, and were named *MtPIN11* (Mt6G011400) and *MtPIN12* (Mt2G038470) (Table 1).

Table 1 Arabidopsis *PIN*s and Medicago *PIN*s in different groups from phylogeny analysis

Group number	Arabidopsis <i>PIN</i> s ( <i>AtPIN</i> s)	<i>AtPIN</i> s gene ID	Medicago <i>PIN</i> s ( <i>MtPIN</i> s)	<i>MtPIN</i> s gene ID
Group 3A And Group 3B	<i>AtPIN8</i> and <i>AtPIN5</i>	At5G15100 and At5G16530	<i>MtPIN8</i> <i>MtPIN11</i> and <i>MtPIN9</i>	Mt7G009370 Mt6G011400 and Mt7G079720
Group 4	<i>AtPIN2</i>	At5G57090	<i>MtPIN2</i> <i>MtPIN7</i> <i>MtPIN12</i>	Mt4G127100 Mt4G127090 Mt2G038470
Group 5	<i>AtPIN1</i>	At1G73590	<i>MtPIN4</i> <i>MtPIN5</i>	Mt6G069510 Mt8G107360
Group 6	--	--	<i>MtPIN10</i>	Mt7G089360
Group 7	<i>AtPIN3</i> <i>AtPIN4</i> <i>AtPIN7</i>	At1G70940 At2G01420 At1G23080	<i>MtPIN1</i> <i>MtPIN3</i>	Mt4G084870 Mt1G030890
Group 8	<i>AtPIN6</i>	At1G77110	<i>MtPIN6</i>	Mt1G029190

The phylogeny of *PIN* genes is studied intensively in higher plants, showing a conserved topology with 6 groups in higher plants (Krecek et al., 2009). *PIN*s can be divided into two major subclasses according to phylogenetic and functional analyses; the endoplasmic reticulum localized PIN5-type (groups 3 and 8; short *PIN*s) and the plasma membrane localized PIN1-type (groups 4 to 7; long *PIN*s).

To establish the relation of Medicago *PIN*s to known *PIN* genes a phylogenetic tree was reconstructed involving *PIN* genes of 29 species representing all major plant lineages (Fig. S1). The Medicago *PIN* genes all belong to the previously identified 6 groups. In comparison to non-legumes *MtPIN*s in group 3 (subgroup 3A), group 4, group 5 and group 7

have been duplicated. These duplications are conserved in other legume species, suggesting a common origin. The newly identified *MtPIN11* is a short *PIN* belonging to subgroup 3A (Fig. S1G), whereas *MtPIN12* is a long *PIN* that groups to group 4 (Fig. S1C). Furthermore, the group 4 genes *MtPIN2* and *MtPIN7* originated from a recent duplication in the *Medicago* lineage. All *Medicago PIN* genes have an orthologue in *Arabidopsis*, with the exception of *MtPIN10* (group 6; Fig. S1B). This gene is also not present in other *Brassicaceae* species.

In this study we focused on the plasma membrane located *PIN*s (*PIN1*-type). These belong to group 4 to 7, and include *MtPIN1*, 2, 3, 4, 5, 7, 10 and 12.

### **Nod factor signalling transiently represses *MtPIN* expression and subsequently induces *MtPIN2* expression**

Rhizobium can only mitotically activate root cells in a specific zone. This is the susceptible zone, which is the region where root hairs emerge and grow. Therefore, we tested by qRT-PCR which *PIN1*-type genes are expressed in this zone using RNA from the susceptible zone as template. This showed that *MtPIN1*, 2, 3, 4 and 10 are expressed in this zone, whereas the expression of *MtPIN5*, 7, and 12 is very low (Fig. S2). Therefore, we further only studied *MtPIN1*, 2, 3, 4 and 10.

To determine the spatial expression pattern of these *MtPIN*s in *Medicago* root, about 2.5 Kbp upstream of the coding region of a *MtPIN* gene was

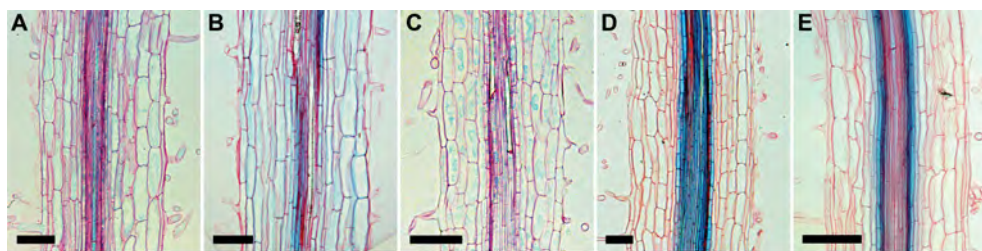


Fig. 2. *MtPIN* promoter derived GUS expression in *Medicago* roots. Longitudinal sections of the root susceptible zone of *MtPIN1::GUS*, *MtPIN2::GUS*, *MtPIN3::GUS*, *MtPIN4::GUS* or *MtPIN10::GUS* expressing roots. (A-C) *MtPIN1*, 2, and 3 are expressed in the cortex and epidermis; (D) *MtPIN4* is expressed in all vascular tissues; (E) *MtPIN10* is expressed in the pericycle. Bar equals to 75  $\mu$ m.

## CHAPTER 4

used to drive the expression of *GUS*. *Agrobacterium rhizogenes* mediated transformation was used to generate transgenic roots. Sections of these roots showed that these 5 *MtPINs* are expressed at a markedly higher level in the meristem than in the susceptible zone (Fig. 2). In the susceptible zone *MtPIN1*, 2, and 3 (Fig. 2A-C) are expressed in the cortex and epidermis; *MtPIN4* (Fig. 2D) is expressed in all vascular tissues and *MtPIN10* (Fig. 2E) is expressed in the pericycle. The expression patterns are described in more detail in Fig. S3.

To test whether auxin accumulation involves a reduction of PIN levels during nodule primordium formation, we first determined whether *MtPIN* expression level is reduced. Our *DR5::GUS* expression studies (Fig. 1) indicated that during nodule primordium formation auxin accumulation precedes cell division. Therefore, we studied *MtPINs* expression during the first 3 hours after Nod factor application by qRT-PCR (Fig. 3). This showed that the expression of *MtPIN1*, 2, 3, 4 and 10 are all reduced at least 2 fold, within 1 h after Nod factor application. However, the expression level soon increased after this reduction. At 3 h after Nod factor treatment *MtPINs* expression levels were similar to control or higher. Especially, *MtPIN2* shows more than 3 fold increase compared to control.

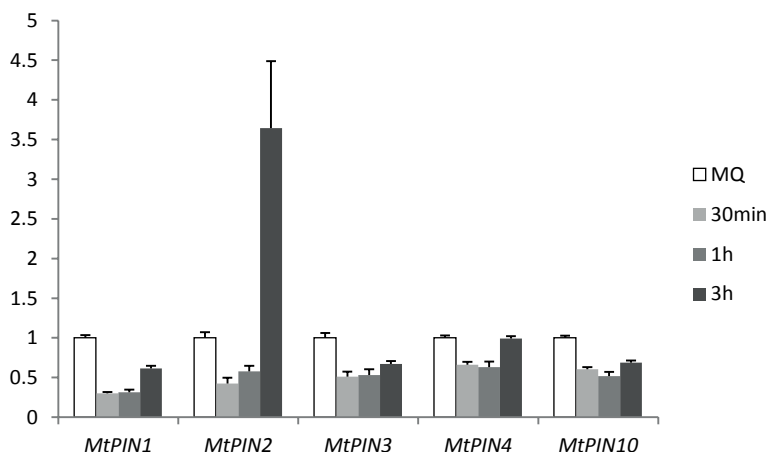


Fig. 3. *MtPIN* expression transiently decreased upon Nod factor treatment. Real time qRT-PCR of *MtPIN1*, 2, 3, 4 and 10 expression at the root susceptible zone treated with *S. meliloti* Nod factor for 30 min, 1 hour, 3 hours and water (MQ) inoculated control.

Data are means  $\pm$  SD.

So, *MtPINs* expression is reduced shortly after Nod factor application, which is consistent with the model. However, markedly before the first divisions have occurred (24 h) the expression of *MtPINs* is up-regulated. This transiently reduced expression happens in a too short time window to visualise it in transgenic roots expressing a *MtPIN::GUS* construct (data not shown). Further, the expression level of the *MtPIN* genes in the susceptible zone, turned out to be too low to visualise the *MtPIN* proteins in a reproducible quantitative manner (see below). However, the increased expression of *MtPIN* genes (after their transiently reduced expression), allowed studies on *MtPINs* during nodule primordium formation.

### ***MtPIN* expression is enhanced during nodule primordium formation**

We determined the spatial expression pattern of *MtPIN1*, *MtPIN2*, *MtPIN3*, *MtPIN4*, and *MtPIN10* during nodule primordium formation, by using transgenic roots containing the *MtPIN::GUS* fusion constructs.

These roots were spot inoculated with *S. meliloti* and root fragments were harvested 1-3 days post inoculation (dpi). Longitudinal sections show that especially *MtPIN2* and *MtPIN10* are highly induced in primordia, whereas the expression of the other 3 *MtPIN* genes is hardly affected (Fig. 4 and Fig. S4). *MtPIN1* (Fig. 4A, B), is expressed at a similar level in nodule primordia as in surrounding non dividing cortical cells, whereas *MtPIN3* (Fig. 4C, D) expression is reduced. *MtPIN4* (Fig. 4E, F) remains active in the endodermis and pericycle derived cells. *MtPIN2* and *MtPIN10* are both induced in the dividing nodule primordium cells (Fig. 4G-L). In the primordium, their expression co-localizes up to stage IV (Fig. 4G, J and Fig. 4H, K). In addition *MtPIN2* is also expressed in the epidermis and some non-dividing outer cortical cells through which the infection thread has passed (Fig. 4G). At stage IV, *MtPIN2* (Fig. 4H) and *MtPIN10* expression is reduced in the centre of the primordia, where cells are infected by infection thread. At stage V-VI, *MtPIN2* (Fig. 4I) is mainly expressed in the nodule meristem and outer cortex cells that are adjacent to the meristem. It is relatively weakly expressed in pericycle derived cells and nodule periphery. In contrast, *MtPIN10* (Fig. 4L) is mainly expressed in pericycle derived cells and cells at the periphery that will differentiate into nodule vascular bundles. It is relatively weakly expressed in the nodule meristem.

## CHAPTER 4

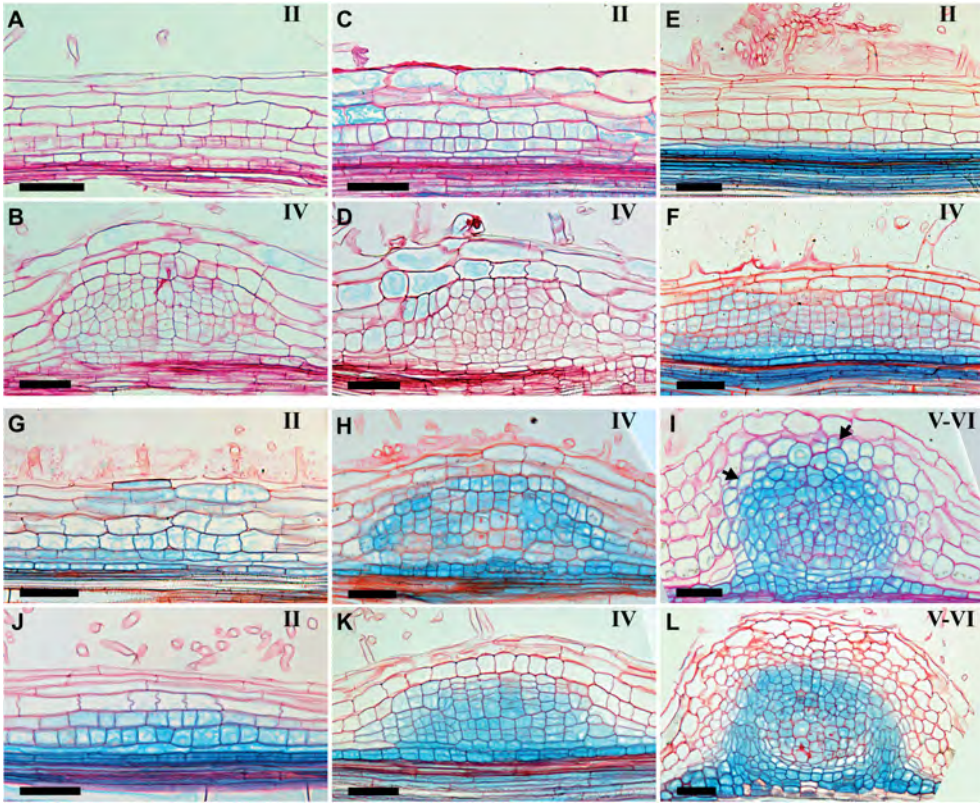


Fig. 4. *MtPIN2* and *MtPIN10* expression are induced in nodule primordium. Longitudinal sections of root nodule primordia expressing (A, B) *MtPIN1::GUS*, (C, D) *MtPIN3::GUS*, (E, F) *MtPIN4::GUS*, (G-I) *MtPIN2::GUS* or (J-L) *MtPIN10::GUS* construct. (A, B) *MtPIN1* is expressed at a similar level in nodule primordia and the surrounding non dividing cortical cells; (C, D) *MtPIN3* expression is reduced in the dividing primordium cells; (E, F) *MtPIN4* remains active in the endodermis and pericycle derived cells. (G, H) *MtPIN2* is expression is induced in dividing primordium cells; outer cortex and epidermis cells which the infection thread has passed. (J, K) *MtPIN10* expression is induced in dividing primordium cells. At stage IV, (H, I) *MtPIN2* and (L) *MtPIN10* expression are reduced in the infected primordium cells. At stage VI, (I) *MtPIN2* is primarily expressed in the nodule meristem and C2 cortex cells (arrows) adjacent to meristem; relatively weak expressed in pericycle derived cells and nodule periphery and infected cells. Whereas (L) *MtPIN10* is primarily expressed in pericycle derived cells and periphery cells that are going to differentiate to nodule vascular bundles of the primordium; relatively weak expressed in the nodule meristem and infected cells.

Bars equal to 75  $\mu$ m.

*MtPIN2* and *MtPIN10* are the highest expressed *PIN* genes during nodule primordium formation. Therefore, these most likely are key players in shaping the auxin landscape during nodule primordium formation. Auxin flow and its accumulation pattern is mainly determined by the (polar) subcellular position of PINs. Therefore, we determined the subcellular localization of *MtPIN2* and *MtPIN10* during nodule primordium development.

### ***MtPIN2* and *MtPIN10* subcellular localization during nodule primordium formation**

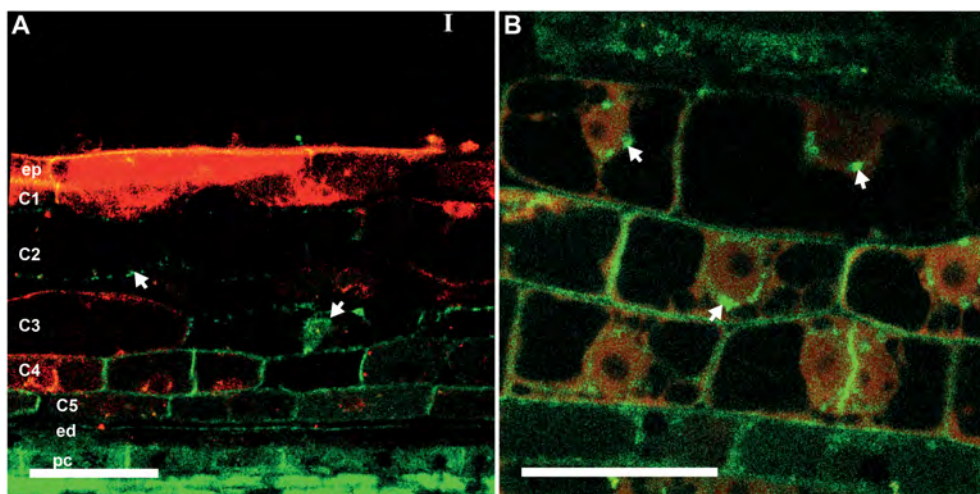


Fig. 5. *MtPIN2* accumulates prior cell division in cortex cells.

(A) *MtPIN2*-GFP accumulates in dividing pericycle cells and non-dividing cortex cells (arrows). (B) It is accumulated in the cytoplasm surrounding the nuclei (arrows) and at the cell plate.

Bar is equal to 60  $\mu$ m in A; 30  $\mu$ m in B.

To determine the localization of *MtPIN2* and *MtPIN10*, *MtPIN2::eGFP* and *MtPIN10::eGFP* protein fusion constructs under the control of their own promoter were made and introduced in *Medicago* roots. In the meristematic region of the root these 2 *MtPIN* proteins can be detected and their polar subcellular location is described in Fig. S5. In the susceptible zone both PIN proteins are reduced to a level that is too low to allow reproducible detection. Therefore, it was not possible to study whether the amount of PIN protein in the plasma membrane is (transiently) reduced upon Nod factor signalling.

## CHAPTER 4

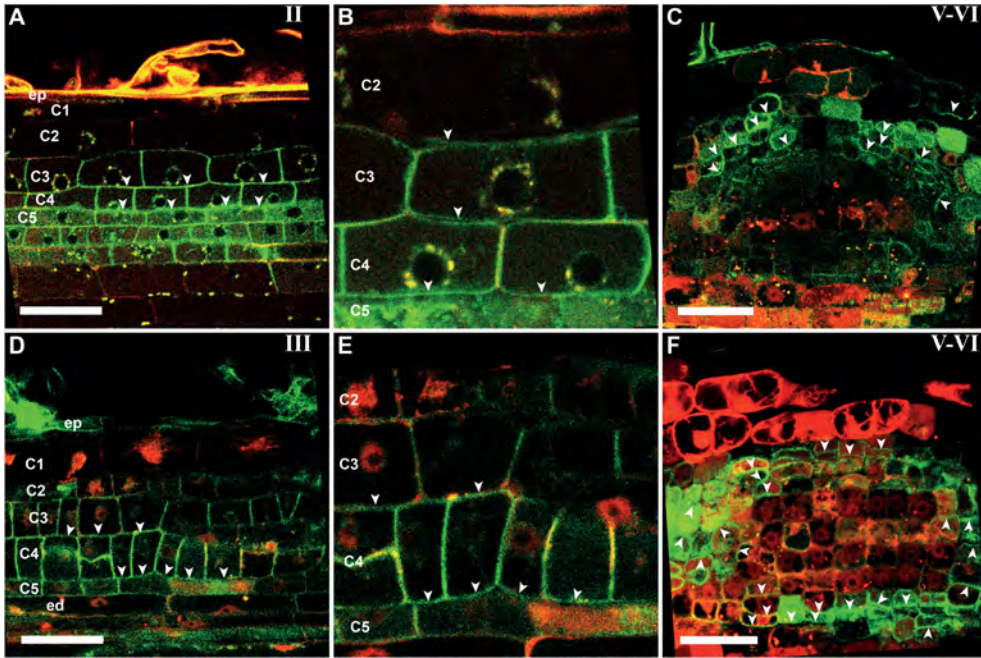


Fig. 6. *MtPIN2* and *MtPIN10* protein localization in nodule primordium.

(A) *MtPIN2* and (D) *MtPIN10* accumulate at the plasma membrane in dividing primordia cells. They are positioned towards the center of the primordium in cells located at the primordium periphery and have no polarity in cells located at the center of the primordium. magnifications of (A) and (D) are shown in (B) and (E), respectively. At stage V-VI, (C) *MtPIN2* is specifically positioned to the nodule meristem in C2 cortex cells adjacent to meristem; it is either positioned towards the nodule center or no polarity in meristematic cells. Whereas (F) *MtPIN10* is facing towards the root vascular bundle in the pericycle derived cells; it is positioned towards the nodule meristem in the cells at periphery that will form the nodule vascular tissues.

White arrowheads indicate the direction of auxin transport.

Bars equal to 60  $\mu\text{m}$ .

We determined the localization of *MtPIN2* and *MtPIN10* in nodule primordium cells. At early stages (I-III, Fig. 5 and Fig. 6A, B, D, E), both PIN GFP fusions accumulate in all nodule primordium cells. At stage I (Fig. 5A) *MtPIN2* accumulates in the dividing pericycle cells. Further, *MtPIN2* starts to accumulate in the cytoplasm in cortical cells that have not yet divided (Fig. 5B). This is also the stage when auxin accumulates in these cells (Fig. 1A). This suggests that in case the start of auxin accumulation is indeed controlled by a transient reduction of PIN levels this reduction will only last for a very short period.

## *Auxin transport during root nodule formation*

At stage IV-V (Fig. 6C), *MtPIN2*:eGFP accumulates in meristem, whereas it only accumulates to a relatively low level at periphery and pericycle derived cell. In contrast, *MtPIN10* (Fig. 6F) accumulates at a relatively high level in pericycle derived cells and periphery, whereas it is only present at a low level in the meristem.

For the subcellular *MtPINs* localization, we analysed several primordia for each stage and results are shown in Fig. 6 and Fig. S6, 7. An overview of the subcellular localization of *MtPIN2* and *MtPIN10* is presented in cartoons for stage II and V, respectively (Fig. 7). At stage I-III, *MtPIN2* and *MtPIN10* co-localise in the dividing primordia cells. They are positioned towards the center of the primordium in cells located at the primordium periphery. In cells located at the center of the primordium, they are equally distributed in the plasma membrane. This subcellular localization probably facilitates transport of auxin to the primordium from the surrounding area and to an equal distribution of auxin in the developing primordia. At later stages (IV-VI), *MtPIN2* in the cortex cells that are adjacent to the meristem,

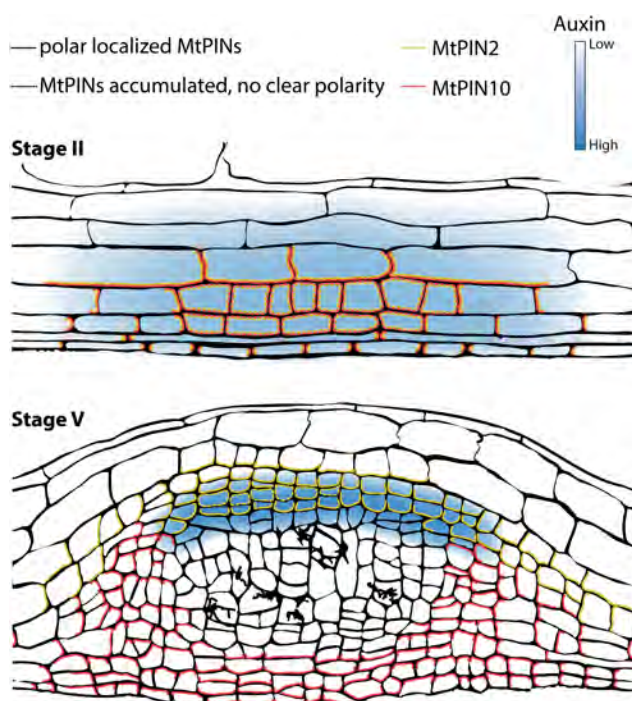


Fig. 7. Conclusion of *MtPIN2* and *MtPIN10* plasma membrane positions and auxin levels at nodule primordium stage II and V.

## CHAPTER 4

is positioned towards the meristem center. In the meristem, *MtPIN2* is positioned either to the nodule center or has no polarity. This indicates that *MtPIN2* maintains the auxin maximum in the meristem. In the pericycle derived cells, *MtPIN10* is especially present at the site facing the root vasculature. This suggests that they could play a role in keeping auxin levels low in the central part of the primordium. In the cells at the periphery that will form the nodule vascular tissues, *MtPIN10* is located especially at the distal lateral site by which auxin is transported from root vasculature to the meristem of the primordium/young nodule. Based on this, we hypothesise that *MtPINs* proteins are specifically expressed and positioned to transport auxin from cortex and root vascular into the nodule primordium. At later stages the position of *MtPIN2* and 10 will lead to an auxin maximum in the meristem.

### ***MtPIN10* is essential for nodule primordium development**

A Medicago *Mtpin10-1* mutant is available (Zhou et al., 2011). Therefore, we could study whether this *PIN* is essential for nodule primordium development. *Mtpin10-1* roots were harvested at different time points after inoculation with rhizobia. Early stages of nodule primordium formation are similar to wt. However, at stage IV-V, (Fig. 8A; about stage IV-V) C4/5 derived cells form about 12 cell layers, which is markedly more than in wt (around 8 cell layers). Further, C3 has formed multiple cell layers

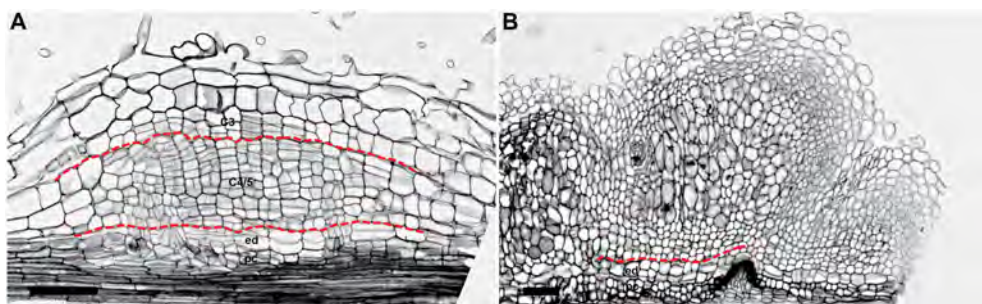


Fig. 8. *Mtpin10-1* nodules.

(A) *Mtpin10-1* nodule primordium has 12 cell layers derived from C4/5. (B) Around 12 non-infected cell layers at the proximal part of the nodule, which are derived from pericycle, endodermis and C4/5 cortex cell layers. And a relatively small meristem. Bars equal to 75  $\mu$ m.

(comparable to wt stage V), but the infection thread has not reached C4/5 derived cells (comparable to wt stage IV). In mature mutant nodules (Fig. 8B), the number of non-infected cell layers at the basis of the nodule is markedly more than in wild type nodules. Together with the pericycle and endodermis derived cells it forms 10-12 non-infected cell layers (wt forms about 6 cell layers). Further, the nodule meristem is relatively small.

## **DISCUSSION**

In this study we precisely determined the accumulation of auxin during different stages of *Medicago* nodule primordium development. We showed that auxin accumulation associates with mitotic activity induced in the three (root) tissues that contribute to primordium formation. Further, we tested whether a local reduction of PIN activity triggers the accumulation of auxin. However, the low level of PIN proteins in the susceptible zone of the root hampered these studies. In contrast, we showed that PIN proteins accumulate in primordium when cell division occurs. This especially involves *MtPIN2* and *MtPIN10*. Based on their expression pattern and subcellular location, we conclude that they control the accumulation of auxin in primordia at early stages of development and the formation of an auxin maximum in the nodule meristem at later stages. Functional analysis of *Mtpin10-1* mutant nodules supports that it is essential for normal primordium development.

### **Auxin accumulation correlates with mitotic activity of the nodule primordium**

In this study we used *DR5::GUS* expression to study auxin accumulates during *Medicago* nodule primordium formation. In general our auxin activity pattern agrees with the results from clover (Mathesius et al., 1998; Huo et al., 2006). It is active in the pericycle and cortex at early stages of primordium formation, whereas at later stages the activity is restricted to the vascular tissue and meristem of the young nodule.

Here, we showed that auxin accumulation (*DR5*) correlated with mitotic activity during nodule formation. During stage I-III auxin accumulates in dividing cells derived from cortex, endodermis and pericycle. At stage IV auxin levels decline in endodermis and pericycle derived cells coinciding with reduced mitotic activity in these cells (Xiao et al., 2014). At stage

## CHAPTER 4

V-VI, auxin is present in the developing vascular bundles, where cell division continued.

Further, at stage V-VI auxin levels in the C4/5 derived cells are markedly decreased, which coincides with their switch from mitosis to endoreduplication. Auxin has been shown to repress the switch from mitosis to endoreduplication in *Arabidopsis* roots (Ishida et al., 2010; Atif et al., 2013). We expect that also in *Medicago* nodules auxin can repress endoreduplication.

### **Auxin accumulation during nodule formation might be triggered by a transient reduction of *PIN* expression**

In this study, we tried to test the theoretical model, which predicts that Nod factor signalling triggers auxin accumulation by locally reducing PIN levels. Unfortunately, low PIN protein levels in the susceptible zone hampered these studies. Although studies on PIN protein levels were technically not possible we could still study the *PIN* transcript levels. This showed that the expression of *PIN* genes is transiently repressed at a stage that markedly precedes the first cell divisions leading to primordium formation. Whether this leads to reduced functional PIN levels in the cells that form a primordium remains to be shown.

In this study we show that *MtPIN2* and *MtPIN10* accumulate in nodule primordia. Accumulation precedes division and (more or less) coincides with auxin accumulation. Therefore, in case PIN levels are transiently reduced to trigger auxin accumulation this can only occur for a very short period. This transient PIN reduction must happen before the auxin accumulation and the first cell divisions.

### **PIN mediated auxin transport is involved in nodule development**

We showed that the levels of *MtPIN2* and *MtPIN10* are increased during nodule primordium development. *MtPIN2* is highly expressed in the meristem and *MtPIN10* is markedly lower. Our studies are in agreement with transcriptome analysis published by Limpens et al (2013). However, more recent transcriptome analyses of *Medicago* indicate that *MtPIN10* is expressed at a high level and *MtPIN2* at a low level in the *Medicago* nodule (Roux et al., 2014). How these transcriptome studies resulted in such

contradicting data is unclear. Further, our study shows that peripheral tissue play an important role in the development of the central tissue. Therefore, transcriptome studies that are merely focused on the central tissue cannot fully reveal mechanisms controlling development of this tissue.

*MtPIN10* is important for nodule primordium development. *Mtpin10-1* nodules show more C4/5 cell division and more non-infected cell layers in the basal part of the nodule primordium. Since cell division is correlated with auxin accumulation during nodule primordia development. This increased cell division most likely is due to a delay in the reduction of the high auxin level in the C4/5 derived cells. Further, the increased number of non-infected cell layers is most likely caused by the continuous cell division in C4/5 at stage IV-V, which will block infection thread growth in these cell layers (Xiao et al., 2014). To test these hypotheses, further study is needed.

## **MATERIALS AND METHODS**

### **Plant materials and bacterial strains**

*M. truncatula* R108 seedlings were used to make the stable *DR5::GUS* transgenic line by using *Agrobacterium tumefaciens* (strain AGL1) according to the protocol described by Chabaud et al. (2003). *M. truncatula* Jemalong A17 plants were used to generate *Agrobacterium rhizogenes* (strain MSU440) mediated transgenic roots as previously described by Limpens et al. (2004) for *MtPIN* promoter GUS and protein GFP fusion constructs. Surface-sterilization and germination of *Medicago* seeds were performed as previously described by Limpens et al. (2004). *Sinorhizobium meliloti* 2011 was used to induce root nodule formation on plates with buffered nod medium (BNM) (Ehrhardt et al., 1992).

### **Constructs**

DNA fragments were amplified from *M. truncatula* genomic DNA using primer combinations listed in Table S1 and *Phusion™ High-Fidelity DNA Polymerase* (Finnzymes). To create the constructs, pENTR™/D-TOPO® Cloning Kits (Invitrogen) and Gateway® technology (Invitrogen) were

## CHAPTER 4

used to generate the entry clone and genetic promoter-GUS or protein-eGFP constructs (Karimi et al., 2002). First, 14 synthetic DR5 DNA fragments (Ulmasov et al., 1997) or the *MtPIN* promoter was introduced in the entry clone. Then, the entry vector was recombined into Gateway®-compatible binary vector pKGW-RR, that contains the GUS reporter gene and *AtUBQ10::DsRED1* as a selection marker (Limpens et al., 2004), by using Gateway® LR Clonase® II enzyme mix (Invitrogen). For *MtPIN* eGFP fusion constructs, the promoter and first part of the DNA fragment was introduced into Gateway® donor vector pENTR2-1, eGFP DNA fragment without start codon were introduced into pENTR1-2 and the rest of the gene which includes the terminator was introduced into pENTR2-3, using Gateway® BP Clonase® II enzyme mix. These entry vectors were recombined into Gateway®-compatible binary vector pKGW-RR-MGW, that contains *AtUBQ10::DsRED1* as a selection marker using Gateway® LR Clonase® II Plus enzyme mix (Invitrogen). Insertion sites for the eGFP reporter in *PIN* genes were selected based on functional AtPINs:GFP protein fusion constructs in Arabidopsis (Xu and Scheres, 2005), which are at position 1237 and 1565 for *MtPIN2* and *MtPIN10*, respectively.

### Histochemical $\beta$ -glucuronidase (GUS) staining

Transgenic plant material containing GUS constructs were incubated in GUS buffer (3% sucrose, 2 mM  $K_3Fe(CN)_6$ , 2 mM  $K_4Fe(CN)_6$ , 10 mM EDTA, and 1 mg/ml X-Gluc salt in 100 mM phosphate buffer solution, pH 7.0) under vacuum for 30 min and then at 37 °C for 3 to 24 h (Jefferson et al., 1987).

### Tissue embedding, sectioning and section staining

Root segments were fixed at 4 °C overnight with 4% paraformaldehyde (w/v), 5% glutaraldehyde (v/v) in 0.05 M sodium phosphate buffer (pH 7.2). The fixed material was dehydrated in an ethanol series and subsequently embedded in Technovit 7100 (Heraeus Kulzer) according to the manufacturer's protocol. Sections (7  $\mu$ m) were made of thin by using a RJ2035 microtome (Leica Microsystems, Rijswijk, The Netherlands), stained 5 min in 0.05% toluidine blue O for wt material and 15 min in 0.1% ruthenium red for transgenic GUS material. Sections were analysed by using a DM5500B microscope equipped with a DFC425C camera (Leica

Microsystems, Wetzlar, Germany).

### **GFP fluorescence sample preparation and confocal microscopy**

Fresh transgenic roots or root nodules were manually sectioned in a longitudinal direction and mounted on microscope slides with phosphate buffer, PH 7.2. Then plant material was immediately observed under a Leica SP2 confocal microscope. GFP is visualized by excitation at 488 nm and by detection at 505–530 nm. DsRED1 is visualized by excitation at 543 nm and by detection at 560–615 nm.

### **ACKNOWLEDGEMENTS**

This research is funded by European Research Council (ERC-2011-AdG-294790) and Graduate School 'Experimental Plant Science'.

### **REFERENCES**

- Andriankaja, A., Boisson-Demier, A., Frances, L., Sauviac, L., Jauneau, A., Barker, D. G. and de Carvalho-Niebel, F.** (2007). AP2-ERF transcription factors mediate nod factor-dependent MtENOD11 activation in root hairs via a novel cis-regulatory motif. *The Plant cell* **19**, 2866-2885.
- Arrighi, J. F., Barre, A., Ben Amor, B., Bersoult, A., Soriano, L. C., Mirabella, R., de Carvalho-Niebel, F., Journet, E. P., Gherardi, M., Huguet, T. et al.** (2007). The *Medicago truncatula* lysine motif-receptor-like kinase gene family includes NFP and new nodule-expressed genes. *Plant physiology* **143**, 1078-1078.
- Atif, R. M., Boulisset, F., Conreux, C., Thompson, R. and Ochatt, S. J.** (2013). In vitro auxin treatment promotes cell division and delays endoreduplication in developing seeds of the model legume species *Medicago truncatula*. *Physiol Plantarum* **148**, 549-559.
- Ben Amor, B., Shaw, S. L., Oldroyd, G. E. D., Maillet, F., Penmetsa, R. V., Cook, D., Long, S. R., Denarie, J. and Gough, C.** (2003). The NFP locus of *Medicago truncatula* controls an early step of Nod factor signal transduction upstream of a rapid calcium flux and root hair deformation. *Plant J.* **34**, 495-506.
- Benkova, E., Michniewicz, M., Sauer, M., Teichmann, T., Seifertova, D., Jurgens, G. and Friml, J.** (2003). Local, efflux-dependent auxin gradients as a common module for plant organ formation. *Cell* **115**, 591-602.
- Bersoult, A., Camut, S., Perhald, A., Kereszt, A., Kiss, G. B. and Cullimore, J. V.** (2005). Expression of the *Medicago truncatula* DM12 gene suggests roles of the symbiotic nodulation receptor kinase in nodules and during early nodule development. *Molecular plant-microbe interactions : MPMI* **18**, 869-876.

## CHAPTER 4

**Chabaud, M., Carvalho-Niebel, F. d. and Barker, D. G.** (2003). Efficient transformation of *Medicago truncatula* cv. Jemalong using the hypervirulent *Agrobacterium tumefaciens* strain AGL1. *Plant Cell Reports* **22**, 46-51.

**Charpentier, M., Bredemeier, R., Wanner, G., Takeda, N., Schleiff, E. and Parniske, M.** (2008). *Lotus japonicus* CASTOR and POLLUX are ion channels essential for perinuclear calcium spiking in legume root endosymbiosis. *The Plant cell* **20**, 3467-3479.

**Deinum, E. E., Geurts, R., Bisseling, T. and Mulder, B. M.** (2012). Modeling a cortical auxin maximum for nodulation: different signatures of potential strategies. *Front in Plant Science* **3**, 96.

**Ehrhardt, D. W., Atkinson, E. M. and Long, S. R.** (1992). Depolarization of *Alfalfa* root hair membrane-potential by *Rhizobium meliloti* Nod factors. *Science* **256**, 998-1000.

**Endre, G., Kereszt, A., Kevei, Z., Mihacea, S., Kalo, P. and Kiss, G. B.** (2002). A receptor kinase gene regulating symbiotic nodule development. *Nature* **417**, 962-966.

**Horvath, B., Yeun, L. H., Domonkos, A., Halasz, G., Gobbato, E., Ayaydin, F., Miro, K., Hirsch, S., Sun, J. H., Tadege, M. et al.** (2011). *Medicago truncatula* IPD3 Is a member of the common symbiotic signaling pathway required for rhizobial and mycorrhizal symbioses. *Molecular Plant Microbe Interactions* **24**, 1345-1358.

**Huo, X., Schnabel, E., Hughes, K. and Frugoli, J.** (2006). RNAi Phenotypes and the Localization of a Protein::GUS Fusion Imply a Role for *Medicago truncatula* PIN Genes in Nodulation. *Journal of plant growth regulation* **25**, 156-165.

**Imaizumi-Anraku, H., Takeda, N., Charpentier, M., Perry, J., Miwa, H., Umehara, Y., Kouchi, H., Murakami, Y., Mulder, L., Vickers, K. et al.** (2005). Plastid proteins crucial for symbiotic fungal and bacterial entry into plant roots. *Nature* **433**, 527-531.

**Ishida, T., Adachi, S., Yoshimura, M., Shimizu, K., Umeda, M. and Sugimoto, K.** (2010). Auxin modulates the transition from the mitotic cycle to the endocycle in *Arabidopsis*. *Development* **137**, 63-71.

**Jefferson, R. A., Kavanagh, T. A. and Bevan, M. W.** (1987). Gus fusions: b-glucuronidase as a sensitive and versatile gene fusion marker in higher-plants. *The Embo Journal* **6**, 3901-3907.

**Kalo, P., Gleason, C., Edwards, A., Marsh, J., Mitra, R. M., Hirsch, S., Jakab, J., Sims, S., Long, S. R., Rogers, J. et al.** (2005). Nodulation signaling in legumes requires NSP2, a member of the GRAS family of transcriptional regulators. *Science* **308**, 1786-1789.

**Karimi, M., Inze, D. and Depicker, A.** (2002). GATEWAY™ vectors for *Agrobacterium*-mediated plant transformation. *Trends Plant Sci* **7**, 193-195.

**Krecek, P., Skupa, P., Libus, J., Naramoto, S., Tejos, R., Friml, J. and Zazimalova, E.** (2009). The PIN-FORMED (PIN) protein family of auxin transporters. *Genome Biology* **10**, 249.

**Levy, J., Bres, C., Geurts, R., Chalhoub, B., Kulikova, O., Duc, G., Journet,**

**E. P., Ane, J. M., Lauber, E., Bisseling, T. et al.** (2004). A putative Ca<sup>2+</sup> and calmodulin-dependent protein kinase required for bacterial and fungal symbioses. *Science* **303**, 1361-1364.

**Limpens, E., Mirabella, R., Fedorova, E., Franken, C., Franssen, H., Bisseling, T. and Geurts, R.** (2005). Formation of organelle-like N<sub>2</sub>-fixing symbiosomes in legume root nodules is controlled by *DMI2*. *P Natl Acad Sci USA* **102**, 10375-10380.

**Limpens, E., Moling, S., Hooiveld, G., Pereira, P. A., Bisseling, T., Becker, J. D. and Kuster, H.** (2013). Cell- and Tissue-Specific Transcriptome Analyses of *Medicago truncatula* Root Nodules. *Plos One* **8**.

**Limpens, E., Ramos, J., Franken, C., Raz, V., Compaan, B., Franssen, H., Bisseling, T. and Geurts, R.** (2004). RNA interference in *Agrobacterium rhizogenes*-transformed roots of *Arabidopsis* and *Medicago truncatula*. *J Exp Bot* **55**, 983-992.

**Marsh, J. F., Rakocevic, A., Mitra, R. M., Brocard, L., Sun, J., Eschstruth, A., Long, S. R., Schultze, M., Ratet, P. and Oldroyd, G. E. D.** (2007). *Medicago truncatula* NIN is essential for rhizobial-independent nodule organogenesis induced by autoactive calcium/calmodulin-dependent protein kinase. *Plant physiology* **144**, 324-335.

**Mathesius, U., Schlaman, H. R. M., Spaink, H. P., Sautter, C., Rolfe, B. G. and Djordjevic, M. A.** (1998). Auxin transport inhibition precedes root nodule formation in white clover roots and is regulated by flavonoids and derivatives of chitin oligosaccharides. *Plant J.* **14**, 23-34.

**Mitra, R. M., Gleason, C. A., Edwards, A., Hadfield, J., Downie, J. A., Oldroyd, G. E. D. and Long, S. R.** (2004). A Ca<sup>2+</sup>/calmodulin-dependent protein kinase required for symbiotic nodule development: gene identification by transcript-based cloning. *P Natl Acad Sci USA* **101**, 4701-4705.

**Murray, J. D., Karas, B. J., Sato, S., Tabata, S., Amyot, L. and Szczyglowski, K.** (2007). A cytokinin perception mutant colonized by *Rhizobium* in the absence of nodule organogenesis. *Science* **315**, 101-104.

**Ovchinnikova, E., Journet, E. P., Chabaud, M., Cosson, V., Ratet, P., Duc, G., Fedorova, E., Liu, W., Camp, R. O. d., Zhukov, V. et al.** (2011). IPD3 controls the formation of nitrogen-fixing symbiosomes in pea and *Medicago* spp. *Molecular Plant Microbe Interactions* **24**, 1333-1344.

**Peret, B., Middleton, A. M., French, A. P., Larrieu, A., Bishopp, A., Njo, M., Wells, D. M., Porco, S., Mellor, N., Band, L. R. et al.** (2013). Sequential induction of auxin efflux and influx carriers regulates lateral root emergence. *Molecular systems biology* **9**, 699.

**Petrasek, J., Mravec, J., Bouchard, R., Blakeslee, J. J., Abas, M., Seifertova, D., Wisniewska, J., Tadele, Z., Kubes, M., Covanova, M. et al.** (2006). PIN proteins perform a rate-limiting function in cellular auxin efflux. *Science* **312**, 914-918.

**Plet, J., Wasson, A., Ariel, F., Le Signor, C., Baker, D., Mathesius, U., Crespi, M. and Frugier, F.** (2011). MtCRE1-dependent cytokinin signaling integrates bacterial and plant cues to coordinate symbiotic nodule organogenesis in *Medicago truncatula*. *Plant J.* **65**, 622-633.

**Radutoiu, S., Madsen, L. H., Madsen, E. B., Felle, H. H., Umehara, Y.,**

## CHAPTER 4

**Gronlund, M., Sato, S., Nakamura, Y., Tabata, S., Sandal, N. et al.** (2003). Plant recognition of symbiotic bacteria requires two LysM receptor-like kinases. *Nature* **425**, 585-592.

**Roth, L. E. and Stacey, G.** (1989). Bacterium release into host cells of nitrogen-fixing soybean nodules the symbiosome membrane comes from three sources. *European Journal of Cell Biology* **49**, 13-23.

**Roux, B., Rodde, N., Jardinaud, M. F., Timmers, T., Sauviac, L., Cottret, L., Carrere, S., Sallet, E., Courcelle, E., Moreau, S. et al.** (2014). An integrated analysis of plant and bacterial gene expression in symbiotic root nodules using laser-capture microdissection coupled to RNA sequencing. *Plant J.* **77**, 817-837.

**Singh, S., Katzer, K., Lambert, J., Cerri, M. and Parniske, M.** (2014). CYCLOPS, a DNA-binding transcriptional activator, orchestrates symbiotic root nodule development. *Cell Host Microbe* **15**, 139-152.

**Smit, P., Raedts, J., Portyanko, V., Debelle, F., Gough, C., Bisseling, T. and Geurts, R.** (2005). NSP1 of the GRAS protein family is essential for rhizobial Nod factor-induced transcription. *Science* **308**, 1789-1791.

**Smit, P., Limpens, E., Geurts, R., Fedorova, E., Dolgikh, E., Gough, C. and Bisseling, T.** (2007). Medicago LYK3, an entry receptor in rhizobial nodulation factor signaling. *Plant physiology* **145**, 183-191.

**Suzaki, T., Yano, K., Ito, M., Umehara, Y., Suganuma, N. and Kawaguchi, M.** (2012). Positive and negative regulation of cortical cell division during root nodule development in *Lotus japonicus* is accompanied by auxin response. *Development* **139**, 3997-4006.

**Turner, M., Nizampatnam, N. R., Baron, M., Coppin, S., Damodaran, S., Adhikari, S., Arunachalam, S. P., Yu, O. and Subramanian, S.** (2013). Ectopic expression of miR160 results in auxin hypersensitivity, cytokinin hyposensitivity, and inhibition of symbiotic nodule development in soybean. *Plant physiology* **162**, 2042-2055.

**Ulmasov, T., Murfett, J., Hagen, G. and Guilfoyle, T. J.** (1997). Aux/IAA proteins repress expression of reporter genes containing natural and highly active synthetic auxin response elements. *The Plant cell* **9**, 1963-1971.

**Vieten, A., Sauer, M., Brewer, P. B. and Friml, J.** (2007). Molecular and cellular aspects of auxin-transport-mediated development. *Trends Plant Sci* **12**, 160-168.

**Vieten, A., Vanneste, S., Wisniewska, J., Benkova, E., Benjamins, R., Beeckman, T., Luschnig, C. and Friml, J.** (2005). Functional redundancy of PIN proteins is accompanied by auxin-dependent cross-regulation of PIN expression. *Development* **132**, 4521-4531.

**Wisniewska, J., Xu, J., Seifertova, D., Brewer, P. B., Ruzicka, K., Blilou, I., Rouquie, D., Benkova, E., Scheres, B. and Friml, J.** (2006). Polar PIN localization directs auxin flow in plants. *Science* **312**, 883-883.

**Xiao, T. T., Schilderink, S., Moling, S., Deinum, E. E., Kondorosi, E., Franssen, H., Kulikova, O., Niebel, A. and Bisseling, T.** (2014). Fate map of *Medicago truncatula* root nodules. *Development* **141**, 3517-3528.

## *Auxin transport during root nodule formation*

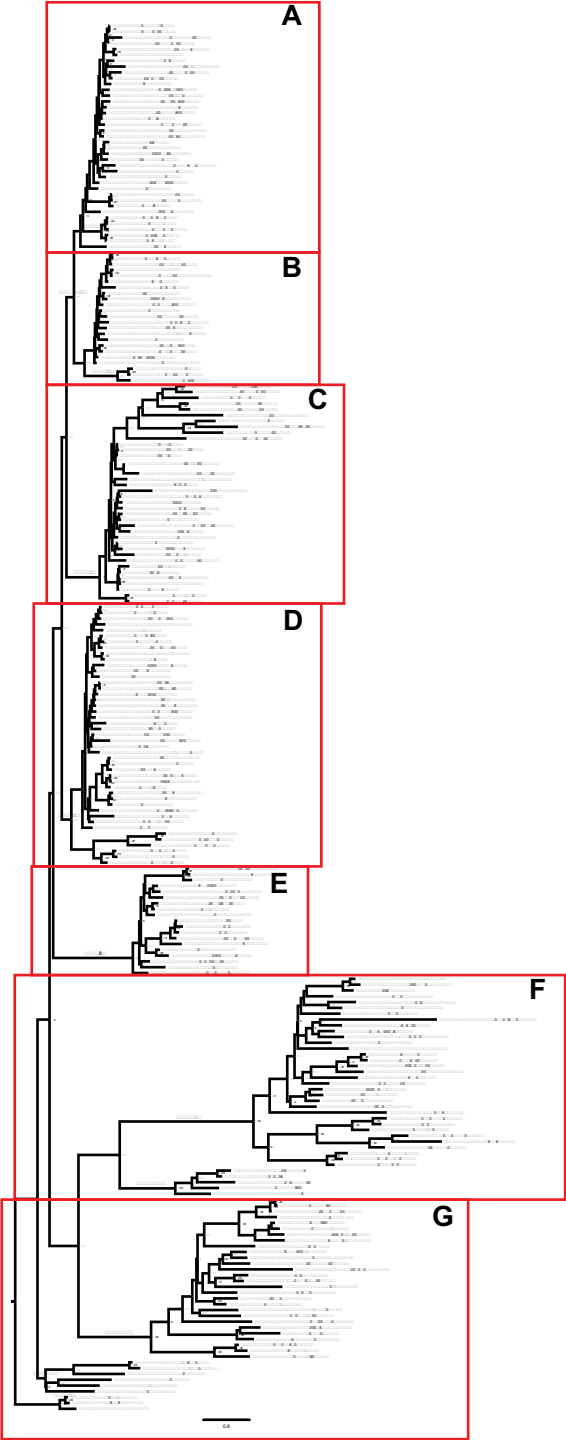
**Xu, J. and Scheres, B.** (2005). Dissection of *Arabidopsis* ADP-RIBOSYLATION FACTOR 1 function in epidermal cell polarity. *The Plant cell* **17**, 525-536.

**Yano, K., Yoshida, S., Muller, J., Singh, S., Banba, M., Vickers, K., Markmann, K., White, C., Schuller, B., Sato, S. et al.** (2008). CYCLOPS, a mediator of symbiotic intracellular accommodation. *P Natl Acad Sci USA* **105**, 20540-20545.

**Zhou, C., Han, L., Hou, C., Metelli, A., Qi, L., Tadege, M., Mysore, K. S. and Wang, Z. Y.** (2011). Developmental analysis of a *Medicago truncatula* smooth leaf margin1 mutant reveals context-dependent effects on compound leaf development. *The Plant cell* **23**, 2106-2124.

# CHAPTER 4

## SUPPLEMENTARY FIGURES AND TABLES



## *Auxin transport during root nodule formation*

1. <i>Arabidopsis thaliana</i>
2. <i>Brassica rapa</i>
3. <i>Capsella rubella</i>
4. <i>Carica papaya</i>
5. <i>Citrus sinensis</i>
6. <i>Cucumis sativus</i>
7. <i>Eucalyptus grandis</i>
8. <i>Fragaria vesca</i>
9. <i>Glycine max</i>
10. <i>Gossypium raimondii</i>
11. <i>Linum usitatissimum</i>
12. <i>Lotus japonicas</i>
13. <i>Lupinus albus</i>
14. <i>Malus domestica</i>
15. <i>Manihot esculenta</i>
16. <i>Medicago truncatula</i>
17. <i>Oryza sativa</i>
18. <i>Phaseolus vulgaris</i>
19. <i>Physcomitrella patens</i>
20. <i>Pisum sativum</i>
21. <i>Populus trichocarpa</i>
22. <i>Prunus persica</i>
23. <i>Ricinus communis</i>
24. <i>Selaginella moellendorffii</i>
25. <i>Solanum lycopersicum</i>
26. <i>Sorghum bicolor</i>
27. <i>Theobroma cacao</i>
28. <i>Vitis vinifera</i>
29. <i>Zea mays</i>

Fig. S1. Phylogenetic analysis of *PIN* genes of 29 species that represent all major plant lineages.

A to G are indicated parts of the overview and show a specific *PIN* group. *Medicago* *PIN* genes are marked within blue squares. Plant species are listed in the table.

Higher plant *PINs* are grouped in 6 groups (groups 3 to 8). Further, *PINs* can be divided into two major subclasses according to phylogenetic and functional analyses; the endoplasmic reticulum localized *PIN5*-type (groups 3 and 8) and the plasma membrane localized *PIN1*-type (groups 4 to 7).

## CHAPTER 4

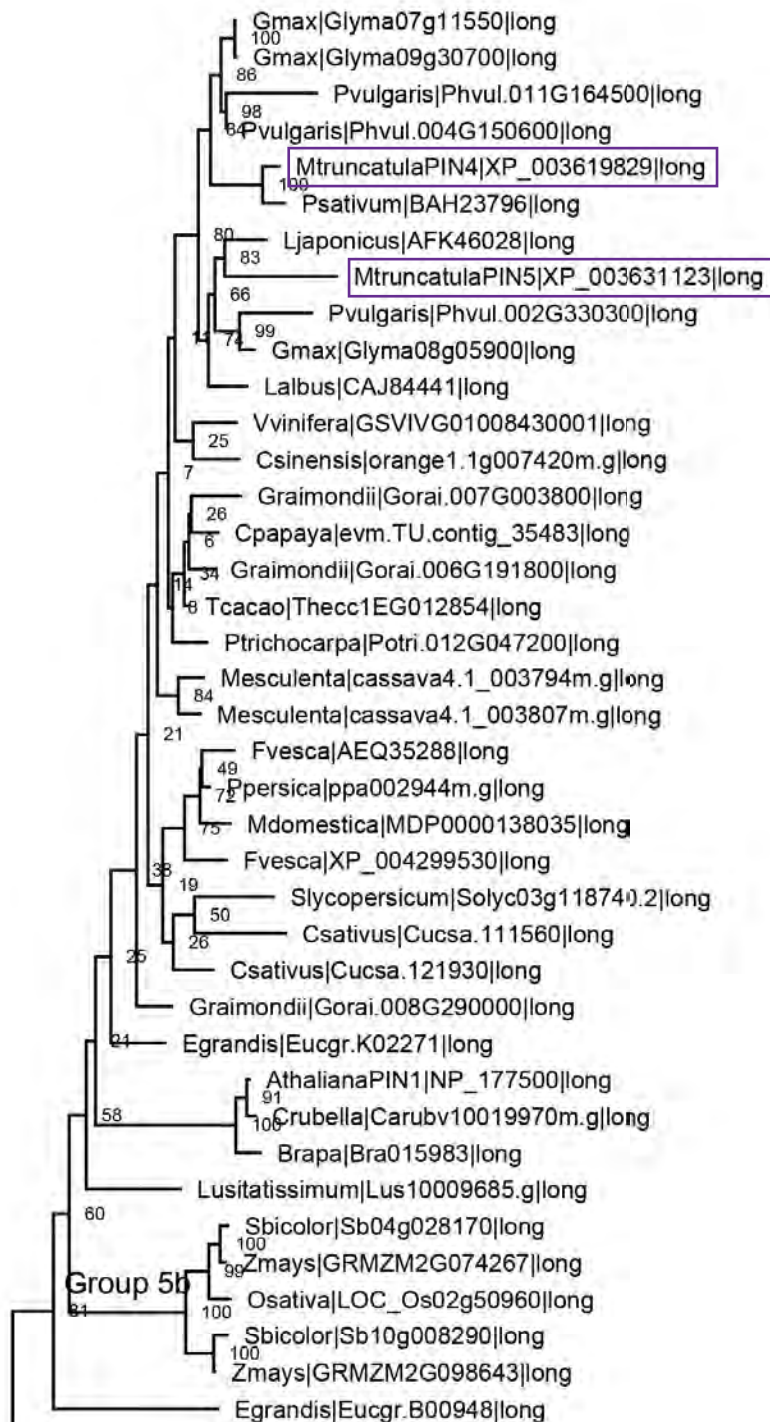


Fig. S1A

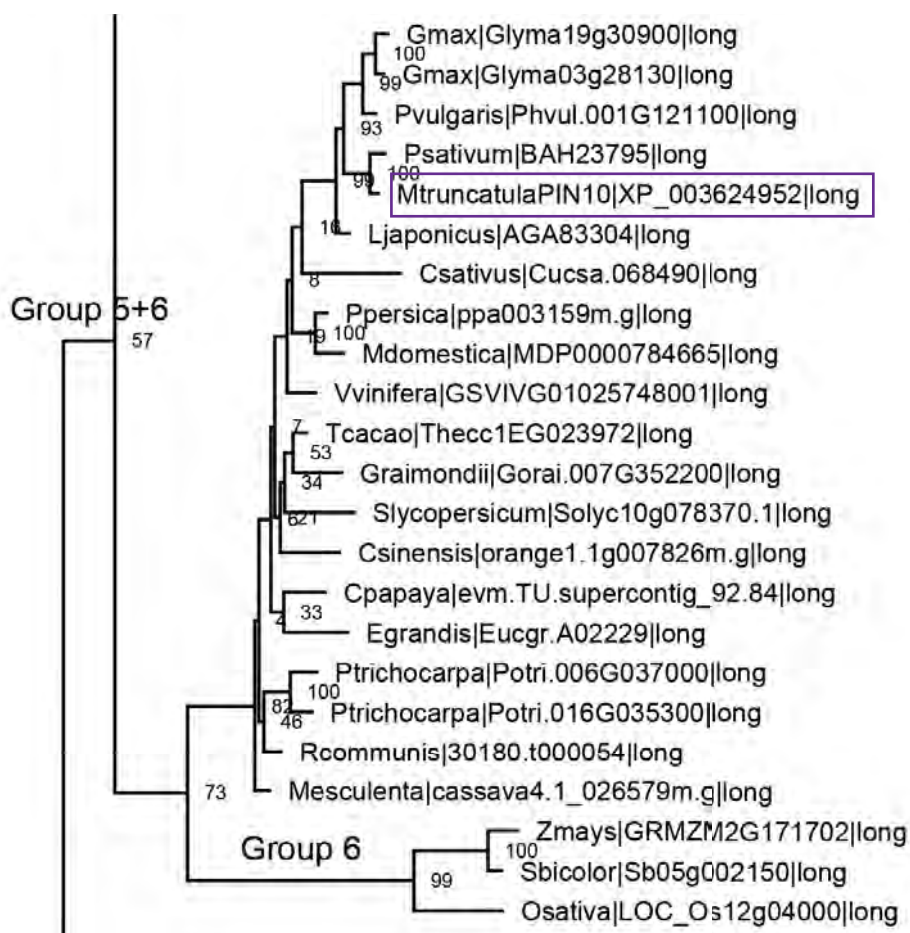


Fig. S1B

# CHAPTER 4

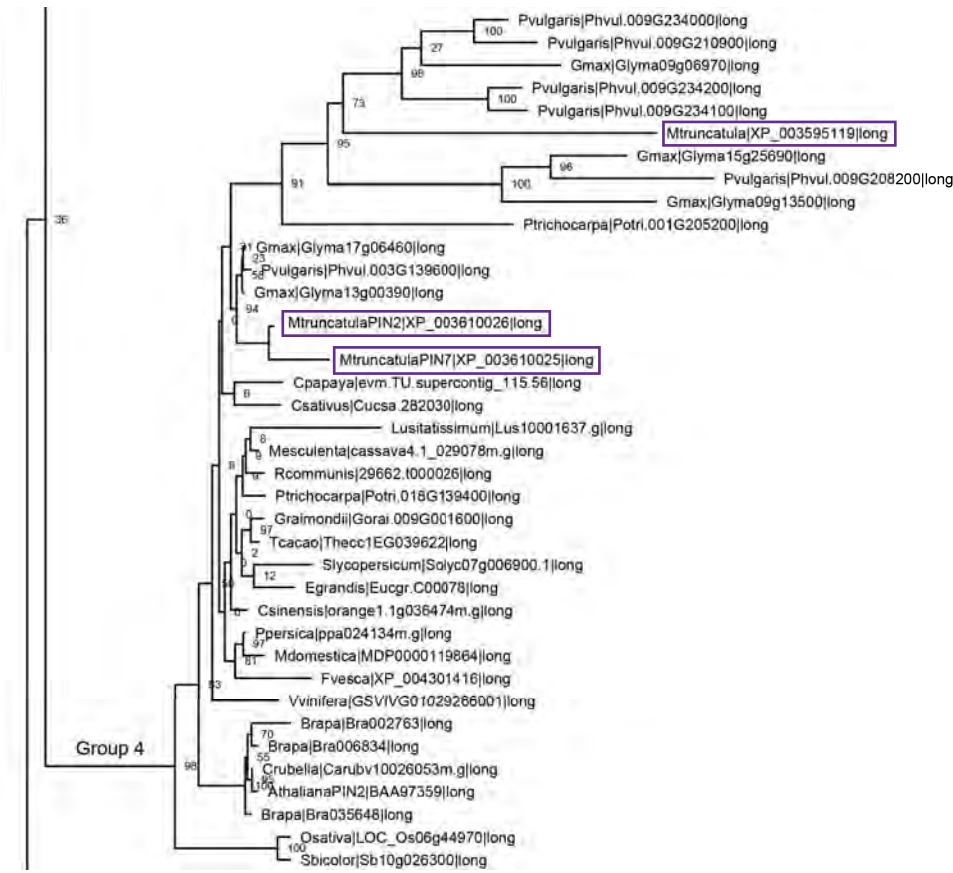


Fig. S1C

# Auxin transport during root nodule formation



Fig. S1D

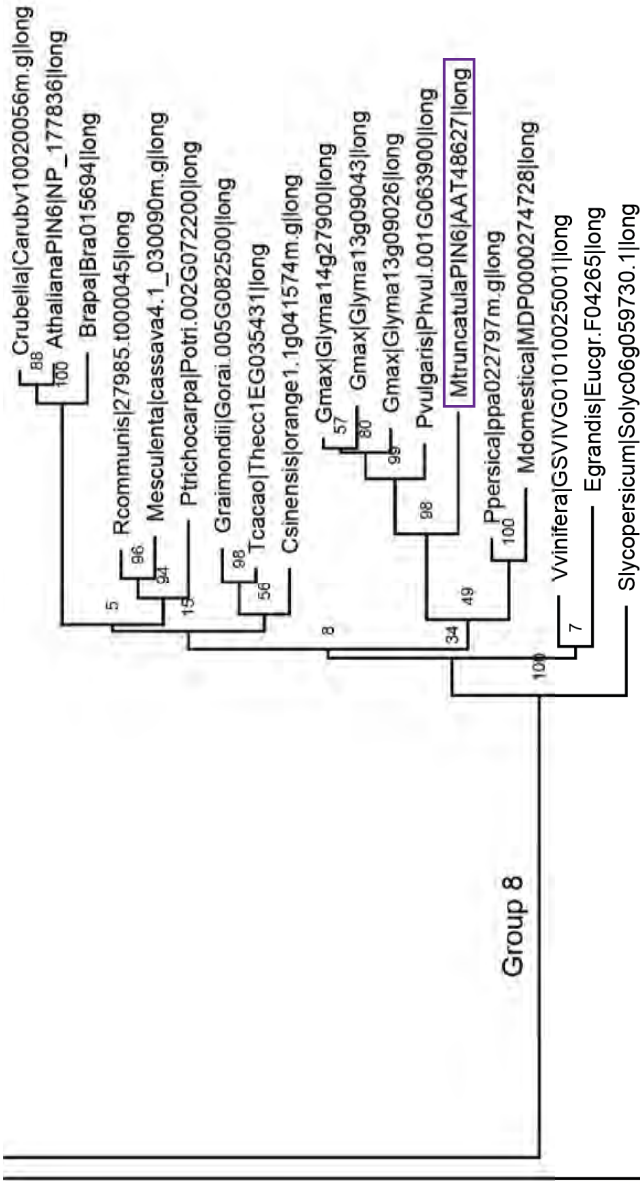


Fig. S1E

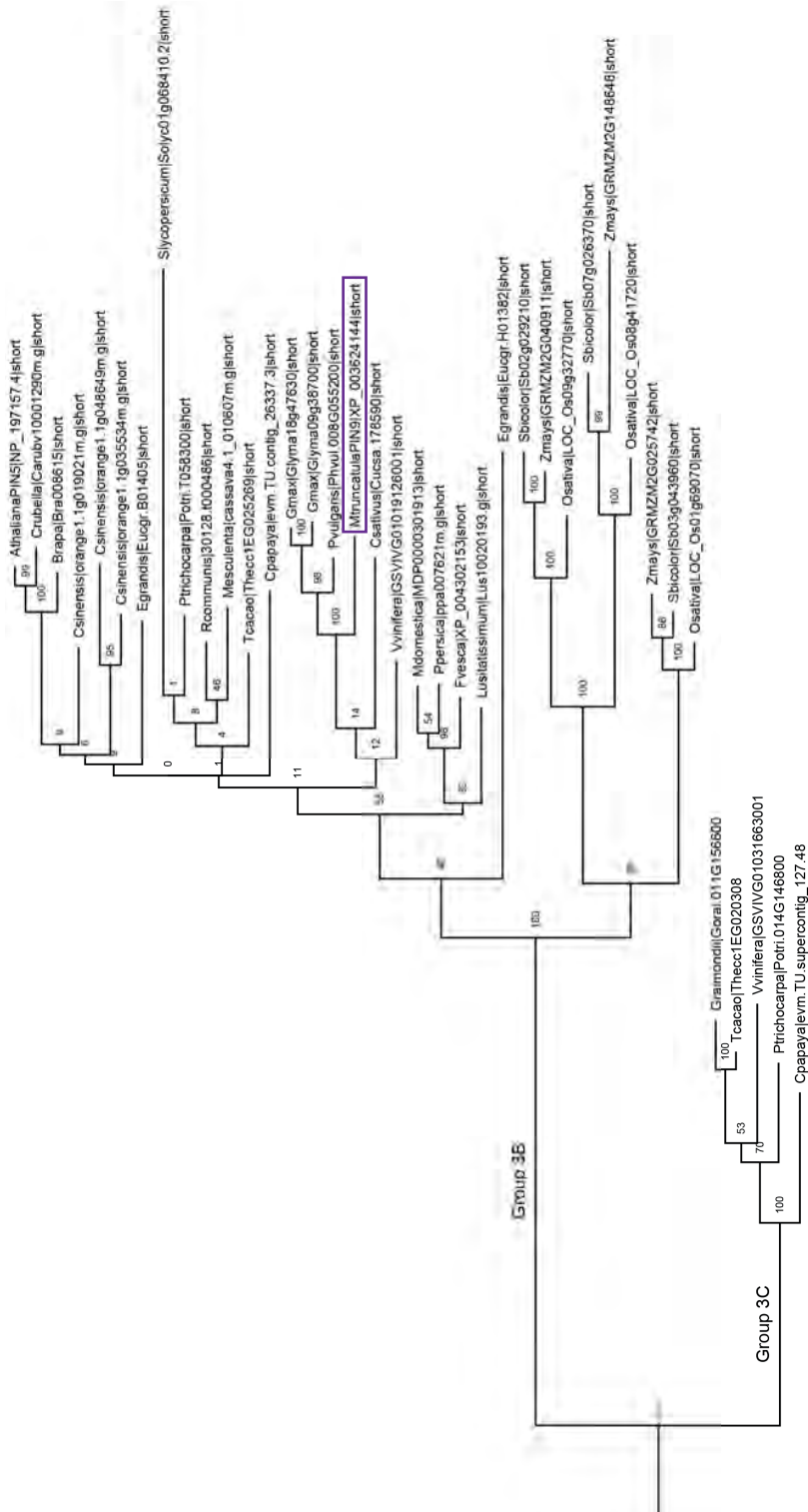


Fig. S1F

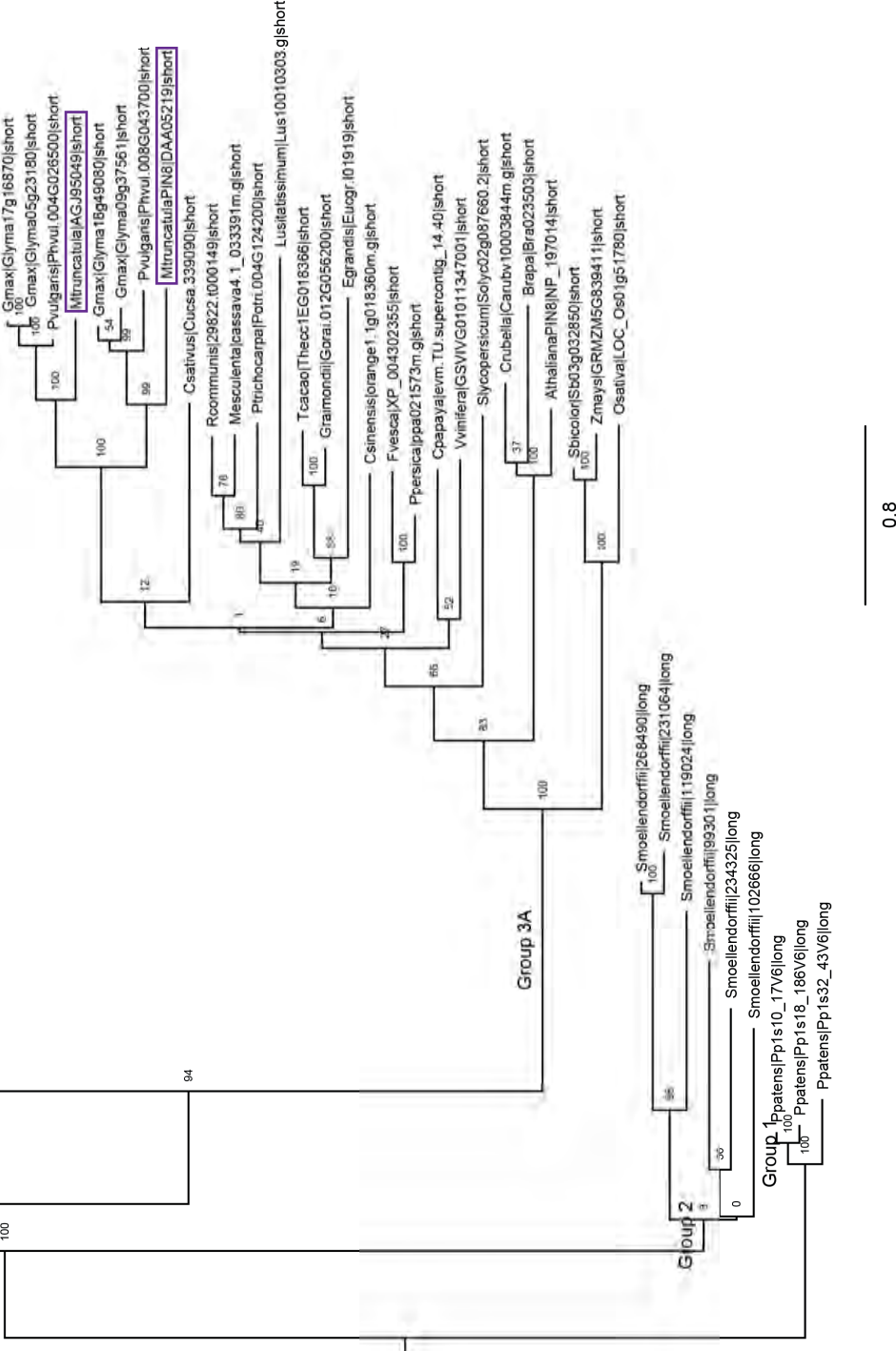


Fig. S1G

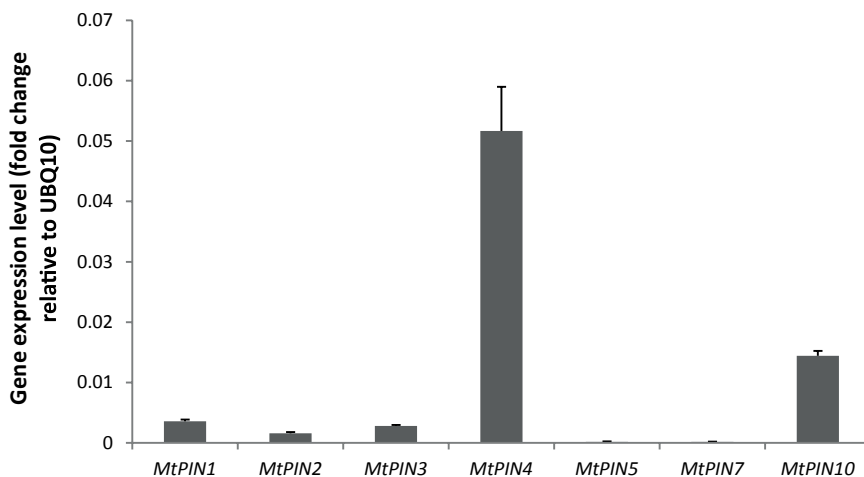


Fig. S2. PIN1-type *MtPINs* qRT-PCR analysis at the Medicago root susceptible zone. *MtPIN1*, 2, 3, 4 and 10 are higher expressed than *MtPIN5* and 7 in Medicago roots. Data are means and  $\pm$ SD.

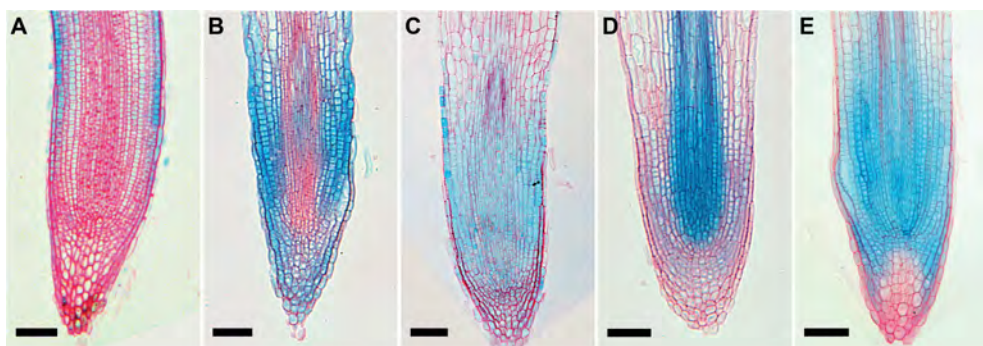


Fig. S3. *MtPIN* promoter::GUS activity in Medicago root meristem region. In the root meristematic region, (B, D, E) *MtPIN2*, 4 and 10 are expressed at a relatively high level compared to (A, C) *MtPIN1* and *MtPIN3*. (A) *MtPIN1* is expressed in epidermis and weakly in root cortex; (B) *MtPIN2* in cortex and epidermis; (D) *MtPIN4* in root vascular bundle; (C) *MtPIN3* and (E) *MtPIN10* are expressed in all root tissues, except root cap and columella cells. Bars equal to 75  $\mu$ m.

# CHAPTER 4

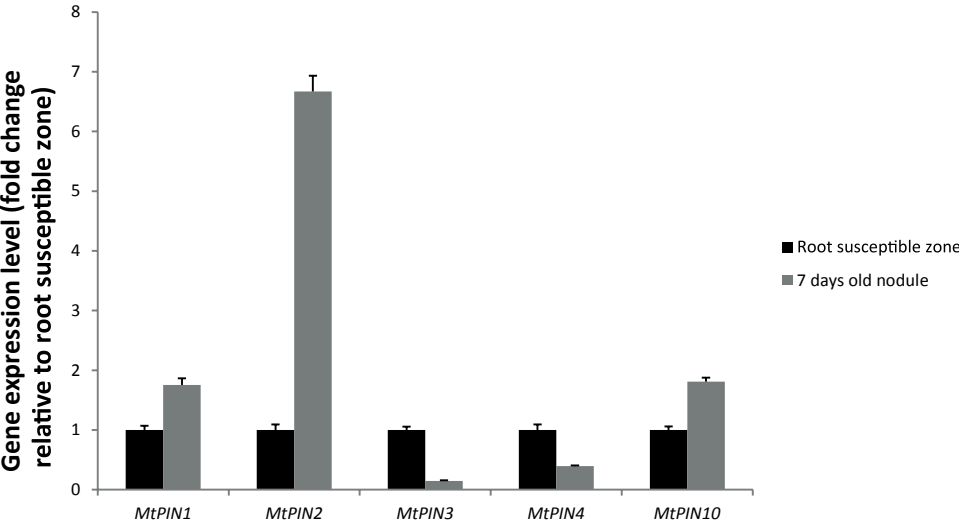


Fig. S4. *MtPINs* expression after 7 days after inoculation. Seven days after spot-inoculation with *S. meliloti* 2011, *MtPIN1*, 2 and 10 expression levels are increased in Medicago root compare to the root susceptible zone, especially, *MtPIN2* (more than 6 fold increase). While, *MtPIN3* and *MtPIN4* expression are reduced. Data are means and +/-SD.

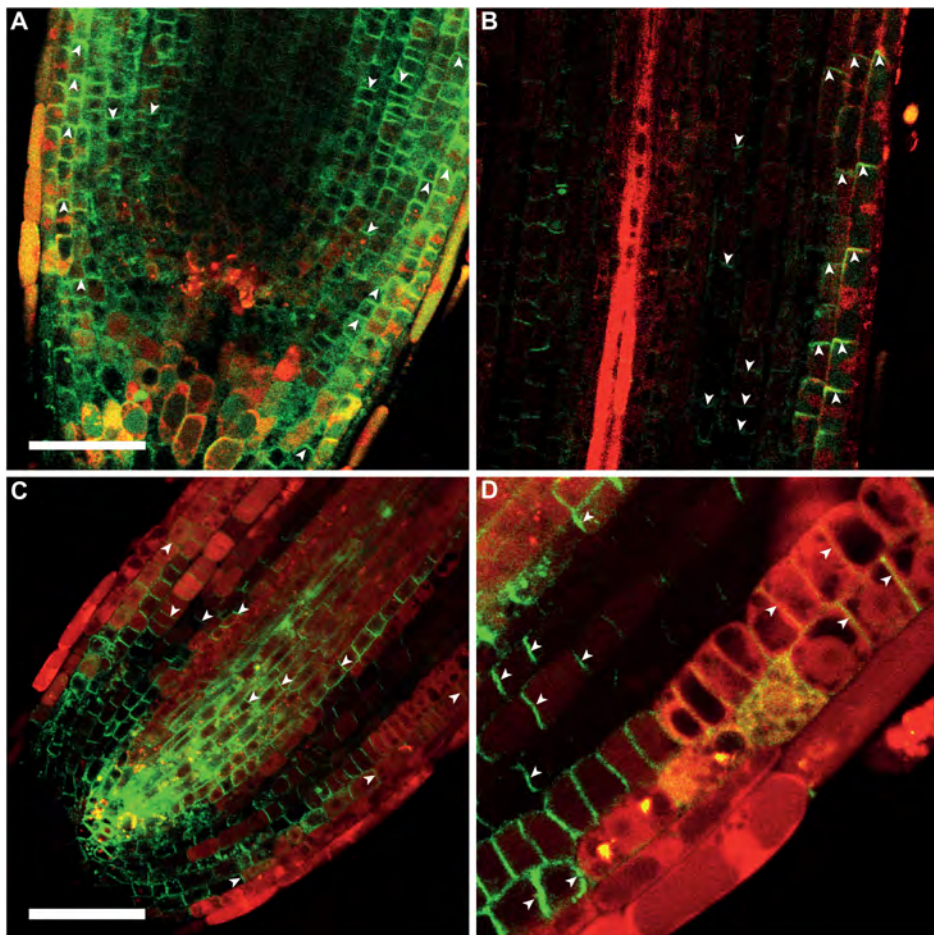


Fig. S5. *MtPIN2* and *MtPIN10* sub-cellular localization in *Medicago* root meristem region. (A, B) *MtPIN2* accumulates in cortex, epidermis and lateral root cap cells. (A) *MtPIN2* is apical localized in the root epidermis and lateral root cap cells; basal localized in the cortex. (B) From the transition zone shoot ward, which is located between the root meristem and elongation zone, *MtPIN2* is apically localized in the outer cortex (about C1 and C2) and remains basal in the inner cortex. (B) Shoot-ward from the transition zone, the PIN level dramatically decreases and no longer detectable. (C, D) *MtPIN10* accumulates in all root tissues of the root meristem region. (C) It is basal localized in the vascular tissues and cortex; apical localized in epidermis and lateral root cap cells. (D) *MtPIN10* level markedly decreased before the meristematic cells enter the transition zone.

Bars equal to 60  $\mu$ m.

# CHAPTER 4

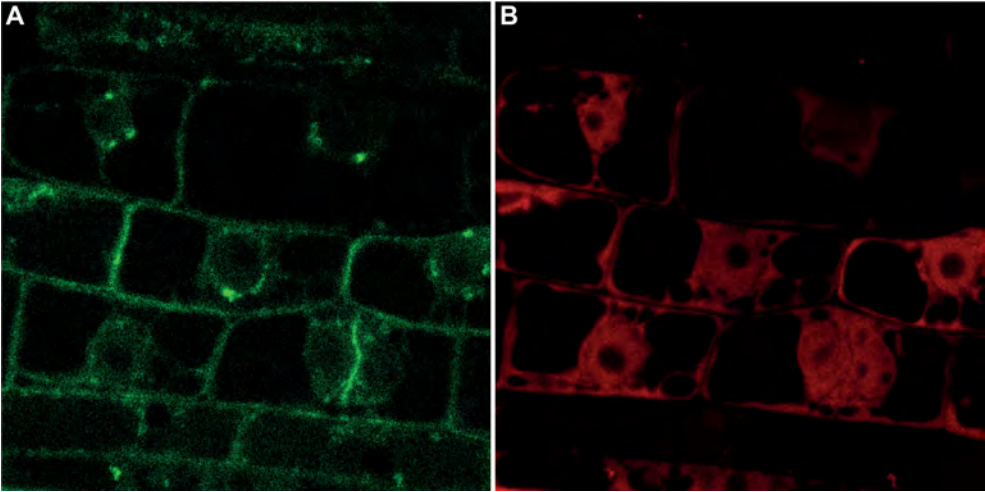


Fig. S6. Split channel of Fig. 5B.

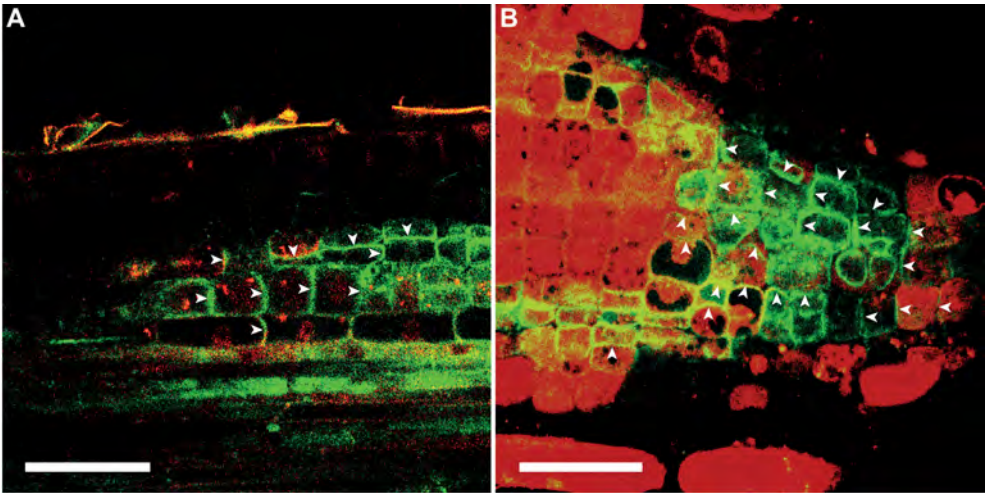


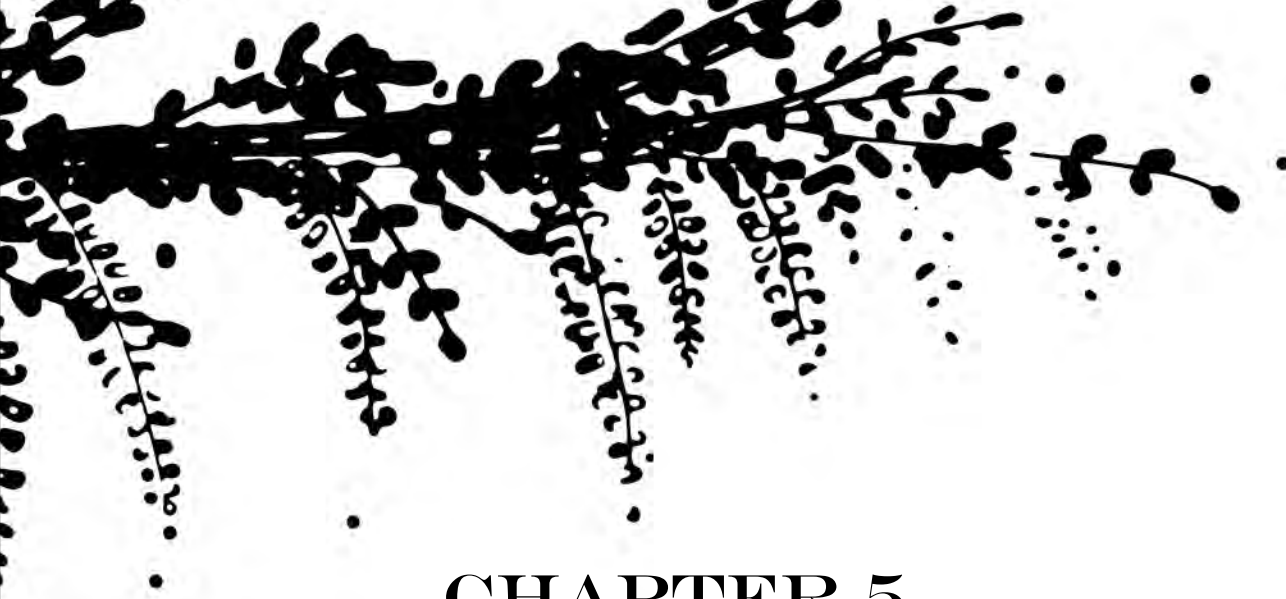
Fig. S7. *MtPIN10* is positioned towards the center of the nodule primordium at the periphery of the nodule primordium. Bars equal to 60  $\mu\text{m}$ .

## *Auxin transport during root nodule formation*

Table S1. Primers for PCR products.

<b>Primers for <i>MtPINs</i> protein GFP fusion constructs</b>	
MtPIN2-F1	GGGGACAACCTTTGTATAGAAAAGTTGCGGACACTATTCTAAGTAGCGTTTG
MtPIN2-R1	GGGGACTGCTTTTTTGTACAAACTTGCCTTTTGATGCAACGGAATTTTC
MtPIN2-F2	GGGGACAGCTTTCTTGTACAAAGTGGGACTGTTACTGAATTGATTGAGAAC
MtPIN2-R2	GGGGACAACCTTTGTATAATAAAGTTGCCAATGCAAAGAATCCACTATG
MtPIN10-F1	GGGGACAACCTTTGTATAGAAAAGTTGCGTGCTCGAATATTAGCCCAAC
MtPIN10-R1	GGGGACTGCTTTTTTGTACAAACTTGCCATAGCTTCACCTTGAGATCCAG
MtPIN10-F2	GGGGACAGCTTTCTTGTACAAAGTGGAGCCAACAACATGCCAC
MtPIN10-R2	GGGGACAACCTTTGTATAATAAAGTTGGTGGCGGAATTCCTC
eGFP-F	GGGGACAAGTTTGTACAAAAAAGCAGGCTCCCGGGGGTACCTGGTGAGCAAG-GGCGAGGA
eGFP-R	GGGGACCACTTTGTACAAGAAAGCTGGGTACTTGTACAGCTCGTCCATGC
<b>Primers for <i>MtPINs</i> promoter GUS fusion constructs</b>	
pMtPIN1-F1	TACAATCCGCTCCTTATCTGTTC
pMtPIN1-R	TTTGATGAAGGCTTTTTTGGA
pMtPIN2-F	GAGGGACAATAGAGGTGTAGAGTTG
pMtPIN2-R	GGTTATAGATAGGTCAAGGTAGATTAGATTAGAC
pMtPIN3-F1	TTAAGATAACCATAGCATGCAGTCAC
pMtPIN3-R	TTTGGATTTTTTGTGTTTTTTTAG
pMtPIN4-F2	TCGTGGTCAAGAACGTTCTC
pMtPIN4-R	GTTTTTGAGTTGAGGTTTGAAGAAG
pMtPIN10-F	TGCTCGAATATTAGCCCAAC
pMtPIN10-R	TTTGTGCTTATTGAAGTTTTG





## CHAPTER 5

### *Root developmental programs shape the Medicago truncatula nodule meristem*

**Henk J. Franssen<sup>1,5</sup>, Ting Ting Xiao<sup>1</sup>, Olga Kulikova<sup>1</sup>, Xi Wan<sup>1,2</sup>,  
Ton Bisseling<sup>1,3</sup>, Ben Scheres<sup>4</sup> and Renze Heidstra<sup>4</sup>**

<sup>1</sup> Laboratory of Molecular Biology, Department of Plant Sciences, Wageningen University, Droevendaalsesteeg 1, 6708 PB Wageningen, The Netherlands

<sup>2</sup> Present address: BGI-Shenzhen, 518083 Shenzhen, China

<sup>3</sup> College of Science, King Saud University, Post Office Box 2455, Riyadh 11451, Saudi Arabia

<sup>4</sup> Laboratory of Plant Developmental, Department of Plant Sciences, Wageningen University, Droevendaalsesteeg 1, 6708 PB Wageningen, The Netherlands

<sup>5</sup> To whom correspondence should be addressed: [henk.franssen@wur.nl](mailto:henk.franssen@wur.nl)

## CHAPTER 5

### SUMMARY

Nodules on the roots of legume plants host nitrogen-fixing rhizobium bacteria. Several lines of evidence indicate that nodules are evolutionary related to roots. We determined whether patterning of the *Medicago truncatula* nodule meristem bears resemblance to that in root meristems through analyses of root meristem expressed *PLETHORA* genes. In nodules, particular *PLETHORA* genes are preferentially expressed in cells positioned at the periphery of the meristem abutting nodule vascular bundles. Their expression overlaps with an auxin response maximum and *WOX5* that marks the root quiescent centre. Strikingly, the cells in the central part of the nodule meristem have a high level of cytokinin and also display *PLETHORA* gene expression. Nodule-specific knock-down of *PLETHORA* genes results in reduced number of nodules and/or in nodules in which meristem activity has ceased. Our nodule gene expression map indicates that the nodule meristem is composed of two domains and that *PLETHORA* genes redundantly function in nodule meristem maintenance.

**Keywords:** *Medicago truncatula*, nodule meristem, *PLETHORA* genes, *DR5*

## **INTRODUCTION**

The interaction between legumes and soil-borne bacteria collectively known as rhizobia leads to the formation of new organs, root nodules (Stougaard, 2001; Limpens and Bisseling, 2003). As nodules are formed on roots it has been hypothesized that the nodule developmental program is derived from the lateral root developmental program (Nutman, 1948; Hirsch et al., 1997; Mathesius et al., 2000; de Billy et al., 2001; Roudier et al., 2003; Bright et al., 2005; Desbrosses and Stougaard, 2011). Recently, the expression of several root meristem regulators has been observed in the nodule meristem (NM) (Osipova et al., 2011; Osipova et al., 2012; Roux et al., 2014), thereby creating molecular support for this hypothesis. However, whether the identified genes function in the formation of NM and root meristem (RM), a prerequisite for concluding that nodule developmental program is derived from that of the root, remained unclear.

Root tissues are continuously replenished by stem cells and in *Arabidopsis* these stem cells are surrounding the quiescent center (QC) cells (Dolan et al., 1993). The QC functions as a so-called organizer and is essential for maintenance of the surrounding stem cells (van den Berg et al., 1997) and together they form the stem cell niche. The daughter cells of these stem cells form files of transit-amplifying cells and together with the stem-cell niche they form the RM (Heidstra and Sabatini, 2014).

Auxin accumulation is critical for the specification of the stem cell niche in the *Arabidopsis* RM that co-localizes with an auxin concentration and response maximum (Sabatini et al., 1999; Blilou et al., 2005; Petersson et al., 2009). Several *Arabidopsis* transcription factors have been identified that are required for proper formation and function of the root stem cell niche, among them WUSCHEL-RELATED-HOMEOBOX 5 (WOX5; Sarkar et al., 2007), SCARECROW (SCR; Di Laurenzio et al., 1996; Sabatini et al., 2003) and four PLETHORAs (PLTs; Aida et al., 2004; Galinha et al., 2007). WOX5 transcript accumulates specifically in the QC and mutant analyses revealed that it functions to preserve QC activity with respect to columella stem cell maintenance (Sarkar et al., 2007). PLTs are part of the small AINTEGUMENTA-like (AIL) gene clade of transcriptional regulators within

## CHAPTER 5

the large AP2/ERF family (Horstman et al., 2014). Among this clade, *PLT1-4* are essential for root formation as their higher order mutants are rootless (Galinha et al., 2007). In double mutants of *plt1/plt2* stem cells and transit-amplifying cells are lost, while ectopic expression of is sufficient to induce root niche formation (Aida et al., 2004; Galinha et al., 2007). This shows that a combination of PLT1 and PLT2 is most indicative for RM activity. A gradient of PLT activity controls root zonation and the highest PLT concentration co-localizes to the stem cell niche (Mähönen et al., 2014).

Legume nodule formation is initiated by dedifferentiation of cortical cells which divide and form the nodule primordium. Upon infection by the microsymbiont, the nodule meristem (NM) is formed at the apex of the primordium (Timmers et al., 1999; Stougaard, 2001; Limpens and Bisseling, 2003). In the model legume *Medicago*, that forms nodules with a persistent meristem at its apex, nodule development can be divided in 6 stages based on the sequential pattern of anti- and periclinal cell division events in inner cortical cell layers C3-C5, endodermis and pericycle (Xiao et al., 2014). The cluster of cells formed up till stage V is called the nodule primordium. It consists of 6-8 cell layers derived from pericycle and endodermis, about 8 cell layers of infected cells derived from the inner cortical cell layers C5 and C4 and a few cell layers derived from cortical cell layer C3 that will develop into the nodule meristem (Xiao et al., 2014). From stage VI onward the *Medicago* nodule apical meristem becomes functional and adds cells to form the different nodule tissues; the central tissue, consisting of infected and non-infected cells, and the peripheral tissues including the nodule cortex, endodermis and parenchyma. The latter contains vascular bundles, that develop from nodule vascular meristems (NVM) (Roux et al., 2014). The part of the NM that adds cells to the central tissue forms a large domain at the apex and is composed of 4-6 cell layers. Transition of meristem cells to the central tissue cells is accompanied with a switch from mitosis to endo-reduplication in the cells that become infected by rhizobia (Cebolla et al., 1999).

Recent studies confirmed the expression of a number of known root meristem regulators in the nodule, among them *MtWOX5*, *MtPLT2* and *MtBBM/PLT4* (Osipova et al., 2011; Osipova et al., 2012; Roux et al., 2014).

These genes appeared to be expressed in the central meristem region and at the tip of the nodule vascular bundles, where also a maximum DR5 activity is observed (Couzigou et al., 2013), suggesting that a root-like developmental program is operational in the NM. To functionally address how the nodule developmental program resembles the root developmental program, we studied the expression of *MtPLT* genes in the NM and the effect of their knock-down on nodule formation. Based on these results we propose that the NM consists of a distinct central and peripheral meristematic domain and four *MtPLT* (*MtPLT1-4*) genes redundantly control nodule formation and NM maintenance. This is reminiscent of the described function of *AtPLT* genes in root development and suggests that rhizobia recruited major regulators of root development.

## RESULTS

### ***MtPLT* genes are required for nodule development and NM maintenance**

Recent studies showed that *MtPLT2* and *MtBBM/PLT4* are expressed in the NM (Limpens et al., 2013; Roux et al., 2014). We asked whether also the *Medicago* orthologs of *AtPLT1* and *AtPLT3* (Aida et al., 2004; Galinha et al., 2007) are expressed in the NM and performed reciprocal BLAST searches using the *AtPLT* protein sequences as a query to identify their homologs in *Medicago* (Table 1). The proposed gene annotations were subsequently used to design primers (Table S2) to enable gene expression studies by qPCR. Our data reveal that all four *MtPLT* genes are expressed in nodules, albeit at lower levels than in roots (Fig. 1A).

Table 1. Accession numbers of *Arabidopsis thaliana* and *Medicago truncatula* *PLETHORA* genes.

	<i>Arabidopsis thaliana</i>	<i>Medicago truncatula</i>
PLT1	At3g20840	MtR_2g098180
PLT2	At1g51190	MtR_4g065370
PLT3	At5g10510	MtR_5g031880
PLT4 (BBM)	At5g17430	MtR_7g080460

Crucial for root growth is the maintenance of the RM, a process for which in *Arabidopsis* four redundantly acting *PLT* genes are essential (Aida et al.,

## CHAPTER 5

2004; Galinha et al., 2007). Therefore, we asked whether down-regulation of *MtPLT* expression will influence nodule growth and whether *MtPLT* genes act redundant. We first reduced the expression of the individual *MtPLT* genes by RNA interference (RNAi) under the control of the 35S promoter by *A. rhizogenes*-mediated root transformation. We analysed nodules formed on at least 15 transgenic roots 15 d post inoculation in two experimental replicas. The level of *MtPLT* gene expression reduction was determined by qPCR on RNA isolated from roots and nodules (Fig. S1A,B). This showed that different degrees of RNA reduction were obtained for the different genes in roots as well as in nodules. However, RNAi did not lead to a significant reduction in nodule number compared to the number of nodules formed on control roots in all replicas (data not shown). Next, we investigated in detail the effect of *MtPLT* knock-down expression on nodule development by analysing serial micro-sections of control and transgenic nodules and counting the cell layers in meristem, infection and the fixation zone (Fig. S2, Table S1). We did not observe significant differences between the number of cell layers in *MtPLT* knock-down and control nodules. Altogether, these results indicate that down-regulation of individual *MtPLT* genes has no large effect on nodule development. Subtle effects, however, may remain uncovered due to the variation between transgenic roots obtained after a hairy root transformation (Limpens et al., 2004).

In contrast to single *plt* mutants, *Arabidopsis* root growth in compound *plt* mutants is severely hampered (Aida et al., 2004; Galinha et al., 2007) indicating redundant activity of *AtPLT* genes. Therefore, it is possible that *MtPLT* genes act redundantly in nodule growth. However, the formation of nodules requires the formation of roots. To demonstrate the effect of reducing gene expression of more than one *MtPLT* in nodules, we conducted RNA interference using the *MtENOD12* promoter. During nodule ontogenesis this gene is activated in the nodule primordium, the NM and in the infection zone of mature nodules (Limpens et al., 2009; Limpens et al., 2013). We tested the effect of simultaneous down-regulation of *MtPLT1* and *MtPLT2* (*MtPLT1i/2i*), *MtPLT3* and *MtPLT4* (*MtPLT3i/4i*) and of all four *MtPLT* genes (*MtPLTi*) in three replicas on nodule growth and development.

The level of down-regulation of the *PLT* genes was determined by qPCR (Fig. 1B-D). We confirmed that *MtPLT1* and *MtPLT2* RNA levels were reduced in transgenic *MtPLT1i/2i* nodules, while *MtPLT3* and *MtPLT4* RNA levels were not (Fig. 1B). Similarly, *MtPLT3* and *MtPLT4* RNA levels were reduced in *MtPLT3i/4i* nodules, while *MtPLT1* and *MtPLT2* RNA levels were not (Fig. 1C). In transgenic *MtPLTi* nodules all *MtPLT* genes were reduced in their expression, albeit to different levels (Fig. 1D). On transgenic quadruple *MtPLTi* roots the number of nodules was reduced by 80% (Mann Whitney test,  $p < 0.001$ ) compared to control roots, while the reduction in the number of nodules formed on transgenic *MtPLT1i/2i* or *MtPLT3i/4i* roots reached 50% (Mann Whitney test,  $p < 0.05$ ).

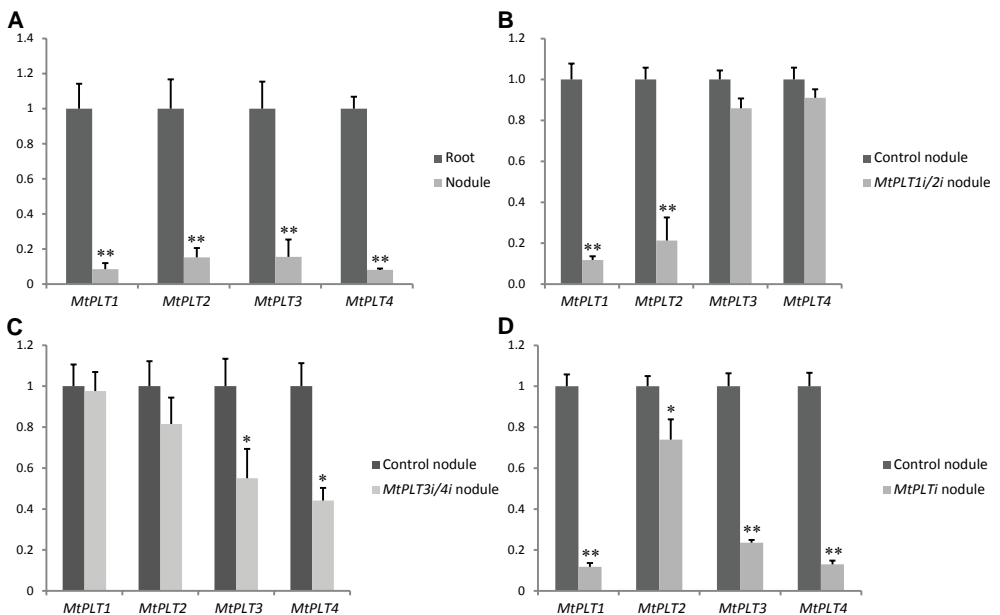


Fig. 1. Quantification of *MtPLT* expression levels in non-transgenic roots and nodules and RNAi nodules.

(A) Relative *MtPLT* expression in 15 d old nodules (grey bar) compared to their expression in roots (black bar) shows that expression in nodules is lower than in roots (expression is normalized to 1 in roots for each *MtPLT* gene); (B-D) Relative *MtPLT* expression (grey bars) in 15 d old transgenic nodules *MtPLT1i/2i* (B); *MtPLT3i/4i* (C) and *MtPLTi* (D) with respect to expression in control nodules (black bars, normalized to 1 for each *MtPLT* gene).

Quantification was normalized using *MtACTIN-2* as reference gene. Bars represent SD of three technical repeats. A representative of three biological replicas is shown. (\* is  $P < 0.05$ , \*\*  $P < 0.001$  in t test).

## CHAPTER 5

All multiple *MtPLT* RNAi transgenic nodules were smaller compared to nodules on control roots. To determine potential causes of the size reduction, we analysed longitudinal sections of transgenic nodules (Fig. 2). Analyses of 20 control nodules, collected per replica, shows that the NM consists of 4-6 cell-layers and the central tissue of 16-19 cell layers distributed over 6-7 cell-layers in the infection zone and 10-12 cell layers in the fixation zone (Fig. 2A). We analysed the transgenic nodules collected from the three replicas, collected 15 days after inoculation and observed a high percentage of phenotypically aberrant nodules (Table 2). We classified the observed phenotypes into two groups: class I nodules in which the number of cell layers in meristem and infection zone is reduced (Fig. 2B) and class II nodules that lack the NM and the infection zone. These class II nodules only consist of 6-8 layers of infected cells (Fig. 2C). Notably, a complete block of meristem formation still allows nodules with 6 layers of infected cells, which are derived from the C4 and C5 cortical cells (Xiao et al., 2014). These results indicate that *MtPLT* activity is needed for proper NM formation and maintenance, but not for infection of primordium cells.

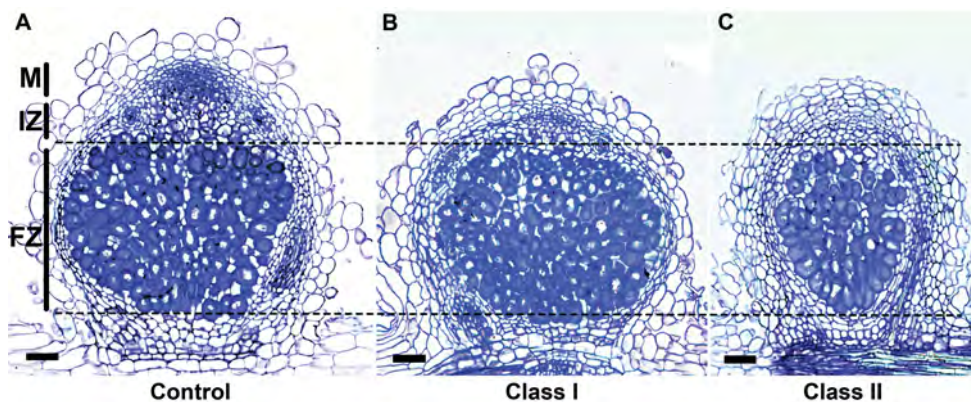


Fig. 2. RNA-interference of *MtPLT* genes affects meristem formation of *Medicago* nodules.

(A) Control wild type nodule. Apart from wild-type looking nodules, two classes of nodules are formed after RNA-interference of more than one *MtPLT* gene. (B) Representative class I nodule. The number of cell layers in meristem (M) and infection zone (IZ) is reduced. (C) Typical class II nodules lacking a meristem. All infected cells in the fixation zone (FZ) originate from primordium cells derived from C4 and C5 cortex layers.

Bars, 75 μm.

In nodules formed on *MtPLT1i/2i* roots, 71% of the affected nodules grouped into class I (n=25 out of 35). This percentage decreases to 64% in *MtPLT3i/4i* nodules (n=9 out of 14) and to 31% in *MtPLTi* nodules (n=5 out of 16, Table 2). In contrast, 69% of the *MtPLTi* nodules fall into class II (n= 11 out of 16, Table 2). These percentages show that the down-regulation of all four *MtPLT* genes simultaneously has a more dramatic effect on meristem formation and maintenance than down-regulation of a combination of only two *MtPLT* genes, indicating that *MtPLT* activity is redundant in nodule development.

Table 2. Percentage of nodules showing phenotypes of class I and class II.

RNAi	N(#)	Phe(#)	% Phe	Class I(#)	Class II(#)	%I	%II
<i>MtPLT1/2i</i>	54	35	65	25	10	71	29
<i>MtPLT3/4i</i>	23	14	61	9	5	64	36
<i>MtPLTi</i>	21	16	76	5	11	31	69

Two types of phenotypes (Phe) were distinguished for *MtPLT* RNAi nodules;

I reduced number of layers in meristem derived from C3 cells, infection zone, and infected primordium cells derived from C4 and C5.

II no meristem, no infection zone, only infected primordium cells; derived from C4 and C5.

N (#) total number of nodules collected over three independent biological replicas.

Phe is the number of nodules with a phenotype

In conclusion, our results show that *MtPLT* genes redundantly affect nodule development through NM formation.

### ***MtPLT* promoter activity marks the Medicago RM**

The striking difference between *PLT*-directed root and nodule growth is that *Mtplt3/4i* affects nodule growth, while in Arabidopsis *plt3/plt4* knock-out mutants minimally affect root growth (Galinha et al., 2007). To seek a putative explanation for this discrepancy, we compared expression patterns of the different *MtPLT* genes by using *pMtPLT::GUS* fusions in nodule and root. In Arabidopsis, *AtPLT3* and *AtBBM/AtPLT4* are expressed in the RM in an overlapping but slightly different pattern compared to *AtPLT1* and *AtPLT2* (Galinha et al., 2007). Before testing the activity of *MtPLT* promoters in the NM, we first identified their activation pattern in the root.

In primary Medicago roots, cell files converge to a group of cells that

## CHAPTER 5

are suggestive to be QC cells (Fig. 3A, arrow). Distal of the QC cells are the columella cells that accumulate starch granules (Fig. 3A). Similar to the pattern observed in *Arabidopsis* (Sabatini et al., 1999), the highest level of *DR5::GUS* expression is detectable in the proposed stem cell niche in *Medicago* roots of plants into which a *DR5::GUS* construct was integrated (Fig. 3B). Comparison of *MtPLT1::GUS* (Fig. 3C), *MtPLT2::GUS* (Fig. 3D), *MtPLT3::GUS* (Fig. 3E) and *MtPLT4::GUS* (Fig. 3F) expression patterns shows that these are mostly overlapping in the RM with the highest activation coinciding with the root stem cell niche. This indicates that the *MtPLT::GUS* and *AtPLT* gene activation patterns (Galinha et al., 2007) are similar in the RM. It has been shown that the activation pattern of *MtWOX5::GUS* also marks the proposed stem cell niche (Osipova et

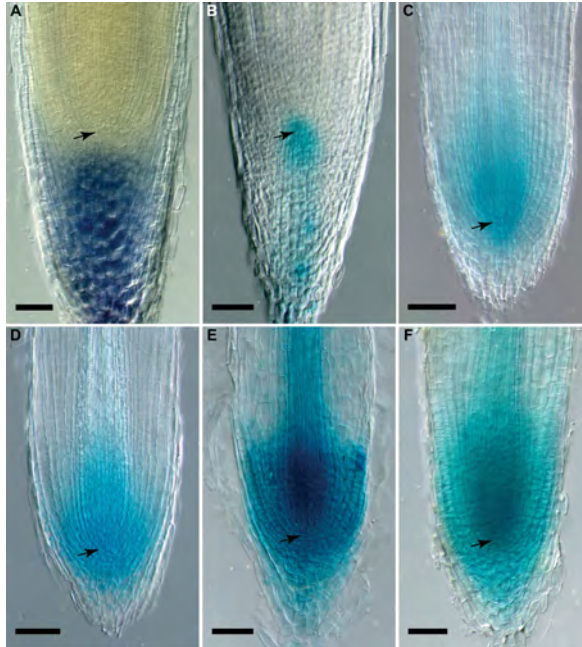


Fig. 3. *GUS* expression patterns of *PLT* and *DR5* promoters in the *Medicago* RM. (A) *Medicago truncatula* root apical meristem stained with Lugol to visualize starch granules. Cell files converge to a central point showing the presence of the presumptive QC cells (arrow). Distally are the columella cells that accumulate starch. (B) In a *DR5::GUS* transgenic root *DR5* is active in a cluster of cells encompassing the QC. (C) *MtPLT1::GUS*, (D) *MtPLT2::GUS*, (E) *MtPLT3::GUS* and (F) *MtPLT4::GUS* expression patterns are overlapping with the highest activity in and around the QC. Arrow indicates the location of the presumptive QC. Bars, 75  $\mu$ m.

al., 2012). Hence, *MtPLT::GUS*, *DR5::GUS* and *MtWOX5::GUS* expression patterns can be used to mark RM-like compartments in Medicago nodule organogenesis.

### ***MtPLT::GUS* promoter activity in nodule primordia**

The dramatic reduction in nodule numbers on the quadruple *MtPLT*i roots indicates that *MtPLT* gene activity is crucial in nodule primordium formation. If so, *MtPLT* genes should be expressed in nodule primordia. To test this, we analysed sections of *pMtPLT::GUS* containing transgenic hairy roots for promoter activation in stage II-V primordia (Xiao et al., 2014). These analyses revealed that the promoters of all four *PLT* genes are indeed activated in primordia (Fig. 4A-D) confirming their crucial role in nodule formation.

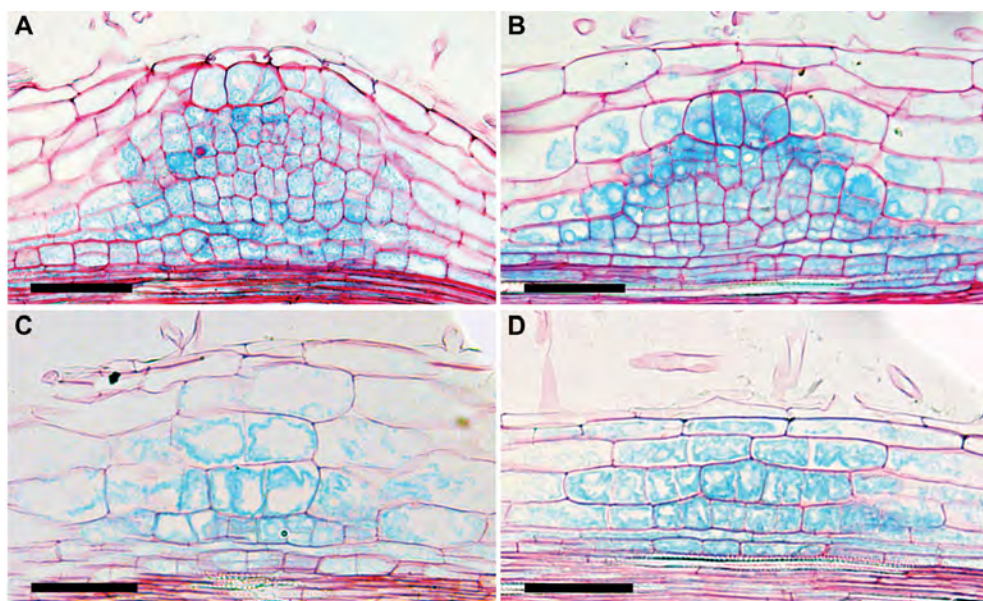


Fig. 4. *MtPLT* genes are activated in the nodule primordium.

(A-D) Examples of nodule primordia of stages II-V (according to Xiao et al., 2014) showing *MtPLT1::GUS* (A, stage IV) *MtPLT2::GUS* (B, stage III) *MtPLT3::GUS* (C, stage II) and *MtPLT4::GUS* (D, stage II) activity.

Bars, 75 μm.

### **Patterns of *MtPLT* activation and auxin-cytokinin response mark distinct meristematic domains in the NM**

## CHAPTER 5

Cells in the *Medicago* NM divide for a prolonged time, suggesting that stem cells may contribute to the maintenance of the NM. *DR5::GFP* (Couzigou et al., 2013) and *MtWOX5::GUS* (Osipova et al., 2012) activation patterns have been allocated to distinct peripheral regions in the NM abutting vascular bundles (Fig. 5A, B arrows). Presuming that *DR5::GUS* and *MtWOX5::GUS* co-localize to areas of stem cell activity in nodules, in analogy to the situation in roots, this observation suggests that stem cells are present in the NM periphery. Strikingly, upon prolonged time of incubation (16 hours) *DR5* activity also becomes detectable throughout the nodule apex (Fig. 5C, arrowhead), including the central part of the NM.

For both *MtPLT1::GUS* and *MtPLT2::GUS*, we observed that GUS activity is highest in discrete domains within the nodule apex (Fig. 5D, E arrows) similar to *DR5* and *MtWOX5* expression (Fig. 5A, B). The domains of high *PLT* promoter activity appear embedded in a region with lower GUS activation

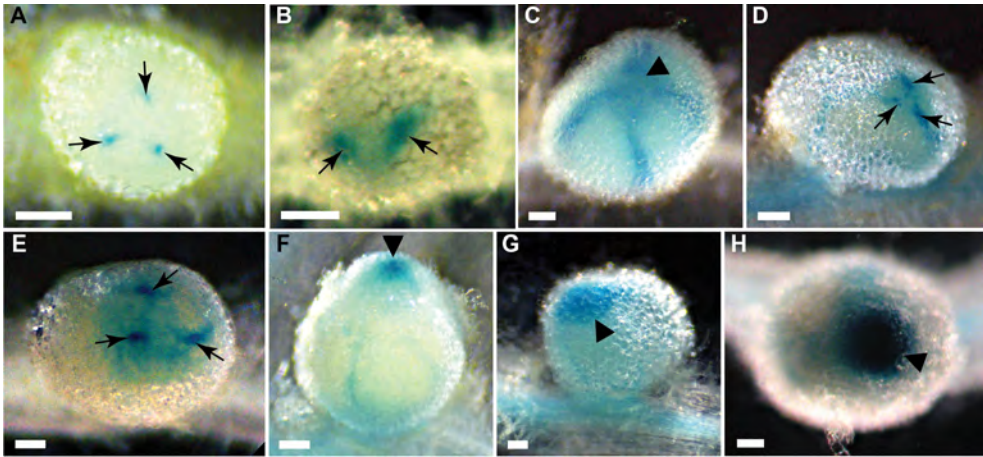


Fig. 5. *DR5*, *MtWOX5*, *MtPLT* and *TCS* promoter activities in nodules.

(A, B) Top view of a *DR5::GUS* nodule (A) and *MtWOX5::GUS* (B) nodule shows GUS activity in distinct regions at the periphery in the NM (arrows). (C) Upon prolonged incubation time GUS activity becomes apparent throughout the NM in *DR5::GUS* nodules (arrowhead). (D, E) Top view on *MtPLT1::GUS* (D) and *MtPLT2::GUS* (E) nodules show highest GUS activity in discrete regions in the periphery in the NM (arrows), with a lower GUS activity throughout the NM (arrowhead). (F, G) *MtPLT3::GUS* (F) and *MtPLT4::GUS* (G) activity throughout the NM (arrowhead). (H) Top view of a *TCS::GUS* nodule marking the whole NM.

Bars, 75  $\mu$ m.

encompassing the NM. In contrast, *MtPLT3::GUS* and *MtPLT4::GUS* are activated throughout the nodule apex (Fig. 5F, G arrowhead).

To determine whether the activation patterns of *DR5::GUS*, *MtWOX5::GUS* and *MtPLT2::GUS* in the NM periphery are overlapping, we analysed serial sections from the nodule apex downwards. A low *DR5* and *MtWOX5* activity is present in a sub-population of cells within the apex adjacent to the vascular bundle (Fig. 6A, D). In subsequent sections, the radial tissue organization of a vascular bundle becomes apparent and all cells of this vascular bundle display *DR5* and *MtWOX5* activity (Fig. 6B, E). Finally, within this radial organized tissue, xylem (thin arrow) and phloem can be discriminated and at this developmental stage, the activity of both *DR5* and *MtWOX5* decreases (Fig. 6C, F). Series of longitudinal sections through *MtPLT2::GUS* nodules reveals that the highest GUS activity is restricted to cells that are contiguous to nodule vascular bundles (Fig.

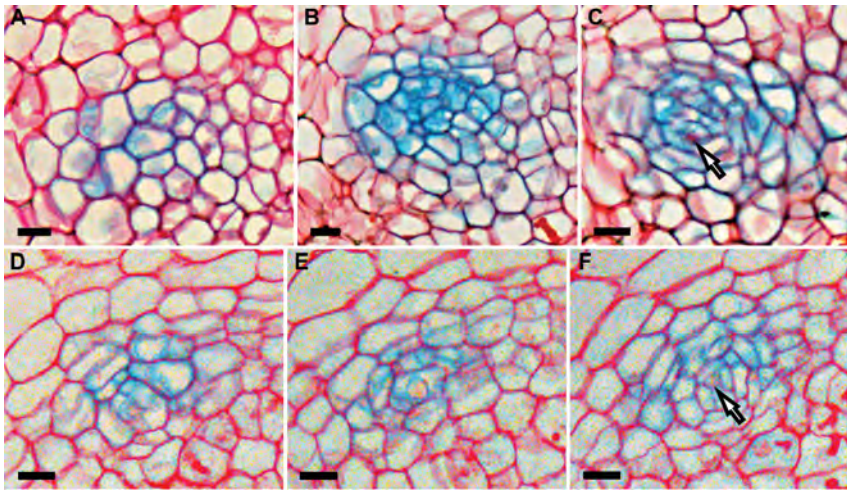


Fig. 6. *DR5::GUS* and *MtWOX5::GUS* expression patterns co-localise in the NVM. (A-C) Serial tangential sections of nodules 2h-incubated in GUS buffer to specifically localize the *DR5::GUS* activation region. A low *DR5* activity first appeared in a group of cells (A) that seemingly are not clonally linked to surrounding cells in the NM. In subsequent sections, *DR5* activity reached a maximum (B) and *DR5* activity remains in cells that are part of the nodule vascular bundle (C). (D-F) Serial tangential sections of *MtWOX5::GUS* nodules shows a pattern comparable to *DR5::GUS*. White arrow indicates differentiation of xylem in the nodule vascular bundle (compare panel A and D, panel B and E, and panel C and F). Bars, 10  $\mu$ m.

## CHAPTER 5

7A-D, arrow), resembling the *DR5* (Fig. 6A-C) and the *MtWOX5* (Fig. 6D-F) promoter activity pattern. These analyses show that *MtPLT2*, *MtWOX5* and *DR5* are active in pro-vascular tissue, in analogy with their expression pattern in *Medicago* roots (Fig. 3B, D; Osipova et al., 2011; Osipova et al., 2012). Sections of *MtPLT3::GUS* and *MtPLT4::GUS* nodules show that both mark the whole NM and, in addition, are also activated in cells of the infection zone (Fig. 7E, F), albeit at lower levels. For *MtPLT4* this is in agreement with the reported expression pattern (Roux et al., 2014).

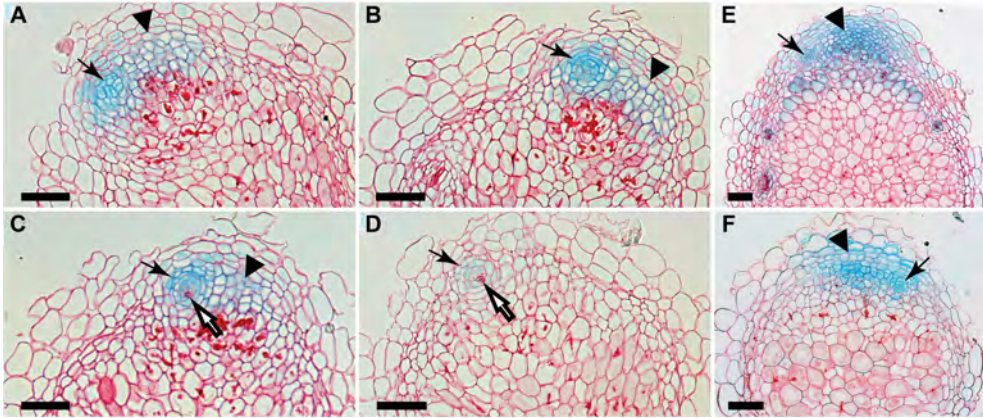


Fig. 7. Distinct *MtPLT::GUS* expression patterns in nodules. (A-D) Serial sections of *MtPLT2::GUS* nodules show that the highest *MtPLT2::GUS* activity is in the NVM (arrows). A lower *MtPLT2::GUS* activity is in the central region of the NM (A-C, arrowhead). *MtPLT3::GUS* (E) and *MtPLT4::GUS* (F) expression patterns are of equal activity in NVM (arrow) and the central part of the NM (arrowhead). White arrow indicates differentiation of xylem in the nodule vascular bundle. Bars, 75  $\mu$ m.

The co-localization of *MtPLTs* and high *DR5* activity in the periphery of the NM suggests that an auxin-driven root-derived developmental program is operational in the nodule. In addition, several genes in the cytokinin signalling cascade are reported to be activated in the NM (Frugier et al., 2008; Plet et al., 2011; Mortier et al., 2014). To determine the cytokinin response distribution in the NM, we studied the expression of *TCS::GUS*, a synthetic cytokinin responsive promoter (Muller and Sheen, 2008), in transgenic *Medicago* roots and nodules. In roots the *TCS::GUS* activation pattern (Fig. 8A) is similar to the activation pattern in *Arabidopsis* roots (Zürcher et al., 2013). In contrast to the *DR5::GUS* activity pattern

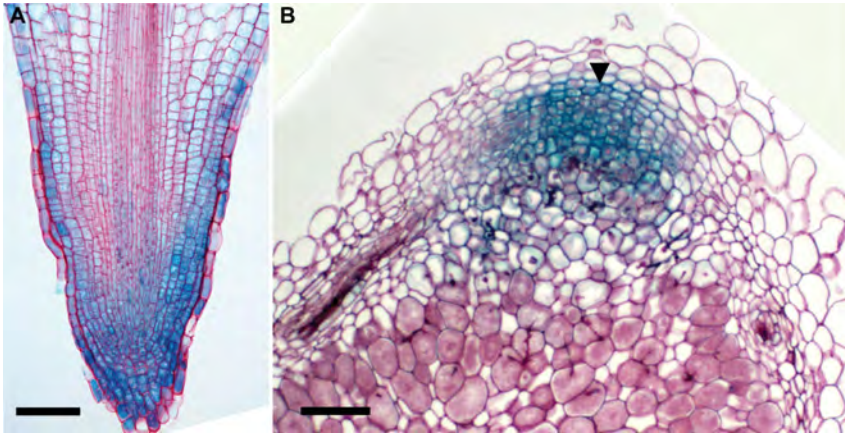


Fig. 8. *TCS::GUS* pattern in *Medicago* root and nodule.

(A) *TCS::GUS* root shows activity in columella and lateral root cap cells. (B) In nodules *TCS::GUS* activity is confined to the central region of the NM.

Bars, 75  $\mu$ m.

(Fig. 5A, C), *TCS::GUS* activation is equally distributed over the apex of the nodules (Fig. 5H). Longitudinal sections of these nodules show that *TCS::GUS* activity is confined to cells in the central part of the NM (Fig. 8B).

In conclusion, based on the activation of root meristem markers *DR5*, *MtWOX5*, *MtPLT1*, *MtPLT2*, *MtPLT3*, *MtPLT4* and *TCS*, gene expression signatures can be distinguished within the NM. One region at the periphery of the nodule that includes the NVM for which the gene activation patterns suggest that an auxin/*PLT*-directed root-like developmental program is active at each of the vascular bundle tips. A second domain is marked by high *TCS*, *MtPLT3* and *MtPLT4* activity. Cells within this second domain are centrally positioned within the NM and give rise to the central tissue. We will refer to this latter domain as the nodule central meristem (NCM). Based on our results we propose that the NM is built up of two adjacent but distinctly operating NVM and NCM.

## DISCUSSION

Down-regulation of four *Medicago* orthologs of *Arabidopsis PLETHORA* genes hampers nodule formation and growth. Therefore we conclude that root developmental programs are used in nodulation. *MtPLT1* and

## CHAPTER 5

*MtPLT2* are highly expressed in regions located at the periphery of the NM corresponding to the NVM. Also the highest auxin response activity and the activation of *MtWOX5::GUS* (Fig. 2B; Osipova et al., 2012; Roux et al., 2014) coincides with the NVM. These expression patterns indicate that the developmental program directing peripheral tissue formation bears similarities to root developmental programs in which *MtPLT* genes are key regulators (Galinha et al., 2007). However, in the absence of a suitable promoter that marks the NVM specifically, the effect of knock-down of *MtPLT* genes could not be tested in the NM periphery.

In addition to the high peripheral NM expression, *MtPLT1* and *MtPLT2* are expressed at lower levels in the central part of the NM, while *MtPLT3* and *MtPLT4* expression levels are comparable in both central and peripheral zones of the NM. In contrast to the peripheral part, characterised by a high auxin response, the central part of the NM is characterised by a higher cytokinin and a lower auxin response. Together these observations indicate that the NM harbours two meristems; one at the periphery, including the NVM (Roux et al., 2014) and the other in the central part, the NCM. Our RNAi studies show that *PLT* genes play a crucial role in NCM formation and maintenance. Interestingly, whereas root growth in *Arabidopsis* that is minimally affected in *plt3/plt4* plants (Galinha et al., 2007), nodule growth is affected in *Mtplt3i/4i* nodules. Therefore, we hypothesise that a *PLT*-directed developmental program is also involved in shaping of NCM.

During ontogenesis *MtPLT* genes are expressed in the nodule primordium including layer C3 from which the future NM will develop. However, in mature nodules *MtPLT1* and *MtPLT2* expression is high in the peripheral region but low in the NCM. This indicates that during nodule formation expression of *MtPLT1* and *MtPLT2* is reduced in the NCM. To what extent the *PLT*-directed programs that shape the NVM and the NCM differ remains to be elucidated. Comparing genes differentially regulated by either set of *MtPLTs* may provide insight into this issue. In addition, identification of genes involved in controlling expression of *MtPLT1/2* and *MtPLT3/4* may uncover how a *PLT*-directed root developmental program is recruited to form the NM and its subdomains. Such knowledge may also uncover mechanisms underlying the communication between the NVM and NCM domains to enable proper nodule growth.

In conclusion our data provide molecular and also mechanistic support that *Rhizobium* has recruited key regulators of root development for nodule formation.

## **MATERIALS AND METHODS**

### **Constructs**

DNA fragments of 1-3 Kb putative promoter regions of *MtPLT* genes were generated via PCR on *Medicago* genomic DNA as a template using Phusion High-Fidelity DNA polymerase (Finnzymes) and specific primers (Table S2). Fragments were cloned into pENTR-D-TOPO (Invitrogen) verified by nucleotide sequence analysis and recombined into the modified Gateway vector pK7GWIWG2(II)-UBQ10::DsRED-GUS-GFP (Karimi et al., 2002).

DNA of single *Medicago MtPLT* genes for RNA-interference constructs were generated via RT-PCR on cDNA made from nodule RNA using Phusion High-Fidelity DNA polymerase (Finnzymes) and gene specific primers (Table S2).

To generate *MtPLT1-MtPLT2* and *MtPLT3-MtPLT4* DNA fragments for double RNA interference constructs the single *MtPLT* DNA fragments were used as a template in a PCR using primer combinations as shown in Table S3. Fragments obtained in this way were diluted 1:500. mixed and used in a subsequent PCR using primers combinations as shown in Table S3. The obtained PCR fragment was cloned into pENTR-D-TOPO and recombined into the Gateway compatible binary vector pENOD12-pK7GWIWG2(II)-UBQ10::DsRED (Limpens et al., 2004; Ivanov et al., 2012) to create the final RNAi construct.

For the quadruple RNAi of *MtPLT* genes, *MtPLT1-MtPLT2* and *MtPLT3-MtPLT4* DNA fragments were amplified using primer combinations shown in Table S3. The obtained fragments were diluted and combined in a second PCR using primers listed in Table S3. The amplified fragment was cloned into pENTR-D-TOPO and then recombined into the Gateway compatible binary vector pENOD12-pK7GWIWG2(II)-UBQ10::DsRED (Limpens et al., 2004; Ivanov et al., 2012).

## CHAPTER 5

### Hairy root transformation

All constructed binary vectors were introduced into *M. truncatula* A17 through *A. rhizogenes*-mediated transformation as described (Limpens et al., 2004). Hybrid plants carrying transgenic roots were grown for 15 days in the presence of *S. meliloti* 2011 to induce nodules. For each experiment, at least 15 individual roots and nodules were examined.

### Histochemical GUS staining

Plant tissues containing promoter-GUS fusion, were incubated in 0.1 M  $\text{NaH}_2\text{PO}_4$ - $\text{Na}_2\text{HPO}_4$  (pH 7) buffer including 3% sucrose, 0.05mM EDTA, 0.5 mg/ml X-gluc, 2.5 mM potassium ferrocyanide and potassium ferricyanide. Incubation (at 37 °C) time varied depending on tissues and different promoter-GUS fusions. GUS stained roots were cleared (2 ml water, 1 ml glycerol, 8 g chloral hydrate). Whole mount pictures of roots were analysed by an Axio Imager A1 microscope (Zeiss, Germany) supplied with Nomarski optics.

### Histological analysis and Microscopy

Root tips and nodules were fixed in 5% glutaraldehyde in 0.1 M phosphate buffer (pH 7.2) at 4 °C overnight, then washed with 0.1 M phosphate buffer 15 min four times and once with  $\text{H}_2\text{O}$  for 15 min, dehydrated for 10 min in 10%, 30%, 50%, 70%, 90% and 100% EtOH, respectively, and embedded in Technovit 7100 (Heraeus Kulzer, Germany). Sections were made of 5-10  $\mu\text{m}$  using a microtome (RJ2035, Leica Microsystems, Rijswijk, The Netherlands), stained either by 0.05% toluidine blue (Sigma, Germany) or 0.1% ruthenium red (Sigma, Germany), mounted in Euparal (Carl Roth, GmbH, Germany), and analysed with a Leica DM5500B microscope equipped with a DFC425c camera (Leica, Microsystems, Wetzlar, Germany). At least 10 GUS-stained nodules from each transformation experiment were sectioned and analysed. Representative sections are depicted.

### ACKNOWLEDGEMENTS

We thank Tom Guilfoyle for sharing DR5 and Bruno Müller for TCS. This work was supported by the Netherlands Organization for Scientific

Research (WOTRO 86-160, X.W.).

## REFERENCES

- Aida, M., Beis, D., Heidstra, R., Willemsen, V., Blilou, I., Galinha, C., Nussaume, L., Noh, Y. S., Amasino, R. and Scheres, B. (2004). The PLETHORA genes mediate patterning of the Arabidopsis root stem cell niche. *Cell* **119**, 109-120.
- Blilou, I., Xu, J., Wildwater, M., Willemsen, V., Paponov, I., Friml, J., Heidstra, R., Aida, M., Palme, K. and Scheres, B. (2005). The PIN auxin efflux facilitator network controls growth and patterning in Arabidopsis roots. *Nature* **433**, 39-44.
- Bright, L. J., Liang, Y., Mitchell, D. M. and Harris, J. M. (2005). The LATD gene of *Medicago truncatula* is required for both nodule and root development. *Molecular Plant Microbe Interactions* **18**, 521-532.
- Cebolla, A., Vinardell, J. M., Kiss, E., Olah, B., Roudier, F., Kondorosi, A. and Kondorosi, E. (1999). The mitotic inhibitor ccs52 is required for endoreduplication and ploidy-dependent cell enlargement in plants. *The Embo Journal* **18**, 4476-4484.
- Couzigou, J. M., Mondy, S., Sahl, L., Gourion, B. and Ratet, P. (2013). To be or root to be: evolutionary tinkering for symbiotic organ identity. *Plant Signal & Behavior* **8**.
- de Billy, F., Grosjean, C., May, S., Bennett, M. and Cullimore, J. V. (2001). Expression studies on AUX1-like genes in *Medicago truncatula* suggest that auxin is required at two steps in early nodule development. *Molecular Plant Microbe Interactions* **14**, 267-277.
- Desbrosses, G. J. and Stougaard, J. (2011). Root nodulation: a paradigm for how plant-microbe symbiosis influences host developmental pathways. *Cell Host Microbe* **10**, 348-358.
- Di Lorenzo, L., Wysocka Diller, J., Malamy, J. E., Pysh, L., Helariutta, Y., Freshour, G., Hahn, M. G., Feldmann, K. A. and Benfey, P. N. (1996). The SCARECROW gene regulates an asymmetric cell division that is essential for generating the radial organization of the Arabidopsis root. *Cell* **86**, 423-433.
- Dolan, L., Janmaat, K., Willemsen, V., Linstead, P., Poethig, S., Roberts, K. and Scheres, B. (1993). Cellular organization of the *Arabidopsis thaliana* root. *Development* **119**, 71-84.
- Frugier, F., Kosuta, S., Murray, J. D., Crespi, M. and Szczyglowski, K. (2008). Cytokinin: secret agent of symbiosis. *Trends Plant Sci* **13**, 115-120.
- Galinha, C., Hofhuis, H., Luijten, M., Willemsen, V., Blilou, I., Heidstra, R. and Scheres, B. (2007). PLETHORA proteins as dose-dependent master regulators of Arabidopsis root development. *Nature* **449**, 1053-1057.
- Heidstra, R. and Sabatini, S. (2014). Plant and animal stem cells: similar yet different. *Nature Reviews Molecular Cell Biology* **15**, 301-312.

## CHAPTER 5

**Hirsch, A. M., La Rue, T. A. and Doyle, J.** (1997). Is the legume nodule a modified root or stem or an organ sui generis? *Crit Rev Plant Sci* **16**, 361-392.

**Horstman, A., Willemsen, V., Boutilier, K. and Heidstra, R.** (2014). AINTEGUMENTA-LIKE proteins: hubs in a plethora of networks. *Trends Plant Sci* **19**, 146-157.

**Ivanov, S., Fedorova, E. E., Limpens, E., De Mita, S., Genre, A., Bonfante, P. and Bisseling, T.** (2012). Rhizobium-legume symbiosis shares an exocytotic pathway required for arbuscule formation. *P Natl Acad Sci USA* **109**, 8316-8321.

**Karimi, M., Inze, D. and Depicker, A.** (2002). GATEWAY™ vectors for Agrobacterium-mediated plant transformation. *Trends Plant Sci* **7**, 193-195.

**Limpens, E. and Bisseling, T.** (2003). Signaling in symbiosis. *Curr Opin Plant Biol* **6**, 343-350.

**Limpens, E., Ivanov, S., van Esse, W., Voets, G., Fedorova, E. and Bisseling, T.** (2009). Medicago N2-fixing symbiosomes acquire the endocytic identity marker Rab7 but delay the acquisition of vacuolar identity. *The Plant cell* **21**, 2811-2828.

**Limpens, E., Moling, S., Hooiveld, G., Pereira, P. A., Bisseling, T., Becker, J. D. and Kuster, H.** (2013). cell- and tissue-specific transcriptome analyses of *Medicago truncatula* root nodules. *PLoS one* **8**.

**Limpens, E., Ramos, J., Franken, C., Raz, V., Compaan, B., Franssen, H., Bisseling, T. and Geurts, R.** (2004). RNA interference in Agrobacterium rhizogenes-transformed roots of Arabidopsis and *Medicago truncatula*. *J Exp Bot* **55**, 983-992.

**Mähönen, A. P., ten Tusscher, K., Siligato, R., Smetana, O., Diaz-Trivino, S., Salojärvi, J., Wachsmann, G., Prasad, K., Heidstra, R. and Scheres, B.** (2014). PLETHORA gradient formation mechanism separates auxin responses. *Nature* **515**, 125-129.

**Mathesius, U., Weinman, J. J., Rolfe, B. G. and Djordjevic, M. A.** (2000). Rhizobia can induce nodules in white clover by "hijacking" mature cortical cells activated during lateral root development. *Molecular Plant Microbe Interactions* **13**, 170-182.

**Mortier, V., Wasson, A., Jaworek, P., De Keyser, A., Decroos, M., Holsters, M., Tarkowski, P., Mathesius, U. and Goormachtig, S.** (2014). Role of LONELY GUY genes in indeterminate nodulation on *Medicago truncatula*. *New Phytol* **202**, 582-593.

**Muller, B. and Sheen, J.** (2008). Cytokinin and auxin interaction in root stem-cell specification during early embryogenesis. *Nature* **453**, 1094-1097.

**Nutman, P. S.** (1948). Physiological studies on nodule formation .1. The relation between nodulation and lateral root formation in red clover. *Ann Bot-London* **12**, 81-96.

**Osipova, M. A., Dolgikh, E. A. and Lutova, L. A.** (2011). Features of the expression of a meristem-specific WOX5 gene during nodule organogenesis in legumes. *Ontogenez* **42**, 264-275.

**Osipova, M. A., Mortier, V., Demchenko, K. N., Tsyganov, V. E., Tikhonovich, I. A., Lutova, L. A., Dolgikh, E. A. and Goormachtig, S.** (2012). WUSCHEL-RELATED HOMEODOMAIN5 gene expression and interaction of CLE peptides with components of the

systemic control add two pieces to the puzzle of autoregulation of nodulation. *Plant Physiol* **158**, 1329-1341.

**Petersson, S. V., Johansson, A. I., Kowalczyk, M., Makoveychuk, A., Wang, J. Y., Moritz, T., Grebe, M., Benfey, P. N., Sandberg, G. and Ljung, K.** (2009). An auxin gradient and maximum in the Arabidopsis root apex shown by high-resolution cell-specific analysis of IAA distribution and synthesis. *The Plant cell* **21**, 1659-1668.

**Plet, J., Wasson, A., Ariel, F., Le Signor, C., Baker, D., Mathesius, U., Crespi, M. and Frugier, F.** (2011). MtCRE1-dependent cytokinin signaling integrates bacterial and plant cues to coordinate symbiotic nodule organogenesis in *Medicago truncatula*. *Plant J* **65**, 622-633.

**Roudier, F., Fedorova, E., Lebris, M., Lecomte, P., Gyorgyey, J., Vaubert, D., Horvath, G., Abad, P., Kondorosi, A. and Kondorosi, E.** (2003). The Medicago species A2-type cyclin is auxin regulated and involved in meristem formation but dispensable for endoreduplication-associated developmental programs. *Plant Physiol* **131**, 1091-1103.

**Roux, B., Rodde, N., Jardinaud, M. F., Timmers, T., Sauviac, L., Cottret, L., Carrere, S., Sallet, E., Courcelle, E., Moreau, S. et al.** (2014). An integrated analysis of plant and bacterial gene expression in symbiotic root nodules using laser-capture microdissection coupled to RNA sequencing. *Plant J* **77**, 817-837.

**Sabatini, S., Heidstra, R., Wildwater, M. and Scheres, B.** (2003). SCARECROW is involved in positioning the stem cell niche in the Arabidopsis root meristem. *Gene Dev* **17**, 354-358.

**Sabatini, S., Beis, D., Wolkenfelt, H., Murfett, J., Guilfoyle, T., Malamy, J., Benfey, P., Leyser, O., Bechtold, N., Weisbeek, P. et al.** (1999). An auxin-dependent distal organizer of pattern and polarity in the Arabidopsis root. *Cell* **99**, 463-472.

**Sarkar, A. K., Luijten, M., Miyashima, S., Lenhard, M., Hashimoto, T., Nakajima, K., Scheres, B., Heidstra, R. and Laux, T.** (2007). Conserved factors regulate signalling in *Arabidopsis thaliana* shoot and root stem cell organizers. *Nature* **446**, 811-814.

**Stougaard, J.** (2001). Genetics and genomics of root symbiosis. *Curr Opin Plant Biol* **4**, 328-335.

**Timmers, A. C. J., Auriac, M. C. and Truchet, G.** (1999). Refined analysis of early symbiotic steps of the Rhizobium-Medicago interaction in relationship with microtubular cytoskeleton rearrangements. *Development* **126**, 3617-3628.

**van den Berg, C., Willemsen, V., Hendriks, G., Weisbeek, P. and Scheres, B.** (1997). Short-range control of cell differentiation in the Arabidopsis root meristem. *Nature* **390**, 287-289.

**Xiao, T. T., Schilderink, S., Moling, S., Deinum, E. E., Kondorosi, E., Franssen, H., Kulikova, O., Niebel, A. and Bisseling, T.** (2014). Fate map of *Medicago truncatula* root nodules. *Development* **141**, 3517-3528.

**Zürcher, E., Tavor-Deslex, D., Lituiev, D., Enkerli, K., Tarr, P. T. and Muller, B.** (2013). A robust and sensitive synthetic sensor to monitor the transcriptional output of the cytokinin signaling network in planta. *Plant Physiol* **161**, 1066-1075.

# CHAPTER 5

## SUPPLEMENTARY FIGURES AND TABLES

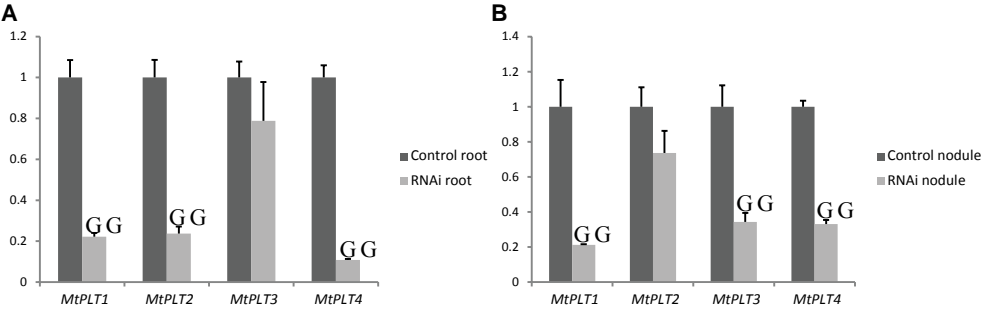


Fig. S1. Quantification of *MtPLT* expression levels. (A, B) Relative *MtPLT* expression in single *MtPLT* RNAi roots (A, grey bar) and 15 d old nodules (B, grey bar) compared to their expression in control roots and nodules (black bar), respectively. Relative expression levels were determined by qPCR and normalized to 1 in control plants for each *MtPLT* gene using *MtACTIN-2*. Bars represent SD of three technical repeats. Shown graphs are a representative of three biological repeats (\* is  $P < 0.05$ , \*\*  $P < 0.001$  in t test).

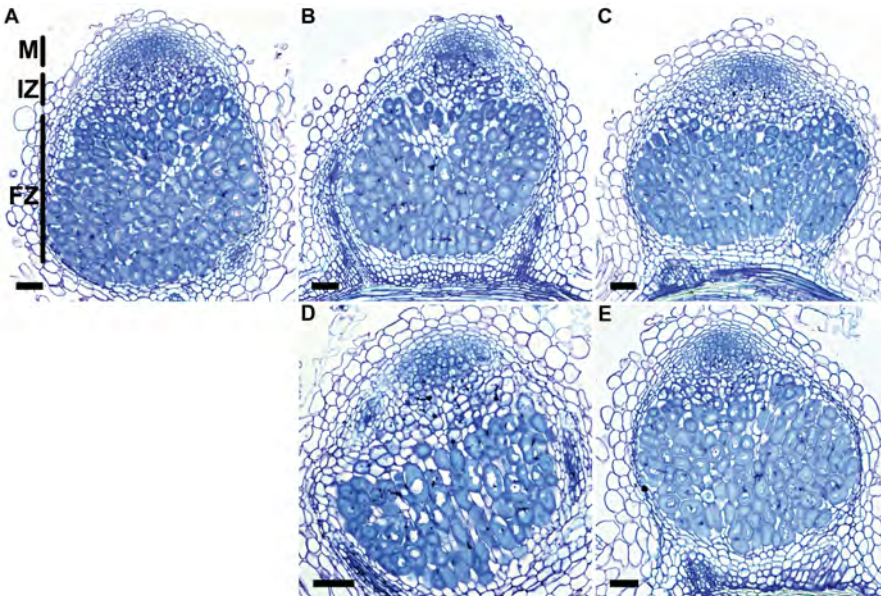


Fig. S2. Longitudinal sections of representative single *MtPLT* RNAi nodules. (A) Control nodule. (B) *MtPLT1i*. (C) *MtPLT2i*. (D) *MtPLT3i*. (E) *MtPLT4i*. All nodules were sampled 15 d after inoculation. For statistics on cell layers per zone see Table S1. M, meristem; IZ, infection zone; FZ, fixation zone. Bars, 75  $\mu\text{m}$ .

## Root nodule meristem formation

Table S1. Analyses of 20 control nodules, collected per replica, shows that the meristem consists of 4-6 cell-layers and the central tissue of 16-19 cell layers distributed over 6-7 cell-layers in the infection zone and 10-12 cell layers in the fixation zone. Compared to control nodules the meristem, infection and fixation zones of single *MtPLT* RNAi nodules consist of a number of cell layers that is within the variation observed in the control. Data was collected in two biological replicas.

	Meristem	Infection zone	Fixation zone	Nodule number
Control	4-6	6-7	10-12	20
<i>MtPLT1i</i>	4-6	6-8	10-14	19
<i>MtPLT2i</i>	4-7	5-7	9-10	17
<i>MtPLT3i</i>	4-5	6-8	8-10	20
<i>MtPLT4i</i>	4-7	7-9	8-12	17

Table S2. Primers used in this study.

Promoters	
MtpPLT1F	caccgacttgacggtgaaggtt
MtpPLT1R	gcacaacctgcattctaaaaagtttact
MtpPLT2F	caccatccaaacacacccttagtc
MtpPLT2R	gagggaatgaaagccagttattgttc
MtpPLT4F	cacctctcaaataagaatttacctccaac
MtpPLT4R	gaaagaaaaaaaaagacaaagagagatcgg
MtpPLT3F	caccttgactcccctcctctcaaag
MtpPLT3R	caaagtcttgaacagaaacaacgg
MtpWOX5F	caccaaccaagccttatcatagtat
MtpWOX5R	gctctctccatatttcaattctaga
Single MtPLTi	
MtPLT2F	cacctgaacacacacaacagcaatgaagtcc
MtPLT2R	gaagttctttgtccaaatgtctctg
MtPLT 1F	cacccttgatgaatagtagtcacaactc
MtPLT 1R	ccttggtacaccacgatatttgatg
MtPLT 4F	caccatcatcatcaacaacacttccc
MtPLT 4R	cctttaatctcactctcacc
MtPLT 3F	caccagcttcctcttcagttg
MtPLT 3R	cactgctactaccaacttc

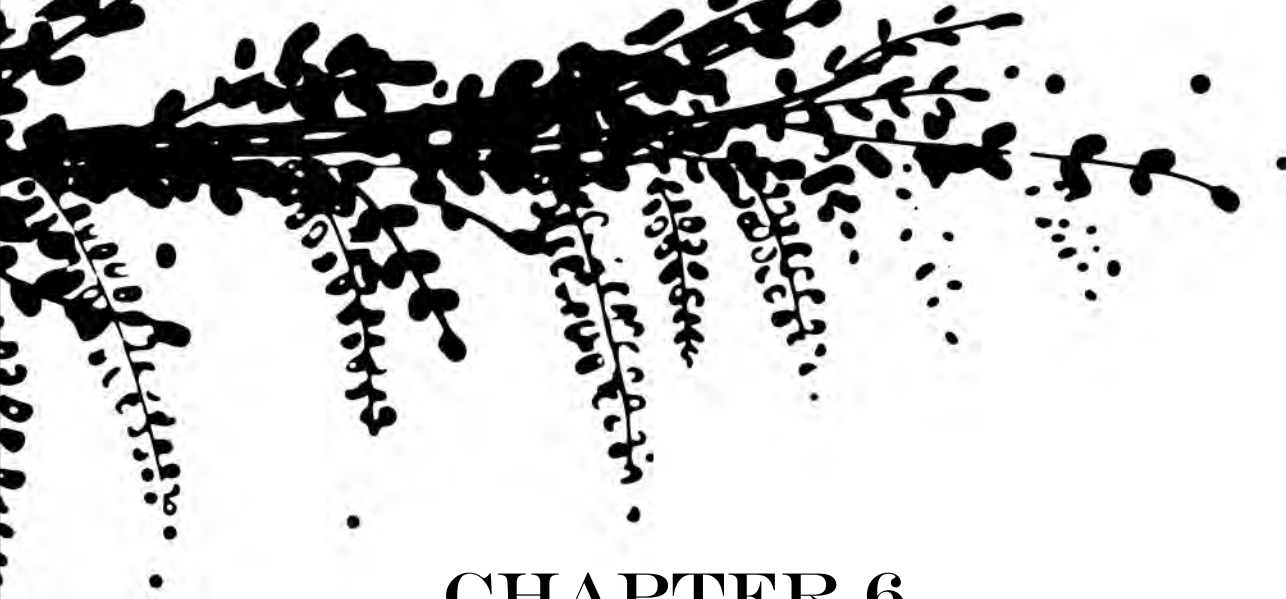
## CHAPTER 5

<b>Double MtPLTi</b>	
MtPLT 1com2R	gttgtgtgtgttcagccttggtacaccacg
MtPLT 2com1F	cgtggtgtaacaaggctgaacacacacaacag
MtPLT 4com3R	caactgaagagcatcatcaacaac
MtPLT 3com4F	gttgtgatgatgctcttcagttg
<b>Quadruple MtPLTi</b>	
12-43F	gggaagtgtgttgagaatagtagtcacaactc
43-12R	gagttgtgactactattctcaacaacacttccc
<b>qPCR primers</b>	
qMtPLT4F	tcacgagggtcatccatttaccga
qMtPLT4R	acatcatatgcctctgctgcctct
qMtPLT1F2	ggacttttggtagcgaggaa
qMtPLT1R2	tttcagcacctcctctctat
qMtPLT2R	gcaatgggtgaggttgtca
qMtPLT2F2	tcgagaaaacgcgaagaaat
qMtPLT3R	gttgctgctgctgctgtaag
qMtPLT3F	tgacgtggaagcgataatga
qMtACT2F	cagatgtggatctccaagggga
qMtACT2R	tgactgaaatatggcacaagactgaga

Table S3. Strategy to obtain *MtPLT* DNA fragments for cloning into RNAi vectors.

Final fragment	Input fragment	First PCR	Second PCR
MtPLT1-MtPLT2	MtPLT1	MtPLT1F+Mt PLT1com2R	MtPLT1F+MtPLT2R
	MtPLT2	MtPLT2com1F+MtPLT2R	
MtPLT3-MtPLT4	MtPLT3	MtPLT3com4F+MtPLT3R	MtPLT4F+ MtPLT3R
	MtPLT4	plt4F+plt4com3R	
MtPLT3-MtPLT4-MtPLT1-MtPLT2	MtPLT1-MtPLT2	12-34F+MtPLT2R	MtPLT3R2+ MtPLT2R
	MtPLT3-MtPLT4	MtPLT3R2+34-12R	





# CHAPTER 6

## *General Discussion*

**Ting Ting Xiao**

Department of Plant Sciences, Laboratory of Molecular Biology, Wageningen  
University, Droevendaalsesteeg 1, 6708 PB, Wageningen, The Netherlands

## CHAPTER 6

The evolution of root nodules, especially, the relationship between root nodule and lateral root, remains a puzzle (Hirsch and La Rue, 1997). Mutant studies are definitely very useful to understand this relationship. However, phenotypes of nodules with disturbed development are often poorly described. In this thesis, I created organ fate maps for both lateral root and root nodule by using the model species *Medicago* (Chapter 2 and Chapter 3). With these as tools, mutants could be properly analyzed. Further, I studied the mechanisms controlling nodule meristem formation and maintenance (Chapter 4 and Chapter 5). In this Discussion I will, among others, discuss the differences and similarities between legume and non-legume root nodule development. I especially focus on nodule vascular bundle and nodule meristem formation. Legumes can form determinate or indeterminate nodules. Indeterminate nodules have a persistent meristem at their apex, whereas determinate nodules have a transient meristem that is only active at early stages (Newcomb et al., 1979). *Medicago* forms indeterminate nodules. When I describe aspects of nodule development in this Discussion it confers to indeterminate nodules. However, as the tissue organization of the 2 nodule types is similar, the development will share a common part.

I will start with a short introduction on non-legume root nodule formation.

### Non-legume nodule formation

N<sub>2</sub>-fixing root nodule symbioses are confined to a single large clade termed the N<sub>2</sub>-fixing clade (Fig. 1) (Soltis et al., 2009; Doyle, 2011), which belongs to the Rosid I clade (Eurosids I/Fabidae/Fabids) (Wang et al., 2009). This N<sub>2</sub>-fixing clade encompasses the Leguminosae (or Fabaceae) in the Fabales order (Fig. 1A), which is the third largest family of flowering plants. The Leguminosae family contains about 700 genera with approximately 20,000 species, of which the majority can be nodulated (Doyle, 2011). In contrast, the non-legume families containing species that can be nodulated, are relatively small and contain in general only a few species that can form the nodule symbiosis. The non-legume plants can establish this nodule symbiosis with rhizobium in the case of *Parasponia* and all others with *Frankia* bacteria. The latter form the so-

called actinorhizal nodules. These non-legumes belong to three different orders, which are Cucurbitales, Fagales and Rosales (Fig. 1). These have more than 170 genera, but only around 300 species belonging to 25 genera are able to form nitrogen fixing nodules.

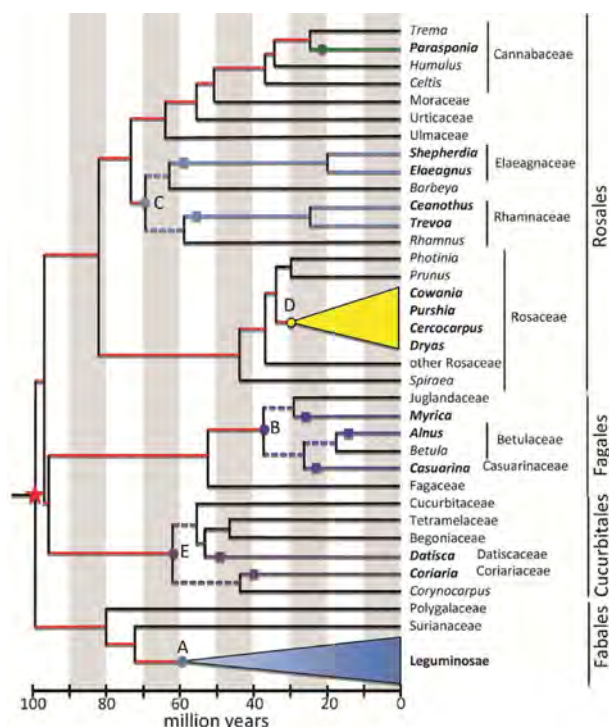


Fig. 1. N<sub>2</sub>-fixing clade.

Nodes marked A through E are Swensen and Benson's (Swensen and Benson, 2008) designations for lineages that can be nodulated; circles associated with letters mark when nodulation evolved in the lineage. An additional origin is indicated for the genus *Parasponia*. Possible additional origins of nodulation within these lineages are indicated by colored boxes, which are placed a short distance from the base of each lineage to indicate that the origin could be anywhere along that branch; dashed lines indicate uncertainty about the date of origin of nodulation between the oldest (circle) and younger (box) date. The origin of the predisposition for nodulation is indicated by a red star. Red lines trace the minimal retention of this predisposition from its origin to the oldest ancestor of each lineage containing nodulated species: the predisposition must have been retained from its origin at least to the common ancestor of each labeled nodes (e.g., node B in Fagales) and *Parasponia*. Topology and dates are from Bell et al. (Bell et al., 2010), with the exception of *Parasponia* and the nodulating species of Rosaceae, which were not included in their analysis. These dates have been estimated by (Doyle, 2011).

## CHAPTER 6

Actinorhizal as well as *Parasponia* root nodules have been characterized as modified lateral roots (Torrey and Callaham, 1979; Lancelle and Torrey, 1985). The cortical cell divisions that have been reported to precede the formation of these modified lateral roots are reported as transient and only facilitating the infection by the bacteria. Therefore they are named pre-nodule. This in a way seems to be lack of biological logic, since all nodulation symbioses appear to be derived from the arbuscular mycorrhiza (AM) fungal symbiosis (Parniske, 2008). In this latter symbiosis exclusively cortical cells are intracellularly infected (Parniske, 2008; Oldroyd et al., 2011; Oldroyd, 2013). Therefore, it is unlikely that cortical cells that form the pre-nodule are just transiently present and do not become part of the real nodule. For this reason, I decided to reexamine whether non-legume nodules are just modified lateral roots. As a first step root nodule and lateral root fate maps are made for the non-legume *Parasponia andersonii* (*Parasponia*).

### **Parasponia root nodule and lateral root fate map**

*Parasponia* belongs to the *Cannabaceae* (Fig. 1). The *Parasponia* nodule symbiosis evolved independent from the legume-rhizobium symbiosis (Lavin et al., 2005; Sprent, 2007; Swensen and Benson, 2008; Wang et al., 2009; Bell et al., 2010; Doyle, 2011). Compared to the nodule symbiosis of model legumes, *Parasponia* nodule symbiosis is rather primitive. A rather broad spectrum of rhizobia is able to infect *Parasponia* via crack entry, unlike the curly root hair entrance in *Medicago* that is restricted to a single rhizobium species (Trinick and Galbraith, 1980; Lancelle and Torrey, 1984; Bender et al., 1987). Further, membrane compartments containing one or a few rhizobia (symbiosomes) are not formed. Instead, long intracellular fixation threads are formed, from which the interaction between rhizobia and host takes place (Lancelle and Torrey, 1984). The crack entry infection strategy is shared with some basal legumes, for example *Arachis* (Chandler, 1978) and *Stylosanthes* (Chandler et al., 1982). However, *Parasponia* nodule histology is distinct from all legumes and will be described in the following section. The *Parasponia* lateral root and root nodule fate maps are shown in Fig. 2 and Fig. 3.

*Parasponia* lateral roots are primarily derived from the pericycle and 4-6

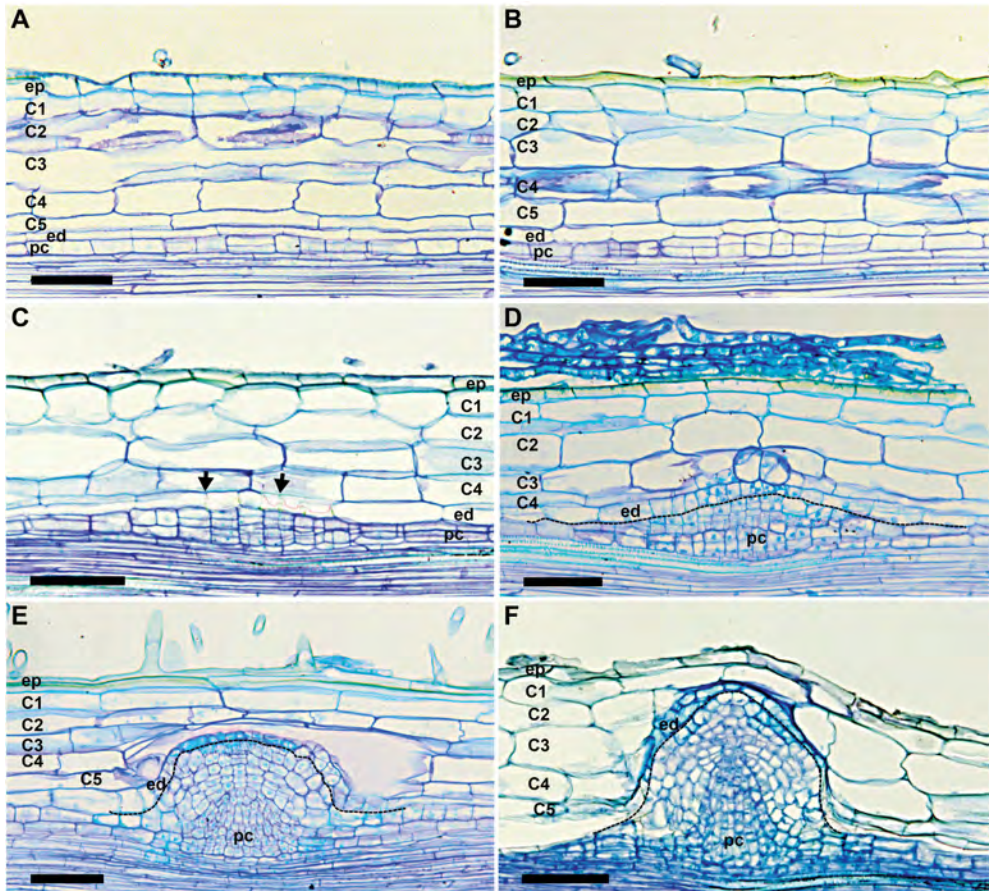


Fig. 2. *Parasponia* lateral root developmental stages.

*Parasponia* lateral root formation involves 4-6 pericycle cells and starts with anticlinal division (A). Periclinal divisions are induced in pericycle and this results in the formation of 2 cell layers (B). Divisions continue in those pericycle cells and form a multi layered primordium (C). Primordium cells derived from the pericycle continue to divide and the endodermis starts to divide anticlinally (arrows) (D). Pericycle derived primordium cells continue to divide and endodermis derived cells differentiate (E). Lateral root primordium starts to resemble a lateral root (F).

Bars, 75  $\mu$ m.

pericycle cells are mitotically activated (Fig. 2). Endodermis cells do divide during initiation of lateral root formation, but only anticlinally (Fig. 2B-F). Ultimately, these cells form the outer most layer of the lateral root primordium (Fig. 2D-F) and later become part of the lateral root cap and columella. Cortex cells do not divide during lateral root formation and so

## CHAPTER 6

do not contribute to the formation of lateral root primordia. Thus, the complete stem cell niche of the *Parasponia* lateral root is derived from the pericycle (Fig. 2E-F). When lateral root primordia have formed 8 cell layers, the different root tissues (epidermis, cortex and vasculature) start to become visible (Fig. 2D).

*Parasponia* root nodule formation starts with cell divisions in the epidermis (Fig. 3A). Then cell divisions are progressively induced in cortical cell layers. Subsequently, the first anticlinal divisions are induced in the pericycle (Fig. 3B). This occurs in at least 8 pericycle cells and so it involves more pericycle cells than during lateral root formation (Fig. 3B, C). In the next stage, cell division continues in the outer cortical cell layers and forms a few centers of cell division. Also the cell division in the pericycle continues, forming a dome-shaped structure (with at least 10 cell layers) in which no specific tissues can yet be discerned (Fig. 3D). Cell division continues in the cell division centers derived from the cortex. The pericycle derived dome-shaped structure starts to elongate and forms the vascular bundle, but an endodermis and cortex are not formed. At the tip of this dome-shaped structure a nodule meristem is formed. It includes cells derived from the pericycle, endodermis, inner cortex and possible also some cells division centers derived from the outer cortex (Fig. 3E). At the next stage the outer cortex derived centers of dividing cells are penetrated by infection threads and fixation threads start to be formed (Fig. 3F) and these cells become an integral part of the lobes with infected cells. The meristem adds cells to different nodule tissues, includes vascular tissue, lobes with infected cells. Our preliminary data shows that the part of the meristem that originated from the root cortex adds cells to the infected lobes. The root endodermis derived cells that flank the pericycle derived vascular tissues differentiate into the endodermis of the nodule vascular bundle (Fig. 3G-I). Casparian strips are formed in these vascular endodermis cells, except in the meristematic region (Fig. 3I). So in contrast to what is published, the modified lateral root that is formed from the pericycle and endodermis does not have any cortical layers. It has been claimed that the cortex of modified lateral root forms the infected lobes (Lancelle and Torrey, 1984). However, it is the mitotically reactivated cortical cells that become infected.

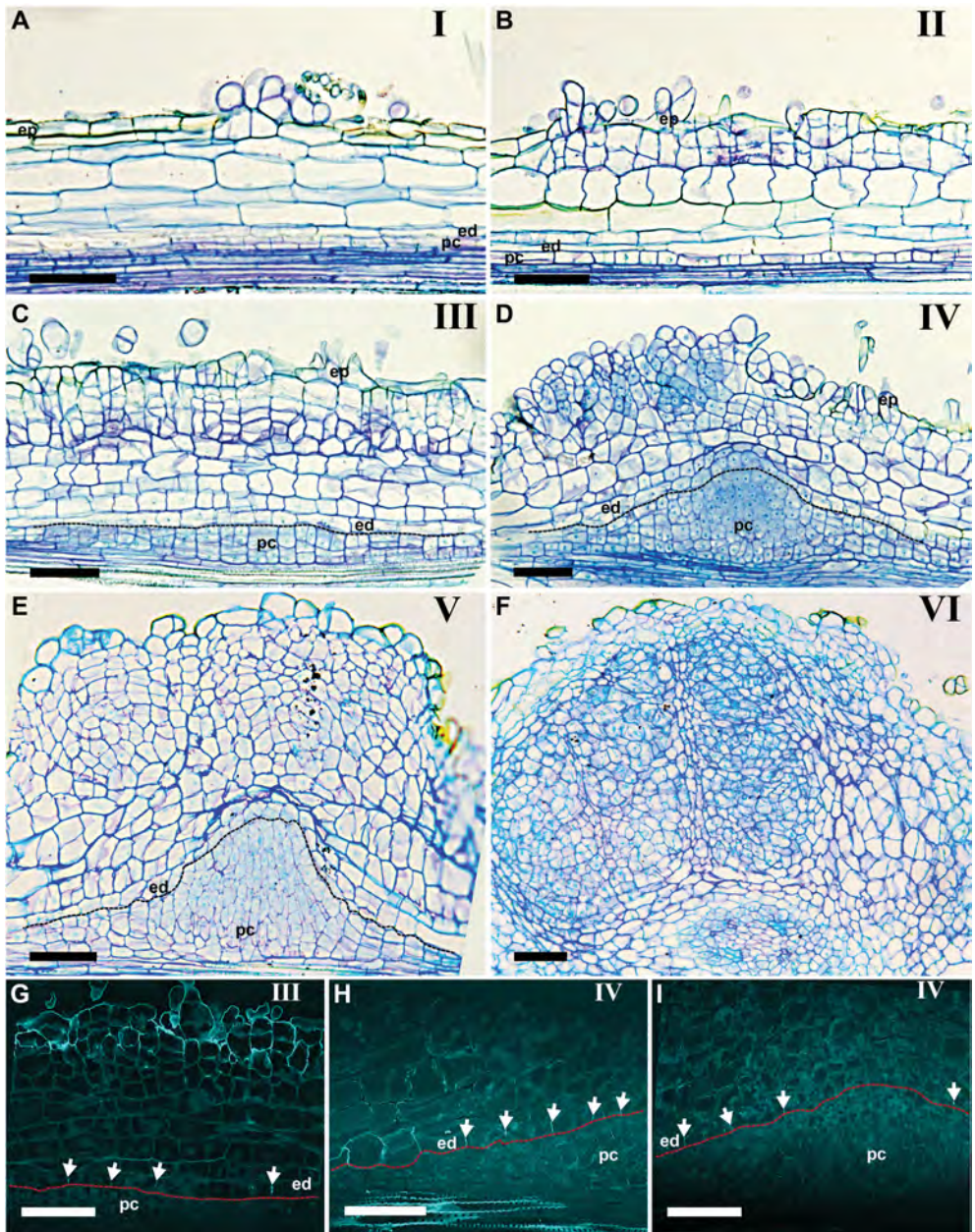


Fig. 3. *Parasponia* root nodule development stages. Nodule formation starts with cell divisions in the epidermis (A). Then cell divisions are induced in outer cortical cell layers and anticlinal divisions are induced in the pericycle in at least 8 cells (B). In the next stage, cell division continues (C) in the outer cortical cell layers and this leads to the formation of a few centers of cell division and in the pericycle a dome-shaped structure is formed (D). Cell division continues in

## CHAPTER 6

the centers with dividing cells (derived from the outer cortex). The pericycle derived dome-shaped structure starts to elongate and forms the vascular bundle. At the tip of this dome-shaped structure a nodule meristem is formed, which includes cells derived from pericycle, endodermis and inner cortex (E). In the outer cortex derived centers of dividing cells fixation threads start to be formed (F). Casparian strips are formed in the endodermis derived cells, except in the meristematic region (G-I). (G) is primordium at stage III; (H-I) are primordia at stage IV.

Bars, 75  $\mu\text{m}$ .

Based on these observations I conclude: 1. Infected cells of *Parasponia* root nodules are derived from root cortex cells that are mitotically activated and this is similar to legume nodule formation. The group mitotically activated cortex cells was named pre-nodule (Lancelle and Torrey, 1985). Because they become part of the infected tissue of the nodule this term is confusing. Therefore I propose not to name them pre-nodule but simply part of the nodule primordium. These cortex derived cells become an integral part of the nodule infected tissue. 2. Different from lateral root formation, during nodule formation the pericycle only forms the vascular bundle and does not form cortex cell layers. Further, nodule vascular and lateral root developments are different from the beginning, as there are more pericycle cells involved in nodule formation (at least 8) than in lateral root formation (4~6). 3. The lateral root meristem is completely derived from the pericycle, but the nodule meristem is formed from a group of cells derived from pericycle, endodermis and cortex. The cortex forms the meristematic part adding cells for bacterial infection. Our studies show that the published description of *Parasponia* nodule development is wrong. As actinorhizal nodule development is supposed to be similar to that of *Parasponia*, it is essential to re-analyze as well.

### **Legume root nodulation is evolutionary more successful than non-legume nodulation**

As described above (section Non-legume nodule formation), the nodulation trait is widely spread within the legume family, whereas in the non-legume families this trait is rather rare. The latter could mean that this trait arose rather recent in evolution or its advantage for the host is less than in legumes. However, the actinorhizal nodulation trait is at least as old as legume nodulation (Fig. 1) (Doyle, 2011; Santi et al., 2013). Therefore,

the nodulation trait is more successful in legumes than in actinorhizal plants, because it is more beneficial to the host.

What could make legume nodulation so successful? A clear difference between legume and non-legume nodules concerns the vascular bundles. Legume nodules have multiple peripheral vascular bundles, whereas non-legume nodules have a central vascular bundle. The peripheral vasculature is relatively close to the gas present in the soil and so oxygen will be rather easily accessible. In contrast, a central vasculature is surrounded by infected cells and this may be a problem. In the infected cells, the respiration rate of the microbes is high, which produce sufficient ATP for the high energy consuming reduction of  $N_2$  to  $NH_3$ . This leads to a low oxygen level in infected cells. In infected legume nodule cells, leghemoglobin is present at high levels to facilitate the transportation of oxygen to the rhizobia at such low oxygen concentrations (Ott et al., 2005). However, nodule vascular bundles do not have a high hemoglobin level to transport oxygen. So, a central vasculature might suffer to some extent from hypoxia. Because oxygen is well available for peripheral vascular bundles, they might function more efficiently than a central vascular bundle that is surrounded by infected cells. Peripheral vascular bundles are present in nodules of the current most basal legumes, like *Arachis* (Chandler, 1978) and *Stylosanthes* (Chandler et al., 1982). This suggests that peripheral vascular bundles are probably formed at the start of the evolution of nodulation in legumes and this could be an important factor that made nodulation so successful in the legume family (Downie, 2014).

### **Similarities and differences between legume and non-legume nodules**

The root nodule fate maps described in this thesis provide further insight into the developmental differences and similarities between legume and non-legume nodules. For both legume and non-legume nodules, infected cells are derived from cortex cells, whereas vascular bundles are derived from different tissue. The legume vascular bundles are mainly derived from mitotically activated cortex cells. In contrast, the non-legume vascular bundles are completely derived from pericycle cells. Further, the

# CHAPTER 6

origin of the meristem in legume and non-legume nodules is different. The legume nodule meristem (indeterminate nodules; Chapter 3) is completely derived from cortex cells. While the non-legume *Parasponia* nodule (section *Parasponia* root nodule and lateral root fate map) meristem is derived from pericycle, endodermis and cortex cells. This difference between legume and *Parasponia* nodules might also be true for actinorhizal nodules, as actinorhizal nodule ontogenesis is most likely similar to that of *Parasponia* (Torrey and Callaham, 1979; Lancelle and Torrey, 1985; Imanishi et al., 2014).

The legume and non-legume root nodule and lateral root fate maps described in this thesis are summarized in Fig. 4. Further discussion on legume and non-legume nodule development will focus on the formation of nodule vascular bundles and meristem.

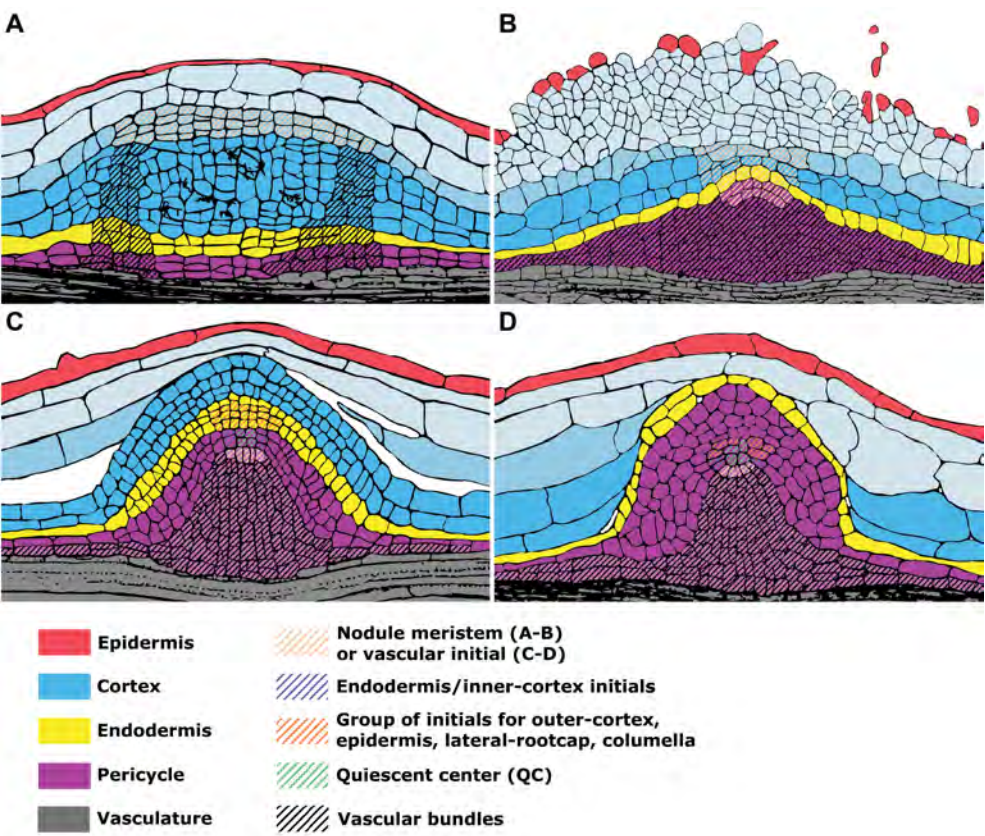


Fig. 4. Legume and non-legume root nodule and lateral root fate maps.

## **Development of nodule vascular bundles**

Legume nodule vascular bundles mainly develop from cortex derived cells and not from pericycle cells. This is not because pericycle cells are not mitotically activated. During nodule primordium formation (Chapter 3) pericycle cells are mitotically active during early stages (I-IV). However, this mitotic activity stops at stage V. In some legume mutants this fails, for example in *lin* (Kiss et al., 2009; Guan et al., 2013). Nodules without LIN have central vascular bundles, which are derived from pericycle cells (Chapter 3), and cortex derived cells do not form vasculature. The origin of these central vascular bundles is similar to the central vascular bundle in non-legume (*Parasponia*) nodules. This suggests that the formation of peripheral vascular bundles requires the repression of mitotic activity in pericycle derived cells at an early stage of legume nodule primordium formation. The vascular bundles in *lin* resemble the *Parasponia* vasculature, which is a modified lateral root. Therefore, it seems that part of the legume nodule development is the suppression of a lateral root program at an early stage of nodule primordium formation. Further, these mutants fail to form peripheral vascular bundles. I propose that this is most likely due to disturbed *PIN* expression (More discussion see next section).

By which mechanism could mitotic activity be suppressed in pericycle derived cells during legume nodule primordium formation? I will first summarize the events that occur simultaneously with this suppression of division. The start of differentiation (including endoreduplication) of infected primordium cells that are derived from the cortex coincides with this suppression. This differentiation seems important for this block of division in the pericycle as in nodules formed by mutants which are blocked in infection, mitotic activity in pericycle derived cells persists. Examples are the *Medicago* mutants *lin* (Kiss et al., 2009) and *vpy-2* (Murray et al., 2011), but it also occurs in *Medicago* nodules formed by *S. meliloti* mutant *exoY*, which is defective in the first step of exopolysaccharide biosynthesis (Kuppusamy et al., 2004; Guan et al., 2013). This mutation leads to abortion of infection in the root hair curl. In these mutant primordia nodule cells remain small, indicating they did not enter endoreduplication, which is part of the differentiation process. I propose that differentiation of the cortex derived primordium cells leads to the suppression the mitotic

## CHAPTER 6

activity of pericycle cells.

What could induce differentiation of the central primordium cells into infected cells? In the nodule, cell differentiation starts in the cell layer that forms the border between the meristem and infection zone. Here, cells become infected, stop dividing and enter endoreduplication. Rhizobia present in infection threads in these cells most likely produce Nod factor (Den Herder et al., 2007). Only in this cell layer the Nod factor receptors NFP and LYK3 accumulate at a relatively high level and it triggers bacteria release from the infection threads (Moling et al., 2014). Those data suggest cell differentiation is induced by Nod factor signaling. This conclusion is also supported by the spontaneous nodules that are induced by dominant active CCaMK constructs (Gleason et al., 2006; Liu, 2014). Dominant active CCaMK activates Nod factor signaling cascade down stream of this kinase.

Dominant active CCaMK induced nodules have many large cells in the nodule center, although these nodules are formed in the absence of bacteria. This large size of the cells in the nodule strongly suggests that they entered endoreduplication and are at least in part differentiated. In these nodules, the pericycle cell divisions are suppressed and peripheral vascular bundles are formed (Gleason et al., 2006; Liu, 2014), like in wt. This suggests that infection by itself is not essential, but the differentiation process that it initiates. From this we conclude that Nod factor signaling induced cell differentiation of the primordium cells leads to periphery vascular bundles formation.

### Formation of nodule meristem

In Chapter 3 we show that the legume nodule meristem is formed from cortex derived cells. The formation of this coincides with the differentiation of the infected cells and the formation of periphery nodule vascular bundles in the primordium. So these three processes somehow are interlinked. Mutant nodule primordia that fail to start differentiation (endoreduplicate) in the central part, such as *lin*, *vpy-2* and *exoY* induced primordia, do neither form a meristem nor peripheral vascular bundles (Chapter 3)

(Guan et al., 2013). So, although the differentiation of infected cells and the formation of a meristem and periphery vascular bundles are spatially separated, these processes appear to be tightly interlinked.

I will first discuss a mechanism by which the formation of nodule vascular bundle and meristem formation might be linked. This is most likely due to the auxin accumulation pattern, which in part is controlled by the transport of auxin through the vascular tissues. In Chapter 4 we show, based on DR5 expression, how auxin accumulates during root nodule primordium development. When bacterial infection occurs in the central part of the nodule primordium (C4/5 derived cells), auxin levels rapidly decrease in these cells. This coincides with a block of mitotic activity and start of differentiation. Concomitantly, at the primordium periphery PINs accumulate and their subcellular position indicates that they facilitate transport of auxin to the future meristem (C3 derived cells). I propose that this high auxin level at the apex is essential to form and maintain the meristem and this would explain why the formation of peripheral vasculature is essential for the formation of a meristem. The next question is how the differentiation of central cells is linked to these 2 processes.

Infection of the primordium center cells (C4/5 derived) triggers their differentiation, which coincides with auxin reduction in those cells. This (in part) might be accomplished by the PINs accumulating at the future meristem and at the basal part of the primordium (Chapter 4). In the future meristem, PINs are positioned to transport auxin into the future meristem. At the basal part of the primordium, PINs are positioned to transport auxin to the root vasculature. However, whether this PIN accumulation is sufficient to trigger a decline in auxin level or how this differentiation of the central cells results in PIN accumulation remains to be solved. Such insight might shed light on how cell differentiation of the center cells is tightly linked to nodule vascular bundle and meristem formation.

In legumes, infection and cell differentiation in the nodule primordium center seems crucial for meristem formation. However, this is probably not the case in non-legume nodule development. In non-legumes the

## CHAPTER 6

pericycle and endodermis derived cells that form the central vasculature also contribute to the nodule meristem. In legume nodules in which infection is blocked the activity of the pericycle/endodermis cells that lead to a central vasculature is even stimulated. This makes it unlikely that in non-legumes infection and the formation of a meristem are linked.

Since there are no non-legume mutants available with blocked infection, it is difficult to study the link between infection and meristem formation genetically. However, in *Parasponia* intracellular infection is blocked (Seifi Kalhor Maryam, personal communication) by high nitrate treatment. In contrast to legumes, nitrate does not block nodulation in *Parasponia*. These nitrate nodules are relatively big, but fixation threads are not formed from the infection threads. Nevertheless a nodule meristem is formed by which big lobes are formed. This provides some support for the idea that nodule meristem and vasculature formation, in non-legumes, are less dependent on intracellular infection. This may add another reason why legume nodulation is more successful than non-legume nodulation. Legumes are able to regulate nodule organogenesis when infection is not successful by blocking meristem formation. In this case a non-profitable investment in nodule formation is reduced. In contrast non-legume nodule seems do not have this ability and therefore is less capable to balance the tradeoff between investment and profit, which is important for successful symbiosis.

### **Nodule and lateral root development**

It has been postulated several times that legume root nodule development is derived from the root developmental program (Hirsch and La Rue, 1997; Gualtieri and Bisseling, 2000; Stougaard, 2001; Roudier et al., 2003; Bright et al., 2005). On the other hand the peripheral location of the legume vascular bundles has also been used to point to a relation with shoot development (Hirsch and La Rue, 1997). Recently, several root apical meristem regulators have been shown to be expressed in the nodule meristem (Osipova et al., 2012; Roux et al., 2014). These genes have first been identified and functionally analyzed in *Arabidopsis*. The genes studied are; *WOX5*, a homeodomain transcription factor expressed in the QC (Forzani et al., 2014); *ACR4*, a receptor kinase controlling

WOX5 expression upon CLE peptide perception (De Smet et al., 2008); PLETHORAs (Chapter 5), AP2/ERF transcription factors (Aida et al., 2004; Galinha et al., 2007); SHORTROOT (SHR) and SCARECROW (SCR), two GRAS-type transcription factors essential for stem cell niche maintenance (Benfey et al., 1993; Di Laurenzio et al., 1996; Heidstra et al., 2004; Lee et al., 2008); JACKDAW (JKD), a C2H2 zinc finger transcription factor that is needed for SCR expression (Ogasawara et al., 2011); EFZ and SMB, two NAC domain TFs involve in lateral root cap and columella production (Willemsen et al., 2008). Within this group of key regulators only WOX5 is really root specific (Nardmann et al., 2009; Majer and Hochholdinger, 2011), whereas the other regulators are also reported to be involved in other developmental processes. The PLTs for example also regulate shoot phyllotaxis (Prasad et al., 2011); ACR4 regulates the ovule and sepal development (Gifford et al., 2003); SHR and SCR play a role in leaf growth (Dhondt et al., 2010).

To compare the developmental programs of nodules and other organs, the nodule meristem organization has to be taken into account. In Chapter 5, we confirmed that the nodule meristem is composed of two types of domains by using WOX5 and PLTs expression patterns (Osipova et al., 2012; Roux et al., 2014). One domain is located at the center of the nodule meristem and adds cells to the central and peripheral tissues. This was named the nodule central meristem. The others are located at the periphery of the nodule meristem and add cells to the vascular bundles. These are named the nodule vascular meristems (Osipova et al., 2012; Roux et al., 2014) (Chapter 5).

When identical genes are expressed in the nodule and root meristem does this mean that the underlying nodule programs are recruited from the root? For example *WOX5* is specifically expressed in the (non-dividing) QC in the root, whereas it is expressed in dividing nodule meristem cells and even in the endodermis of the vasculature (Roux et al., 2014). Such observations are for sure not sufficient to conclude that the QC developmental program is recruited for the development of nodule meristem as well as endodermis of the vascular bundle. In Chapter 5 we conclude that nodule development has recruited key regulators of root development, based on WOX5 and PLTs expression. However, to obtain

## CHAPTER 6

insight in whether and how a developmental program has been coopted, it is essential that studies are not restricted to single components, but that regulatory networks are analyzed.

Non-legume nodules have been described as modified lateral roots, based on their structure and development (Torrey and Callaham, 1979; Hirsch and La Rue, 1997; Imanishi et al., 2014). The Parasponia nodule fate map that I describe in this thesis shows that at least the work on Parasponia is not correct. However, it is still consistent with the conclusion that development of the central nodule vascular bundle is coopted from root development. This conclusion is especially based on the observation that the central vascular bundle and lateral root are both derived from the pericycle. However, a comparison at the molecular level, using regulators as described above, has not been performed. In none of transcriptome studies on non-legume nodules, attention was given to the nodule meristem or vascular bundles (Hochoer et al., 2006; Hochoer et al., 2011; Demina et al., 2013). So a comparison at the molecular level of root and nodule development in non-legumes remains to be done.

### **Symbiotic cells are derived from the root cortex**

There is increasing evidence that supports the hypothesis that nodule symbiosis evolved from the AM symbiosis. In legumes the Nod factor signaling pathway most likely evolved from the Myc factor signaling pathway. This conclusion is based on the fact that many components of the Nod factor signaling cascade are also essential for the interaction with AM fungi. Further, the structure of Nod factors and a class of Myc factors is very similar (Maillet et al., 2011). In non-legumes this has been less well studied, but knockdown of the *SymRK* orthologue in *Casuarina glauca* (*CgSymRK*) (Gherbi et al., 2008) or the orthologue of a Nod factor receptor in Parasponia (*PaNFP*) (den Camp et al., 2011) inhibit both nodulation and AM colonization. Similar results were found in *Casuarina glauca* with the orthologue of *CCaMK* (Svistoonoff et al., 2013). On the cellular level there are also similarities. In most, if not all, these endosymbiotic interactions, the cell cycle machinery is activated in root cortical cells. During nodule symbioses cell division is induced in cortex cells and mycorrhiza infected

root cortex cells have entered endoreduplication (Bainard et al., 2011). So in both cases entry into the cell cycle is induced, but only during nodule formation the mitotic cycle is completed. Further, in *Medicago* *MtVAMP72s* are required for both rhizobium and AM fungal symbiosis, which indicates that they share the same exocytotic pathway (Ivanov et al., 2012). In this thesis, root nodule fate maps showed that the symbiotic root nodule cells (infected cells) are derived from root cortex in both legume and the non-legume *Parasponia*. I assume this also holds for actinorhizal nodules. So, it seems probable that all these endosymbiotic interactions share with AM fungal symbiosis that especially root cortical cells (or cells derived of it) can be intracellularly infected. In case nodules are formed also cells derived from a newly formed meristem can be infected.

The studies described in this thesis have strengthened the conclusion that nodule endosymbiotic interactions in plants are derived from the ancient AM fungal symbiosis. We showed that the root cortical cells which is the only cell type that can be intracellularly infected by mycorrhizal fungi, is also intracellularly infected in the non-legume symbiosis of *Parasponia* and rhizobia. However, a striking difference between the nodule and AM fungal symbioses is that the bacteria inducing a nodule symbiosis are never intracellularly accommodated in an existing root cortical cell. In all cases at least these cortical cells have been mitotically activated. So, a major question that remains to be answered is what changes have to be induced in cortical cells to allow intracellular infection by bacteria. In addition to mechanisms related to nodule organogenesis it also is very important to understand by which mechanism plant cells control intracellular infection by bacteria.

## REFERENCES

Aida, M., Beis, D., Heidstra, R., Willemsen, V., Blilou, I., Galinha, C., Nussaume, L., Noh, Y. S., Amasino, R. and Scheres, B. (2004). The PLETHORA genes mediate patterning of the Arabidopsis root stem cell niche. *Cell* **119**, 109-120.

Bainard, L. D., Bainard, J. D., Newmaster, S. G. and Klironomos, J. N. (2011). Mycorrhizal symbiosis stimulates endoreduplication in angiosperms. *Plant Cell Environ* **34**, 1577-1585.

## CHAPTER 6

**Bell, C. D., Soltis, D. E. and Soltis, P. S.** (2010). The age and diversification of the angiosperms re-revisited. *Am J Bot* **97**, 1296-1303.

**Bender, G. L., Goydych, W., Rolfe, B. G. and Nayudu, M.** (1987). The role of rhizobium conserved and host specific nodulation genes in the infection of the non-legume *Parasponia andersonii*. *Mol Gen Genet* **210**, 299-306.

**Benfey, P. N., Linstead, P. J., Roberts, K., Schiefelbein, J. W., Hauser, M. T. and Aeschbacher, R. A.** (1993). Root development in Arabidopsis: four mutants with dramatically altered root morphogenesis. *Development* **119**, 57-70.

**Bright, L. J., Liang, Y., Mitchell, D. M. and Harris, J. M.** (2005). The LATD gene of *Medicago truncatula* is required for both nodule and root development. *Molecular Plant Microbe Interactions* **18**, 521-532.

**Chandler, M. R.** (1978). Some observations on infection of *Arachis hypogaea* L. by rhizobium. *J Exp Bot* **29**, 749-755.

**Chandler, M. R., Date, R. A. and Roughley, R. J.** (1982). Infection and root-nodule development in *Stylosanthes* species by rhizobium. *J Exp Bot* **33**, 47-57.

**De Smet, I., Vassileva, V., De Rybel, B., Levesque, M. P., Grunewald, W., Van Damme, D., Van Noorden, G., Naudts, M., Van Isterdael, G., De Clercq, R. et al.** (2008). Receptor-like kinase ACR4 restricts formative cell divisions in the Arabidopsis root. *Science* **322**, 594-597.

**Demina, I. V., Persson, T., Santos, P., Plaszczyca, M. and Pawlowski, K.** (2013). Comparison of the nodule vs. root transcriptome of the actinorhizal plant *Datisca glomerata*: actinorhizal nodules contain a specific class of defensins. *Plos One* **8**.

**den Camp, R. O., Streng, A., De Mita, S., Cao, Q. Q., Polone, E., Liu, W., Ammiraju, J. S. S., Kudrna, D., Wing, R., Untergasser, A. et al.** (2011). LysM-type mycorrhizal receptor recruited for rhizobium symbiosis in nonlegume *Parasponia*. *Science* **331**, 909-912.

**Den Herder, J., Vanhee, C., De Rycke, R., Corich, V., Holsters, M. and Goormachtig, S.** (2007). Nod factor perception during infection thread growth fine-tunes nodulation. *Molecular Plant Microbe Interactions* **20**, 129-137.

**Dhondt, S., Coppens, F., De Winter, F., Swarup, K., Merks, R. M. H., Inze, D., Bennett, M. J. and Beemster, G. T. S.** (2010). SHORT-ROOT and SCARECROW regulate leaf growth in Arabidopsis by stimulating S-phase progression of the cell cycle. *Plant Physiology* **154**, 1183-1195.

**Di Laurenzio, L., Wysocka Diller, J., Malamy, J. E., Pysh, L., Helariutta, Y., Freshour, G., Hahn, M. G., Feldmann, K. A. and Benfey, P. N.** (1996). The SCARECROW gene regulates an asymmetric cell division that is essential for generating the radial organization of the Arabidopsis root. *Cell* **86**, 423-433.

**Downie, J. A.** (2014). Legume nodulation. *Current Biology* **24**, R184-R190.

**Doyle, J. J.** (2011). Phylogenetic perspectives on the origins of nodulation. *Molecular Plant Microbe Interactions* **24**, 1289-1295.

**Forzani, C., Aichinger, E., Sornay, E., Willemsen, V., Laux, T., Dewitte, W. and Murray, J. A. H.** (2014). WOX5 suppresses CYCLIN D activity to establish quiescence at the center of the root stem cell niche. *Current Biology* **24**, 1939-1944.

**Galinha, C., Hofhuis, H., Luijten, M., Willemsen, V., Blilou, I., Heidstra, R. and Scheres, B.** (2007). PLETHORA proteins as dose-dependent master regulators of Arabidopsis root development. *Nature* **449**, 1053-1057.

**Gherbi, H., Markmann, K., Svistoonoff, S., Estevan, J., Autran, D., Giczey, G., Auguy, F., Peret, B., Laplace, L., Franche, C. et al.** (2008). SymRK defines a common genetic basis for plant root endosymbioses with *arbuscular mycorrhiza* fungi, *rhizobia*, and *frankia* bacteria. *P Natl Acad Sci USA* **105**, 4928-4932.

**Gifford, M. L., Dean, S. and Ingram, G. C.** (2003). The Arabidopsis ACR4 gene plays a role in cell layer organisation during ovule integument and sepal margin development. *Development* **130**, 4249-4258.

**Gleason, C., Chaudhuri, S., Yang, T. B., Munoz, A., Poovaiah, B. W. and Oldroyd, G. E. D.** (2006). Nodulation independent of rhizobia induced by a calcium-activated kinase lacking autoinhibition. *Nature* **441**, 1149-1152.

**Gualtieri, G. and Bisseling, T.** (2000). The evolution of nodulation. *Plant Mol Biol* **42**, 181-194.

**Guan, D., Stacey, N., Liu, C. W., Wen, J. Q., Mysore, K. S., Torres-Jerez, I., Vernie, T., Tadege, M., Zhou, C. N., Wang, Z. Y. et al.** (2013). Rhizobial infection is associated with the development of peripheral vasculature in nodules of *Medicago truncatula*. *Plant Physiology* **162**, 107-115.

**Heidstra, R., Welch, D. and Scheres, B.** (2004). Mosaic analyses using marked activation and deletion clones dissect Arabidopsis SCARECROW action in asymmetric cell division. *Gene Dev* **18**, 1964-1969.

**Hirsch, A. M. and La Rue, T. A.** (1997). Is the legume nodule a modified root or stem or an organ sui generis? *Crit Rev Plant Sci* **16**, 361-392.

**Hocher, V., Auguy, F., Argout, X., Laplace, L., Franche, C. and Bogusz, D.** (2006). Expressed sequence-tag analysis in *Casuarina glauca* actinorhizal nodule and root. *New Phytol* **169**, 681-688.

**Hocher, V., Alloisio, N., Auguy, F., Fournier, P., Dumas, P., Pujic, P., Gherbi, H., Queiroux, C., Da Silva, C., Wincker, P. et al.** (2011). Transcriptomics of actinorhizal symbioses reveals homologs of the whole common symbiotic signaling cascade. *Plant Physiology* **156**, 700-711.

**Imanishi, L., Perrine-Walker, F. M., Ndour, A., Vayssieres, A., Conejero, G., Lucas, M., Champion, A., Laplace, L., Wall, L. and Svistoonoff, S.** (2014). Role of auxin during intercellular infection of *Discaria trinervis* by *Frankia*. *Frontiers in plant science* **5**, 399.

**Ivanov, S., Fedorova, E. E., Limpens, E., De Mita, S., Genre, A., Bonfante, P. and Bisseling, T.** (2012). Rhizobium-legume symbiosis shares an exocytotic pathway required for arbuscule formation. *P Natl Acad Sci USA* **109**, 8316-8321.

## CHAPTER 6

Kiss, E., Olah, B., Kalo, P., Morales, M., Heckmann, A. B., Borbola, A., Lozsa, A., Kontar, K., Middleton, P., Downie, J. A. et al. (2009). LIN, a novel type of U-Box/WD40 protein, controls early infection by rhizobia in legumes. (Special Issue: Legume biology.). *Plant Physiology* **151**, 1239-1249.

Kuppusamy, K. T., Endre, G., Prabhu, R., Penmetsa, R. V., Veereshlingam, H., Cook, D. R., Dickstein, R. and VandenBosch, K. A. (2004). LIN, a *Medicago truncatula* gene required for nodule differentiation and persistence of rhizobial infections. *Plant Physiology* **136**, 3682-3691.

Lancelle, S. A. and Torrey, J. G. (1984). Early development of rhizobium induced root nodules of *Parasponia rigida*. 1. Infection and early nodule initiation. *Protoplasma* **123**, 26-37.

Lancelle, S. A. and Torrey, J. G. (1985). Early development of rhizobium induced root nodules of *Parasponia rigida*. 2. Nodule morphogenesis and symbiotic development. *Canadian Journal of Botany* **63**, 25-35.

Lavin, M., Herendeen, P. S. and Wojciechowski, M. F. (2005). Evolutionary rates analysis of Leguminosae implicates a rapid diversification of lineages during the tertiary. *Syst Biol* **54**, 575-594.

Lee, H., Kim, B., Song, S. K., Heo, J. O., Yu, N. I., Lee, S. A., Kim, M., Kim, D. G., Sohn, S. O., Lim, C. E. et al. (2008). Large-scale analysis of the GRAS gene family in *Arabidopsis thaliana*. *Plant Mol Biol* **67**, 659-670.

Liu, W. (2014). Comparative and functional analysis of NODULATION SIGNALING PATHWAY 1 (NSP1) and NSP2 in rice and *Medicago*. *PhD thesis*.

Maillet, F., Poinot, V., Andre, O., Puech-Pages, V., Haouy, A., Gueunier, M., Cromer, L., Giraudet, D., Formey, D., Niebel, A. et al. (2011). Fungal lipochitooligosaccharide symbiotic signals in *arbuscular mycorrhiza*. *Nature* **469**, 58-63.

Majer, C. and Hochholdinger, F. (2011). Defining the boundaries: structure and function of LOB domain proteins. *Trends Plant Sci* **16**, 47-52.

Moling, S., Pietraszewska-Bogiel, A., Postma, M., Fedorova, E., Hink, M. A., Limpens, E., Gadella, T. W. J. and Bisseling, T. (2014). Nod factor receptors form heteromeric complexes and are essential for intracellular infection in *Medicago* nodules. *Plant Cell* **26**, 4188-4199.

Murray, J. D., Muni, R. R. D., Torres-Jerez, I., Tang, Y. H., Allen, S., Andriankaja, M., Li, G. M., Laxmi, A., Cheng, X. F., Wen, J. Q. et al. (2011). Vapyrin, a gene essential for intracellular progression of arbuscular mycorrhizal symbiosis, is also essential for infection by rhizobia in the nodule symbiosis of *Medicago truncatula*. *Plant J* **65**, 244-252.

Nardmann, J., Reisewitz, P. and Werr, W. (2009). Discrete shoot and root stem cell-promoting WUS/WOX5 functions are an evolutionary innovation of angiosperms. *Mol Biol Evol* **26**, 1745-1755.

Newcomb, W., Sippell, D. and Peterson, R. L. (1979). The early morphogenesis of *Glycine max* and *Pisum sativum* root nodules. *Canadian Journal of Botany* **57**, 2603-

2616.

**Ogasawara, H., Kaimi, R., Colasanti, J. and Kozaki, A.** (2011). Activity of transcription factor JACKDAW is essential for SHR/SCR-dependent activation of SCARECROW and MAGPIE and is modulated by reciprocal interactions with MAGPIE, SCARECROW and SHORT ROOT. *Plant Mol Biol* **77**, 489-499.

**Oldroyd, G. E. D.** (2013). Speak, friend, and enter: signalling systems that promote beneficial symbiotic associations in plants. *Nat Rev Microbiol* **11**, 252-263.

**Oldroyd, G. E. D., Murray, J. D., Poole, P. S. and Downie, J. A.** (2011). The rules of engagement in the legume-rhizobial symbiosis. *Annual Review Genetics* **45**, 119-144.

**Osipova, M. A., Mortier, V., Demchenko, K. N., Tsyganov, V. E., Tikhonovich, I. A., Lutova, L. A., Dolgikh, E. A. and Goormachtig, S.** (2012). WUSCHEL-RELATED HOMEBOX5 gene expression and interaction of CLE peptides with components of the systemic control add two pieces to the puzzle of autoregulation of nodulation. *Plant Physiology* **158**, 1329-1341.

**Ott, T., Dongen, J. T. v., Gunther, C., Krusell, L., Desbrosses, G., Vigeolas, H., Bock, V., Czechowski, T., Geigenberger, P. and Udvardi, M. K.** (2005). Symbiotic leghemoglobins are crucial for nitrogen fixation in legume root nodules but not for general plant growth and development. *Current Biology* **15**, 531-535.

**Parniske, M.** (2008). *Arbuscular mycorrhiza*: the mother of plant root endosymbioses. *Nat Rev Microbiol* **6**, 763-775.

**Prasad, K., Grigg, S. P., Barkoulas, M., Yadav, R. K., Sanchez-Perez, G. F., Pinon, V., Blilou, I., Hofhuis, H., Dhonukshe, P., Galinha, C. et al.** (2011). Arabidopsis PLETHORA transcription factors control phyllotaxis. *Current Biology* **21**, 1123-1128.

**Roudier, F., Fedorova, E., Lebris, M., Lecomte, P., Gyorgyey, J., Vaubert, D., Horvath, G., Abad, P., Kondorosi, A. and Kondorosi, E.** (2003). The Medicago species A2-type cyclin is auxin regulated and involved in meristem formation but dispensable for endoreduplication-associated developmental programs. *Plant Physiology* **131**, 1091-1103.

**Roux, B., Rodde, N., Jardinaud, M. F., Timmers, T., Sauviac, L., Cottret, L., Carrere, S., Sallet, E., Courcelle, E., Moreau, S. et al.** (2014). An integrated analysis of plant and bacterial gene expression in symbiotic root nodules using laser-capture microdissection coupled to RNA sequencing. *Plant J* **77**, 817-837.

**Santi, C., Bogusz, D. and Franche, C.** (2013). Biological nitrogen fixation in non-legume plants. *Ann Bot-London* **111**, 743-767.

**Soltis, D. E., Albert, V. A., Leebens-Mack, J., Bell, C. D., Paterson, A. H., Zheng, C. F., Sankoff, D., dePamphilis, C. W., Wall, P. K. and Soltis, P. S.** (2009). Polyploidy and angiosperm diversification. *Am J Bot* **96**, 336-348.

**Sprent, J. I.** (2007). Evolving ideas of legume evolution and diversity: a taxonomic perspective on the occurrence of nodulation. *New Phytol* **174**, 11-25.

## CHAPTER 6

**Stougaard, J.** (2001). Genetics and genomics of root symbiosis. *Curr Opin Plant Biol* **4**, 328-335.

**Svistoonoff, S., Benabdoun, F. M., Nambiar-Veetil, M., Imanishi, L., Vaissayre, V., Cesari, S., Diagne, N., Hoher, V., de Billy, F., Bonneau, J. et al.** (2013). The independent acquisition of plant root nitrogen-fixing symbiosis in Fabids recruited the same genetic pathway for nodule organogenesis. *Plos One* **8**.

**Swensen, S. M. and Benson, D. R.** (2008). Evolution of actinorhizal host plants and frankia endosymbionts. In *Nitrogen-fixing actinorhizal symbioses*, (ed. K. Pawlowski and W. E. Newton), pp. 73-104. Dordrecht, the Netherlands: Springer.

**Torrey, J. G. and Callaham, D.** (1979). Early nodule development in *Myrica gale*. *Botanical Gazette* **140**, S10-S14.

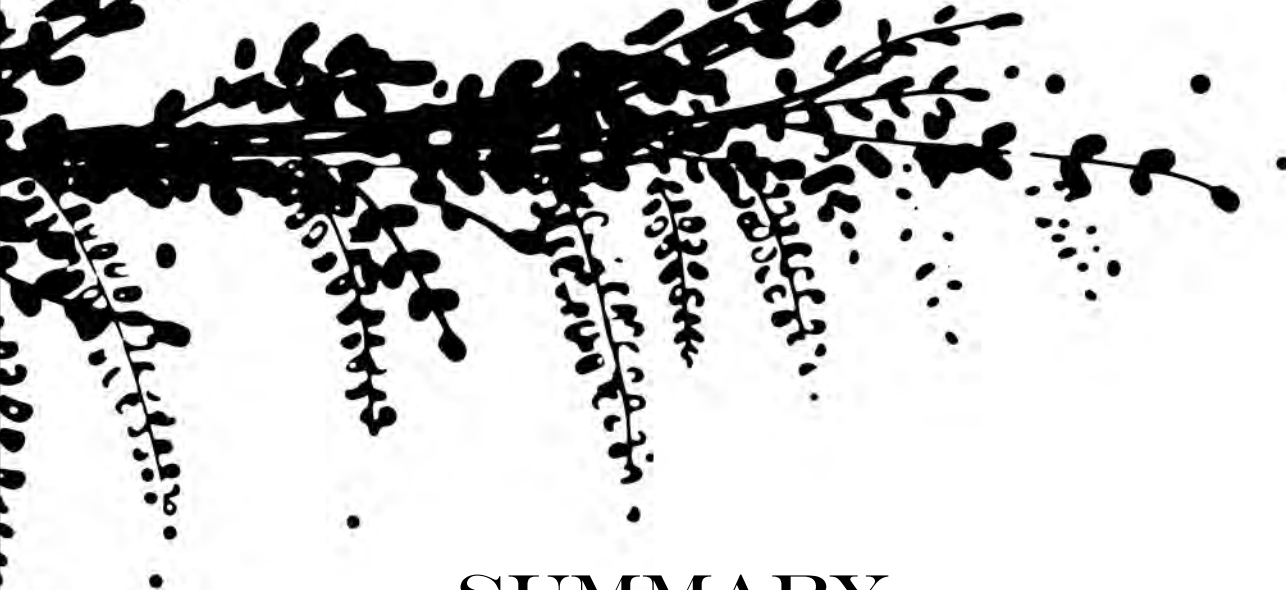
**Trinick, M. J. and Galbraith, J.** (1980). The Rhizobium requirements of the non-legume *Parasponia* in relationship to the cross-inoculation group concept of legumes. *New Phytol* **86**, 17-26.

**Wang, H. C., Moore, M. J., Soltis, P. S., Bell, C. D., Brockington, S. F., Alexandre, R., Davis, C. C., Latvis, M., Manchester, S. R. and Soltis, D. E.** (2009). Rosid radiation and the rapid rise of angiosperm-dominated forests. *P Natl Acad Sci USA* **106**, 3853-3858.

**Willemsen, V., Bauch, M., Bennett, T., Campilho, A., Wolkenfelt, H., Xu, J., Haseloff, J. and Scheres, B.** (2008). The NAC domain transcription factors FEZ and SOMBRERO control the orientation of cell division plane in *Arabidopsis* root stem cells. *Dev Cell* **15**, 913-922.







# SUMMARY

## SUMMARY

Root nodule endosymbiosis, which evolved from the more ancient endosymbiosis arbuscular mycorrhizal symbiosis, is formed in a group plants that belong to a single clade, the  $N_2$ -fixing clade. In this endosymbiosis the host plant interacts with soil borne nitrogen fixing bacteria, which are collectively known as rhizobium and Frankia. They are able to trigger the formation of a novel plant organ the root nodule. It is a special organ that is formed to host the bacteria. In these nodules the bacteria convert  $N_2$  into ammonia providing a fixed nitrogen source to its host. In return, the plant supports the bacteria with carbohydrates. Although root nodules often thought to have a close relationship with lateral roots, the ontogeny of these two organs in legume plant was not known. During my PhD research I focused on the development of these two organs in nodulating plants.

It is well known that *Arabidopsis* lateral roots completely originate from pericycle cells and it has almost become a dogma that this is also the case in other plant species. However, in legumes the ontogeny of lateral roots was not well studied. In this thesis it is shown that during *Medicago* lateral root development, in addition to the pericycle, also endodermis and cortex contribute to lateral root development. The pericycle derived cells form part of the stem cell niche, but interestingly, the endodermis derived cells also form about half of the initials of the stem cell niche. This means part of these endodermis cells were really dedifferentiation and obtained a stem cell nature. This is the first time that it is shown that fully differentiated cells dedifferentiate and become stem cells during dicot lateral root formation.

In the *Medicago* root nodule fate map we showed that the nodule meristem originates from the third cortical layer, while several cell layers at the base of the nodule are directly formed from cells of the inner cortical layers, root endodermis and pericycle. The latter 2 differentiate into the uninfected tissues that are located at the base of the mature nodule, whereas the cells derived of the inner cortical cell layers (C4/5) form about 8 cell layers of infected cells. This means that the middle cortical cells (C3) dedifferentiate to form the nodule meristem, while the endodermis trans-differentiates into parenchyma and vascular endodermis. The peripheral vascular bundles are formed from cortex derived cells. Using this fate

## SUMMARY

map we reanalysed several mutants, among others the *lin* mutant. This forms nodules with central vascular bundle derived from pericycle and a meristem is not formed. This indicates that nodule development requires suppression of mitotic activity in the pericycle derived cells division at an early stage of development. Another example is *nf-ya1*, it makes small nodules that contain well-infected inner cortex derived cells. However, bacterial release is blocked in cells derived from the meristem. Based on this we conclude intracellular release of rhizobia in primordium cells and daughter cells of the meristem are regulated in different manners.

Auxin plays a critical role in plant organ organogenesis and root nodules are no exception. Some studies have shown that auxin accumulates during nodulation by using reporter constructs. Previously, it has been postulated by theoretical modelling that the accumulation of auxin during nodulation is induced by a local reduction of PIN (auxin efflux carriers) activity. In this thesis this model is tested. However, this study was hampered due to the low level of *MtPIN* proteins in the susceptible zone of the root. It is still possible that the PIN levels are transiently reduced, but we showed that at a rather early stage (before divisions have occurred) PIN proteins start to accumulate during primordium formation. To correlate PIN accumulation with the auxin landscape, we first analysed the auxin accumulation pattern during the nodule primordium developmental stages, by using *DR5::GUS* as reporter system. This showed that auxin accumulation associates with mitotic activity within the primordium. Then, *MtPINs* expression was studied. This showed that at initial stages (Stage I-III) these *MtPINs* accumulate in all primordium cells. At later stages (IV-VI), *MtPIN10* mainly expressed at the nodule periphery and *MtPIN2* predominantly expressed at the future meristem (middle cortex derived cells). The subcellular position of the PINs in these primordium areas make it very likely that they play a key role in creating the auxin landscape in the primordium.

It has been suggested that nodule development is closely related to that of lateral roots. I studied whether the Medicago nodule meristem shares molecular markers with the root meristem, by studying the expression and function of *PLETHORA* genes in the root nodule meristem. Nodule-specific knockdown of *PLETHORA* genes resulted in a reduced number of nodules and in nodules the meristem size is reduced. Hence, we conclude that

## SUMMARY

Medicago recruited some key regulators of root development for nodule development. To investigate further the relationship between lateral root and nodule development, we made a lateral root and nodule fate map of *Parasponia*. This is a non-legume plant that makes nodules. These studies showed that the nodule central vascular bundle is completely derived from the pericycle similar as its lateral root, however, the infected cells originated from cortex. The latter showed that the published characterisation of *Parasponia* nodule ontogeny is wrong.

At the end of this thesis is a discussion based on the data we obtained in this thesis and the literature related to it. Mutant nodules which cannot form peripheral vascular bundles, such as *lin*, *vpy-2* and rhizobium *exoY* induced nodules, never form a meristem. To explain this tight link I proposed a putative mechanism. The high auxin level at the apex is most likely essential to form and maintain the meristem. PINs accumulate at the nodule periphery where the peripheral vasculature is formed. Further, their subcellular position indicates that auxin is transported towards the meristem. This PIN accumulation pattern in the peripheral vasculature could explain this tight link between the formation of peripheral vasculature and meristem.

The legume nodulation trait is markedly more wide spread than nodulation in non-legumes. This suggests that the nodulation trait is evolutionary more successful in legumes. I discussed that the peripheral vascular bundles may contribute to this success. Another reason might be that legumes have a mechanism in place to stop nodule development when infection is not successful. So a non-profitable investment in nodule formation is reduced in legume plants. Such a mechanism seems absent in the non-legume *Parasponia*.

The idea that root nodule symbiosis is derived from mycorrhizal symbiosis is supported by several studies. In the case of the rhizobium legume symbiosis it is for example clear that the cell type that can be intracellularly infected is the root cortex. However, a major difference is that rhizobia can only enter these cells after they have been mitotically activated. It had been reported that in non-legumes cortical cells of a newly formed modified lateral root could be infected which seemed strikingly different

## SUMMARY

from the rhizobium-legume interaction. However, the fate map of Parasponia nodules, described in this thesis, clearly showed that also in this interaction mitotically activated cortical cells are the prime targets for intracellular infection. This indicates that the mechanism by which cortical cells are modified to become susceptible for intracellular infection might be shared by the different nodule symbioses.





## SAMENVATTING

# SAMENVATTING

Wortelknolsymbiose, de samenwerking tussen plant en bacteriën in de knollen, is geëvolueerd uit de endosymbiotische interactie van mycorrhiza schimmels en planten. Wortelknolsymbiose is tijdens de evolutie een aantal malen onafhankelijk bij verschillende soorten ontstaan, maar alle planten die een knolsymbiose aangaan behoren tot dezelfde clade, d.w.z. ze stammen af van de zelfde evolutionaire voorouder. Dit wordt de N-fixatie clade genoemd. De bacteriën die een wortelknolsymbiose kunnen vormen zijn of rhizobia- of Frankia- bacteriën. Deze bacteriën induceren de vorming van een nieuw orgaan, de wortelknol. In deze wortelknollen vinden de bacteriën de juiste omgeving om atmosferische stikstof om te zetten in ammonia, die gebruikt kan worden door de gastheer. Als tegenprestatie voorziet de plant de bacteriën van koolhydraten.

Vaak wordt gesuggereerd dat wortelknollen gemodificeerde zijwortels zijn. Echter, de basis voor deze veronderstelling is zeer gering aangezien zelfs de ontogenie van deze twee organen in vlinderbloemige planten niet bekend was. Tijdens mijn PhD-onderzoek heb ik mij gericht op de ontwikkelingsbiologie van deze twee organen in planten die wortelknollen kunnen maken.

Zijwortels van *Arabidopsis* – een niet-vlinderbloemige - ontstaan alleen uit cellen van de pericykel. De gedachte dat dit ook bij andere planten het geval is, is algemeen aanvaard. Echter, in vlinderbloemigen was de ontogenie van zijwortels niet eerder bestudeerd. In dit proefschrift wordt beschreven dat in *Medicago* naast de pericykel ook de endodermis en cortex bijdragen aan de ontwikkeling van zijwortels. De cellen van de pericykel vormen een deel van de nieuwe stamcelniche. Maar ook cellen afkomstig van de endodermis dragen bij aan de vorming van de stamcelniche. Dit is de eerste keer dat is aangetoond dat bij de vorming van zijwortels volledig gedifferentieerde cellen geherprogrammeerd worden tot stamcellen.

Ook voor *Medicago*-wortelknollen is een gedetailleerde fate map gemaakt. Een fate map laat zien van welke wortel cellen de verschillende knoldelen afkomstig zijn. Deze fate map toont aan dat naast de cortex ook de mitotisch geactiveerde endodermis en pericykel bijdragen aan vorming van de knol. Deze cellen vormen de niet-geïnfecteerde weefsels aan de basis van de knol. *Medicago*-knollen hebben een persistent meristeem aan de apex. Dit meristeem wordt gevormd uit de middelste corticale cellaag.

## SAMENVATTING

De mitotisch geactiveerde binnenste corticale cellagen veranderen direct in ongeveer acht cellagen met geïnfecteerde cellen. Deze cellagen zijn dus niet afkomstig van het meristeem. Deze gedetailleerde fate map van de knol blijkt een krachtig instrument om knolfenotypes van mutanten nauwkeurig te beschrijven.

Bij de ontwikkeling van planten speelt het plantenhormoon auxine een cruciale rol. Dit is ook bij wortelknolvorming het geval. Hierbij worden gebieden met een hoge auxine concentratie gecreëerd door met behulp van b.v. auxine efflux carriers (PINs) auxine gericht naar deze gebieden te transporteren. Twee *Medicago*-PINs blijken een belangrijke rol te spelen bij de vorming van een auxinemaximum in het knolmeristeem. Dit zijn *MtPIN10* en *MtPIN2*. *MtPIN* wordt vooral gevormd in de knolperiferie en is zodanig gepositioneerd dat het het transport van auxine van de wortel naar het knolmeristeem faciliteert. *MtPIN2* is gelokaliseerd in het meristeem. En de sub-cellulaire lokalisatie draagt bij aan een ophoping van auxine in het meristeem.

Om de relatie van knol- en zijwortelvorming te bestuderen is er gebruik gemaakt van de *PLETHORA*-genen, die een belangrijke rol spelen bij zijwortelvorming. Een verminderde expressie van deze genen verlaagt het aantal knollen dat gevormd wordt. Verder missen deze knollen vaak het apicale meristeem.

Vlinderbloemige wortelknollen hebben vaatbundels die aan de periferie van de knol gelegen zijn. Dit is een belangrijk verschil met wortelknollen van niet-vlinderbloemigen. Deze laatsten vormen allemaal knollen met een centraal gelegen vaatbundel. Een gedetailleerde fate map van knollen van de niet-vlinderbloemige *Parasponia* laat zien dat deze vaatbundel een gemodificeerde zijwortel is. Ik bediscussieer in dit proefschrift hoe de perifere positie van de vaatbundels kan bijdragen aan het evolutionaire succes van knolvorming binnen de vlinderbloemige planten. Dit in tegenstelling tot de centrale vaatbundel bij niet-vlinderbloemigen.





## • ACKNOWLEDGEMENTS

## ACKNOWLEDGEMENTS

This thesis could never been accomplished without the help from so many people. Here, I would like to express my gratefulness and appreciation to my supervisors, colleagues, friends, family and who has ever accompanied me during this journey in any possible way.

Frist of all, thank you Ton, for giving me this great opportunity to be a member of Molbi, for supervising me during my PhD study period, for teaching me how to think, how to write, how to present and for all these interesting discussions and chats we had. Thanks to my daily supervisors. Henk, thank you for encouraging me to continue when I feel depressed, for your nice advises and all discussions we had. Rene, thank you for teaching me how to present and advising me on my project.

Here, I would like to thank all the others who helped or collaborated in these works from this thesis. Olga, either in the lab or in my life there are so many thanks to you. Thanks also to Marijke, Carolien, Cao, Robin, Eva, Stefan, Andreas and all students who helped me in the lab such as Pauline, David.....

Thanks to my pervious colleagues and friends: Chunting, Wei, Silvester, Sergey, Gerben, Alessandra, Evgenia, Adam, Rik O., Aleksandr, Arend, Maryam..... Thanks to my current colleagues and friends: Maria, Marie-Jose, Jan V., Jan H., Elena, Defeng, Huchen, Trupti, Xu, Fengjiao, Tian, Rik H., Guiling, Erik, Joan..... Thanks to my friends from the neighbor groups: Sabine, Du, Kunkun, Serena, Luca, Ikram, Bandan, Long, Kris, Jeroen, Olga, Juliane, Ying, Bela..... And thanks to every one that we enjoyed our coffee breaks together.

Thanks to these who supported me from the beginning of my life in Wageningen: Bai Yuling, Hanzi, Suxian, Nini, 幸晃, 静惠, Yu-wei, Xiaoli, Peng Ying, Wei, Jim, Luc, Emma, Ciska..... Thanks to my lovely friends: Zhu Feng, Yehua, Yanxia, Huihui, Cheng Xi, Xianwen, Yunmeng, Yuanyuan, Bobo, Chen Xi, Weicon, Song Wei, Jimmy, Ya-Fen, Yang Ting, Liu Qing, Wang Yan, Xu Xuan, He Jun, Xiaohua, Bai Bing, Lin Ke, Ningwen, Junwei, Yanli, Wei Zhen, Jianhua, Zhang Zhao, Chenlei, Lisha, Pingping, Lemeng, Chunxu, Qin Wei, Li Na, Du Yu, Bi Guozhi, Xiaoqian, Kaile, Xiaoxue, Shuhang, Yiqian, Ligu, Chen Hsuan, MoMo, 佳諭, 家愷, Drik..... And thanks to all my friends with who shared party or dinner together and

## ACKNOWLEDGEMENTS

accompanied me during my life in the Netherlands.

My special acknowledgments to my dear paranymphs I-Chiao and Arjan. My dear I-Chiao, I am so lucky to have you as my friend. You are such a thoughtful and grateful person, I enjoyed every minute we spend together..... Dear Arjan, really nice to work with you in the lab and also thank you for “endure” my nonsensical humor for so long :).....

致我亲爱的家人：

谢谢爸爸们、妈妈们和甲子对我的支持、理解与包容，你们是我的动力，特别谢谢爸爸在我失落时对我的鼓励；谢谢小倩、小房、小维尼，有了你们让我安心的远行；谢谢爱我的外公（对不起，没能守候在您的身边）、外婆；谢谢爱我的爷爷、奶奶；谢谢爱我小姨，姨父，舅舅，叔叔们，婶婶们，姑姑，姑父，还有我亲爱的兄弟姐妹们。。。。。。

Ting Ting Xiao

Wageningen

15-04-2015



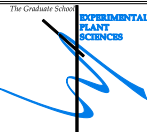


# CURRICULUM VITAE

## CURRICULUM VITAE

Ting Ting Xiao was born on 12<sup>th</sup> of July 1984 in Zibo, Shandong, China. She finished her high school education in 2003, in Zichuan NO. 1 Middle School. The same year, she started her 4 years Bachelor education in the College of Horticulture Science and Engineering of Shandong Agriculture University. There she worked in the laboratory of Prof. Chengshu Zheng on ornamental flower blossom physiology. After she got her Bachelor degree in 2007, she moved to the Netherlands and obtained her Master education in Wageningen University from 2008 till 2010 on Plant Breeding. There she specialized herself in marker-trait association mapping in tetraploid rose population and molecular marker development and recombination screening in tomato (F2 population generated from the cross between *Solanum chilense* and MoneyMaker) for TYLCV resistance gene *Ty-1*. After she obtained her Master degree in 2010, she got an opportunity to work as a PhD student in the Laboratory of Molecular Biology of Wageningen University. There, from 2010 till 2015, she mainly focused on plant lateral root organ development, under the supervision of promoter Prof. dr. Ton Bisseling and co-promoters Dr. Henk Franssen and Dr. ir. Rene Geurts. In this thesis, results during her PhD period were presented.

Education Statement of the Graduate School  
Experimental Plant Sciences



Issued to: Ting Ting Xiao  
Date: 20 May 2015  
Group: Laboratory of Molecular Biology  
University: Wageningen University & Research Centre

1) Start-up phase	date
First presentation of your project	
PINs expression during nodule formulation	Oct 15, 2010
Writing or rewriting a project proposal	
MSc courses	
Laboratory use of isotopes	
Radiation course, level 5 B	Apr 2011
Subtotal Start-up Phase	3.0 credits*
2) Scientific Exposure	date
EPS PhD student days	
EPS PhD student day, Leiden	Nov 21, 2013
Get2Gether Event, Soest	Jan 29-30, 2015
EPS theme symposia	
EPS Theme 1 Symposium Developmental Biology of Plants, Leiden	Jan 20, 2011
EPS Theme 1 Symposium Developmental Biology of Plants, Wageningen	Jan 19, 2012
EPS Theme 1 Symposium Developmental Biology of Plants, Leiden	Jan 17, 2013
EPS Theme 1 Symposium Developmental Biology of Plants, Leiden	Jan 24, 2014
NWO Lunteren days and other National Platforms	
ALW meeting 'Experimental Plant Sciences', Lunteren	Apr 19-20, 2010
ALW meeting 'Experimental Plant Sciences', Lunteren	Apr 04-05, 2011
ALW meeting 'Experimental Plant Sciences', Lunteren	Apr 02-03, 2012
ALW meeting 'Experimental Plant Sciences', Lunteren	Apr 22-23, 2013
ALW meeting 'Experimental Plant Sciences', Lunteren	Apr 14-15, 2014
Seminars (series), workshops and symposia	
Symposium on the plant endomembrane system, Amsterdam	Jul 02, 2010
Centre for Biosystems Genomics (CBSG) Technology Symposium, Wageningen	Nov 25, 2010
EPS symposium Plant Breeding in the Genomics Era, Wageningen	Nov 25, 2011
Seminar Prof. Doris Wagner, Wageningen	Jul 10, 2012
Two Seminars: Prof.dr. Howard S. Judelson and Dr. Rays H.Y. Jiang, Wageningen	May 07, 2013
Seminar Eric Kramer, Wageningen	Jul 02, 2013
Start symposium Plant Developmental Biology	Oct 14, 2013
Seminar Ying Zeng, Wageningen	Oct 24, 2013
Seminar on Bioinformatics, Wageningen	Nov 11, 2014
Seminar Prof. dr. Jiayang Li, Wageningen	Nov 15, 2013
Seminar Prof. dr. Wim van den Ende, Wageningen	Dec 13, 2013
Seminar Saskia Hogenhout, Amsterdam	Mar 07, 2014
Plant Sciences Seminar Mutualism in Action, Wageningen	Mar 11, 2014
Seminar Prof. Sophien Kamoun, Wageningen	May 28, 2014
Seminar Prof. dr. Claus Schwechheimer, Wageningen	Oct 21, 2014
Seminar plus	
International symposia and congresses	
Plant Vascular Development Conference, Vienna, Austria	Jul 01-02, 2012
The 23rd International Conference on Arabidopsis Research (ICAR), Vienna, Austria	Jul 03-07, 2012
4th European Retreat for PhD Students in Experimental Plant Sciences, Norwich, UK	Aug 15-17, 2012
10th European Nitrogen Fixation Congress (ENFC), Munich, Germany	Sep 02-05, 2012
13th Symposium on Biological Nitrogen Fixation With Non-Legumes (BNF), Munich, Germany	Sep 06-07, 2012
5th European Retreat for PhD Students in Experimental Plant Sciences, Ghent, Belgium	Jul 23-26, 2013
The 3rd ASian Conference on Plant-Microbe Symbiosis and Nitrogen Fixation (3APMNF), Chengdu, China	Oct 28-31, 2014
The 14th International Symposium on Nitrogen Fixation with Non-Legumes, Tenerife, Spain	Oct 31-Nov 03, 2014
Presentations	
Poster presentations at Lunteren Auxin and root nodule initiation	Apr 04-05, 2011
Oral presentation at EPS Theme 1 Symposium, Leiden	Jan 17, 2013
Oral presentation ALW meeting, Lunteren	Apr 23, 2013
Oral presentation at the 3APMNF Conference	Oct 30, 2014
IAB interview	
Meeting with a member of the International Advisory Board of EPS	Nov 14, 2012
Excursions	
Excursion to Rijk Zwaan, De Lier	Sep 27, 2013
Subtotal Scientific Exposure	20.3 credits*
3) In-Depth Studies	date
EPS courses or other PhD courses	
The legume-rhizobium symbiosis: from molecules to farmers' fields	Oct 18-22, 2010
Utrecht Summer School: Environmental Signaling	Aug 22-24, 2011
Microscopy and Spectroscopy in Food and Plant Sciences	May 06-09, 2014
Journal club	
Member of literature discussion group at laboratory of Molecular Biology	2010-2014
Individual research training	
Subtotal In-Depth Studies	6.6 credits*
4) Personal development	date
Skill training courses	
ExPeCtationS Day (EPS Career Day), Wageningen	Nov 18, 2011
Techniques for Writing and Presenting Scientific Papers	Oct 16-19, 2012
Information literacy	Apr 10-11, 2013
Chinese Association of Life-Sciences in the Netherlands Annual Meeting, Wageningen	Nov 09, 2013
Writing Grant Proposals, Wageningen	Apr 07-Jun 09, 2015
Organisation of PhD students day, course or conference	
Membership of Board, Committee or PhD council	
Subtotal Personal Development	4.4 credits*
<b>TOTAL NUMBER OF CREDIT POINTS*</b>	<b>34.4</b>
Herewith the Graduate School declares that the PhD candidate has complied with the educational requirements set by the Educational Committee of EPS which comprises of a minimum total of 30 ECTS credits	
* A credit represents a normative study load of 28 hours of study.	



This work was preformed at Laboratory of Molecular biology, Wageningen University, with support from Graduate School of Experimental Plant Sciences of the Netherlands.

Cover design: Xue Ping Xiao

Lay out: Ting Ting Xiao

Printed by: Proefschriftmaken.nl || Uitgeverij BOXPress

